Modeling the Kinetics of Bimolecular Reactions

Antonio Fernández-Ramos

Departamento de Quimica Fisica, Universidade de Santiago de Compostela, 15782 Santiago de Compostela, Spain

James A. Miller and Stephen J. Klippenstein†

Combustion Research Facility, Sandia National Laboratories, Livermore, California 94551-0969

Donald G. Truhlar*

Department of Chemistry and Supercomputing Institute, University of Minnesota, Minneapolis, Minnesota 55455-0431

Received October 3, 2005

Contents

1. Introduction 4518
2. Gas-Phase Thermal Reactions 4518
   2.1. Thermodynamics: Enthalpies and Free Energies of Reaction 4518
   2.2. Kinetics 4520
      2.2.1. Arrhenius Parameters and Free Energy of Activation 4520
      2.2.2. Collision Theory 4521
   2.3. Saddle Points and Potential Energy Surfaces 4523
   2.4. Rate Theory for Simple Barrier Reactions 4531
      2.4.1. Conventional Transition State Theory 4531
      2.4.2. Variational Transition State Theory 4532
      2.4.3. Anharmonicity 4538
      2.4.4. Tunneling, Recrossing, and the Transmission Coefficient 4541
      2.4.5. Improvements in VTST Methodology 4545
      2.4.6. Reduced-Dimensionality Theory 4546
      2.4.7. Direct Dynamics Calculations 4547
      2.4.8. Fully Quantal Calculations 4547
   2.5. Bimolecular Reactions over Potential Wells 4548
      2.5.1. RRKM Assumption 4548
      2.5.2. Variational Transition State Theory for Barrierless Addition Reactions 4549
      2.5.3. Master Equation and Its Application to Reactions over Potential Wells 4553
      2.5.4. Energy Transfer 4554
      2.5.5. Solving the Master Equation 4556
3. Gas-Phase State-Selected Reactions and Product State Distributions 4562
   3.1. Electronically Adiabatic Reactions 4563
   3.2. Electronically Nonadiabatic Reactions 4564
4. Condensed-Phase Bimolecular Reactions 4568
   4.1. Reactions in Liquids 4568
   4.2. Reactions on Surfaces and in Solids 4570
   4.3. Tunneling at Low Temperature 4571
5. Concluding Remarks 4572
6. Glossary of Acronyms 4572
7. Acknowledgments 4572
8. References 4572

* To whom correspondence should be addressed.
† Current address: Chemistry Division, Argonne National Laboratory, Argonne, IL 60439 USA.

1. Introduction

This review is concerned with the theoretical and computational modeling of bimolecular reactions, especially with generally applicable methods for kinetics (i.e., overall rates as opposed to detailed dynamics). It includes a basic theoretical framework that can be used for gas-phase thermal reactions, gas-phase microcanonical and state-selected reactions, and condensed-phase chemical reactions. The treatment of gas-phase thermal reactions includes separate discussions of simple direct reactions over a barrier, which usually have tight transition states and reactions proceeding over a chemical potential well, which can have a number of additional complications, such as barrierless addition potentials (which generally have loose, flexible transition states), competitive reaction pathways, isomerizations between multiple wells, and pressure-dependent energy transfer processes. The section on thermal reactions has a heavy emphasis on (generalized) transition state theory (TST) including multidimensional tunneling because this theory provides the best available method to calculate thermal rate constants for all but the very simplest systems. The section on state-selective reactions and product state distributions includes an introduction to the theory of electronically nonadiabatic reactions and coupled potential energy surfaces, as required for modeling photochemical and chemiluminescent reactions. The section on bimolecular reactions in liquid solution considers diffusion control and equilibrium and nonequilibrium solvation.

2. Gas-Phase Thermal Reactions

2.1. Thermodynamics: Enthalpies and Free Energies of Reaction

The rate constant (or, equivalently, rate coefficient) for a pressure-independent bimolecular reaction is defined experimentally as follows. Two substances A and B (reactants)

10.1021/cr050205w CCC: $59.00 © 2006 American Chemical Society
Published on Web 11/08/2006

Antonio Fernández-Ramos was born in Ourense (Galicia), Spain in 1970. He received his B.A. in Chemistry in 1993 and his Ph.D. in 1998 from the Universidade de Santiago de Compostela, the latter under the direction of Miguel A. Ríos and Jesús Rodríguez. He started his postdoctoral training as Visiting Fellow of the Steacie Institute for Molecular Sciences of Ottawa from 1998 to 2000, and he has worked in collaboration with Zorka Smedarchina, Willem Siebrand, and Marek Zgierski in the development of an approximate method to model proton transfer reactions at low temperatures. In 2001, he was awarded a postdoctoral grant of the Fundaçao para a Ciencia e a Tecnologia of Portugal to work in the Universidade de Coimbra with Antonio Varandas. He has been regularly collaborating with Donald G. Truhlar since 2000 in the improvement of some aspects of variational transition state theory. Since 2001 he is a "Ramón y Cajal" associate researcher at the Universidade de Santiago de Compostela. His research interests are computational chemistry and chemical reaction dynamics. He has authored over 50 publications and has been awarded with the Spanish Royal Society of Chemistry Award to young scientists in 2003. He has been married to María del Carmen Feijoo since 1995.

undergo an elementary gas-phase reaction

$$A + B \rightleftarrows C_1 + \cdots + C_n \qquad (2.1.1)$$

where C_1, ..., C_n are products. Equation 2.1.1 with $n = 3$ implies that three products are formed from two reactants. This happens quite frequently in very exothermic reactions, where a product can be formed with a very large amount of internal energy, enough that the molecule can dissociate spontaneously before it is stabilized by collisions with other molecules. One might view this physically as a two-step process: $A + B \rightarrow C_1 + C_2C_3^*$ followed by $C_2C_3^* \rightarrow C_2 + C_3$. Similarly, again for $n = 3$, the reverse formally termolecular reactions may be described as two bimolecular reactions. (We shall not be concerned with the mechanism of termolecular reactions in this review.)

Number densities, that is, concentrations (denoted [A], [B], ...) can be monitored as a function of time and fitted to the phenomenological second-order rate law

$$-\frac{d[A]}{dt} = k[A][B] - k'\prod_{i=1}^{n}[C_i] \qquad (2.1.2)$$

where k and k' are the forward and reverse temperature-dependent rate constants (or rate coefficients), respectively. The equilibrium constant, K, for the process is given by the quotient of the forward and reverse rate constants,[1] and the reaction quotient is defined by

$$Q_K = \frac{\prod_{i=1}^{n}[C_i]}{[A][B]} \qquad (2.1.3)$$

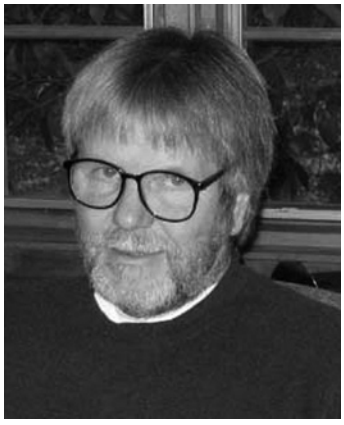

James A. Miller was born in Huntington, WV in 1946. He received his bachelor's degree from the University of Cincinnati and his Ph.D. from Cornell University in 1974. He has worked at Sandia National Laboratories in Livermore, CA. since that time. He was part of the founding staff of the Combustion Research Facility in 1980 and has had the title "Distinguished Member of the Technical Staff" since 1989. His research interests are principally in combustion chemistry and theoretical chemical kinetics. He has published extensively in both the physical chemistry and combustion literature. He is best known for his work on the nitrogen chemistry of combustion and the gas-phase chemistry leading to soot formation. His paper "Mechanism and Modeling of Nitrogen Chemistry in Combustion" [Miller, J. A.; Bowman, C. T. *Prog. Energy Combust. Sci.* **1989**, *15*, 287–338] is the single most cited paper ever to appear in any combustion journal. His 1992 paper "Kinetic and Thermodynamic Issues in the Formation of Aromatic Compounds in Flames of Aliphatic Fuels" [Miller, J. A.; Melius, C. F. *Combust. Flame* **1992**, *91*, 21–39] is the most cited paper to appear in the journal *Combust. Flame* in its 49-year history. He is a Fellow of the American Physical Society and a member of the American Chemical Society, the American Association for the Advancement of Science, and The Combustion Institute, from whom he received the Silver Medal in 1990 and the Lewis Gold Medal in 2006. He has been married to Connie Miller since 1971. They have two children, Abigail and Nathan, both of whom are budding scientists.

Usually the rate constant is measured under conditions where the second term in eq 2.1.2 is negligible. In this case, k gives the total rate constant for formation of all products. Complications arise if the states of A or B are not thermally equilibrated or if back reaction occurs from unequilibrated products.[1]

The temperature-dependent equilibrium constant is related to the standard-state Gibbs free energy of reaction, $\Delta G_T^o(T)$ at temperature T by

$$K = Q_K^o(T)\exp[-\Delta G_T^o/RT] \qquad (2.1.4)$$

where R is the gas constant, Q_K^o is the value of the reaction quotient at the standard state, and

$$\Delta G_T^o(T) = \Delta H_T^o(T) - T\Delta S_I^o \qquad (2.1.5)$$

where ΔH_T^o and ΔS_T^o are the standard-state enthalpy and entropy of reaction, respectively. The standard state for gas-phase molecules can be an ideal gas at a partial pressure of 1 atm or any stated concentration, e.g., 1 cm^3 $molecule^{-1}$ or 1 mol L^{-1}; the standard-state for liquid-phase solutes can be an ideal solution with a concentration of 1 mol L^{-1}, etc.

In general, the free energy change upon reaction is

$$\Delta G = RT\ln\frac{Q_K}{K} \qquad (2.1.6)$$

If the free energy change is zero, the reaction is at

Stephen J. Klippenstein was born in Winnipeg, Canada in 1960. He received a B.Sc. in chemistry and mathematics from the University of British Columbia, Canada, in 1983 and a Ph.D. in Chemistry from Caltech in 1988 under the direction of R. A. Marcus. After one year of postdoctoral research at the University of Colorado, Boulder, he joined the faculty in the Department of Chemistry at Case Western Reserve University, in 1989. He remained there until 2000, when he moved to the Combustion Research Facility, at Sandia National Laboratories in Livermore, CA. In 2005, shortly after writing this review, he moved to the Chemistry Division of Argonne National Laboratory, where he is currently a Senior Chemist in the Chemical Dynamics in the Gas-Phase Group. His research interests are in theoretical gas-phase chemical kinetics with particular emphasis on the modeling of reactions of importance in combustion chemistry. In 2004, he received the O. W. Adams award from Sandia, for outstanding achievement in combustion science. He has been married to Gloria Klippenstein since 1985, and they have four children, Kenneth, Jennifer, Edwin, and Ashley.

Donald G. Truhlar was born in Chicago in 1944. He received a B.A. in chemistry from St. Mary's College of Minnesota in 1965 and a Ph.D. from Caltech in 1970 under the direction of Aron Kuppermannn. He has been on the faculty of the University of Minnesota since 1969, where he is currently Regents Professor of Chemistry, Chemical Physics, Nanoparticle Science and Engineering, and Scientific Computation. His research interests are theoretical and computational chemical dynamics and molecular structure and energetics. He is the author of over 800 scientific publications, and he has received several awards for his research, including a Sloan Fellowship, Fellowship in the American Physical Society and the American Association for the Advancement of Science, an NSF Creativity Award, the ACS Award for Computers in Chemical and Pharmaceutical Research, the Minnesota Award, the National Academy of Sciences Award for Scientific Reviewing, the ACS Peter Debye Award for Physical Chemistry, the Schrödinger Medal of The World Association of Theoretical and Computational Chemists, and membership in the International Academy of Quantum Molecular Science. He has been married to Jane Truhlar since 1965, and he has two children, Sara Elizabeth Truhlar and Stephanie Marie Eaton Truhlar.

equilibrium. If ΔG_T° or ΔG is negative, the reaction may be called exergonic (work-producing), and if either of these quantities is positive, the reaction may be called endergonic (work-consuming).

The enthalpy of reaction (heat of reaction at constant pressure) is negative for an exothermic reaction (which releases heat) and positive for an endothermic reaction (which absorbs heat) and can be obtained at a given temperature from the enthalpies of formation of the reactants and products. For an electronically adiabatic reaction, the enthalpy of reaction at 0 K may be calculated quantum mechanically as the change in Born−Oppenheimer electronic energy (which includes nuclear repulsion) plus the change in zero point vibrational energy. The Born−Oppenheimer electronic energy is the potential energy surface for nuclear motion. A reaction with a negative potential energy of reaction is called exoergic, and one with a positive energy of reaction is called endoergic. A reaction with a negative change in free energy is called exergonic, and one with a positive change in free energy is called endergonic.

The enthalpy of reaction can also be computed by Hess's law as the sum of the heats of formation of the products minus the sum of the heats of formation of reactants. Recent progress in electronic structure calculations[2] allows one to compute enthalpies of formation with chemical accuracy[3] (~1 kcal/mol) for most systems with up to about 50 electrons.[4] For larger systems, one should probably judge the accuracy in terms of kcal/mol per bond. Transition metals provide a more severe test, and typical errors of even the best methods are often several kcal/mol per bond.

2.2. Kinetics

2.2.1. Arrhenius Parameters and Free Energy of Activation

From a phenomenological point of view, numerous experiments have shown that the variation of the rate constant with temperature can be described by the Arrhenius equation[5]

$$k = A \exp(-E_a/RT) \qquad (2.2.1)$$

where A is the preexponential or frequency factor, which may have a weak dependence on temperature, and E_a is the activation energy. A plot of ln k versus $1/T$ is called an Arrhenius plot. If a reaction obeys the Arrhenius equation, then the Arrhenius plot should be a straight line with the slope and the intercept being $-E_a/R$ and A, respectively. The activation energy can be very roughly interpreted as the minimum energy (kinetic plus potential, relative to the lowest state of reactants) that reactants must have to form products (the threshold for reaction), and the preexponential factor is a measure of the rate (collision frequency) at which collisions occur. A more precise interpretation of E_a was provided by Tolman,[6,7] who showed that the Arrhenius energy of activation is the average total energy (relative translational plus internal) of all reacting pairs of reactants minus the average total energy of all pairs of reactants, including nonreactive pairs. The best way to interpret A is to use transition state theory, which is explained below.

Although transition state theory will be presented in detail in Sections 2.4 and 2.5, it is useful to anticipate here the general form of the result. For bimolecular reactions, TST yields an expression of the form

$$k(T) = \frac{1}{\beta h}\gamma(T)K^\circ \exp(-\Delta G_T^{\ddagger,\circ}/RT) \qquad (2.2.2)$$

where $\Delta G_T^{\ddagger,o}$ is the quasithermodynamic free energy of activation, and $\gamma(T)$ is a transmission coefficient, K^o is the reciprocal of the standard state concentration, h is Planck's constant, and β is $1/k_BT$, where k_B is Boltzmann's constant. (Note that some formulations include a symmetry number σ that counts equivalent paths to the transition state; however, we omit this and include symmetry numbers in $\Delta G_T^{\ddagger,o}$, which is equivalent[8,9] and allows symmetry effects to be included by the same methods that are well established for real equilibria.) It is common practice, especially for reaction kinetics in the liquid phase, to write eq 2.2.2 as

$$k(T) = \frac{1}{\beta h} K^o \exp(-\Delta G_{act}^o(T)/RT) \qquad (2.2.3)$$

where $\Delta G_{act}^o(T)$ is the phenomenological free energy of activation. Clearly

$$\Delta G_{act}^o(T) = \Delta G_T^{\ddagger,o} - RT \ln \gamma(T) \qquad (2.2.4)$$

2.2.2. Collision Theory

In this section, we briefly discuss collision theory. Collision theory is necessary if one wants to discuss differential cross sections or most state-selected phenomena,[10] but the present article is more focused on thermally averaged rate constants. For rate constants, it has been emphasized that collision theory and transition state theory make the same predictions if the same criterion is used for reaction.[11] However, the theories are also complementary in that one or another may be more convenient for a specific application. Furthermore, collision theory can be used to provide a foundation for deriving transition state theory.[12−14] We consider collision theory first.

Simple collision theory provides useful insight into the temperature dependence and magnitude of bimolecular rate constants. There are several possible outcomes for a collision of atom or molecule A in internal state i with molecule B in internal state j:

(i) Elastic collision: Neither the arrangement (composition and bonding pattern), nor the internal state of the molecules, nor the relative translational energy changes; the only change is in the direction of their relative motion.

(ii) Inelastic collision: The two molecules retain their arrangement but change their internal states.

(iii) Reactive collision: The two molecules react to form one or more new molecules, for example, C in internal state m and D in the internal state n.

In case (iii), where a number of A(i) are incident in a beam with relative velocity V_R upon a scattering zone containing B(j), we may define the state-selected rate constant k_{ij} and reaction cross section σ_{ij} such that

$$k_{ij}(V_R) = V_R \sigma_{ij}(V_R) \qquad (2.2.5)$$

The average reaction cross section σ_r is obtained by averaging over all the reactants internal states:

$$\sigma_r = \sum_{i,j} w_i^A w_j^B \sigma_{ij}(V_R) \qquad (2.2.6)$$

where w_i^A and w_j^B represent the Boltzmann weighting factors of the i and j reactant internal states, respectively. The thermal rate constant for the process is given by averaging $V_R\sigma_r$ over an equilibrium Maxwell−Boltzmann distribution of V_R; the result is[12,15,16]

$$k = \beta\left(\frac{8\beta}{\pi\mu}\right)^{1/2} \int_0^\infty dE_{rel} E_{rel} \sigma_r(E_{rel}) \exp(-\beta E_{rel}) \qquad (2.2.7)$$

where

$$E_{rel} = \mu V_R^{\ 2}/2 \qquad (2.2.8)$$

is the relative translational energy, with μ being the reduced mass of relative translational motion.

It is also possible to obtain state-selected thermal rate constants by considering separately each of the internal states

$$k_{ij} = \beta\left(\frac{8\beta}{\pi\mu}\right)^{1/2} \int_0^\infty E_{rel} \sigma_{ij}(E_{rel}) \exp(-\beta E_{rel}) dE_{rel} \qquad (2.2.9)$$

Sometimes it is also useful to define the reaction probability P_R as a function of the impact parameter b, which is defined as the distance of closest approach between the two molecules in the absence of interparticle forces. The probability of reaction decreases to zero for large b. Actually, we can consider a value of $b = b_{max}$ after which the reaction probability is negligible, and the reaction cross section is given by

$$\sigma_r = 2\pi \int_0^{b_{max}} P_R(b) b db \qquad (2.2.10)$$

The simplest model is to consider the reactants as hard spheres that do not interact with each other if the intermolecular distance is larger than the arithmetic average d of their diameters, and so $P_R(b > d) = 0$, but that react at all shorter distances so $P_R(b \le d) = 1$. For this case the reaction cross section is πd^2, and by applying eq 2.2.7 one finds that the reaction rate equals

$$k(T) = \left(\frac{8}{\pi\mu\beta}\right)^{1/2} \pi d^2 \qquad (2.2.11)$$

The thermally averaged value of the relative speed is

$$\bar{V}_R = \left(\frac{8}{\pi\mu\beta}\right)^{1/2} \qquad (2.2.12)$$

so that eq 2.2.11 can be rewritten as

$$k = \bar{V}_R \pi d^2 \qquad (2.2.13)$$

In other words, k is usually the thermal average $\overline{V_R\sigma_r}$ of $V_R\sigma_r$, but if σ_r is independent of relative speed, then k becomes $\bar{V}_R\sigma_r$. Equation 2.2.11 does not account for the observed experimental behavior described by the Arrhenius equation, since it predicts a temperature dependence of $T^{1/2}$ for the rate constant.

An improvement of this model is the reactive hard spheres model in which it is assumed that the reaction occurs if $\mu V_{LOC}^2/2$ exceeds a threshold energy E^0, where V_{LOC} is the relative velocity along the line of centers, i.e., in the direction connecting the centers of the two spheres. This velocity depends on the impact parameter so that the reaction is assumed to occur if

$$E^o \le E_{rel}(1 - b^2/d^2) \qquad (2.2.14)$$

Then the reaction cross section is

$$\sigma_r = \pi b_{max}{}^2 = \pi d^2(1 - E^o/E_{rel}) \qquad (2.2.15)$$

and the rate constant is

$$k(T) = \pi d^2\left(\frac{8}{\pi\mu\beta}\right)^{1/2} \exp(-\beta E^o) \qquad (2.2.16)$$

which is similar to the Arrhenius expression and predicts a variation with temperature of $T^{1/2}$ for the preexponential factor. A problem with the reactive hard spheres model is that it does not predict the preexponential factor is much smaller than the gas-kinetic collision rate, although one finds experimentally that this is often the case. To solve this problem, a multiplicative empirical steric factor p was introduced into the rate constant (2.2.16). The main problem with these models is that they do not consider that a molecule may react only when it is oriented in a particular manner, nor do they account for the shapes and rotational−vibrational motions of the reactants. These limitations are overcome by transition state theory.

Analytical expressions have been given for the thermal rate constants using other forms for σ_r.[17,18]

One case where reactions often occur without a barrier (and hence where collision theory can be particularly useful) is the collision of an ion with a neutral molecule. A useful simple model for this case is the Langevin model,[19−21] which assumes that the ion is a point charge and the molecule is a structureless sphere with polarizability α. It is assumed that at long range only the ion-induced dipole attractive term in the potential is important; the effective potential is then given by

$$V_{eff} = -\frac{1}{2}\frac{\alpha q^2}{r^4} + \frac{L^2}{2\mu r^2} \qquad (2.2.17)$$

where r is the distance between collision partners, q is the charge of the ion, and L is the orbital angular momentum. (In later sections, the classical L^2 is replaced by the quantal $l(l + 1)$, where l is the orbital quantum number.) The first term in eq 2.2.17 is the ion-induced dipole potential, and the second term is the centrifugal potential. Because $L = \mu V_R b$ and using (2.2.8), we obtain

$$V_{eff}(r) = -\frac{1}{2}\frac{\alpha q^2}{r^4} + E_{rel}\left(\frac{b}{r}\right)^2 \qquad (2.2.18)$$

The effective potential in eq 2.2.18 has a single maximum at a radius r_* given by

$$r_* = \frac{1}{b}\left(\frac{\alpha q^2}{E_{rel}}\right)^{1/2} \qquad (2.2.19)$$

and the effective potential at the maximum is

$$V_{eff,*} = \frac{E_{rel}{}^2 b^4}{2\alpha q^2} \qquad (2.2.20)$$

The critical impact parameter b_* is obtained from $V_{eff,*}$ and is given by[21]

$$b_* = (2\alpha q^2/E_{rel})^{1/4} \qquad (2.2.21)$$

and the reaction cross section is

$$\sigma = \pi b_*{}^2 = \pi\left(\frac{2\alpha q^2}{E_{rel}}\right)^{1/2} \qquad (2.2.22)$$

Thus, $V_R\sigma_r$ in eq 2.2.5 is independent of V_R. If $E_{rel} < V_{eff,*}$, the centrifugal barrier cannot be penetrated (if tunneling is neglected), and no reaction occurs. If $E_{rel} = V_{eff,*}$ the ion is captured into a circular orbit of radius r_* around the molecule. Finally, if $E_{rel} > V_{eff,*}$ the ion can move inside the centrifugal barrier, and the reaction probability is assumed to be equal to unity.

The thermal rate constants obtained by the Langevin model are independent of temperature and velocity and are given by

$$k_L = 2\pi\left(\frac{\alpha q^2}{\mu}\right)^{1/2} \qquad (2.2.23)$$

For some reactions involving nonpolar molecules, the Langevin model cross sections agree quite well with experiment even at translational energies up to 5 eV,[22,23] but in general the model is only valid when the cross sections exceed the hard-sphere cross sections. The hard-sphere diameter for an ion can be estimated in various ways, for example, by computing the potential energy curve or potential energy surface for its interaction with a neon atom, whose hard-sphere radius is known. At large E_{rel}, b_* becomes less than the sum d of the effective hard-sphere radii of the collision partners so a better model is

$$\sigma_r = \max\begin{cases}\pi(2\alpha q^2/E_{rel})^{1/2} \\ \pi d^2\end{cases} \qquad (2.2.24)$$

An analogue of the Langevin ion−dipole model for neutral reactions without a barrier (the most common examples of these are many radical−radical reactions) is the Gorin model which replaces $-\alpha q^2/2r^4$ in eq 2.2.17 by $-(C_6/r^6)$[24−29] where C_6 is a constant. With the Gorin model, the thermal rate constant is given by

$$k_{Gorin}(T) = \sqrt{\frac{\pi}{\mu}}2^{11/6}\Gamma\left(\frac{2}{3}\right)(C_6)^{1/3}(k_B T)^{1/6} \qquad (2.2.25)$$

This predicts a centrifugal barrier at much smaller R than that of the Langevin model, and it is much less likely that actual molecules can be treated as structureless and isotropic at this distance than the ion−molecule partners can be treated as structureless and isotropic at their centrifugal barrier. Therefore, reactions between neutral molecules are less likely than ionic reactions to be dominated by the long-range force law. It has been suggested that a steric factor can be used to correct for such deficiencies,[30] but such corrections tend to be purely empirical, providing little physical insight. More sophisticated methods for treating both neutral and ionic reactions without a barrier are considered in Section 2.5.

The Langevin model and later improvements are still useful for current work and are widely used; however, analytic collision theory has been largely overtaken by more detailed and accurate TST calculations and by the use of classical trajectory calculations. The latter allow the study of the dynamics at the microscopic level (differential cross sections, total cross sections, product energy distributions, etc., ...), as well as at the macroscopic level (thermal rate constants by numerical or Monte Carlo integration of eq 2.2.7), by solving the classical equations of motion. To run

the trajectories, a potential energy surface should be supplied (its construction is discussed in the next section) together with the initial conditions for the coordinates and momenta. To sample as much as possible of the initial phase space (coordinates and momenta) and to get meaningful results, many trajectories (usually thousands or tens of thousands) should be run. Often one restricts the initial vibrational energies in the various vibrational modes to their allowed quantized values, and when this is done the method is usually called the quasiclassical trajectory (QCT) method.[31] QCT calculations can give accurate results when dynamical quantum effects such as zero point energy, tunneling, and resonances are not important. Methods[32−35] for trajectory calculations and a summary of classical models[36] for reactive collisions are available in reviews in other books.

For thermal rate constants of most chemical reactions, trajectory calculations suffer from two major defects: (i) failure to maintain zero point energy in modes transverse to the reaction coordinate, and (ii) inability to include tunneling. Defect (i) has been called "nonadiabatic leak," and it tends to make trajectory-calculated rate constants too large.[31] Several methods have been proposed for alleviating this, but none are satisfactory.[37] There have also been attempts to add tunneling to trajectory calculations, and a recent study suggests that such methods deserve further investigation.[38]

Even more accurate information can be obtained by performing quantum mechanical scattering calculations.[39−53] For systems with only a few atoms, one can even calculate converged reaction cross sections and rate constants for a given potential energy surface. For example, very accurate calculations are available for the D + H_2[50,51] and H + H_2[53] reactions. A recent review includes applications to bimolecular reactions with up to six atoms.[47] The early work on applying scattering theory to chemical reaction rates involved first calculating converged state-to-state cross sections[49] and then summing these over product states and averaging them over thermal initial conditions. More recent work calculates the converged thermal constant without generating or even implicitly converging the state-to-state details. This kind of treatment is based on time-dependent flux correlation functions,[54,55] which can be calculated by time-dependent[56] or time-independent[57] quantum mechanics. We return to this topic in Section 2.4.7.

2.3. Saddle Points and Potential Energy Surfaces

In many cases, it is possible to separate the motion of the electrons from the motion of the nuclei, because the nuclei move more slowly due to their higher mass. The condition for the motion of both particles to be separable is that the nuclear motion should proceed without change in the quantum state of the electron cloud and, in this case, the potential energy is only a function of the nuclear coordinates. This approximation is known as the Born−Oppenheimer or electronically adiabatic approximation, and it is equivalent to assuming that the motion of the atoms does not cause real or virtual transitions between different electronic states. This condition is met if the electronic states are well separated from each other. In this review, except in Section 3.2 and one paragraph of Section 4.1, we consider systems in the ground electronic state for which the Born−Oppenheimer approximation is valid.

The study of the dynamics of a chemical reaction requires knowledge of the potential energy surface (PES) for nuclear motion. The PES is the potential energy as a function of the nuclear coordinates of the system. According to the Born−Oppenheimer approximation,[58−62] it is equal to the adiabatic electronic energy, including nuclear repulsion. The electronically adiabatic energy E of the system is given by

$$E = T_R + V_{NR}(R) + E_\gamma^{(el)}(R) \qquad (2.3.1)$$

where $\mathbf{R}$ is the set of $3N - 6$ independent coordinates, $T_\mathbf{R}$ is the nuclear kinetic energy, and $V_{NR}(\mathbf{R})$ and $E_\gamma^{(el)}(\mathbf{R})$ are the nuclear Coulombic repulsion energy and the electronic energy, respectively. The subscript on $E_\gamma^{(el)}$ denotes the electronic quantum number, and we consider this to be the ground state ($\gamma = 1$). Thus, the potential energy for the motion of the nuclei is

$$V(\mathbf{R}) = V_{NR}(\mathbf{R}) + E_1^{(el)}(\mathbf{R}) \qquad (2.3.2)$$

In the case of a bimolecular reaction, the PES should cover the range of geometries from separated reactants through the strong interaction region and on to the separated products. If the two fragments A and B are very far apart, there is no interaction between them and the potential energy is the sum of the potential energies of the fragments. When the fragments approach, there is interaction between their electronic clouds until a common electronic cloud is formed. The forces due to the electron cloud change during this process, and these forces are the gradient field of the PES.

Since $E_\gamma^{(el)}$ is an eigenvalue of the electronic Hamiltonian, the PES can be obtained by electronic structure calculations. Some workers divide electronic structure methods into ab initio and semiempirical. "Models which utilize only the fundamental constants of physics are generally termed ab initio; if some parameters are introduced which are determined by fitting to some experimental data, the methods are semiempirical."[3] Although purists prefer ab initio methods, it is usually necessary, except for very small systems, to use semiempirical methods to obtain satisfactory results, either semiempirical molecular orbital theory or high-level correlated methods with semiempirical parameters. Furthermore, even when high-level ab initio methods are affordable, they are usually less efficient than semiempirical methods.

Hartree−Fock (HF) theory[63−65] and Møller−Plesset second-order perturbation theory[66,67] (MP2) are examples of low-level ab initio methods; the former is inaccurate because of the neglect of electronic correlation, but it can be improved (and, as a bonus, made less expensive) if some matrix elements are substituted by empirical parameters. Two of the most successful of the semiempirical methods are the AM1[68] and PM3[69] semiempirical molecular orbital methods, implemented in the popular MOPAC program[70] and many other electronic structure packages. These methods, however, are often not accurate enough for practical work.

Higher accuracy can be obtained by including electron correlation and extending the basis sets used in the calculation. To use a method that accounts for *all* the electron correlation, like full configuration interaction with a large one-electron basis set, is feasible only for very small systems, and the increase of either the level of correlation or the basis set increases the cost of the calculation. Low-order treatments of correlation energy, as in MP2, are quantitatively inaccurate for kinetics, and higher-order correlated wave function theory, such as coupled cluster theory[71,72] with single and double excitations and a quasiperturbative treatment of selected connected triple excitations,[73] called CCSD(T), is

slowly convergent with respect to increasing the size of the one-electron basis set. However, if one can afford CCSD(T) calculations with two or more basis sets one can often extrapolate to the infinite-basis (IB) limit, also called the complete-basis-set (CBS) limit, and this often yields results good to 1 kcal/mol.[74,75]

Although CCSD(T) is generally very useful, it does not describe bond breaking accurately if one considers bond distances larger than those in typical atom-transfer transition states. For such applications as well as some other "multireference" situations, a "completely renormalized" (CR) coupled cluster theory is more accurate.[76−78]

A variety of one-electron basis sets are available. A major breakthrough in understanding basis-set convergence was provided by analyzing atomic natural orbitals,[79] and this led to Dunning's correlation-consistent polarized (cc-p) basis sets,[80] which are available in sequences of increasing quality, e.g., valence double-ζ (cc-pVDZ), valence triple-ζ (cc-pVTZ), valence quadruple-ζ (cc-pVQZ), etc.[81] When systematic sets of diffuse functions are included, a prefix aug- is added (denoting "augmented").[82] Less systematic, but often more economical, basis sets were developed by Pople and co-workers. For example, 6-31+G(d,p)[83] is an economical alternative to aug-cc-pVDZ, and MG3S[84] is an economical alternative to aug-cc-pVTZ. For H though Si, MG3S is the same as 6-311+G(3d2f,2df,2p),[83] whereas for P through Cl it differs from G3Large[85] by the deletion of core polarization functions on nonhydrogenic atoms and diffuse functions on H. We note that the versatile 6-31+G(d,p) basis has also been called DIDZ ("desert-island double-ζ") to denote its general usefulness, and MG3S could similarly be called DITZ.[86] Some workers prefer other basis sets such as 6-311++G(d,p)[83] which is correlation inconsistent but nevertheless often gives reasonably well-converged geometries or vibrational frequencies at lower expense than aug-cc-pVTZ. Another useful "inconsistent" basis is 6-311+G(3df,2pd).[4] The popular 6-31G(d) and 6-31+G(d,p) basis sets, the balanced 6-31B(d) basis set,[87] the economical MIDI![88] and MIDIY[89] basis sets, split-valence polarized (SVP) basis,[90] and the core-pruned general contractions[91] may be useful for calculations on large molecules.

Another useful strategy is to use semiempirical models that employ correlated wave functions. Typically, these methods involve carrying out the calculation at more than one level ("level" = electron correlation method plus one-electron basis set), and there are several successful multilevel methods such as the scaling-all correlation (SAC) method,[92−97] the complete basis set (CBS) methods,[98−100] the multicoefficient correlation methods (MCCM),[87,96,97,101−105] including multi-coefficient Gaussian-3,[97,103] scaled Gaussian-3 (G3S),[106,107] scaled and extended Gaussian-3 (G3SX),[108] the balanced multi-coefficient coupled cluster singles and doubles method[87] (BMC−CCSD), multi-coefficient Gaussian-2[102] (MCG2), the original Gaussian-2 (G2)[109] and Gaussian-3 (G3)[85,107] methods, and the Weizmann-1 (W1) and Weizmann-2 (W2) methods.[110] These methods use different schemes and different empirical data to extrapolate to full electron correlation and an infinite basis set. Methods employing lower (and hence more affordable) levels[87,97,101,108] may be especially well suited to kinetics applications; these are sometimes called reduced-order methods. A review is available.[111]

As an example of high-level calculations applied to a difficult case, Table 1 compares the transition state geometries and classical barrier heights for the $F + H_2 \rightarrow HF + H$ reaction as calculated by five high-level methods: scaling external correlation[112,113] (SEC), multireference configuration interaction with single and double substitutions[114] (MR-CISD), multi-coefficient Gaussian-3[115] (MCG3), multireference coupled cluster[116] (MRCC), fixed-node diffusion quantum Monte Carlo[117] (FN-DQMC), and r_{12}-averaged coupled-pair functional[118] (r_{12}-ACPF-2) calculations. The values of the classical barrier height are tabulated in all cases both with and without the relativistic spin−orbit contribution of 0.39 kcal/mol. The table shows good convergence of the most complete calculations[114−118] and reasonable agreement with the original calculations that predicted a bent transition state,[112,113] in contrast to the collinear transition state that had been inferred from semiempirical valence bond calculations,[119] unconverged ab initio calculations,[120] and molecular beam experiments.[121]

Table 1. Electronic Structure Calculations of the Bond Lengths (Å), Bond Angle (deg), and Barrier Height (kcal/mol) of the Saddle Point of the $F + H_2 \rightarrow HF + F$ Reaction

				$V^{\ddagger}$	
method	F−H	H−H	F−H−H	nonrel	rel
SEC	1.61−1.64	0.74−0.76	104−130	1.0−1.3	1.4−1.7
MR-CISD	1.55	0.77	119	1.5	1.9
MCG3[a]	1.51	0.775	128	2.8	3.2
MRCC	1.54	0.77	118	1.5	1.9
FN-DQMC	1.53	0.77	118	1.4	1.8
*r*12-ACPF-2	1.53	0.77	117	1.4	1.8

[a] Version 2s.

The electronic structure methods in the previous paragraphs all involve wave function theory (WFT). A different approach, less expensive in computer time, is based in the Kohn−Sham implementation of density functional theory (DFT),[122,123] especially hybrid DFT[124] and hybrid meta DFT[125] methods, which are versions of DFT with nonlocal density functionals. These methods account for the electron correlation energy and part of the electron exchange energy through functionals of the density and density gradient (DFT), through such functionals plus nonlocal exchange operators (hybrid DFT), and through such functionals plus nonlocal exchange operators and functionals of the kinetic energy density (hybrid meta DFT).

Some of the most useful hybrid DFT functionals, based on nonlocal exchange and on the density and magnitude of the local gradient of the density, are the B3LYP,[126] mPW1PW91,[127] MPW1K,[128] PBE1PBE,[129,130] and B97-2[131] functionals. Successful hybrid meta DFT methods include B1B95,[86,132] TPSSh,[125] BB1K,[132,133] MPW1B95,[134] MPWB1K,[134] BMK,[135] PW6B95,[136] PWB6K,[136] and M05-2X.[137] DFT calculations employing the above functionals with basis sets such as 6-31+G(d,p) and MG3 can be very useful for calculating geometries of stationary points (saddle points[138] and equilibrium geometries of reactants and products) at which more accurate energetic calculations (such as extrapolated CCSD(T) or MCCM calculations) may be carried out. Such DFT calculations can also be very useful for calculating vibrational frequencies of large molecules and saddle points. One advantage of DFT methods is that one can obtain reliable results with smaller basis sets than are required for reliable WFT calculations.

Another encouraging approach is the doubly hybrid DFT method,[139] which is a combination of SAC and hybrid or hybrid meta DFT. A problem with DFT-type methods is that

they are not systematically improvable, although the predictions of DFT can be systematically improved by combining them with successively higher levels of MCCMs.[140] Furthermore, over time the density functionals have been improved by better parametrizations.

Because the stationary points are often used to characterize the general features of a PES, algorithms for optimizing stationary points are very important. These have recently been reviewed.[141] Methods for finding reaction paths are also important, and the most commonly used methods require that one first find a saddle point. More recently, nudged elastic band methods have been developed that can compute a reaction path without first finding a saddle point.[142−146]

Almost all density functionals involve some empirical elements and should not be called ab initio; some workers call them "first principles" methods, although the precise boundary between first principles and other principles is not clear.

In summary, a wide variety of quantum chemical methods can allow us to obtain potential energy surfaces with high accuracy, the limitation being the size of the system, although the DFT-type methods can be applied to fairly big systems.

Trajectory simulations require knowledge of the PES over broad ranges of configuration space. More limited PES information is generally required for TST calculations, but the amount of required information does increase with the sophistication of the TST method. Various methods have been developed to obtain an accurate representation of the computed PES with the least computational effort. Reviews of PESs for reactive systems are available,[147,148] but progress since then is substantial.

In general, the first step is to locate all the stationary points important for the reaction. A particular geometry is a stationary point of the PES if the first derivatives of the potential (gradient) with respect to all the nuclear coordinates are zero

$$\frac{\partial V(\mathbf{R})}{\partial \mathbf{R}} = 0 \qquad (2.3.3)$$

In other words, all the forces on the atoms in the molecule are null. The nature of stationary points is determined by the eigenvalues of the Hessian matrix, which is the matrix of second derivatives with respect to nuclear coordinates. The stationary points are classified as minima, saddle points, and hilltops.

A geometry is a minimum (also called an equilibrium structure) when $3N - 6$ eigenvalues of the Hessian matrix are positive for a system with N atoms. The number of Cartesian coordinates is $3N$; we exclude the six eigenvalues that correspond to overall translation and rotation. For linear structures, there are only two rotational degrees of freedom so $3N - 6$ and $3N - 7$ become $3N - 5$ and $3N - 6$, respectively. The PES will usually (the major exception being radical−radical reactions) have van der Waals minima formed by intermolecular attraction before and/or after the collision, and in addition it sometimes has deeper minima due to chemical bonding; these are called wells. For nearly thermoneutral reactions, one expects van der Waals minima for both reactants and products, but for very exothermic reactions the reactants may come together without a transition state and without a reactant van der Waals complex.

When one says saddle point with no modifier, one usually means first-order saddle point. An nth-order saddle point in the PES is a geometry with n negative eigenvalues of the Hessian (again after excluding the six zero translations and rotations). Saddle points with $n > 1$ are also called hilltops. The most important saddle points are the first-order saddle points, for which only one eigenvalue is negative. The eigenvectors of the Hessian matrix at a stationary point are called normal coordinates.[149,150] A first-order saddle-point is a minimum of the PES with respect to $3N - 7$ normal vibrational coordinates, but a maximum with respect to the other one.

For a simple barrier reaction, there is only one first-order saddle-point which is a maximum with respect to this "reaction coordinate" of the process. This saddle point is commonly called a transition state, and the potential energy at this geometry minus the potential energy of the equilibrium reactants is the classical barrier height of the reaction, which, as discussed above, is a zero-order approximation to the activation energy in the Arrhenius equation. Therefore, a good PES should have chemical accuracy at least at the stationary points.

The simplest bimolecular reactions are atom−diatom reactions. The first quantum mechanical model for a reactive PES was derived for this kind of system by London,[151] based on the valence bond method for the $H + H_2$ exchange reaction,[152] and this became the basis of the London-Eyring-Polanyi (LEP),[153] London-Eyring-Polanyi-Sato (LEPS),[154,155] and extended-LEPS[156,157] potential energy surface fitting functions. The extended-LEPS model has three adjustable parameters (called the Sato parameters) that allow one to fit the location of the potential energy barrier and its height. This kind of PES, although historically very important, cannot represent most atom−diatom reactions accurately due to its lack of flexibility,[158] but it is still frequently useful for providing insight into reaction mechanisms. Examples are provided by recent studies of product energy release in the $H + HBr \rightarrow H_2 + Br$ reaction[159] and vibrationally inelastic and reactive probabilities for the N and N_2 degenerate rearrangement (exchange reaction).[160,161]

In current practice, due to the high accuracy that can be obtained from electronic structure calculations, the strategies used to construct polyatomic PESs are usually based on electronic structure calculations. The most straightforward procedure is called direct dynamics.[162−167] Direct dynamics is defined as "the calculation of rates or other dynamical observables directly from electronic structure information, without the intermediacy of fitting the electronic energies in the form of a potential energy function."[164] This is sometimes dubbed "on the fly" dynamics because every time the dynamics algorithm requires an energy, gradient, or Hessian, it is calculated "on the fly" by electronic structure methods. A difficulty, though, is that chemical accuracy requires high levels of electronic structure theory, and even for very small systems high levels of electronic structure theory are expensive in terms of computer time. The cost is higher for trajectory calculations than for variational transition state theory, and for this reason early direct dynamics trajectory calculations were based on neglect-of-differential-overlap approximations[168] or the Hartree−Fock approximation[169,170] and were limited to ensembles of short-time trajectories.

A recent example of a medium-level ab initio direct dynamics calculation on a bimolecular reaction is provided by a recent calculation on the gas-phase $Cl^- + CH_3Cl$ S_N2 reaction.[171] Although the level of theory chosen, MP2/6-31G(d), does not usually provide chemical accuracy for either barrier heights or anion thermochemistry (it does better

for a degenerate rearrangement like $Cl^- + CH_3Cl$), the trajectories required 92 h of computer time even with a step size large enough to allow energy nonconservation up to 0.6 kcal/mol. Such high costs are often reflected in sparse sampling to keep the total effort affordable. In the case at hand, only three bimolecular collisions were calculated. Also at the QCT/MP2 level, Liu et al.[172] studied the zero-point energy effect on quasiclassical trajectories for the bimolecular reaction of formaldehyde cation with D_2. Another possibility is to use density functional theory which, in general, can be quite accurate, or higher-level correlation methods. For instance, Camden et al.[173−175] carried out B3LYP/6-31G(d,p) calculations for a QCT direct dynamics study of $H + CD_4$. Yu et al.[176] studied the OH + HOCO reaction by using the SAC-MP2[92] method, which generally provides more accurate energies than the MP2 method. The scaling factor of SAC was obtained by minimizing the differences between this method and a coupled-cluster method.

For the purpose of evaluating cost/accuracy quotients of various electronic structure levels that might in principle be used for direct dynamics calculations, Zhao and one of the authors[177] applied several levels of electronic structure theory to five relevant databases, and the results are summarized in Table 2. The table shows mean unsigned errors (i.e., mean absolute deviations from best estimates) for five databases: AE6 for atomization energies of neutral main-group molecules,[178] EA13 for electron affinities of atoms and small molecules,[84] BH6 for barrier heights of bimolecular hydrogen-atom transfer reactions,[178] HAT12 for barrier heights of bimolecular neutral heavy-atom transfer reactions,[179] and NS16 for barrier heights of bimolecular anionic nucleophilic substitution reactions.[179] Table 3 shows mean signed errors for the same five databases. Table 2 also includes relative costs (in computer processor time) for evaluating the energy of a typical transition state configuration by each of the methods. Tables 2 and 3 show that MP2 calculations, although widely employed for direct dynamics, are not reliable for kinetics because they systematically overestimate barrier heights. SAC methods give improved accuracy but are still not as accurate as the best DFT method, MO5−2X. The older, but more popular B3LYP density functional is also less accurate than MO5−2X, and it systematically underestimates barrier heights. Boese et al. have commented,[180] "Very often, because of sheer user inertia, first-generation functionals are applied rather than the more accurate second-generation functionals."

Table 2. Mean Unsigned Errors (kcal/mol) and Costs (relative units) of Several Electronic Structure Levels

level	AE6[a]	EA13	BH6	HAT12	NS16	cost[b]
MP2/6-31G(d)	8.0	27.5	6.8	12.4	8.0	1.0
MP2/6-31+G(d)	8.2	10.2	6.6	12.5	2.3	1.4
MP2/6-31+G(d,p)	5.1	10.0	5.5	12.6	2.2	1.9
MP2/6-31+G(d,2p)	4.3	9.6	4.0	12.0	2.2	2.8
MP2/6-31++G(d,p)	5.3	10.0	5.4	11.2	2.2	2.3
MP2/6-311++G(d,p)	5.0	10.2	4.6	12.6	3.3	3.4
MP2/6-311++G(2df,2pd)	1.5	4.8	3.3	11.1	0.6	33.8
SAC-MP2/6-31G(d)	4.1	24.3	5.2	13.3	8.9	1.5
SAC-MP2/6-31+G(d,p)	2.1	7.8	4.2	12.1	2.9	2.8
SAC-MP2/6-31+G(d,2p)	1.6	7.8	2.7	11.5	2.8	3.9
B3LYP/6-31+G(d,p)	1.5	3.2	5.0	8.8	3.6	3.2
B3LYP/MG3S	0.7	2.3	4.7	8.5	3.3	11.0
M05−2X/6-31+G(d,p)	1.4	3.0	1.6	2.5	1.7	4.3
M05−2X/MG3S	0.7	2.0	1.4	2.0	1.5	15.6

[a] The mean unsigned error for atomization energies is on a per bond basis. [b] The cost for each method is the computer time for a single-point gradient calculation at a generalized transition state of the $OH^- + CH_3F$ S_N2 reaction divided by the computer time for the same calculation at the MP2/6-31G(d) level with the same computer program and same computer, averaged over two computers (IBM Power4 and SGI Itanium 2).

Table 3. Mean Signed Errors (kcal/mol) of Several Electronic Structure Levels

level	AE6[a]	EA13	BH6	HAT12	NS16
MP2/6-31G(d)	−8.0	27.5	6.8	12.0	−2.2
MP2/6-31+G(d)	−8.2	10.2	6.6	12.1	1.1
MP2/6-31+G(d,p)	−5.1	9.9	5.5	12.6	1.1
MP2/6-31+G(d,2p)	−4.3	9.5	4.0	12.0	1.0
MP2/6-31++G(d,p)	−5.3	9.9	5.4	11.2	1.1
MP2/6-311++G(d,p)	−5.0	10.2	4.6	12.6	3.3
MP2/6-311++G(2df,2pd)	−0.7	4.7	3.3	11.1	0.6
SAC-MP2/6-31G(d)	−1.0	24.3	5.2	11.5	−3.6
SAC-MP2/6-31+G(d,p)	−0.5	7.2	4.2	12.1	0.3
SAC-MP2/6-31+G(d,2p)	−0.3	7.2	2.7	11.5	0.3
B3LYP/6-31+G(d,p)	−1.5	−2.5	−5.0	−8.8	−3.6
B3LYP/MG3S	−0.6	−1.5	−4.7	−8.5	−3.3
M05−2X/6-31+G(d,p)	−1.4	−0.1	−0.6	1.1	−0.6
M05−2X/MG3S	0.0	0.5	−0.4	1.2	−0.8

[a] The mean unsigned error for atomization energies is on a per bond basis.

When high-level direct dynamics is not feasible, high-level electronic structure calculations can still be used in various other ways. For example, they can be used (i) as data for "fitting" or "interpolation" to a given analytical function or (ii) as data for parametrizing lower level electronic structure methods, which can then be used to perform the direct dynamics calculations. We will return to case (ii) in the final two paragraphs of this section; next, though, we consider several approaches for case (i).

In case (i), we say that the analytical function "fits" the ab initio data when the potential obtained by the function does not necessarily match the ab initio data and that it "interpolates" when it does match at the data points.[181]

A fitting (or interpolation) method is called global when the resulting PES is fit for all accessible ranges of the interesting coordinates. One can also construct semiglobal and local fits. The terms "global" and "local" will be used in the following paragraphs though to distinguish different ways to interpolate. A global interpolant is a single function that covers all the regions of the potential that are relevant to the dynamics and that is determined using all the data. In contrast, an interpolation method is called local when the potential at a given point is determined only by the ab initio points that are in its vicinity. Especially for interpolation, the distinction between these kinds of fits and interpolations is not, however, as clear-cut as it might first seem because in all methods the interpolation or fit is a stronger function of nearby data than far away data, and as the dependence on distance away becomes steeper, a method becomes more local. In recent years, the increasing accuracy of WFT calculations for small systems has been responsible for the appearance of many interpolation algorithms.[182−257]

In general, when a number of scattered ab initio points are fitted to an analytical function, the method is global. On the other hand, methods that interpolate between electronic structure points may be global (polynomials,[242,252] splines,[182,183,187,237,258,259] reproducing kernel Hilbert space,[192,217,226] or Shepard interpolation[260]) or local.

The first type of PESs used for reaction dynamics were analytical global functions (for instance, the extended LEPS function mentioned above), often with parameters that were

fit to available spectroscopic or thermochemical data (such as bond energies), dynamics data (such as barrier heights inferred from rate constants), electronic structure data, or some combination. Sometimes the early PESs had qualitative flaws.[157] For example, LEPS functions do not include dispersion interactions, and often the van der Waals well is missing or is qualitatively inaccurate. It has been pointed out that a reactive surface should have a qualitatively correct well in about the right place so that the repulsive interaction energy decreases to about the right value at about the right place.[261] The width of the energy barrier depends on the location of van der Waals well, and thus the correct calculation of the tunneling probabilities, especially at low energy, is sensitive to the quality of modeling this feature.[262,263]

Over the years, several new methods have been developed for the global representation of a PES, especially for atom−diatom reactions. For some simple reactions, like the H + H_2 bimolecular reaction, there are several PESs, which have been recently reviewed by Aoiz et al.[264] The most accurate H + H_2 potential energy surface has been used for converged quantum mechanical dynamics calculations of the rate constant.[53] Below, we briefly describe some of the general techniques to build global PES from scattered electronic structure calculations.

The diatomics-in-molecules (DIM) method,[265−267] a form of semiempirical valence bond theory, allows one to build a Hamiltonian for a polyatomic system based on information about the diatomic fragments. It relates the Hamiltonian matrix elements of the polyatomic system to those of its diatomic subsystems, for which matrix elements depend on a single interatomic distance. The DIM representation has been used, for instance, to study the $O(^1D) + H_2 \rightarrow OH +$ H bimolecular reaction.[268,269] The DIM method reduces to a LEPS-type potential for three-body systems with one active *s* electron on each center.[152,270]

In the many-body expansion (MBE)[184] method, the potential for a polyatomic system of *N* atoms is given by a sum of terms corresponding to atoms, its diatomic subsystems, triatomic subsystems, tetra-atomic subsystems, etc. For instance, for a tetratomic system ABCD, there are four monatomic terms, $V_A^{(1)}$, $V_B^{(1)}$, $V_C^{(1)}$, and $V_D^{(1)}$, six diatomic terms of the type AB, AC, AD, BC, BD, and CD, four triatomic terms of the type ABC, ABD, ACD, and BCD and one four-body term. The monatomic terms are simply the energies of the separated atoms, the two-body terms are potentials for diatomics, and the higher order terms include interaction potentials among three and four atoms, respectively. Varandas et al.[271] used MBE potentials together with the DIM approach to fit the ground and first excited state of the water molecule. Their PES also includes a function that allows switching between the two electronic states. Liu et al.[272] have used the MBE method to study the recombination reaction between hydroxyl radicals and nitrogen dioxide to form nitric acid. The MBE method has the advantage that the terms can be used for any system containing the same fragments. For instance, if an MBE potential for water is available, it provides several of the terms in a potential for the reaction HO + $H_2 \rightarrow H_2O$ + H, including all the one-body and two-body terms and one of the three-body terms. Mielke, Garrett, and Peterson[273] showed for the H + H_2 reaction that the many-body decomposition is also useful for extrapolation of ab initio data. Lakin et al.[225] and Troya et al.[235] applied the MBE method to the OH + CO and F + CH_4 reactions, respectively.

Varandas and co-workers have pioneered a version of the MBE method, called the double many-body expansion (DMBE) method,[274−278] in which the interaction energy is divided into two independent expressions that are called Hartree−Fock and dynamical correlation terms, respectively. This method has the advantage that the functional forms of the two contributions can be different and that each term can be fitted independently to different ab initio levels. A summary of the application of DMBE to four-atom bimolecular reactions has been given by Varandas.[277] Paniagua and co-workers developed a similar method, but in this case the polynomial expressions for the two-body and three-body terms[279,280] can be extended in a systematic way to larger systems.[281] Recently, Hayes et al.[282] have used this method to fit 3230 ab initio geometries to study the F + HCl → HF + Cl reaction.

Some global fitting methods, mainly for atom−diatom reactions, are based on Morse-type potentials. Wall and Porter[283] used a rotating Morse (RM) function to construct the potential energy surface for collinear atom−diatom A + BC → AB + C reactions, and this was used for the first semiquantitative fit to the PES of the collinear H + H_2 reaction.[284] Bowman and Kuppermann[285] improved the RM model by performing a cubic spline interpolation of the Morse parameters along the rotating angle. This approach is called rotated Morse-splines (RMS) method. Wright and Gray[286] extended its applicability by including not only the swing angle but also the bond angle to take into account bent geometries. This functional form has been used to model the PES of some atom−diatom systems.[287−291] Garrett et al.[292] combined the RM method with the bond-energy-bond-order (BEBO)[293] method for the Cl + H_2 system. Related to the RMS approach are the rotated bond order (ROBO)[188] and the largest-angle generalization of rotating bond order (LAGROBO)[198,201] methods. The bond-order (BO) for two atoms n_{ij} is given by[294]

$$n_{ij} = \exp[-\beta_{ij}(R_{ij} - R_{ij}^0)] \qquad (2.3.4)$$

where R_{ij} and R_{ij}^0 are the internuclear distance and the equilibrium internuclear distance, respectively, and β_{ij} is a parameter related to the harmonic frequency, reduced mass, and dissociation energy of the diatom. In the ROBO method, as in the RMS method, the potential is written as a sum of a radial function multiplied by an angular function plus an interaction term. The LAGROBO functional is a weighted sum of the ROBO functions for the different rearrangement channels of the system (3 for a triatomic system and 12 for a four-atom system). This method was recently applied to the OH + HCl reaction.[230] For systems with more than four atoms, García et al.[251] developed an approximate method based partly on the LAGROBO method and partly on the MBE method, which they applied to build the PES for the hydrogen abstraction reaction from methane by chlorine. Duin et al.[295] proposed an extension of molecular mechanics to reactive systems by using bond orders.

Related to the above methods is the reduced dimensionality (RD) approach developed by Clary and co-workers[213,231,234,245,257] to study hydrogen abstraction reactions. These reactions are all of the type D−H + A → D + H−A (D and A are the donor and acceptor atoms, respectively, and H is hydrogen) and the RD potential is constructed from a sum of two 2D-Morse functions, which are given in

hyperspherical coordinates. The objective is to obtain a PES for evaluating the thermal rate constants by conventional transition state theory but calculating the cumulative reaction probability of this two-dimensional (2D) reduced Hamiltonian by a quantum mechanical method.

Other techniques make use of high-order polynomials to fit the global PES. Millam et al.[206] developed a fitting method based on a fifth-order polynomial function. It has the advantage that can be used to run trajectories with larger step sizes. Medvedev, Harding, and Gray[256] calculated ~79 000 ab initio points to construct a global analytic function based on a sixth-order polynomial plus three additional polynomial functions to reproduce the CH_3 minimum and the asymptotes of the $H_2 + CH(^2\Pi) \rightarrow H + CH_2(\tilde{X}^3B_1)$ bimolecular reaction. Bowman and co-workers[238,242,247,252] used an approach in which the ab initio data are globally fitted to a permutational symmetry invariant polynomial. The potential is given by

$$V = p(x) + \sum_{i<j} q_{i,j}(x) y_{i,j} \tag{2.3.5}$$

where $p(x)$ and $q_{i,j}(x)$ are polynomials, and $y_{i,j} = [R_{i,j}]^{-1} \exp(-R_{i,j})$. The polynomials are built in a way that ensures invariance under permutation of like nuclei. The method has been tested in the construction of the potential energy surfaces for $O(^3P) + C_3H_3$ and $H + CH_4$ reactions,[247,252] respectively. For the latter, the authors calculated a large number of ab initio points, which they fitted to the above expression to study the abstraction and exchange reactions by running quasiclassical trajectories.

Rogers at al.[296] compared a potential made by combining the extended LEPS function with two high-order polynomials to an RMS potential for the $O(^3P) + H_2$ reaction. They obtained excellent accuracy (about 0.3 kcal/mol) between the PESs by adding virtual points and localized Gaussians, which eliminated some unphysical features of the original potentials.

All the global fitting methods described above, with the exception of the MS methods, require the optimization of adjustable parameters. Those parameters are usually obtained by performing a least squares (LS)[184−186] fitting of electronic structure data, which is not always easy. In contrast, spline functions[182,183,258,259,297] interpolate the data instead of fitting them. A difficulty is that splines need a fair amount of data over a regular grid, and their application has been limited to two or three dimensions. Recently, Rheinecker, Xie, and Bowman[237] carried out dynamics calculations of the $H_3O^+ + H_2O$ proton-transfer reaction in reduced dimensionality. Those authors considered three coordinates, i.e., those of the donor, the acceptor, and the transferred particle, which were fitted to a three-dimensional (3D) spline.

The reproducing kernel Hilbert space (RKHS)[192] method, like spline interpolation, is an interpolation method, but with the advantage that some constraints, like smoothness and good asymptotic behavior, are explicitly taken into account. On the other hand, the number of ab initio points needed to do the interpolation grows exponentially with the dimensions of the system and the method works best if the data are provided over a rectangular grid. This approach is usually combined with the MBE method and each of the many-body expansion terms are given by RKHS interpolation, i.e., the N-body term of the expansion for a regular grid is given by

$$V^{(N)}(x_1,x_2,...x_N) = \sum_{i_1}^{M_1}\sum_{i_2}^{M_2}...\sum_{i_N}^{M_N} \alpha_{i_1,i_2,...i_N} \prod_{j=1}^{N} q_i(x_j^{i_j},x_j) \tag{2.3.6}$$

where $\mathbf{x} = (x_1, x_2,..., x_N)$ is the set of N independent coordinates, M_1, M_2, ..., M_N are the numbers of ab initio points along each coordinate, $q_j(x_j^{i_j},x_j)$ is a one-dimensional (1D) reproducing kernel for each variable $x_j^{i_j}$, and $\alpha_{i_1,i_2,...,i_N}$ are coefficients that can be obtained by solving a set of linear equations.[215] The RKHS method has been applied to several triatomic systems as for instance the $N(^2D) + H_2$, $C(^1D) + H_2$ and $O(^3P) + HCl$ bimolecular reactions.[219,221,227] Balabanov et al.[249] also applied this interpolation method to several reactive channels of the ground-state of the $HgBr_2$ system, i.e., abstraction of a bromine atom ($HgBr + Br \rightarrow Hg + Br_2$), exchange [$HgBr(1) + Br(2) \rightarrow HgBr(2) + Br(1)$], and insertion ($HgBr + Br \rightarrow HgBr_2$) reactions, respectively. Recently, Ho and Rabitz[226] introduced a new formulation of the RKHS method called reproducing kernel Hilbert space high dimensional model representation (RKHS−HDMR), which allows one to reduce multidimensional integrations to independent lower dimensional problems. So far it has been tested for the $C(^1D) + H_2$ reaction,[226] although in principle it is easier to extend to higher dimensional systems than the original RKHS method.

Analytic potentials for reactive degrees of freedom can be combined with nonreactive force fields (molecular mechanics) to treat more complex reactions[210,214,241,244,297−300] (as discussed further below).

Next we turn our attention to local methods based on interpolation and specifically those based on Shepard interpolation,[259,260] which was pioneered by Ischtwan and Collins.[189,218] In their work, electronic structure methods are used to calculate Hessians at many points, typically selected on the basis of trajectory calculations,[190,194−197,199,200,204,207,209,212,218,222,232,246,248,250] and the PES is represented by a weighted average of the Taylor series T_i about each electronic structure point where a Hessian is calculated:

$$V = \sum_{i=1}^{N} W_i(\mathbf{R}) T_i(\mathbf{R}) \tag{2.3.7}$$

T_i is a Taylor series expansion around point $\mathbf{R}_i$ truncated to second order, and N is the number of points where a Taylor series is available. The normalized weighting factor W_i weights the contribution of the Taylor expansion about $\mathbf{R}_i$ and is given by

$$W_i(\mathbf{R}) = \frac{\upsilon_i(\mathbf{R})}{\sum_{j=1}^{N} \upsilon_j(\mathbf{R})} \tag{2.3.8}$$

Data points that have a geometry close to $\mathbf{R}$ have a larger weight than those with very different geometries. This is achieved by the weighting function

$$\upsilon_i = \frac{1}{|\mathbf{Z}(\mathbf{R}) - \mathbf{Z}(\mathbf{R}_i)|^{2p}} \tag{2.3.9}$$

where p is a parameter that determines how quickly the weighting function drops off, and $\mathbf{Z}$ is a suitable function of

R. In particular, the PES is built in coordinates that are reciprocals of the internal coordinates. The normalized weighting factor should provide a smooth interpolation between nearby points even when they are far away from the geometry of interest. Alternative weighting functions can also be considered.[191,211] The Shepard interpolation method for generating PESs for trajectory calculations is featured in a recent review.[220]

One of the advantages of this method and of Shepard interpolation in general is that regions that are irrelevant to the dynamics may be ignored and new electronic structure points may be readily incorporated to improve the PES. Yagi et al.[216] and Oyanagy et al.[254] have used Shepard interpolation based on fourth-order Taylor expansion to obtain highly accurate PESs. Very recently,[246] the Shepard method has been extended to study diabatic potential energy surfaces, which are discussed later in this section and also in Section 3.2. Thompson and Collins[195] also developed techniques called "rms sampling" and "*h*-weight" to successively improve and "grow" the PES.

The Shepard interpolation method needs not only the energy but also the gradient and the Hessian at every data point. One way to overcome some of the high computational requirements of the method is to combine Shepard interpolation with an interpolating moving least-squares method to evaluate the gradients and Hessians. The combined IMLS/Shepard procedure has been applied to some atom−diatom reactions such as the LiH + H and $O(^1D) + H_2$ reactions.[215,224] Other authors[228,229,236,239,240,253] have simply used the IMLS method to interpolate PESs, because Shepard interpolation can be considered a zero-degree IMLS and a first-degree IMLS solves the "flat-spot" problem.

Another method that makes use of Shepard interpolation is multiconfiguration molecular mechanics method (MCMM).[210,214,241] This method is based on semiempirical valence bond theory,[151−158,181,265−270,274,297−307] and the PES is built starting with a molecular mechanics potential V_{11} valid in the reactant-valley well and a molecular mechanics potential V_{22} valid in the product-valley well. The Born−Oppenheimer potential energy is represented at any geometry **R** as the lowest eigenvalue of the 2 × 2 electronically diabatic matrix **V**

$$\mathbf{V} = \begin{pmatrix} V_{11}(\mathbf{R}) & V_{12}(\mathbf{R}) \\ V_{12}(\mathbf{R}) & V_{22}(\mathbf{R}) \end{pmatrix} \qquad (2.3.10)$$

In this context, a diabatic potential is one that corresponds to a particular bonding arrangement or valence bond structure.

The lowest eigenvalue of eq 2.3.10 is

$$V(\mathbf{R}) = \frac{1}{2}\{(V_{11}(\mathbf{R}) + V_{22}(\mathbf{R})) - [(V_{11}(\mathbf{R}) - V_{22}(\mathbf{R}))^2 + 4V_{12}(\mathbf{R})^2]^{1/2}\} \qquad (2.3.11)$$

where $V_{12}(\mathbf{R})$ is called the resonance energy function or resonance integral. An estimate of $V_{12}(\mathbf{R})$ is obtained from the scheme proposed by Chang and Miller.[306,307] In their approach, the resonance integral is expressed as

$$V_{12}(\mathbf{R})^2 = [V_{11}(\mathbf{R}) - V(\mathbf{R})][V_{22}(\mathbf{R}) - V(\mathbf{R})] \qquad (2.3.12)$$

In the MCMM method, this equation is used for each of the *n* ab initio points, for which we know the energy, gradients, and Hessians, and for a given point *i* the potentials are expanded in Taylor's series $V(\mathbf{R};i)$, $V_{11}(\mathbf{R};i)$, and $V_{22}(\mathbf{R};i)$, to second order about the $\mathbf{R}(i)$ geometry. Each Hessian generates a Taylor's series of $V_{12}(\mathbf{R})$ about another point. These series are joined by Shepard interpolation, and the new resonance integral $V_{12}^S(\mathbf{R})$, is given by

$$V_{12}^S(\mathbf{R}) = \sum_{i=1}^{n} w_i(\mathbf{R}) V'_{12}(\mathbf{R};i) \qquad (2.3.13)$$

where $w_i(\mathbf{R})$ is a weighting function, and $V'_{12}(\mathbf{R},i)$ is a modified quadratic form obtained from the Taylor series expansion about the point *i*. The weighting function is taken to be as smooth as possible consistent with conditions required for eq 2.3.13 to be a true interpolant of energies, gradients, and Hessians. The weighting function is usually a function of the bond-forming and bond-breaking distances. The MCMM method uses redundant internal coordinates because they have the advantage of being rotationally invariant. As is Collins's method, the MCMM method is systematically improvable, and we can sample only the parts of the PES relevant to the dynamics.

A key advantage of the MCMM method is that it makes use of molecular mechanics and therefore can deal with quite large systems. The use of molecular mechanics in a valence bond context for representing potential energy surfaces was suggested in various ways in pioneering studies by Coulson and Danielsson,[301] Raff,[297] Warshel and Weiss,[298,299,308,309] and others[300,303,310−315] and it is useful to add some perspective on these approaches. First of all, as emphasized recently by Shurki and Crown,[314] incorporating valence-bond configuration-mixing elements in a model allows one to work explicitly with "the pictorial resonance structures we usually think of as chemists" and thereby "enables us to understand in detail the mechanism of barrier formation by following the energies of the VB structures and the resulting mixing of states along the reaction coordinates." Thus, valence bond theory is a powerful tool for obtaining insight. Furthermore, it provides very useful nonpairwise-additive functional forms for fitting PESs since it naturally builds in the saddle point structure of chemical reactions. Indeed, as mentioned above, there is a long history of this kind of usage of valence bond theory,[151−158,181,265−270,274,302−304] especially for small systems.

Espinosa-Garcia and co-workers[316−320] have used LEPS-type potential energy surfaces augmented by molecular mechanics terms to study polyatomic systems, mainly abstraction reactions of the type $CH_4 + X \rightarrow CH_3 + HX$ and $CX_3Y + H \rightarrow$ products, where X, Y = F, Cl, Br, or I. These surfaces are formulated as a sum of three terms:

$$V = V_{str} + V_{val} + V_{op} \qquad (2.3.14)$$

where V_{str} is a LEPS-type semiempirical valence bond potential, V_{val} is the potential for harmonic valence bending, and V_{op} is the out-of-plane bending term.

A natural way to extend such treatments to larger systems is to write[297,300]

$$V = V_{VB}^A + V_N^B \qquad (2.3.15)$$

where V_{VB}^A is a valence bond potential energy function for the reactive part of the subsystem where bond rearrangement occurs (subsystem A, as indicated in the superscript), V_N is a nonreactive (N) potential function of the type[321] widely

used to treat molecular vibrations and vibrational spectroscopy, and the nonreactive subsystem is labeled B. If we use a two-state valence model, eq 2.3.10 can be written as

$$V = \text{mineiv}\begin{pmatrix} V_{RR}^{A} & V_{RP}^{A} \\ V_{RP}^{A} & V_{PP}^{A} \end{pmatrix} + V_{N}^{B} \qquad (2.3.16)$$

or

$$V = \text{mineiv}\begin{pmatrix} V_{RR}^{A} + V_{N}^{B} & V_{RP}^{A} \\ V_{RP}^{A} & V_{PP}^{A} + V_{N}^{B} \end{pmatrix} \qquad (2.3.17)$$

where mineiv **V** denotes the minimum eigenvalue of matrix **V**. The subscripts refer to reactant (R) and product (P). Nonreactive potential functions are usually written as a sum of (often harmonic) potentials for individual stretches, bends, torsions, and other nonbonded interactions, and such potential functions were originally obtained from vibrational spectroscopy.[321] They were also used to rationalize the rate of bimolecular reactions.[322,323] More recently, such potential energy functions have been widely parametrized in a way designed to be transferable for the prediction of structure and conformational energy, with less emphasis on vibrational spectra;[324−330] such potential functions are usually called molecular mechanics (MM). Since an MM potential function corresponds to a definite bonding arrangement, it can be associated with a single valence bond configuration.

Warshel and Weiss[298,299,308,309] proposed a method that is equivalent to replacing the diagonal elements in eq 2.3.17 by molecular mechanics potentials (V^{AB}) for the reactants (subscript R) and products (subscript P) of the combined AB system:

$$V = \text{mineiv}\begin{pmatrix} V_{R}^{AB} & V_{RP}^{A} \\ V_{RP}^{A} & V_{R}^{AB} \end{pmatrix} \qquad (2.3.18)$$

The idea that potential energy functions for large systems can be approximated by mixing molecular mechanics potential functions is a powerful one. Warshel and Weiss call this the empirical valence bond method (EVB). Although this name has now become well established, it continues to cause confusion of the same type that would be engendered if a specific kind of semiempirical molecular orbital theory were designated empirical molecular orbital (EMO) theory. To avoid confusion of the generic and the specific, we use the phrase "semiempirical valence bond"[157] to refer to the generic class of empirical or semiempirical (these words mean essentially the same thing) valence bond theories.

Warshel and co-workers usually parametrize V_{RP}^{A} as a constant or a two-parameter function depending on one of the coordinates of subsystem A. This is not guaranteed to give the correct global behavior of V, but it is serviceable, especially since "the main point of the EVB method is not in its gas-phase surface but rather in its treatment of the solvent."[308] Other workers, however, have employed the formalism with more elaborate fitting methods.[315] Chang and Miller[306] attempted to make the EVB form more systematic by replacing V_{RP}^{A} by V_{RP}^{AB} and making a multidimensional Gaussian approximation to V_{RP}, and they claimed that their resulting expression for the potential energy reduces properly to the appropriate limits for reactants and products, but it does not because approximately half the coefficients of the quadratic terms in the multidimensional Gaussian are positive, whereas they assumed that they are all negative.

The MCMM method presented above also has the form of eq 2.3.18, and it provides a systematic way to parametrize the EVB method. The use of MM in this method helps in two ways. First of all, it makes it possible to interpolate V_{12}, rather than V; V_{12} is much smoother. Second, the molecular mechanics terms describe the variation of the potential as a function of the spectator degrees of freedom quite well, and so one does not need to add Hessian points with various values of the spectator coordinates to incorporate that variation. It is possible to save further computational expense by using electronic structure theory to calculate partial Hessians involving only the most critical degrees of freedom.[241] Recently, the MCMM method has also been applied to the barrierless BH_5 dissociation reaction[233] and to proton-transfer reaction in the water trimer. [255]

The MCMM method, although based completely on ab initio electronic structure calculations, is not a straight direct-dynamics method because an algorithm for interpolation is needed to calculate geometries that are not available in the initial set of input data. An alternative approach that avoids interpolation is the hybrid VB/MM method of Shurki and Crown.[314] This method combines molecular mechanics for the diagonal elements with a "standard" ab initio valence bond package for the off-diagonal elements, thereby avoiding parametrization as well as interpolation. An empirical combined valence bond molecular mechanics (CVBMM) method has also been proposed.[300] In this method, the VB part is an extension of the semiempirical VB methods that were originally developed for small systems.

As discussed above, another alternative is to avoid both MM and interpolation and to use straight direct dynamics to build the PES, that is, to calculate "on the fly" every energy, gradient, or Hessian needed for the dynamics calculation. Unfortunately, this cannot be done economically if the level of ab initio theory employed includes much of the electronic correlation and involves large basis sets. One possibility is to use a neural network for function approximation; this combines[243] electronic structure calculations with sampling methods that make use of molecular dynamics calculations to sample important parts of the PES in a similar way to how they are used by Collins and co-workers[218] for Shepard interpolations.

Another possibility is to do high level ab initio calculations at the stationary points (reactants, products, and transition state) and try to find a lower-level method that provides similar energies and geometries. Sometimes it is possible to find a low-level ab initio method that fulfills the requirement; however, if the system is relatively big even a low-level ab initio method can be impractical. A common approach is to use semiempirical molecular orbital theory instead of ab initio or DFT methods.[331,332] As mentioned in Section 2.1, some of the integrals evaluated in the ab initio methods are replaced by parameters in some of the semiempirical methods; in other semiempirical methods, the parameters are scaling factors or occur in additive terms. In any of these methods, the parameters can be optimized in a general way against a broad or representative database, or they can be modified to reproduce the energetics, some frequencies (for instance the imaginary frequency at the transition state), and/or some key geometric parameters important for a specific reaction or range of reactions. In general, these parameters are reaction dependent, and therefore this produces a semiempirical

method with specific reaction parameters (SRPs). This approach is quite flexible, and since its introduction in 1991[164] many groups have used it to obtain potentials for classical trajectories or to evaluate thermal rate constants.[174,175,333−335] The use of genetic algorithms to optimize the SRPs is especially powerful.[336,337]

An example of a reaction where various approaches may be compared is $H + CH_4 \rightarrow H_2 + CH_3$. A sequence of successively improved semiempirical valence bond surfaces[218,297,338,339] eventually led to the refined surface of Espinosa-Garcia,[339] which has been employed for several approximate quantal[340] and quasiclassical[171−173,341] studies. Some of the trajectory studies[171−173] were compared to direct dynamics with B3LYP. Unfortunately, the Espinosa-Garcia surface has a classical barrier height of only 12.9 kcal/mol, whereas the current "best estimate" is 14.8 kcal/mol;[342] B3LYP has a similar deficiency since it has a barrier of 9.4 kcal/mol, which is not surprising since Table 2 shows that B3LYP systematically underestimates barrier heights for hydrogen transfers. Direct dynamics calculations of rate constants were carried out with multicoefficient correlation methods with specific reaction parameters, in particular, MCG3-SRP, which yielded the most accurate available potential energy surface for any reaction with this many atoms.[342] Later quantum mechanical calculations with a fitted ab initio surface gave similar results.[343] Another fitted ab initio potential energy surface in good agreement with the MCG3-SRP one has been published more recently.[252]

2.4. Rate Theory for Simple Barrier Reactions

2.4.1. Conventional Transition State Theory

The variation of a thermal rate constant with temperature can be described phenomenologically in terms of the Arrhenius equation (see eq 2.2.1), which contains the activation energy as a key parameter. Transition state theory also centers attention on the activation process. The transition state divides phase space (the space of atomic coordinates and momenta) into a reactants region and a products region with a "dividing surface" normal to the reaction coordinate. (Technically, we might say dividing hypersurface, but "surface" is a less formal shorthand for "hypersurface.") In some cases, the reaction-coordinate definition and dividing-surface definition depend only on atomic coordinates (not on atomic coordinates and momenta), in which case the dividing surface becomes a surface in coordinate space, a special case of a surface in phase space.

A number of implicit assumptions are needed to derive the conventional TST expression, in particular (1) that the Born−Oppenheimer approximation is valid; (2) that the reactant molecules are distributed among their states in accordance with a Maxwell−Boltzmann distribution (this is called the local-equilibrium approximation; the word "local" is needed because reactants are not in equilibrium with products); (3) that a dynamical bottleneck can be identified such that once the reacting trajectories reach the dynamical bottleneck, they proceed to products without ever returning (and similarly any product trajectories that reach the dynamical bottleneck proceed straight to reactants without returning to the bottleneck); (4) that quantum effects may be added by replacing the classical partition functions that result from the above assumptions by quantum mechanical partition functions; and (5) that the dynamical bottleneck (transition state) may be identified as a coordinate-space hypersurface that divides reactants from products and that passes through a saddle point orthogonal to its imaginary-frequency normal mode, which is the reaction coordinate. [Looking ahead, variational transition state theory will retain assumptions (1−4) but improve on (5).]

The classical TST expression to evaluate thermal bimolecular rate constants is[344,345]

$$k^{\ddagger}(T) = \frac{1}{\beta h}\frac{Q_C^{\ddagger}(T)}{\Phi_C^{R}(T)}\exp(-\beta V^{\ddagger}) \qquad (2.4.1)$$

where $V^{\ddagger}$ is the barrier height from reactants to the transition state, $Q_C^{\ddagger}(T)$ is the classical (C) partition function of the transition state, and $\Phi_C^{R}(T)$ is the reactants classical partition function per unit volume. Conventional TST requires a very limited knowledge of the PES, namely, the transition state energy and the partition functions at the reactants and transition state. Thus, conventional TST states that thermal rate constants can be calculated by focusing exclusively on the saddle point, and if we are only interested in the total rate constant, what happens before or after is irrelevant.

TST also introduces the concept of "reaction coordinate" and the assumption that motion along it can be separated from all the other degrees of freedom. It has been recognized since the early days of TST that the choice of the reaction coordinate is crucial. Since the reaction coordinate is the degree of freedom normal to the transition state, which is a surface, a choice of transition state is equivalent to choosing a reaction coordinate plus choosing the location of a surface along this coordinate. In Section 2.4.2, we will consider choosing the transition state that way. First though, it is useful to comment on notation. When we choose the transition state as normal to the imaginary frequency normal mode coordinate of the saddle point structure and locate it so it cuts that coordinate at the saddle point, we often call this the conventional transition state. Any other choice is called a generalized transition state. In variational transition state theory, we will have a criterion for choosing the best of these generalized transition states, and that is called the variational transition state. Very often though, one just says transition state, and the meaning (conventional, generalized, or variational) is supposed to be clear from the context.

Equation 2.4.1 can be reformulated in quasithermodynamic terms by using the connection between the equilibrium constant and the Gibbs standard free energy. Thus, we rewrite eq 2.4.1 as

$$k^{\ddagger}(T) = \frac{1}{\beta h}K^{\ddagger}(T) \qquad (2.4.2)$$

where $K^{\ddagger}$ is a quasiequilibrium constant for forming the transition state; the "quasi" refers to the important[346] distinction that the transition state is not a true thermodynamic species because it is missing one degree of freedom. (Recall that a hypersurface, such as a transition state, has one less degree of freedom than the volume in which it is embedded.) Then by analogy to true thermodynamic relations, we can write

$$k(T) = \frac{1}{\beta h}K^{o}\exp[-\Delta G^{\ddagger,o}/RT] \qquad (2.4.3)$$

Equation 2.4.3 provides the historical motivation for the widespread use of eq 2.2.3 and can be written as

$$k^{\ddagger}(T) = \frac{1}{\beta h} K^{o} \exp[\Delta S^{\ddagger,o}/R] \exp[-\Delta H^{\ddagger,o}/RT] \quad (2.4.4)$$

If we use a standard state of 1 atm and equate this to the Arrhenius equation, standard thermodynamic analysis yields[347,348]

$$\Delta H^{\ddagger,o} = E_a - 2RT \quad (2.4.5)$$

and[343]

$$A = \left(\frac{K^{o} e^{2}}{\beta h}\right) \exp(\Delta S^{\ddagger,o}/R) \quad (2.4.6)$$

or

$$\Delta S^{\ddagger,o} = R \ln(\beta h A/K^{o}) - 2R \quad (2.4.7)$$

where K^{o} is the reciprocal of the concentration that corresponds to a pressure of 1 atm at temperature T.

2.4.2. Variational Transition State Theory

Transition state theory can be derived from a dynamical approach by statistical mechanics. In the quasiequilibrium formulation given above, the emphasis is on the equilibrium distribution in the dividing surface that separates reactants from products and on the statistical character of the equilibrium approximation, and the factor $1/\beta h$ can be obtained from simple models of reaction coordinate motion. In contrast, in the dynamical formulation of the theory, TST is derived, including the $1/\beta h$ factor, by a rigorous statistical mechanical calculation of the flux through a phase-space or coordinate-space dividing surface. In the latter approach, developed by Horiuti,[349] Wigner,[350] and Keck[351,352] (see also Pechukas,[353] Tucker and Truhlar,[354] Garrett,[355] and Garrett and Truhlar[356]), the TST rate constant is the one-way equilibrium flux coefficient through the dividing surface. Then, the fundamental assumption of transition state theory is that this one-way flux through the dividing surface equals the net flux. This will be true if all trajectories that cross the dividing surface in the direction of products originated at reactants and will not cross this surface again before leading to products. Pechukas and Pollak argued convincingly that, in a classical world, conventional transition state theory is accurate near the threshold of a chemical reaction.[357−359]

The motion of an N-atom system on a PES can be described in terms of $3N$ atomic coordinates, or, in particular mass-scaled Cartesian coordinates. These coordinates[360] are the same as mass-weighted Cartesian coordinates[149] but with a mass factor of $\mu^{-1/2}$. If $S_{i,\gamma}$, for $\gamma = x, y, z$, are the Cartesian coordinates of atom i with respect to a fixed origin or with respect to the center-of-mass of the system, the mass-scaled coordinates are defined as

$$R_j = \left(\frac{m_i}{\mu}\right)^{1/2} S_{i\gamma}; \quad i = 1,...,N; \quad \gamma = x,y,z; \quad j = 1... 3N \quad (2.4.8)$$

For a bimolecular reaction, it is sometimes convenient to define the scaling mass μ as the reduced mass of the relative motion of reactants, $\mu = m_A m_B/(m_A + m_B)$, where m_A and m_B are the masses of the reactants A and B, respectively. Alternatively, it is very popular to set μ equal to 1 amu. In this system of coordinates the kinetic energy associated with the nuclear motion is diagonal and has the same mass μ associated with motion in any direction (which is why the coordinates are called isoinertial), and so the $3N$-dimensional motion of the many-atom system governed by the PES $V(R_{i\gamma})$ is equivalent to the motion of a point mass on $V(\mathbf{R})$, where $\mathbf{R}$ denotes the collection of the R_j coordinates. An orthogonal transformation of these coordinates provides new coordinates, for example, mobile coordinates,[361] that are also isoinertial.

Isoinertial coordinates have many advantages, and they will be used throughout this review. A trivial advantage is that they make it easier to write down and derive many of the dynamical equations. A more fundamental advantage is that they allow a multiparticle generalization of concepts such as centrifugal forces; for example, the tendency of a bobsled to veer off its minimum energy path toward the convex side of the path has an analogue for chemical reactions that may be expressed quantitatively in terms of the curvature of the reaction path in isoinertial coordinates.[362−364] Furthermore, dividing surfaces orthogonal to the minimum-energy path in isoinertial coordinates have been found to be very good dividing surfaces for TST.[365]

Next, following previous presentations,[352,354] we derive variational transition state theory for a system described by classical mechanics. From a classical mechanical point of view, a reactive system of N atoms can be fully described at a given time t by a $6N$-dimensional point $(\mathbf{p},\mathbf{R})$ in phase space and the Hamiltonian

$$H(\mathbf{p},\mathbf{R}) = T(\mathbf{p}) + V(\mathbf{R}) \quad (2.4.9)$$

The density $\rho(\mathbf{p},\mathbf{R})$ of phase points in the ensemble satisfies the continuity equation

$$\frac{\partial \rho}{\partial t} + \nabla \cdot \rho \mathbf{v} = 0 \quad (2.4.10)$$

where $\mathbf{v}$ is the generalized velocity of a point in phase space and $\nabla\cdot$ is the generalized divergence operator.

By following the flow of points between different regions in phase space, it is possible to study the course of the chemical reaction in this ensemble.[349,352,354,366] First consider a volume Ω in phase space corresponding to reactants. The integration of eq 2.4.10 over this volume yields,

$$-\frac{\partial}{\partial t}\int_{\Omega} d^{6N}\tau \rho = \int_{\Omega} d^{6N}\tau \nabla \cdot \rho \mathbf{v} \quad (2.4.11)$$

where

$$d^{6N}\tau = \prod_{i=1}^{3N} dp_i dR_i \quad (2.4.12)$$

The left-hand-side of eq 2.4.11 is the time derivative of the number N^{R} of reactant systems in the ensemble in the volume Ω, and so

$$-\frac{dN^{R}}{dt} = \int_{\Omega} d^{6N}\tau \nabla \cdot \rho \mathbf{v} \quad (2.4.13)$$

Then the integral of eq 2.4.13 can be transformed into a surface integral using Gauss' theorem, yielding

$$-\frac{dN^{R}}{dt} = \int_{S} ds \rho(\mathbf{v}\cdot\mathbf{n}) \quad (2.4.14)$$

where ds is a differential element of area belonging to the transition state surface S, and $\mathbf{n}$ is a unit vector orthogonal

to the surface S that points out of the volume Ω. The surface is a $(6N-1)$-dimensional hyperplane (the dividing surface) that separates reactants from products, and all the flux from the volume Ω passes through it. Therefore, eq 2.4.14 equals the one-way flux F_+ (the + sign indicates that the flux is calculated in the forward direction, that is, from reactants to products) through this hyperplane:

$$F_+ = \int_{S_+} ds \rho(\mathbf{v}\cdot\mathbf{n}) \tag{2.4.15}$$

where S_+ is the portion of the phase space dividing surface for which $(\mathbf{v}\cdot\mathbf{n}) > 0$.

Next rotate the axes so that one of the $3N$ new coordinates is perpendicular to the dividing surface. This coordinate is our reaction coordinate and will be labeled as z; the remaining coordinates are called $\mathbf{u} = u_1, u_2, \ldots u_{3N-1}$, and their conjugate momenta are called $\mathbf{p_u}$. Since we are assuming here that z is a rectilinear coordinate (an assumption that will be relaxed later in the review), the dividing surface is a hyperplane. The value of z at the dividing surface will be denoted as z_*. By construction:

$$\mathbf{v}\cdot\mathbf{n} = \frac{dz}{dt} = \frac{p_z}{\mu} > 0 \tag{2.4.16}$$

where p_z is the momentum conjugate to z. By separating this coordinate and momentum from the rest, the one-way flux is given by

$$F_+ = \int_{z=z_*} d^{6N-2}\tau \int_0^\infty dp_z \rho \frac{p_z}{\mu} \tag{2.4.17}$$

Now, if we assume that the internal degrees of freedom of the reactants are in thermal equilibrium, the density of states corresponds to a Boltzmann distribution

$$\rho = \rho_0 \exp[-\beta H] \tag{2.4.18}$$

so that

$$N^R = \rho_0 \int_\Omega d^{6N}\tau \exp[-\beta H] \tag{2.4.19}$$

and the one-way flux through the dividing surface is given by

$$F_+ = \rho_0 \int d^{6N-2}\tau \exp[-\beta H^{GT}(\mathbf{u},\mathbf{p_u}; z = z_*)] \int_0^\infty dp_z \frac{p_z}{\mu} \exp[-\beta p_z^2/2\mu] \tag{2.4.20}$$

The superscript GT indicates that the dividing surface at z is a generalized transition-state, and $z = z_*$ because the integral is over the surface at this particular value of z. The integration over p_z leads to the one-way flux through the generalized transition-state at $z = z_*$

$$F^{GT}(T,z_*) = \rho_0 k_B T \int d^{6N-2}\tau \exp[-\beta H^{GT}(\mathbf{u},\mathbf{p_u}; z = z_*)] \tag{2.4.21}$$

For a bimolecular reaction, the classical mechanical rate constant is given in terms of the flux from reactants to products by

$$k_C(T) = \frac{F(T)}{V[A][B]} = \frac{F(T)V}{N_A N_B} \tag{2.4.22}$$

where V is the volume, and the subscript on the left-hand side reminds us that we are using classical mechanics here. In the reactant region, the reactants are independent of each other, and the Hamiltonian that describes them is separable in the coordinates of A and B. Using this separability and eq 2.4.19, we can write

$$N_A N_B = \rho_0 h^{3n_A} V \Phi_C^A(T) h^{3n_B} V \Phi_C^B(T) \tag{2.4.23}$$

where Φ_C^A and Φ_C^B are classical partition functions of both reactants per unit volume.

On the other hand, if we make the TST assumption and replace $F(T)$ by $F^{GT}(T, z_*)$ in eq 2.4.22 and define a generalized transition-state "partition function" that has the potential energy $V_{RP}(z = z_*)$ as its zero of energy, we obtain

$$\Phi_C^{GT}(T,z_*) = \frac{\exp[V_{RP}(z = z_*)]}{V h^{(3N-1)}} \int d^{6N-2}\tau \exp[-\beta H^{GT}(\mathbf{u},\mathbf{p_u}; z = z_*)] \tag{2.4.24}$$

Then eq 2.4.22 becomes

$$k_C^{GT}(T,z_*) = \frac{1}{\beta h} \frac{\Phi_C^{GT}(T,z_*)}{\Phi_C^A(T)\Phi_C^B(T)} \exp[-\beta V_{RP}(z = z_*)] \tag{2.4.25}$$

It is useful to separate the overall translation from the partition functions, since it is irrelevant. Taking into account that

$$\Phi_{trans}^X(T) = (2\pi m_X/h^2\beta)^{3/2} \tag{2.4.26}$$

where X is GT, A, or B, the ratio of all translational partition functions is

$$\frac{1}{\Phi_{rel}(T)} = \left(\frac{h^2\beta}{2\pi\mu}\right)^{3/2} \tag{2.4.27}$$

and the thermal rate constant for a bimolecular reaction can be rewritten as

$$k_C^{GT}(T,z_*) = \frac{1}{\beta h} \frac{Q_C^{GT}(T,z_*)}{\Phi_C^R(T)} \exp[-\beta V_{RP}(z = z_*)] \tag{2.4.28}$$

where Q_C^{GT} is the partition function defined by

$$\Phi_C^{GT}(T,z_*) = \Phi_{trans}^{GT}(T) Q_C^{GT}(T,z_*) \tag{2.4.29}$$

and

$$\Phi_C^R(T) = \Phi_{rel}(T) Q_C^A(T) Q_C^B(T) \tag{2.4.30}$$

We have presented the derivation of eq 2.4.28 because it is the central result of TST. Using standard statistical mechanical relations,[367,368] one can show that eq 2.4.28 is equivalent to eq 2.2.2 with $\gamma(T) = 1$. In classical mechanics the TST rate constant would be the exact local-equilibrium result if all the trajectories that cross the dividing surface in the direction of products originated on the reactant side and, having crossed once, never return. Then $F^{GT}(T, z_*) > F(T)$,

and the TST rate constant provides an upper bound to the true classical rate constant. The "quasiequilibrium hypothesis" assumed by Eyring in his formulation of TST is thus equivalent to the "nonrecrossing" condition, and it is exact if all of the systems that cross the dividing surface in the direction of products do so only once. Transition state theory is sometimes incorrectly categorized as a nondynamical statistical theory. Actually, it is a statistical dynamical theory in that the problem of evaluating the one-way flux through a dividing surface by running classical trajectories on a $3N$-dimensional potential energy surface is reduced to a local quasiequilibrium calculation.

The next step is to find good practical methods for choosing the dividing surface so that the local one-way flux equals, to a good approximation, the global net flux. The method for this that we discuss is the one proposed by Garrett and Truhlar.[360,365,369] The dividing surface is perpendicular to the minimum energy path (MEP) through isoinertial coordinate spaces; this path[370,371] is also called the intrinsic[372] reaction path. The MEP is chosen as the path of steepest descent, starting at the transition state, in isoinertial coordinates. In general, the distance along the MEP is denoted by s, with the saddle point at $s = 0$, the reactants region corresponding to $s < 0$, and the products region corresponding to $s > 0$. For a reacting system composed of N atoms with the $3N$ mass-scaled coordinates $\mathbf{R}$, it is possible to rotate and translate these coordinates in such a way that the rotated coordinate z is tangent to the MEP at s, with the value of zero at the point of tangency and with coordinates $\{u_1(s),...u_{3N-1}(s)\}$ that are orthogonal to the MEP at s. Although the MEP follows a curved path, it is possible to define, at each value of s, a Cartesian coordinate system that has one coordinate directed along the MEP at s; this set of coordinates $\{u_1(s),...u_{3N-1}(s), s\}$ are called local natural collision coordinates. The position of a particular dividing surface along the MEP will be determined by the s value at which it intersects the MEP. Hereafter, we designate as $\mathbf{x}(s)$ the set of isoinertial mass-scaled Cartesian coordinates along the MEP.

With these considerations, we can write an expression similar to eq 2.4.28 but with the rate constant as function of s

$$k_C^{GT}(T,s) = \frac{1}{\beta h}\frac{Q_C^{GT}(T,s)}{\Phi_C^R(T)}\exp[-\beta V_{MEP}(s)] \quad (2.4.31)$$

As discussed in the paragraph below eq 2.4.30 the rate constant calculated this way is always larger than (or equal to) the correct classical mechanical local-equilibrium result. Therefore we want to minimize the calculated rate constant. The resulting rate expression is known as canonical variational transition state theory (CVTST) or simply canonical variational theory (CVT);[365,369,373] the resulting rate constant is

$$k_C^{CVT}(T) = k_C^{GT}(T,s_*^{CVT}) = \min_s k_C^{GT}(T,s) \quad (2.4.32)$$

where $s = s_*^{CVT}$ is the optimized position of the dividing surface. This condition is equivalent to

$$\frac{\partial}{\partial s}[k_C^{GT}(T,s)]|_{s=s_*^{CVT}} = 0 \quad (2.4.33)$$

with the condition that the second derivative is greater than zero. One should also remember the condition that the dividing surface must separate the reactant region of configuration space or phase space from the product region. Then the classical mechanical CVT rate constant is given by

$$k_C^{CVT}(T) = \frac{1}{\beta h}\frac{Q_C^{GT}(T,s=s_*^{CVT})}{\Phi_C^R(T)}\exp[-\beta V_{MEP}(s_*^{CVT})] \quad (2.4.34)$$

To provide physical insight into this minimization process, we write eq 2.4.34 in a quasithermodynamic form like eq 2.4.3, yielding

$$k_C^{GT}(T,s) = \frac{K^{\ddagger,o}}{\beta h}\exp[-\Delta G_C^{GT,o}(T,s)/RT] \quad (2.4.35)$$

where $K^{\ddagger,o}$ is the reciprocal of the standard-state concentration, and $\Delta G_C^{GT,o}(T,s)$ is a quasithermodynamic quantity, as discussed above. Condition (2.4.33) is equivalent to

$$\frac{\partial}{\partial s}[\Delta G_C^{GT,o}(T,s)]|_{s=s_*^{CVT}} = 0 \quad (2.4.36)$$

and therefore CVT is equivalent to a maximum free energy of activation criterion.[12,360,365,369,374-377] (except for a Jacobian factor[378-381] discussed in Section 2.4.5). The canonical variational transition state location is a compromise of an "entropic" factor associated with the partition functions and an "energetic" factor associated with the exponential factor,[382] whereas the conventional transition state location is entirely determined by the energetic criterion, which puts it at the highest energy point on the minimum energy path, i.e., at the saddle point.

In summary, we have reduced the problem of running trajectories on a "global" $3N$ potential energy surface to the evaluation of the flux through a $(3N - 1)$-dimensional dividing surface. To find a reasonably accurate dividing surface in a practical way, one computes a minimum energy path and searches for the optimum dividing surface from a one-parameter sequence of hypersurfaces orthogonal to this path. A hypersurface defined this way is almost surely not the best choice in every case; however, for reactions with tight saddle points it is usually very good.

The MEP, defined as above, can be calculated by the solution of the steepest-descents equation

$$\frac{d\mathbf{x}}{ds} = -\hat{\mathbf{g}} \quad (2.4.37)$$

where $\hat{\mathbf{g}} = \mathbf{g}/|\mathbf{g}|$ is the normalized gradient of the potential. The first step along the MEP starting from the saddle point cannot be calculated this way because the gradient at any stationary point is zero. At the saddle point, the direction along the MEP is given by the unbound normal coordinate associated with the imaginary frequency. Finding this direction requires the force constant matrix (or Hessian) $\mathbf{F}$ at the transition state structure $\mathbf{x}^{\ddagger}$; since the elements of the force constant matrix are second partial derivatives of the potential, this matrix is also called the Hessian. The force constant matrix is diagonalized by the orthogonal transformation

$$\mathbf{L}(\mathbf{x}^{\ddagger})^{\dagger}\mathbf{F}(\mathbf{x}^{\ddagger})\mathbf{L}(\mathbf{x}^{\ddagger}) = \Lambda(\mathbf{x}^{\ddagger}) \quad (2.4.38)$$

where † indicates transpose, $\mathbf{L}(\mathbf{x}^{\ddagger})$ is the orthonormal matrix of eigenvectors whose columns $\mathbf{L}_m(\mathbf{x}^{\ddagger})$ correspond to the normal-mode directions at the saddle point and $\Lambda(\mathbf{x}^{\ddagger})$ is a

diagonal matrix that contains the eigenvalues called $\lambda_m(0)$, which are the normal-mode force constants at the saddle point, and are related to the normal-mode frequencies by

$$\omega_m(\mathbf{x}^{\ddagger}) = \left(\frac{\lambda_m(\mathbf{x}^{\ddagger})}{\mu}\right)^{1/2}, m = 1, ..., 3N \quad (2.4.39)$$

At the saddle point there are $F - 1$ positive eigenvalues corresponding to the modes perpendicular to the reaction coordinate (hereafter F is the number of normal mode vibrations, equal to $3N - 6$ for a nonlinear molecule and $3N - 5$ for a linear molecule since five modes for a linear molecule and six for a nonlinear molecule correspond to the overall translations and rotations) and one negative eigenvalue (denoted $\lambda_F(\mathbf{x}^{\ddagger})$), corresponding to the reaction coordinate. This normal-mode has an imaginary frequency $\omega^{\ddagger}$ with an eigenvector $\mathbf{L}_F(\mathbf{x}^{\ddagger})$ in the direction of the reaction coordinate. Then, the first step along the MEP can be taken along this eigenvector[360,383]

$$\mathbf{x}(s_1 = \pm\delta s) = \mathbf{x}^{\ddagger} \pm \delta s \mathbf{L}_F(s^{\ddagger}) \quad (2.4.40)$$

where the sign indicates whether the direction is toward reactants or toward products. The procedure just presented corresponds to using a quadratic expansion of the potential at the saddle point; another possibility is to use a cubic expansion around the saddle point.[384]

After the first step, the gradient is no longer zero and the next steps can be taken in the direction of the normalized gradient. One of the simplest algorithms is the Euler single-step method or Euler steepest-descent (ESD) method[162] in which the next geometry along the MEP is calculated as

$$\mathbf{x}(s_j = s_{j-1} \pm \delta s) = \mathbf{x}(s_{j-1}) \mp \delta s \frac{\mathbf{g}[\mathbf{x}(s_{j-1})]}{|\mathbf{g}[\mathbf{x}(s_{j-1})]|} \quad (2.4.41)$$

This algorithm requires quite small steps and therefore a large number of potential energy gradient evaluations. This is not a problem if the PES is given in analytical form, but it can be very time-consuming for high-level direct dynamics. Improvements to this method and other more efficient methods that may use larger steps are described elsewhere.[141,162,384−389] Some of these algorithms, such as the Page-McIver method,[384] make use of Hessians, $\mathbf{F}(s)$, along the MEP.

To calculate the vibrational part of $Q_C^{GT}(T,s)$ in eq 2.4.31 we need to obtain generalized normal-mode frequencies along the reaction path. These are called generalized because true normal-mode analysis is only defined at stationary points and for systems that are not missing any degrees of freedom. The elimination of the reaction coordinate is accomplished by rotating the coordinate system[369] or by a projection operator;[390] here we describe the latter method. It involves diagonalizing the projected Hessian matrix, $\mathbf{F}^P(s)$, which is obtained from[383,390]

$$\mathbf{F}^P(s) = [\mathbf{1} - \mathbf{P}(s)]\mathbf{F}(s)[1 - \mathbf{P}(s)] \quad (2.4.42)$$

where $\mathbf{P}$ is a matrix that projects onto the direction along the reaction path and onto the overall translations and rotations. The diagonalization is carried out in the same way as for stationary points, with an orthogonal transformation of the type

$$\mathbf{L}^{GT}(s)^{\dagger}\mathbf{F}^P(s)\mathbf{L}^{GT}(s) = \Lambda(s) \quad (2.4.43)$$

and the eigenvalues $\lambda_m(s)$ are related to the generalized normal-mode frequencies $\omega_m(s)$ by

$$\omega_m(s) = \left(\frac{\lambda_m(s)}{\mu}\right)^{1/2}, m = 1, ..., 3N \quad (2.4.44)$$

where $F - 1$ positive values correspond to the generalized frequencies of the bound normal modes at that point on the MEP and the remaining $3N - F + 1$ eigenvalues are zero. The directions along the various generalized normal modes m are given by the corresponding columns of the $\mathbf{L}^{GT}(s)$ matrix.

In the above discussion, TST has been derived by using classical mechanics, but for most reactions quantum effects, especially zero-point energy and sometimes tunneling, cannot be ignored. Next we consider including these quantum effects.

Quantum effects can be included in an ad hoc way in CVT for the normal modes perpendicular to the reaction coordinate by adiabatic quantization of their partition functions. Here adiabatic means that, at each value of s, the energy levels of motions transverse to the reaction coordinate are quantized as if motion along the reaction coordinate were infinitesimally slow. The resulting transition state theory expressions are called quasiclassical, and we drop the subscript C.

The chief quantum effect on the reaction coordinate is penetration through the barrier (tunneling effect), which is most readily treated by using a semiclassical model. The quantum effects on the reaction coordinate are included through a multiplicative ground-state (/G) semiclassical transmission factor $\kappa^{CVT/G}(T)$, and therefore adding quantum effects to eq 2.4.34 yields

$$\kappa^{CVT/G}(T) = \kappa(T)k^{CVT}(T) \quad (2.4.45)$$

where κ is a transmission coefficient that accounts for tunneling, and

$$k^{CVT}(T) = \frac{1}{\beta h}\frac{Q^{GT}(T,s = s_*^{CVT})}{\Phi^R(T)}\exp[-\beta V_{MEP}(s_*^{CVT})] \quad (2.4.46)$$

We will defer discussion of κ and tunneling to Section 2.4.4 and focus here on the rest of the quantized formalism.

In eq 2.4.46, $Q^{GT}(T,s)$ and $\Phi^R(T)$ are the quantum mechanical partition functions for the generalized transition state and reactants, respectively, where

$$Q^{GT}(T,s) = Q_{el}^{GT}(T)Q_{vib}^{GT}(T,s)Q_{rot}^{GT}(T,s) \quad (2.4.47)$$

and

$$\Phi^R(T) = \Phi_{rel}(T)Q_{el}^A(T)Q_{vib}^A(T)Q_{rot}^A(T)Q_{el}^B(T)Q_{vib}^B(T)Q_{rot}^B(T) \quad (2.4.48)$$

where Φ_{rel} is the relative translational partition function per unit volume given by eq 2.4.27 and Q_{el}, Q_{vib}, and Q_{rot} are the electronic, vibrational, and rotational partition functions, respectively. Notice that we have now removed the subscripts C, and all partition functions are now to be computed in principle from quantized energy levels. In practice, it is almost always a good approximation to still treat rotation as classical, but quantization of vibrations is very important.

In eqs 2.4.47 and 2.4.48 we ignore the coupling between the electronic, vibrational, and rotational partition functions.

The electronic partition function of the generalized transition state is given by

$$Q_{\mathrm{el}}^{\mathrm{GT}}(T,s) = \sum_{\gamma=1} d_{\gamma}^{\mathrm{GT}}(s) \exp\{-\beta[V_{\gamma}(s) - V_{\mathrm{MEP}}(s)]\} \tag{2.4.49}$$

where

$$V_{\gamma}(s) = E_{\gamma}^{(\mathrm{el})}(s) + V_{\mathrm{NR}}(s) \tag{2.4.50}$$

where γ is the electronic quantum number with $\gamma = 1$ being the ground state so that

$$V_{\mathrm{MEP}}(s) = V_1(s) = \mathrm{V}(s) \tag{2.4.51}$$

with all quantities in eqs 2.4.49−2.4.51 being evaluated on the MEP, and where $d_{\gamma}^{\mathrm{GT}}(s)$ is the degeneracy of the electronic state γ. Usually we approximate $Q_{\mathrm{el}}^{\mathrm{GT}}(T,s)$ by $Q_{\mathrm{el}}^{\mathrm{GT}}(T, s = 0)$.

For the rotational partition function $Q_{\mathrm{rot}}^{\mathrm{GT}}(T,s)$, since the rotational levels are generally close together, we approximate the quantal partition function by the classical one. It has been shown for atom−diatom reactions that this approximation gives an error in CVT rate constants of not more than about 1% for room temperature and above.[28] For a linear generalized transition state, the classical rotation partition is given by

$$Q_{\mathrm{rot}}^{\mathrm{GT}}(T,s) = \frac{2I(s)}{\hbar^2 \beta \sigma_{\mathrm{rot}}} \tag{2.4.52}$$

where $I(s)$ is the moment of inertia, and σ_{rot} is the rotational symmetry number. For a nonlinear GTS the rotational partition function is

$$Q_{\mathrm{rot}}^{\mathrm{GT}}(T,s) = \left[\left(\frac{2}{\hbar^2\beta}\right)^3 \pi I_{\mathrm{A}}(s) I_{\mathrm{B}}(s) I_{\mathrm{C}}(s)\right]^{1/2} / \sigma_{\mathrm{rot}} \tag{2.4.53}$$

where I_{A}, I_{B}, and I_{C} are the principal moments of inertia.

The vibrational partition function at a generalized transition state is evaluated within the harmonic approximation by

$$Q_{\mathrm{vib}}^{\mathrm{GT}}(T,s) = \prod_{m=1}^{F\text{-}1} Q_{\mathrm{vib},m}^{\mathrm{GT}}(T,s) \tag{2.4.54}$$

with $Q_{\mathrm{vib},m}^{\mathrm{GT}}(T,s)$ being the vibrational partition function of mode m,

$$Q_{\mathrm{vib},m}^{\mathrm{GT}}(T,s) = \sum_{n_m} \exp[-\beta E_{\mathrm{vib},m}^{\mathrm{GT}}(n_m,s)] \tag{2.4.55}$$

where the harmonic vibrational energy of level n,

$$E_{\mathrm{vib},m}^{\mathrm{GT}}(n_m,s) = \left(n_m + \frac{1}{2}\right)\hbar\omega_m(s) \tag{2.4.56}$$

is measured at the bottom of the local vibrational well, that is, at $V_{\mathrm{MEP}}(s)$. The sum of eq 2.4.55 should finish with the last term for which $E_{\mathrm{vib},m}^{\mathrm{GT}}(n_m,s)$ is less than the lowest bond dissociation asymptote of the system,[365,391,392] or it could also include all the quasibound states that are effectively bound on the time scale of stabilizing collisions; but instead, if we assume that the contribution from high energy levels is negligible, the sum can be extended to include all the harmonic levels, and eq 2.4.55 can be replaced by the analytical expression

$$Q_{\mathrm{vib},m}^{\mathrm{GT}}(T,s) = \frac{\exp[-(1/2)\beta\hbar\omega_m(s)]}{\{1 - \exp[\beta\hbar\omega_m(s)]\}} \tag{2.4.57}$$

In the case of the reactants, the partitions functions are given by similar expressions to those just presented but using the equilibrium moments of inertia and the equilibrium frequencies of each of the reactants.

The incorporation of quantum effects in the partition functions for the bound degrees of freedom allow us to include the zero-point energy to the classical potential along the PES. Since we are assuming that the generalized normal-mode frequencies follow the reaction coordinate adiabatically (the reaction coordinate is formally considered the slowest motion at a dynamical bottleneck), we can define the vibrationally adiabatic ground-state potential curve, $V_{\mathrm{a}}^{\mathrm{G}}(s)$ as

$$\mathrm{V}_{\mathrm{a}}^{\mathrm{G}}(s) = V_{\mathrm{MEP}}(s) + E_{\mathrm{int}}^{\mathrm{G}}(s) \tag{2.4.58}$$

where $E_{\mathrm{int}}^{\mathrm{G}}(s)$ is the total vibrational zero-point energy:

$$E_{\mathrm{int}}^{\mathrm{G}}(s) = \sum_{m=1}^{F\text{-}1} E_{\mathrm{vib},m}^{\mathrm{GT}}(n_m = 0,s) \tag{2.4.59}$$

and in the harmonic approximation $E_{\mathrm{int}}^{\mathrm{G}}(s)$ is simply:

$$E_{\mathrm{int}}^{\mathrm{G}}(s) = (1/2)\sum_{m=1}^{F\text{-}1} \hbar\omega_m(s) \tag{2.4.60}$$

The maximum of the vibrationally adiabatic potential coincides with the maximum of the Gibbs free energy of activation at $T = 0$ K.[28] Anharmonicity may have an important influence on the computed thermal rate constant, and in the next subsection we describe different methods to include anharmonicity.

Another way of improving CVT is to consider a microcanonical ensemble, that is, an ensemble in which the system is characterized by a given total energy rather than by a temperature (as in a canonical ensemble). Such a treatment is more complete than using a canonical ensemble because it takes account of the conservation of the total energy in each collision. The resulting rate constant is called microcanonical variational transition state theory or simply microcanonical variational theory (μVT). To derive the μVT rate constant we start from eqs 2.2.6 and 2.2.7. In eq 2.2.6, the Boltzmann weighting factors represent the fraction of reactant molecules in a given internal state when the system is in thermal equilibrium

$$w_k^{\mathrm{X}} = \frac{d_k^{\mathrm{X}} e^{-\beta E_{\mathrm{int},k}{}^{\mathrm{X}}}}{Q_{\mathrm{int}}^{\mathrm{X}}(T)} \tag{2.4.61}$$

where X is A if k is i and where X is B if $k = j$; d_k^{X} is a degeneracy; and $E_{\mathrm{int},k}^{\mathrm{X}}$ and $Q_{\mathrm{int}}^{\mathrm{X}}(T)$ are the internal energy of the reactant X in state k and the internal partition function at temperature T, respectively. Therefore

$$Q_{\mathrm{int}}^{\mathrm{X}}(T) = \sum_k d_{\mathrm{int},k}^{\mathrm{X}} \exp[-\beta E_k^{\mathrm{X}}(T)] \tag{2.4.62}$$

Thus, the total rate constant is related to the state-selected rate constants by

$$k(T) = [Q^{\mathrm{A}}_{\mathrm{int}}(T)Q^{\mathrm{B}}_{\mathrm{int}}(T)]^{-1}\sum_{i,j} d^{\mathrm{A}}_i d^{\mathrm{B}}_j k_{ij}(T) \exp[-\beta(E^{\mathrm{A}}_{\mathrm{int},i} + E^{\mathrm{B}}_{\mathrm{int},j})] \quad (2.4.63)$$

Following Appendix I of ref 383 then leads to an expression of the thermal rate constant as a function of the state-selected reaction probability P^J_α

$$k(T) = \frac{1}{\beta h \Phi^{\mathrm{R}}(T)}\sum_J (2J+1)\sum_{ijlm_l}\int_0^\infty P^J_{ijlm_l}(E)\exp(-\beta E)\beta dE \quad (2.4.64)$$

where l is the quantum number associated with L, and m_l is the projection of this orbital quantum number on an arbitrary space-fixed axis,

$$E = E_{\mathrm{rel}} + E^{\mathrm{A}}_{\mathrm{int},i} + E^{\mathrm{B}}_{\mathrm{int},j} \quad (2.4.65)$$

and $P^J_{ijlm_l}$ is the reaction probability as a function of the rotational and vibrational quantum numbers of reactants and also l, m_l, and total angular momentum J. The factor of $2J + 1$ results from a sum over $2J + 1$ values of M_J, the component of J on an arbitrary space-fixed axis, since the probabilities are independent of M_J. Let α denote the collective set of quantum numbers $ijlm_l$. Then J, M_J, and α represent a "channel" specified by a complete set of quantum numbers labeling the initial state of a collision.

Next define the J-resolved cumulative reaction probability $N^J(E)$ as[393−396]

$$N^J(E) = \sum_{ijlm_l} P^J_{ijlm_l}(E) = \sum_\alpha P^J_\alpha(E) \quad (2.4.66)$$

in terms of which eq 2.4.64 can be rewritten as

$$k(T) = \frac{1}{\beta h \Phi^{\mathrm{R}}(T)}\sum_J (2J+1)\int_0^\infty N^J(E)\exp(-\beta E)\beta dE \quad (2.4.67)$$

Summing over J gives

$$k(T) = \frac{1}{\beta h \Phi^{\mathrm{R}}(T)}\int_0^\infty N(E)\exp(-\beta E)\beta dE \quad (2.4.68)$$

where the cumulative reaction probability is[397−399]

$$N(E) = \sum_J (2J+1)N^J(E) = \sum_J\sum_{M_J}\sum_\alpha P^{JM\mathrm{J}}_\alpha(E) \quad (2.4.69)$$

This result is exact.

The transition state theory approximation to eq 2.4.68 is

$$k^{\mu\mathrm{VT}}(T) = \frac{1}{\beta h \Phi^{\mathrm{R}}(T)}\int_0^\infty N^\ddagger(E)\exp(-\beta E)\beta dE \quad (2.4.70)$$

Each of the probabilities in eqs 2.4.64 and 2.4.66 satisfies

$$0 \le P^J_{ijlm_l} \le 1 \quad (2.4.71)$$

These probabilities are labeled by the quantum numbers that describe the initial state of a collision. We could instead specify the probabilities by a complete set of quantum numbers J, M_J, and $\tilde{\alpha}$ that label the members of a complete basis set at the transition state. Then eq 2.4.69 would be

$$N(E) = \sum_J\sum_{M_J}\sum_{\tilde{\alpha}} P^{JM_J}_{\tilde{\alpha}}(E) \quad (2.4.72)$$

The transition state approximation is to replace this by

$$N^\ddagger(E) = \sum_J\sum_{M_J}\sum_{\tilde{\alpha}} \Theta(E - E^{JM_J}_{\tilde{\alpha}}) \quad (2.4.73)$$

where Θ is the Heaviside function, and $E^{JM_J}_{\tilde{\alpha}}$ is the energy of state $\tilde{\alpha}$ with rotational quantum numbers J and M_J at the transition state.

Actually $P^{JM_J}_{\tilde{\alpha}}(E)$ is not a physical observable, and it is not well defined, but its only purpose is to motivate eq 2.4.73. In this equation, $E^{JM_J}_{\tilde{\alpha}}$ is not actually well-defined either (since the transition state has a finite lifetime), but we have already used transition state energy levels in computing canonical partition functions, so that is not a serious limitation. Furthermore, in Section 3.1, we will see that accurate quantum mechanical scattering calculations lend support to the existence of quantized energy levels of the transition state.

If we designate $N^{\mathrm{GT}}_{\mathrm{vr}}(E,s)$ as the number of vibrational−rotational states with energy less than E at a given generalized transition state, then

$$N^\ddagger(E) = N^{\mathrm{GT}}_{\mathrm{vr}}(E,s) \quad (2.4.74)$$

Microcanonical variational theory is given by minimizing the value of $N^{\mathrm{GT}}_{\mathrm{vr}}(E,s)$, that is

$$N^{\mu\mathrm{VT}}(E) = \min_s N^{\mathrm{GT}}_{\mathrm{vr}}(E,s) \quad (2.4.75)$$

or equivalently

$$\left.\frac{\partial N^{\mathrm{GT}}_{\mathrm{vr}}(E,s)}{\partial s}\right|_{s=s_*{}^{\mu\mathrm{VT}}(E)} = 0 \quad (2.4.76)$$

The derivation above shows why a minimum-number-of states criterion should be preferred to a minimum-density-of-states criterion to evaluate the microcanonical rate constant.[369]

Again we assume that rotation and vibration are separable with vibrational quantum numbers denoted **n**. This yields for $N^{\mathrm{GT}}_{\mathrm{vr}}(E,s)$:

$$N^{\mathrm{GT}}_{\mathrm{vr}}(E,s) = \sum_{\mathbf{n}} \Theta[E - V_{\mathrm{MEP}}(s) - E^{\mathrm{GT}}_{\mathrm{vib}}(\mathbf{n},s)]N^{\mathrm{GT}}_{\mathrm{rot}}[E - V_{\mathrm{MEP}}(s) - E^{\mathrm{GT}}_{\mathrm{vib}}(\mathbf{n},s),s] \quad (2.4.77)$$

where for $N^{\mathrm{GT}}_{\mathrm{rot}}(E,s)$ we use the classical approximation.[383]

If we calculate $N^{\mathrm{GT}}_{\mathrm{vr}}(E, s = s_*^{\mathrm{CVT}})$ we obtain the CVT thermal rate constant. Another possibility is to optimize the generalized transition state microcanonically for energies up to the microcanonical variational threshold energy and canonically for higher-energy contributions. This leads to the improved canonical variational theory (ICVT),[383,400] which has the same threshold as μVT but the calculations are almost as simple as for CVT. One can easily show that

$$k^{\mathrm{CTST}} \ge k^{\mathrm{CVT}} \ge k^{\mathrm{ICVT}} \ge k^{\mu\mathrm{VT}} \quad (2.4.78)$$

where CTST denotes conventional TST, i.e., the dividing surface at the saddle point.

Full details of VTST calculations are given elsewhere.[383,401,402]

Next we present some examples to illustrate the difference between conventional TST, CVT, and μVT. Fernández-Ramos et al.[403] used ab initio dual-level direct dynamics to study the $Cl + C_2H_6 \rightarrow ClH + C_2H_5$ hydrogen abstraction reaction. Low-level calculations were performed by MP2/aug-cc-pVDZ electronic structure method,[404] and the high-level calculations were performed using the infinite basis (IB) electronic structure method[75,405] to correct the low-level energies. Although a transition state was located for this abstraction reaction, after the ZPE contributions are included there is no barrier in the effective potential along the reaction coordinate, so important variational effects are expected.

Both V_{MEP} and the vibrationally adiabatic potential

$$\Delta V_a^G(s) = V_a^G(s) - V_a^G \text{ (reactants)} \qquad (2.4.79)$$

are plotted along the path in Figure 1. At room temperature the maximum of the free energy (see eq 2.4.36) is located

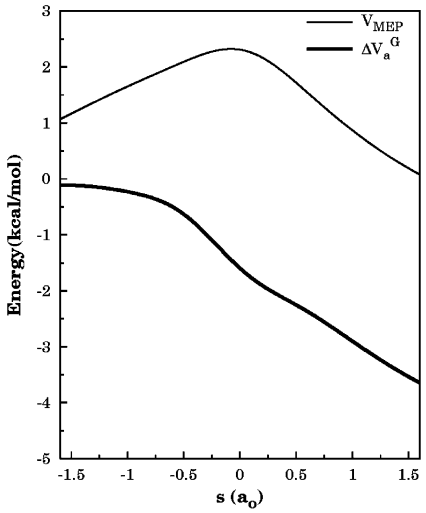

Figure 1. Plots of V_{MEP} and relative vibrationally adiabatic potential ΔV_a^G along the reaction path for the $Cl + C_2H_6 \rightarrow ClH + C_2H_5$ hydrogen abstraction reaction.

at $s_*^{CVT} = -0.364$ a_0, whereas $s_*^{\mu VT}$ is energy dependent (see eq 2.4.76). Figure 2 shows the variation of $s_*^{\mu VT}$ with energy; it moves in the interval $[-0.70\ a_0, -0.22\ a_0]$ at low energies and remains almost constant above 55 kcal/mol, where the zero of energy is the potential energy at the equilibrium structure of reactants. Despite the variation of $s_*^{\mu VT}$, the CVT and μVT rate constants are quite similar at room temperature with values of 6.54×10^{-11} and 6.08×10^{-11} cm^3 molecule^{-1} s^{-1}, respectively, and at higher temperatures they are even closer. This example shows that even for reactions with variable transition states the CVT rate constants are reasonable and economical alternatives to μVT rate contants. However, the conventional TST rate constant is 2.33×10^{-10} cm^3 molecule^{-1} s^{-1} and seriously overestimates the experimental[406] value of 5.75×10^{-11}.

Another interesting example is the comparison of CVT, ICVT, and μVT with QCT for the room-temperature abstraction of a bromine atom in the bimolecular $HgBr + Hg \rightarrow Hg + Br_2$ reaction.[249] In this case, the QCT rate constants

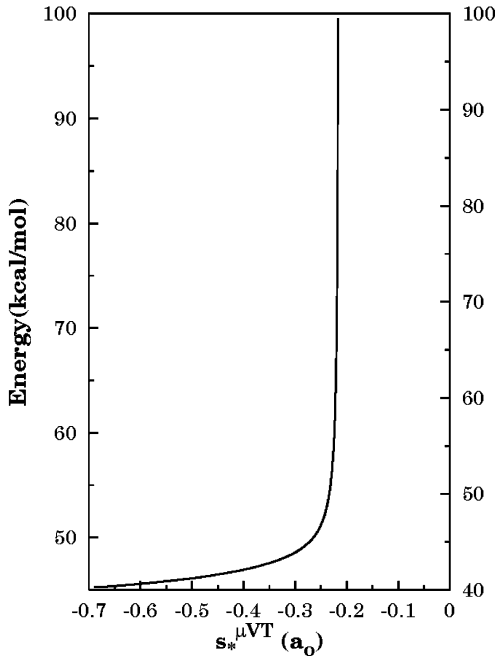

Figure 2. Variation with energy of the location of the minimum sum of states for the $Cl + C_2H_6 \rightarrow ClH + C_2H_5$ reaction.

are smaller than the CVT, ICVT, and μVT rate constants by factors of 1.58, 1.36, and 1.16, respectively.

For cases in which the transition state is "tight" and no light particle participates in the reaction, so tunneling is not important, conventional TST can still provide a reliable determination of thermal rate constants, and it also provides insight into reaction mechanisms.[407]

In the examples just discussed, VTST is applied to study a particular system, so if we want to study another system, even if similar, the entire procedure, starting with building the potential energy surface, has to be repeated. To make it easier to study a series of reactions, Truong and coworkers[408−412] have presented a method called reaction class transition state theory (RC-TST), which profits from recognizing the common aspects of a given set of chemical reactions. Thus, reactions with similar characteristics form what is called a class, and it is expected that they also share some similarity in their kinetics parameters. The procedure involves accurate calculations for one of the reactions, called the principal reaction, and all the other thermal rate constants are obtained from empirical relations. Truong applied these ideas to hydrogen abstraction reactions by hydrogen atoms with encouraging results.[408−412]

An important point to keep in mind in using either conventional or variational transition state theory is that extra assumptions are required to predict more than the overall reaction rate. We will present some discussion of product state distributions in Section 3. Sometimes not only the product states but even the identity of the products is inaccessible. This problem arises if two or more products share a given transition state. This can occur if the reaction path bifurcates after the transition state.[413−421]

2.4.3. Anharmonicity

Conventionally, one would compute the reactant partition function accurately by a sum over states, although in practice this has only recently become possible for molecules with more than 3−4 atoms.[422] An alternative method to compute accurate vibrational−rotational partition functions is the

Feynman path integral method, and this approach has been applied to compute converged partition functions for H_2O_2,[423] the first molecule with a torsion for which an accurate partition function corresponding to a known potential energy surface is available. More recently, converged vibrational partition functionals have also been computed for ethane.[424] Before discussing these methods though, we consider some simpler approximations.

The vibrational partition functions discussed in the previous section are based on the harmonic approximation for all the normal modes orthogonal to the reaction path. In this approach, the partition function is separable and the potential due to a given normal mode m is given by

$$V^{(m)}[s,u_m(s)] = (1/2)k_{mm}(s)[u_m(s)]^2 \quad (2.4.80)$$

where k_{mm} is the principal (the two subscripts are the same) normal-coordinate force constant, and $u_m(s)$ is the normal-mode coordinate for a geometry $\mathbf{x}$ close to $\mathbf{x}(s)$, specifically,

$$u_m(s) = [\mathbf{x} - \mathbf{x}(s)]\mathbf{L}_m^{\mathrm{GT}}(s) \quad (2.4.81)$$

2.4.3.1. Principal Anharmonicity. In general the vibrational degrees of freedom of the stationary points and generalized transition states along the path are bound by an anharmonic potential:

$$V^{(m)}[s,u_m(s)] = \frac{1}{2}k_{mm}(s)[u_m(s)]^2 + k_{mmm}(s)[u_m(s)]^3 + k_{mmmm}(s)[u_m(s)]^4 + \cdots \quad (2.4.82)$$

where $k_{mmm}(s)$ and $k_{mmmm}(s)$ are the third and fourth principal normal mode force constants. These force constants can be obtained from numerical derivatives of analytic gradients.[383] One difficulty with using this expansion is that the cubic term is always unbounded from below, and the quartic term is unbounded from below if k_{mmmm} is negative. It therefore requires finesse to include anharmonicity in a practical scheme.

One approach commonly used to treat anharmonicity is to assume that the normal modes are independent (not coupled), so the partition function may still be evaluated by eq 2.4.54. This section begins with independent normal-mode (INM) methods, and within the INM framework we discuss Morse and quartic anharmonicity,[360] together with the Wentzel−Brillouin−Kramers (WKB) method[425−427] and the anharmonicity of bond torsional modes.

To evaluate the energy levels of the 1D potential (2.4.82) one possibility is to replace that potential by a Morse function:[428]

$$V^{(m)}[s,u_m(s)] \cong D_e(s)\{\exp[-\beta_M^{(m)}(s)u_m(s)] - 1\}^2 \quad (2.4.83)$$

where $D_e(s)$ is the dissociation energy for the vibrational potential on the PES:

$$D_e = D - V_{MEP}(s) \quad (2.4.84)$$

and D is the lowest dissociation energy of the system. The range parameter $\beta_M^{(m)}$ is given by

$$\beta_M^{(m)}(s) = [k_{mm}(s)/2D_e(s)]^{1/2} \quad (2.4.85)$$

so the potential has the correct force constant at the minimum. The Morse model in which the parameters D_e and $\beta_M^{(m)}$ are chosen this way is known as Morse approximation I.[360,365,429] The energy levels of this potential are given by[428]

$$E_{vib,m}^{GT}(n,s) = \hbar\omega_m(s)(n_m + 1/2)[1 - x_M^{(m)}(s)(n_m + 1/2)] \quad (2.4.86)$$

where n_m is the level index, and $x_M^{(m)}(s)$ is the anharmonic constant given by

$$x_M^{(m)}(s) = \hbar\omega_m(s)/4D_e(s) \quad (2.4.87)$$

This Morse model does not give any improvement for modes in which $k_{mmm}(s) = 0$, such as the bending modes of linear systems, out-of-plane modes of planar systems, and certain stretching motions. This kind of mode can be treated by a quadratic-quartic model with

$$V^{(m)}[s,u_m(s)] \cong \frac{1}{2}k_{mm}(s)[u_m(s)]^2 + k_{mmmm}(s)[u_m(s)]^4 \quad (2.4.88)$$

which can sometimes be accurately approximated by a perturbation-variation method to obtain the energy levels.[430,431] A centrifugal oscillator treatment provides a more accurate approximation.[432] Anharmonicity of bending modes is often dominated by quartic anharmonicity, and it can be very significant, especially at high temperature.[431]

The anharmonicity can be also treated by the WKB approximation.[425−427] Since this method is more expensive, it might be used only for finding the zero-point energy of some or all the normal modes. For several atom−diatom reactions, the results obtained by VTST improve if the WKB method is used to treat anharmonicity instead of the Morse model.[427]

Another important source of error in calculating vibrational partition functions is the inapplicability of the harmonic oscillator (HO) approximation for low-frequency torsional modes. Such modes show a hindered rotation transition from HO behavior at low temperature to free internal rotation at high temperature. An interpolatory function that is reasonably accurate has the form[433]

$$Q_m^{HR} \approx Q_m^{HO} f_m \quad (2.4.89)$$

where Q_m^{HR} is the approximate hindered-rotor (HR) partition function, Q_m^{HO} is the harmonic oscillator partition function, and f_m is an interpolating function given by

$$f_m = \tanh Q_m^{FR} w_m \quad (2.4.90)$$

The interpolating function approaches unity when $w_m = h\omega_m/k_BT$ goes to infinity, and it approaches $Q_m^{FR}w_m$ when w_m goes to zero, with Q_m^{FR} being the free-rotor (FR) partition function. For small values of w_m the interpolating function deviates only quadratically from its limiting form.

Assuming that the torsional degree of freedom is separable, that the reduced moment of inertia for the hindered rotor is independent of torsion angle and is known, and that the torsion potential is the lowest-order cosine potential with the correct periodicity, results obtained by this formula were tested against the tables of Pitzer and Gwinn,[434,435] and the accuracy obtained was encouraging. However, the separability approximation and the simplification of the torsional potential may cause errors as large as or larger than the

principal anharmonicity, so this success for a separable torsion may be irrelevant. Furthermore, the reduced moment of inertia is not independent of torsion angle, and even for the equilibrium geometry it is not trivial. In a series of articles, Pitzer and co-workers derived various approximate and exact expressions for decoupling the internal rotor from the external rotor, including the case of multiple rotors.[436−439] East and Radom have recently provided a useful summary of their key results.[440] Robertson and Wardlaw provide an alternative viewpoint[441] whose extension to all modes could prove useful in considering nonrigid effects.

In a later publication Chuang and Truhlar[442] and Katzer and Sax[443] extended the above formulation to nonsymmetric torsional modes. Furthermore, McClurg et al.[444] and Ayala and Schlegel[445] have suggested alternative procedures involving the Pitzer-Gwinn approximation with a reference potential. A goal of the Chuang-Truhlar and Ayala-Schlegel work was to provide an automated general method, especially for overcoming the fact that internal rotors are usually coupled to other low-frequency modes and sometimes coupled to high-frequency modes, but the methods remain unvalidated. Further work is required to obtain satisfactory practical procedures.[446]

When there is a high barrier between torsional minima at the transition state, one can, as a first approximation, add the rate constants for the different conformers of the transition state with each treated harmonically.[447]

For applying eq 2.4.70, it is necessary to calculate the number of states. Counting methods[448,449] and the Whitten-Rabinovitch method[450] are the most popular methods employed. At the classical level, it is important to have a procedure for estimating the density of states for hindered internal rotors. Forst,[451] Knyazev,[452,453] and McClurg[454] have provided approximate expressions for the density of states via inverse Laplace transforms of the canonical partition functions. The Pitzer-Gwinn approximation has also been employed at the microcanonical level,[455] with simple configurational integrals providing the classical state densities.[456] Jordan et al. determined analytic classical partition functions and densities of states for a variety of hindering potentials.[457] Knyazev and Tsang have recently generalized their results for internal rotor state densities to obtain an algorithm for deriving approximate quantum anharmonic state densities for arbitrary potential energy forms.[458] The algorithm is based on classical phase space integrals coupled with quantum corrections obtained via the Pitzer-Gwinn approximation and inverse Laplace transforms of the canonical partition functions. At the classical level, accurate numbers of states are easily expressed in terms of phase space integrals that can generally be reduced to just configurational integrals.[459]
Monte Carlo evaluation provides a standard procedure for evaluating the multidimensional configuration integrals. Direct evaluation (without fitting the potential energy surface) is feasible up to at least five atoms. Densities of states can be obtained via either numerical or analytic differentiation. Quantum corrections may be implemented with a microcanonical version of the Pitzer-Gwinn approximation. Alternatively, the usual Pitzer-Gwinn approximation could be applied to the classically evaluated canonical partition functions, followed by inverse Laplace transforms. Parneix and co-workers propose a different approach based on the temperature dependence of the average energy,[460] and Börjesson et al.[461] proposed a power-law form with the parameters determined from thermodynamic data.

2.4.3.2. Mode−Mode Coupling. In a full treatment of anharmonicity, one cannot consider the modes one at a time. For example, in addition to torsions, which are 1D internal rotations, one must also sometimes consider 2D internal rotations, especially for association reactions, and approximate formulas have been developed.[462,463] More sophisticated methods for association reactions are presented in Section 2.5.2.

Another kind of anharmonicity corresponds to mode−mode coupling. This involves cross terms (or nonprincipal force constants) that may couple vibrational modes to each other[464,465] and to rotational modes.[431] Unless one includes mode−mode coupling, attempts to include anharmonicity are almost as likely to make the calculations less accurate than more accurate because anharmonicity cancels out to some extent between the reactant and the transition state partition functions. Anharmonicity in low-frequency bends and torsions that occur in the transition state but not the reactant are not subject to this cancellation, and anharmonicity in such modes can be an important source of error in transition state theory. These modes, however, are particularly difficult to treat because of mode−mode coupling.

The simplest method to treat anharmonicity quantum mechanically including mode−mode coupling is perturbation theory,[466−470] and a particularly effective way to use perturbation theory is as follows (this is called simple perturbation theory or SPT[471]). In this approach, we write the potential energy function for a polyatomic molecule as

$$V = V_e + \frac{1}{2}\sum_{m=1}^{F} \mu\omega_m{}^2 u_m{}^2 + V_{Anh} \qquad (2.4.91)$$

where V_e is the energy at the equilibrium geometry, and V_{Anh} contains all the anharmonic terms. The harmonic partition function of eq 2.4.54 can be rewritten as

$$Q_{vib} = \frac{\exp(-\beta E_0)}{\prod_{m=1}^{F}[1 - \exp(-\beta\Delta_m)]} \qquad (2.4.92)$$

where E_0 is the harmonic zero-point energy of the normal modes, and Δ_m is the lowest excitation energy of mode m. In SPT, these quantities are obtained by second-order perturbation theory (PT2)[466−470] by going to second order in cubic force constants and to first order in quartic ones. The method has been tested[466−473] for several cases where accurate partition functions were available, and it was found to be efficient and to represent a considerable improvement over the INM approximation.

One could also consider using perturbation theory for higher-energy levels, as opposed to just the zero-point level and fundamentals in eq 2.4.92. This presents two problems. First, perturbation theory tends to diverge for the higher levels, and it is much less accurate than for the low levels. Second, calculating only the zero point energy and fundamentals by perturbation theory requires only a subset of the force constants and is therefore more economical and feasible. Thus, SPT should not be considered a shortcut but rather an algorithm designed to enhance accuracy and efficiency.

For some molecules, the dominant error in vibrational pertubation theory is caused by Fermi resonances and other similar resonances since the original method has singularities when there are resonances, that is, when one frequency is a ratio of integers times the other. The PT2 method has been

corrected[474] to remove these singularities in an automatic way.

Four other approaches to including anharmonicity that include mode−mode coupling are vibrational configuration interactions,[422,424,475−477] Feynman path integrals,[423,478−484] and the Pitzer−Gwinn approximation,[434,485] and Einstein−Brillouin−Keller (EBK) quantization.[486]

Vibrational configuration interaction[422,424,475−477] (VCI) is straightforward in that vibrational−rotational energy levels are calculated variationally, and the partition function is obtained by summing eigenvalues. However, without using special techniques VCI rapidly becomes unaffordable as the molecule size increases. The largest molecule for which vibrational−rotational partition functions have been computed by summing converged vibrational−rotational eigenvalues is CH_4.[422] The first simplification one can make is to assume separable rotation. With this approximation, converged vibrational partition functions have been calculated for C_2H_6 using VCI.[424] This is a difficult problem because it involves 18 vibrational degrees of freedom, one which is a large-amplitude torsion, but its solution was made possible by using a hierarchical expansion[475] of the potential. Future progress is possible as the potentiality of this method is still largely untapped.

Feynmann path integrals[423,478−484] allow the direct computation of partition functions without separating rotation from vibration and without converging or even calculating individual energy levels. The method has been applied successfully to H_2O,[480,482] H_2S,[482] H_2Se,[482] H_2O_2,[423] and seven isotopologs of H_2O_2. Note that the tetra-atomic cases involve a large-amplitude torsion. The key to further success with this method is the development and exploitation of improved sampling[423] and extrapolation[481,483] algorithms.

The Pitzer−Gwinn method[434,485] is computationally less demanding than VCI or path integrals. It provides a reasonably accurate way to include mode−mode coupling effects at high temperature.[424]

The EBK quantization method has been employed[486] (with total angular momentum equal to zero) in the flexible transition state model discussed further in Section 2.5.2.

An interesting example of a 2D treatment of coupled hindered internal rotors is provided by the reaction of ethylene with butylbenzene, as recently studied by Van Speybroeck and co-workers.[487] For this reaction, the net effect of the potential couplings on the canonical rate coefficients corresponds to a reduction in the rate coefficient by only about 30%, due in part to some cancellation of errors in the partition functions for the transition state and the reactants.

The anharmonic effects on Al_3 clusters were estimated to be factors of 2.5 to 2.9.[488]

2.4.4. Tunneling, Recrossing, and the Transmission Coefficient

The above treatment assumes reactants at local equilibrium and separable, classical reaction coordinate motion. One may attempt to remove these deficiencies by multiplying the VTST rate constant by a correction factor, called the transmission coefficient as in eq 2.2.2. Although the various physical effects that may be included in a transmission coefficient are not independent, it is useful for discussion purposes[489] to separate them qualitatively as follows:

$$\gamma(T) = g(T)\Gamma(T)\kappa(T) \qquad (2.4.93)$$

where $g(T)$ corrects for nonequilibrium reactants, $\Gamma(T)$ corrects for nonseparability of the reaction coordinate at the classical level, and $\kappa(T)$ corrects for quantum effects on the reaction coordinate. If the reaction coordinate truly were classical and separable, there would be no recrossing; thus $\Gamma(T)$ may be considered a recrossing correction. If the reaction coordinate were classical, there would be no tunneling and no diffractive reflection from the barrier; thus $\kappa(T)$ may be considered a correction for these effects—for simplicity it is often called a tunneling correction. Note that even if one neglects recrossing, it is important to include the nonseparability of the reaction coordinate at the quantal level; thus $\kappa(T)$ should be multidimensional. In the rest of this section, we consider further the factors in eq 2.4.93, starting with $\Gamma(T)$ and then considering $\kappa(T)$ and $g(T)$.

The thermal rate constants derived so far in this review are based on the fundamental assumption of TST, namely, that there is a dynamical bottleneck located at the transition state (conventional TST) or at a generalized transition state obtained by a canonical (CVT) or microcanonical (μVT) criterion, respectively. In the latter cases, the dividing surface is optimized variationally to minimize the recrossing. Placing the transition state at the location that maximizes the free energy of activation (see eq 2.4.36) is equivalent to minimizing recrossing and therefore to maximizing Γ. This perspective on VTST was first proposed by Evans,[490] and it provides a key conceptual framework for modern variational transition state theory.[491] However, we still may have some classical recrossing at the location of the best variational transition state because we do not allow the transition state dividing surface to be completely optimized as an arbitrary function of coordinates. In fact, as long as we continue to assume that classical mechanics is applicable, we could in principle make the dividing surface more and more general, until it depends on all coordinates and all momenta, which would eventually allow us to totally eliminate recrossing. This is not really an option once we quantize the vibrations within the dividing surface because practical (which usually means separable—at least until we get to Section 2.5) approximations to the quantized energy levels are valid only for simple dividing surfaces, and thus some recrossing remains. Although practical experience for simple barrier reactions has shown that recrossing effects can usually be made small even with very manageable prescriptions (such as hyperplanes in coordinate space) for the dividing surface, there are approaches, like the unified statistical model[492,493] (US), the canonical unified statistical model[383,494] (CUS), and the unified dynamical model[383,495−497] (UD), that can be used to account for the recrossing that remains after the variational transition state has been optimized within some set of necessarily restricted choices for the dividing surface.

The US[492,493] and CUS[383,494] models have been proposed to describe reactions with more than one bottleneck. The thermal rate constant for this model is given by[494]

$$k^{\mathrm{US}}(T) = \frac{Q_{\mathrm{el}}^{\mathrm{GT}}(T)}{\beta h \Phi^{\mathrm{R}}(T)} \int_0^\infty N_{\mathrm{vr}}^{\mathrm{US}}(E) \exp(-\beta E)\beta dE \qquad (2.4.94)$$

where

$$N_{\mathrm{vr}}^{\mathrm{US}}(E) = N_{\mathrm{vr}}^{\mu\mathrm{VT}}(E)\Gamma^{\mathrm{US}}(E) \qquad (2.4.95)$$

and $\Gamma^{\mathrm{US}}(E)$ is the US recrossing factor defined as[493]

$$\Gamma^{\mathrm{US}}(E) = 1 + \frac{N_{\mathrm{vr}}^{\mu}\mathrm{VT}(E)}{N_{\mathrm{vr}}^{\mathrm{min}}(E)} - \frac{N_{\mathrm{vr}}^{\mu\mathrm{VT}}(E)}{N_{\mathrm{vr}}^{\mathrm{max}}(E)} \quad (2.4.96)$$

where $N_{\mathrm{vr}}^{\mathrm{min}}(E)$ is the second lowest minimum of $N_{\mathrm{vr}}^{\mathrm{GT}}(E, s)$ and $N_{\mathrm{vr}}^{\mathrm{max}}(E)$ is the maximum of $N_{\mathrm{vr}}^{\mathrm{GT}}(E, s)$ that lies between the two minima. It should be noticed that the US calculation is nonvariational, although it always satisfies that $k^{\mathrm{US}}(T) \leq k^{\mu}{}_{\mathrm{VT}}(T)$. The same analysis can be applied to a canonical ensemble by defining canonical probabilities in terms of canonical-ensemble averages of the flux through these surfaces.[494] The resulting canonical unified statistical (CUS) thermal rate constant assumes the form

$$k^{\mathrm{CUS}}(T) = k^{\mathrm{CVT}}(T)\Gamma^{\mathrm{CUS}}(T) \quad (2.4.97)$$

with $\Gamma^{\mathrm{CUS}}(T)$ being the CUS recrossing factor.

The CUS result can yield a reduction in the rate coefficient of no more than a factor of 2 relative to the minimum of the VTST treatments of the two individual bottlenecks. In contrast, at the microcanonical level there is no such limit on the magnitude of the effect of the unified statistical treatment. Indeed, in a recent treatment of the addition of OH to C_2H_4, the unified statistical treatment yielded a reduction by more than a factor of 10.[498] However, the CUS and US methods, although nonvariational, may be more accurate that CVT and μVT methods when the reaction has several bottlenecks. An example is the VTST study of the $H + O_3 \rightarrow HO + O_2$ reaction carried out by Fernández-Ramos and Varandas[499] using a DMBE potential energy surface for the dynamics calculations. The reaction has a very low barrier and two dynamical bottlenecks near to the transition state structure. The μVT and US rate constants were compared with QCT calculations in the temperatures interval 100−700 K. The μVT values were about a factor of 2 larger than the QCT ones, whereas the US ones are only about 1.4 times larger than the QCT calculations, as can be seen in Figure 3.

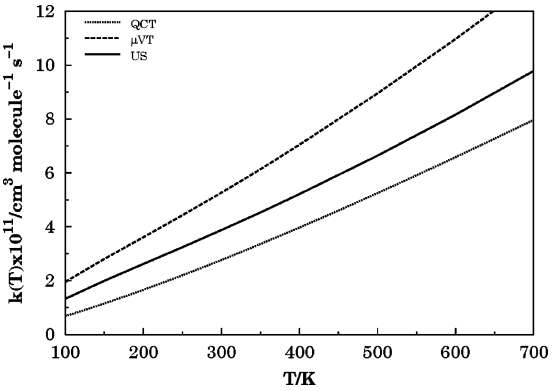

Figure 3. Arrhenius plot comparing μVT, US, and QCT methods for the $H + O_3 \rightarrow OH + O_2$ reaction.

When there are both consecutive and competitive dynamical bottlenecks, one may use the competitive canonical unified statistical (CCUS) model.[413,500,501]

Whereas the US and CUS models involve statistical estimates of recrossing probabilities, it is also possible to use trajectories for this purpose. Keck[502,503] and Anderson[504−506] showed how trajectories can be used to calculate a correction for the breakdown of the TST assumption in a classical mechanical context. In fact, this is a convenient way to do trajectory calculations for gas-phase reaction processes because it involves starting the trajectories at the transition state, which is a form of rare event sampling and is very efficient. A quantized version of this approach is called the unified dynamical (UD) theory. In the UD model the recrossing corrections to VTST are evaluated from trajectories beginning at a quantized variational transition state.[383,495−497] The short-time dynamics in the vicinity of a localized dynamical bottleneck determines the rate. A key source of potential error in this approach is that even though the trajectories are quantized at the variational transition state, classical mechanical dynamics does not preserve this quantization as they evolve in time.

In eq 2.4.45, the VTST thermal rate constants include the quantization of vibrations orthogonal to the reaction path by using quantum instead of classical partition functions. But with $\kappa = 1$, the reaction coordinate is still treated classically, and therefore tunneling is neglected. One way of correcting this deficiency is to include a multiplicative transmission coefficient $\kappa^{\mathrm{X/Y}}$ such that the resulting rate constant is given by

$$k^{\mathrm{X/Y}}(T) = \kappa^{\mathrm{X/Y}}(T)k^{\mathrm{X}}(T) \quad (2.4.98)$$

where X indicates the variational method used (CVT, ICVT, or μVT), and Y indicates the approach used to treat tunneling. In the case of conventional TST we have

$$k^{\ddagger/\mathrm{Y}}(T) = \kappa^{\ddagger/\mathrm{Y}}(T)k^{\ddagger}(T) \quad (2.4.99)$$

One of the first and simplest methods of calculating tunneling in conventional TST is by using the semiclassical Wigner correction, which involves an expansion in $\hbar$ and is given by:[507]

$$\kappa^{\ddagger,\mathrm{W}}(T) = 1 + \frac{1}{24}|\hbar\omega^{\ddagger}\beta|^2 \quad (2.4.100)$$

where $\omega^{\ddagger}$ is the imaginary frequency at the transition state. This correction is very approximate since it represents truncating a power series in $\hbar$ after the first two terms; it should not be used when $\kappa^{\ddagger,\mathrm{W}}$ is $\tilde{>}$ 1.2. Furthermore, even then, it is only valid when the contributions due to tunneling come only from the transition state region and the potential around it can be well approximated by an inverted parabola. At the same time, the reaction path curvature has to be negligible.

A better approximation, even when the reaction path curvature is neglected, is to assume that the bound degrees of freedom follow the reaction coordinate adiabatically and we can treat tunneling along the reaction coordinate by calculating the probability of penetration through a 1D potential with an effective reduced mass. This assumption is equivalent to treating the reaction coordinate as a slow motion with respect to the bound degrees of freedom,[362,371,508] which is reasonable when reaction-coordinate motion corresponds to a threshold. Specifically, the potential along the reaction coordinate would be given by

$$V_{\mathrm{a}}(\mathbf{n},J,s) = V_{\mathrm{MEP}}(s) + E_{\mathrm{int}}^{\mathrm{GT}}(\mathbf{n},J,s) \quad (2.4.101)$$

where

$$E_{\mathrm{int}}^{\mathrm{GT}}(\mathbf{n},J,s) = E_{\mathrm{vib}}^{\mathrm{GT}}(\mathbf{n},s) + E_{\mathrm{rot}}^{\mathrm{GT}}(J,s) \quad (2.4.102)$$

A further approximation would be to assume that at low temperatures the system is in its ground state and so the potential governing the motion along the reaction coordinate is the ground-state vibrationally adiabatic potential, $V_{\mathrm{a}}^{G}(s)$,

which is given by eq 2.4.58. A justification for this ground-state approximation is postponed until Section 3.1. The ground-state transmission coefficient is given by the ratio of the thermally averaged ground-state quantal transmission probability $P^G(E)$ to the thermally averaged ground-state transmission probability evaluated with the assumption of classical reaction coordinate motion, $P_C^G(E)$:[401,491]

$$\kappa^{X/G}(T) = \frac{\int_0^\infty P^G(E)\exp(-\beta E)dE}{\int_0^\infty P_C^G(E)\exp(-\beta E)dE} \quad (2.4.103)$$

In the case of the CVT, the classical transmission probability is approximated by

$$P_C^G(E) = \Theta\{E - V_a^G[s_*^{CVT}(T)]\} \quad (2.4.104)$$

where $V_a^G(s)$ was defined in eq 2.4.58.

The transmission coefficient for the CVT thermal rate constant[400] is readily obtained by substituting eq 2.4.101 into eq 2.4.103, yielding

$$\kappa^{CVT/G}(T) = \beta\exp\{\beta V_a^G[s_*^{CVT}(T)]\}\int_0^\infty P^G(E)\exp(-\beta E)dE \quad (2.4.105)$$

For the ICVT and μVT the classical transmission probability is[383]

$$P_C^G(E) = \Theta\{E - V^{AG}\} \quad (2.4.106)$$

where V^{AG} is the maximum of the ground-state vibrationally adiabatic potential, and the substitution into eq 2.4.103 yields, for instance, for μVT, the following transmission coefficients:

$$\kappa^{\mu VT/G}(T) = \kappa^{CVT/G}(T)\frac{\exp\{\beta V_a^G[s_*^{CVT}(T)]\}}{\exp(-\beta V^{AG})} \quad (2.4.107)$$

The ratio in the above equation accounts for the different thresholds in ICVT and μVT as compared to CVT.

In practical work, the transmission probability is evaluated semiclassically, which is known to yield results within ~15% of the accurate quantal values.[400,509,510] The theory takes its simplest form when the curvature of the reaction path is small[390,511] because under that condition it is a good approximation to assume that motion is vibrationally adiabatic along the entire tunneling path. Then the effective barrier for ground-state tunneling is given by $V_a^G(s)$, the maximum value of which is called V_a^{AG} or V^{AG}. The semiclassical probability for energies below V^{AG} is given by

$$P^{SAG}(E) = \{1 + \exp[2\theta(E)]\}^{-1} \quad (2.4.108)$$

where $\theta(E)$ is the imaginary-action integral

$$\theta(E) = \hbar^{-1}\int_{s_<}^{s_>}\{2\mu[V_a^G(s) - E]\}^{1/2}ds \quad (2.4.109)$$

which is 2π times the magnitude of the imaginary action integral between the classical turning points $s_<$ (reactants side) and $s_>$ (products side) of the effective potential.

To carry out the Boltzmann average, one also needs to evaluate the tunneling probability at energies $E > V^{AG}$ to incorporate nonclassical reflection. If the potential V_a^G is assumed parabolic around its maximum, the semiclassical probability can be approximated for energies above but near V^{AG} by[512]

$$P^{SAG}(V^{AG} + \Delta E) \cong 1 - P^{SAG}(V^{AG} - \Delta E) \quad (2.4.110)$$

where $\Delta E = E - V^{AG}$. The presence of the Boltzmann factor in eq 2.4.103 allows one to use eq 2.4.110 well above the barrier, and therefore the semiclassical probability in the whole range of energies is given by

$$P^{SAG}(E) = \begin{cases} 0, & E < E_0 \\ \{1 + \exp[2\theta(E)]\}^{-1} & E_0 \le E \le V^{AG} \\ 1 - P^{SAG}(2V^{AG} - E) & V^{AG} \le E \le 2V^{AG} - E_0 \\ 1, & 2V^{AG} - E_0 < E \end{cases} \quad (2.4.111)$$

where

$$E_0 = \max\begin{cases} V_a^G(s = -\infty) \\ V_a^G(s = +\infty) \end{cases} \quad (2.4.112)$$

When the transmission coefficient is calculated along the MEP with eq 2.4.103 and the probabilities of eq 2.4.111, but in absence of reaction path curvature, the result[400] is called the zero-curvature tunneling (ZCT) transmission coefficient.

A more accurate way of treating tunneling is to include the reaction-path curvature, which is physically meaningful if computed in an isoinertial coordinate system such as used in this review. Let $\mathbf{x}(s)$ denote the geometry in isoinertial coordinates at a point that is located at a distance s along the MEP. The curvature vector $\kappa(s)$ of the reaction path at this geometry is given by the second derivative of the geometry $\mathbf{x}(s)$ with respect to s, i.e.,

$$\kappa(s) = d^2\mathbf{x}/ds^2 \quad (2.4.113)$$

The reaction path curvature may be calculated by formulas given elsewhere.[387,390] For a bimolecular reaction of the type A + BC → AB + C, where A, B, and C may be atoms or groups of atoms, we define the skew angle as the angle between the A-to-BC vector and the C-to-AB vector. This angle (in isoinertial coordinates) is given by

$$\beta = \cos^{-1}\sqrt{\frac{m_A m_C}{(m_A + m_B)(m_C + m_B)}} \quad (2.4.114)$$

The skew angle is related to the reaction-path curvature by[185]

$$\left[\int_{-\infty}^{+\infty}\kappa(s)ds\right]\cdot\frac{d\mathbf{x}^R}{ds} = \left(\frac{d\mathbf{x}^P}{ds} - \frac{d\mathbf{x}^R}{ds}\right)\cdot\frac{d\mathbf{x}^R}{ds} = -(1 + \cos\beta) \quad (2.4.115)$$

where $\mathbf{x}^R$ and $\mathbf{x}^P$ are the geometries in the reactant and product valleys, respectively.

From eq 2.4.114, it is clear that the skew angle lies in the range $0 < \beta < \pi/2$, and thus the absolute value of eq 2.4.115 is between one and two. Thus, small skew angles and therefore large curvature occur when m_B is much smaller than m_A and m_C. Marcus and Coltrin[513] optimized the tunneling path for a collinear atom−diatom reaction semiclassically and found that reaction path curvature leads to a negative centrifugal effect, i.e., the particle "cuts the corner" and moves toward the inside of the MEP. This motion

shortens the tunneling paths thereby increasing the tunneling probability.

If the curvature is small, it is possible to treat this effect of the reaction path curvature by using an effective mass for the reaction-path motion. Specifically, this effective mass is a function of the reaction path curvature.[360,511,514] The final version of this approach[401,402,515] is called the small-curvature tunneling (SCT) approximation, and the effective mass is given by

$$\mu(s) = \mu \prod_{m=1}^{F-1} \min\begin{cases} \exp\{-2\bar{a}(s) - [\bar{a}(s)]^2 + (\mathrm{d}\bar{t}/\mathrm{d}s)^2\} \\ 1 \end{cases} \tag{2.4.116}$$

where $\bar{t}(s)$ is a suitably averaged value of the mass-scaled normal coordinate u_m at the zero-point-energy turning point of mode m on the concave side of the MEP, and $\bar{a}(s)$ is a suitably averaged value of

$$a_m(s) = -\kappa_m(s) t_m(s) \tag{2.4.117}$$

where $\kappa_m(s)$ is the component of the reaction-path curvature vector $\kappa(s)$ in the direction of mode m. Note that the corner cutting due to the negative centrifugal effect raises the tunneling probability, contrary to earlier[516] assumptions. This is because the path is shortened but not enough to raise the effective potential for tunneling. If one cuts the corner in any mode by more than the distance to the vibrational turning point, this would not be true.

The SCT approximation breaks down when the reaction path curvature is large, and corner cutting is so severe as to raise the effective potential or cause the breakdown of the $s,u1,u2,...$ coordinate system. When corner cutting is severe the SCT approximation can seriously underestimate the tunneling probability. The large curvature tunneling (LCT) methods[383,401,402,517−524] were developed to evaluate transmission factors for these types of reactions. In these methods, a series of tunneling energies E_{tun} are considered with values less than or equal to V^{AG}. During the approach stage of a given collision, the reactants are treated as if they proceed vibrationally adiabatically. This is not correct if one is concerned with state-to-state reactivity, but it does not cause significant error in the cumulative reaction probability. This vibrationally adiabatic treatment is applied along the MEP in the exoergic direction until the tunneling energy matches the vibrationally adiabatic potential curve, that is,

$$V_{\mathrm{a}}^{G}(\tilde{s}_0) = E_{\mathrm{tun}} \tag{2.4.118}$$

where $\tilde{s}_0 < 0$ is the classical turning points of the reaction-coordinate motion on the reactant side. In the next stage of the collisions tunneling is assumed to occur, without assuming vibrational adiabaticity, along the reaction path and along straight-line paths that connect the reactants valley turning point to a products valley turning point. Specifically, the linear paths connect the point $\tilde{s}_0$ on the reactant side to a point ($\tilde{s}_1 > 0$) with an identical value of eq 2.4.118 on the product side.

The primitive tunneling amplitude $T_{\mathrm{tun}}(\tilde{s}_0)$ along the straight tunneling path initiating at $\tilde{s}_0$ is approximated semiclassically as

$$T_{\mathrm{tun}}(\tilde{s}_0) = \exp[-\theta(\tilde{s}_0)] \tag{2.4.119}$$

in which $\theta(\tilde{s}_0)$ is the 1D imaginary action integral along the path and is given by an imaginary action integral over the straight-line path. The integral is divided into three parts that correspond to three different regions along the straight tunneling path. Region I corresponds to an adiabatic region where the information needed to evaluate the imaginary action integral can be extrapolated from information along the MEP in the reactant valley, Region III is similarly related to the product valley. Region II corresponds to a nonadiabatic region and the contributions to the imaginary-action integral from this region are calculated from the actual potential at a point on the tunneling path (without any quadratic potential approximation) and from correction potentials V_{corr} that take into account the zero-point energy of the modes that are still within their turning points at the boundaries of Region II. Version 4 of the LCT method, also called the LCG4 method,[402,523] uses more stringent requirements than version 3 (also called LCG3) for a point to be considered in the vibrationally adiabatic region. The LCG4 transmission factors are always smaller than or equal to the LCG3 transmission factors. Although the LCG4 method is currently recommended as the default large-curvature tunneling method, it is not always more accurate than LCG3.[525]

The final result includes tunneling into a set of states in which a vibrationally diabatic mode of the products is excited,[401,402] and the tunneling probability is appropriately uniformized.[401,402,521]

Figure 4 shows the different kinds of tunneling paths to illustrate the above discussion.

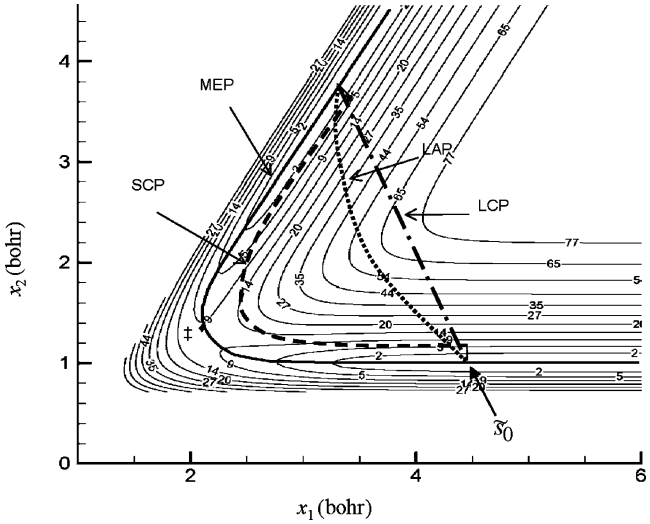

Figure 4. Contour plot of a model bimolecular reaction that indicates the possible tunneling paths at a given tunneling energy as discussed in Section 2.4.4. MEP is the minimum-energy path, SCP is a schematic small-curvature tunneling path (actually, the SCT approximation does not correspond to a uniquely defined path), LCP is a large-curvature tunneling path, and LAP is a least-imaginary-action path.

Liu et al.[522] applied the LCG3 method to the $CF_3 + CD_3H \rightarrow CF_3H + CD_3$ and $CF_3 + CD_3H \rightarrow CF_3D + CD_2H$ reactions. (A later study with a more accurate potential function found less tunneling for this reaction.[524]) They found that for these systems the reaction occurs mainly through large-curvature tunneling paths with a small contribution (around 1%) of tunneling into vibrationally excited states of the products. It is interesting to notice that for evaluating kinetic isotope effects the representative tunneling path (the dominant path at the energy at which the integrand of the numerator of eq 2.4.103 has a maximum) may be close to a large-curvature tunneling path when the hydrogen is trans-

ferred but to a small-curvature tunneling path when the transferred atom is deuterium. Furthermore, even for a given isotope, the type of tunneling path that gives the most tunneling may depend on energy. To take account of this possibility a new approximation for the transmission factor, called microcanonical optimized multidimensional tunneling or μOMT, was introduced.[522] This transmission factor is obtained at every energy by taking the maximum of the SCT and LCT tunneling probabilities, i.e.,

$$P^{\mu\mathrm{OMT}}(E) = \max\begin{cases} P^{\mathrm{LCT}}(E) \\ P^{\mathrm{SCT}}(E) \end{cases} \qquad (2.4.120)$$

In principle the "most accurate" transmission factor would be obtained, at every energy, by finding the path that minimizes the imaginary action integral.[518] This least-action path would be a compromise between the energetically most favorable path along the MEP and the energetically less favorable but shortest path, which is included in the LCT calculations. The evaluation of the least-action path involves a search that can be computationally expensive. The μOMT transmission factors are less computationally intensive, and it has been shown by an extensive comparison with accurate quantum chemical thermal rate constant calculations for atom−diatom reactions[526] that they are accurate enough for almost all practical work, although a recent study[525] showed that sometimes the full least-action method is more accurate.

Recently, it has been possible to extend these tests of the μOMT tunneling approximation to reactions of larger molecules by comparing to calculations[52,527,528] that provide numerically converged quantum dynamical rate constants for a given potential energy surface. The μOMT results are in excellent agreement with the quantum ones for $H + CH_4 \rightarrow H_2 + CH_3$, which has a skew angle of $\beta = 47$ deg and is dominated by small-curvature tunneling,[529,530] and in good agreement for $O + CH_4$, which has $\beta = 20$ deg and for which tunneling is better taken into account by the large-curvature approximation.[531]

A tunneling mechanism not included in the above discussions is tunneling enhanced by resonances below the quasiclassical threshold energy; this subject has received considerable recent attention.[532−542]

Next we turn attention to the factor $g(T)$ in eq 2.4.93. In TST it is assumed that the observed one-way rate constants should be well approximated by the one-way rate constants corresponding to internal states of reactants being at equilibrium. By Liouville's theorem, if reactants have an equilibrium distribution then this distribution should evolve to an equilibrium distribution in other parts of the phase space,[543] such as, for instance, the transition state, and the "quasiequilibrium assumption" of the TST holds. Actually, for gas-phase bimolecular reactions the TST provides an upper bound to the observed rate constant if collisions are efficient enough to maintain the thermal distribution of reactants. A quantitative estimate of the effect of internal-state (rotational and vibrational) nonequilibrium on the rate constants for the fast, bimolecular, reversible hydrogen-transfer reaction

$$Cl + HBr \rightleftarrows ClH + Br$$

was carried out by Lim and Truhlar.[544] Those authors found out that nonequilibrium effects for this reaction are negligible when product concentrations are negligible. This conforms to the usual assumption, but it does not exclude the possibility that nonequilibrium effects could be more important for other possible assumptions about the state-to-state reaction probabilities and energy transfer probabilities. Nevertheless, it is reasonable to assume that the local equilibrium of reactants is maintained for the case of simple barrier reactions that do not proceed on every collision.

In analyzing experimental data, some workers set the experimental rate constant equal to eq 2.4.35 without a transmission coefficient. This produces a phenomenological free energy of activation with two kinds of contributions: the quasithermodynamic contribution of eq 2.4.35 and another contribution called nonsubstantial.[382,489,545] The quasithermodynamic part is related to partition functions by quasithermodynamic generalizations of the equations for chemical substances and, as may be derived from the quasiclassical analogues of eqs 2.4.34−2.4.36, it may be written

$$\Delta G^{\ddagger}_{\mathrm{sub}}(T) = V_{\mathrm{MEP}}(s_*^{\mathrm{CVT}}) - RT\,ln\,\frac{Q^{\mathrm{CVT}}(T)}{\Phi^{\mathrm{R}}(T)K^{\ddagger,\mathrm{o}}} \qquad (2.4.121)$$

where the nonsubstantial part may be written

$$\Delta G^{\ddagger}_{\mathrm{nonsub}}(T) = -RT\,ln\,\gamma(T) \qquad (2.4.122)$$

2.4.5. Improvements in VTST Methodology

In this section, we consider two kinds of improvements:[402] (1) more general dividing surfaces based on curvilinear coordinates or optimizing the orientation of the dividing surface, and (2) interpolation schemes that improve the computational efficiency of the method.

In Section 2.4.2, we assumed a planar (hyperplanar) dividing surface, but in many respects this is unsatisfactory. First of all, a hyperplane in coordinate space does not always separate reactants from products, even if it intersects the MEP at a right angle. This usually does not cause a problem though if we use physically correct models for partition functions, such as the harmonic oscillator model or the Morse model.[365,429]

A more serious problem is the nonphysical nature of the vibrational frequencies for planar dividing surfaces.[546] This can be circumvented by using curvilinear coordinates defined in terms of valence coordinates (bond stretches, bends, and torsions) to define the dividing surface.[465,546−549] This yields more physical harmonic frequencies and is therefore often more important than including anharmonicity. Recently, in a very significant advance, a procedure has been developed for also including anharmonicity when using such curvilinear coordinates.[465]

A third problem when using curvilinear reaction coordinates (and hence curved dividing surfaces) is that equations such as 2.4.25, 2.4.28, 2.4.31, 2.4.34, and 2.4.35 are no longer strictly valid. One must also include a Jacobian factor to account for the curved nature of the dividing surface.[378−381] For dividing surfaces defined in terms of valence coordinates, the factor is reasonably close to unity.[378,381]

VTST is much less time-consuming than trajectory calculations, and, when tunneling is included, it is usually more accurate. However, VTST calculations (like trajectory calculations) can still be expensive if the system under study is big, since VTST requires the evaluation of gradients and Hessians at more than just stationary points (whereas trajectory calculations require extensive sampling of initial

conditions and long time integrations). Several techniques have been developed in the past few years to reduce the number of electronic structure calculations needed for VTST and tunneling calculations without loss of accuracy.

One technique involves the reorientation of the dividing surface (RODS) to maximize the free energy at each calculated point. The RODS algorithm[388] considers trial dividing surfaces that are hyperplanes in **x** and that pass through a point on a reaction path, which need not be a converged MEP. The orientation of the dividing surface (with normal vector $\hat{\mathbf{n}}$) is optimized to maximize the free energy of the generalized transition state at a given point along the MEP. The standard-state optimized generalized free energy (corresponding to optimized generalized transition state theory or OGT) value is given by

$$G^{\mathrm{OGT},0}(T) = \max_{\hat{\mathbf{n}}} G^{\mathrm{GT},0}(T,\hat{\mathbf{n}}) \qquad (2.4.123)$$

This algorithm can be combined with the traditional Euler steepest-descent algorithm to calculate accurate and computationally efficient VTST rate constants using large step sizes.[389] Although in principle this algorithm should give more accurate results because of the greater degree of optimization of the dividing surface, the main effect is actually to eliminate instabilities in the calculated reaction path and generalized normal-mode frequencies and to allow efficient calculations with larger step sizes. At low temperatures this procedure leads to rate constants converged to ~15% with a step size of around 0.05 a_0, whereas at high temperatures a step size of around 0.15 a_0 is enough to get rate constants with the same degree of precision as the full calculation.

Another possibility is to use an interpolating function over a given number of points along the MEP. One approach, called interpolated variational transition state theory by mapping (IVTST-M),[550] interpolates the potential $V_{\mathrm{MEP}}(s)$, the determinant $|\mathrm{I}(s)|$ of the moment of inertia tensor, the frequencies $\omega_m(s)$, and the curvature components $B_{m,F}(s)$ not as functions of s but as functions of z, where z is a new variable that always has a finite value (in a bimolecular reaction s has infinite values ($-\infty$ and $+\infty$) at the reactants and the products). The parameter z is determined as

$$z = \frac{2}{\pi}\arctan\left(\frac{s - s_0}{L}\right) \qquad (2.4.124)$$

with s_0 and L being two parameters obtained from the forward and reverse barrier heights. The new $V_{\mathrm{MEP}}(z)$, $|\mathrm{I}(z)|$, $\omega_m(z)$, and $B_{m,F}(z)$ functions are interpolated by using splines under tension.

Instead of using functions to interpolate the calculated electronic structure points it may be better to interpolate them with a MEP obtained from low-level electronic structure calculations. One method based on this dual-level approach is variational transition state theory with interpolated corrections (VTST-IC).[551−554] In this method, correction procedures are applied to the calculated energy, frequencies, and moment-of-inertia determinant along the MEP. The corrections are calibrated such that the corrected results match the accurate values at those selected points, and they correspond to interpolating these corrections at other points. When the corrections involve data from higher-level optimizations of the stationary points, the method is called VTST-IOC,[554] a special case of VTST with interpolated corrections. This method is based on the correction at three points, in particular, the saddle point and two stationary points, one on each side of the MEP. If corrections were made at nonstationary points, they would be based on reaction paths calculated at the higher level. The interpolated optimized energies (IOE) approach is a particular case of IOC in which only the energies and moment-of-inertia determinants are corrected, but the corrected energies are based on geometries optimized at the higher level. Finally, if the correction is based on single-point energies using higher-level electronic structure calculations, the method is called VTST-ISPE (VTST with interpolated single-point energies). González-García et al.[555] used the ISPE dual-level methodology to study the dimethyl sulfoxide reaction with OH. This important reaction in atmospheric chemistry has three possible products. The global rate was obtained by applying the CCUS theory.[413] The CUS theory[383,494,556,557] was employed to calculate the thermal rate constants for individual reactions because the free energy profile shows several dynamic bottlenecks.

Of all the methods that allow greater efficiency, probably the most promising is the MCMM method[210,214,241] described in Section 2.3, because it accurately reproduces the stationary points, it can be used with large steps, and it can be improved by adding more points to the MEP until one obtains convergence in the calculated thermal rate.

It is also possible to use interpolation methods to evaluate the large curvature transmission factors. In computer time, the most expensive part of the evaluation of this kind of transmission factor is the calculation of energies in the nonadiabatic region, because single-point energy calculations are needed to evaluate the imaginary action integral. The computer time can be reduced by using a spline under tension to interpolate the linear path within the nonadiabatic region. This algorithm is called interpolated large curvature tunneling in one dimension (ILCT1D).[558] Tests carried out on five bimolecular reactions indicated that the ILCT1D algorithm reduces the evaluations of the LCT transmission factors by about five times, with results similar to the full calculations. An even less expensive algorithm (in computer time) involves using 2D interpolation to interpolate not only along the linear path variable ξ, but also along different tunneling energies. The calculated points are interpolated by a 2D spline under tension. This method[524] is called ILCT2D. It has been tested for several CF3 + hydrocarbon reactions and is about 30 times faster than the full LCT algorithm and about 5 times faster than the ILCT1D method with an average deviation from the full LCT results of less than 1%.

2.4.6. Reduced-Dimensionality Theory

Variational transition state theory may be derived by assuming that vibrations transverse to the reaction coordinate are adiabatic,[365,429,559] although it is not necessary to assume vibrational adiabaticity to derive VTST. Hofacker was the first to make a detailed study of the vibrational adiabaticity and nonadiabaticity of the modes transverse to a reaction coordinate;[560] Wu and Marcus continued this work.[561] Since then the concept has been widely invoked. Assuming a quantitative requirement for zero point energy of stretch[562,563] and bend[563] vibrations can be quite accurate in the threshold region that controls thermal bimolecular rate constants. However, stretch vibrations are only approximately adiabatic in a global sense, even when the reaction appears to be vibrationally adiabatic in terms of initial and final states[516,563,564]

and bending vibrations are more complicated; the latter show propensities (but not strict selection rules) to couple to selected asymptotic rotational quantum numbers.[516,565−567]

Based in part on their success in transition state theory, vibrational adiabaticity and the separable rotation approximation are sometimes used to reduce the dimensionality in non-TST calculations. Several combinations of these and other approximations, including also sudden approximations, that reduce the dimensionality of reactive collisions have been developed.[46,213,231,234,237,245,257,568−599] Clary and co-workers have developed general reduced-dimensionality methods for atom−molecule reactions that treat the dynamics in 2 or 3 active degrees of freedom and assume vibrational adiabaticity with no curvature coupling to the active degrees for the other degrees of freedom.[213,231,234,245,257,591,592,594,597,599] Although it is an advantage to use full quantum mechanics rather than semiclassical approximations in the active degrees of freedom, the neglect of curvature coupling in all but a few degrees of freedom may make the tunneling calculations less accurate than the SCT and LCT approximations, with which direct dynamics calculations have been applied to systems of similar size as those in the reduced-dimensionality calculations and also to larger systems (see Section 2.4.7). A convenient advantage of VTST/MT over reduced-dimensionality approximations is that the same formalism can be applied to different kinds of reactions, e.g., both H + C_2H_4 → C_2H_5 and H + C_2H_6 → H_2 + C_2H_5. Nevertheless, the reduced-dimensionality method of Clary and co-workers is a major advance in systematic methodology for dimensionality reduction, and it can also be applied to certain state-selected processes.

2.4.7. Direct Dynamics Calculations

Direct dynamics with VTST/MT has now become a widely used method for calculating rate constants of bimolecular reactions in the gas phase without dimensionality reduction. Although the present review is mainly concerned with methodology, and not with complete lists of applications, Table 4 provides some prototype examples[162,164,210,214,235,522,523,549,551,600−650] of applications of VTST/MT to reactions with rate-limiting potential energy barriers.

2.4.8. Fully Quantal Calculations

In addition to the approximate calculations discussed so far, one may also calculate rate constants by converged quantum mechanical scattering theory or converged quantum statistical mechanics.[44,45,48] These results are exact within some numerical tolerance for a given PES, although usually only for total angular momentum equal to zero; contributions to the rate constant from higher total angular momenta can be obtained by the separable rotation approximation.[651] So far such calculations have been limited to systems with six or less atoms. We especially call attention to prototype calculations for H + H_2 → H_2 + H,[53,652−654] D + H_2 → DH + H,[655,656] Cl + H_2 → HCl + H,[657] O + HD → OH + D and OD + H,[658] OH + H_2 → H_2O + H,[57,659−661] H + CH_4 → H_2 + CH_3,[662,663] and O + CH_4 → OH + CH_3.[664]

Even with modern computer capabilities, direct calculation of enough state-selected reaction probabilities or rate constants to compute a thermal rate constant by Boltzmann averaging over reactant states is very expensive for four or more atoms, especially with two or more nonhydrogen atoms, as illustrated in a recent paper on the OH + CO → H + CO_2 reaction.[665] Therefore, the calculation of rate constants from the cumulative reaction probability or the flux autocorrelation functions is preferred for larger systems.[54,56,57,659,662−664,666−671]

The time correlation function approach is well suited not only to gas-phase reactions[54−57,652,654,655,658,666−671] but also

Table 4. Prototype Applications of VTST/MT to Gas-Phase Bimolecular Reactions

MT method	reaction	ref
ZCT	OH + CH_3CH_2F → CH_3CHF + H_2O	603
SCT	H + $SiCl_4$ → $SiCl_3$ +HCl	622
	H + C_2H_4 → C_2H_5	612
	H + $C_2H_5SiH_2$ → C_2H_5SiH + H	633
	H + NF_3 → NF_2 + HF	616
	H + $(CH_3)_3GeH$ → $(CH_3)_2Ge$ + H_2	626
	H + $(CH_3)_3GeD$ → $(CH_3)_2Ge$ + HD	625
	H + $(CH_3CH_2)_2SiH_2$ → $(CH_3CH_2)_2SiH$ + H_2	636
	O + CH_3CHF_2 → CH_3CF_2 + OH	638
	Cl + CH_3Cl → CH_2Cl + HCl	647
	Cl + C_2H_5Cl → CH_3CHCl + H′Cl	649
	Cl^- + CH_3→ $ClCH_3$ + Cl′$^-$	164
	Cl^- + CH_3Br → $ClCH_3$ + Br^-	600
	OH + HCl → C_1 + H_2O	602
	OH + D_2O → OD + HDO	610
	OH + CD_4 → CD_3 + HDO	628
	OH + $^{13}CH_4$ → $^{13}CH_3$ + H_2O	642
	OH + CH_3Cl → CH_2Cl + H_2O	647
	OH + CH_3SH → CH_3S + H_2O	631
	OH + CH_3OCl → CH_2OCl + H_2O	644
	OH + $CH_3C(O)CH_3$ → $(CH_3)_2C(O)OH$	627
	OH + $(CH_3)_2SiH_2$ → $(CH_3)_2SiH$ + H_2O	645
	OH + $HOCH_2C(O)H$ → $HOCH_2CO$ + H_2O	640, 643
	OH + (*cyclo*-C_3H_5)$CH(CH_3)_2$ → (*cyclo*-C_3H_5)$C(CH_3)_2$ + H_2O	648
	HF + H_2SiLiF → H_3SiF + LiF	646
	C_2H + H_2 → H + C_2H_2	614
	NO_2 + CH_2O → CHO + HONO	629
	CH_3 + H_2 → H + CH_4	162
	CH_3 + CH_2O → CHO + CH_4	635
	CH_3 + $(CH_3)2O$ → CH_3OCH_2 + CH_4	630
	CH_3 + C_2H_5OH → CH_3CHOH + CH_4	639
	$CH_3Cl(H_2O)$ + $NH_3(H_2O)$ → $(CH_3NH_3^+)(Cl^-)(H_2O)_2$	605
	C_6H_5 + $(CH_3)_2CO$ → $CH_3C(O)CH_2$ + C_6H_6	632
OMT	H + H_2S → HS + H_2	615
	H + CH_4 → CH_3 + H_2	624
	H + CH_3OH → CH_2OH + H_2	611
	H + N2H_4 → H_2NNH + H_2	549
	O + CD4 → CD_3 + OD	607
	F + CH_4 → CH_3 + HF	641[a]
	Cl + $^{13}CH_4$ → $^{13}CH_3$ + HCl	606
	Cl + C_2H_6 → C_2H_5 + HCl	403
	OH + H_2 → H + H_2O	623[a]
	OH + NH_3 → NH_2 + H_2O	601
	OH + CH_3F → CH_2F + H_2O	608
	OH + CH_2F2 → CHF_2 + H_2O	621
	OH + CF_3CH_3 → CF_3CH_2 + H_2O	618
	OH + C_3H_8 → $(CH_3)_2CH$ + H_2O	212
	OH + CHF_3 → CF_3 + H_2O	619
	OH + C_8H_{18} → C_8H_{17} + H_2O	613
	HBr + HCCH → H_2CCHBr	604
	C_2H + H_2 → C_2H_2 + H	614
	CH_2Cl + CH_3F → CH_2F + CH_3Cl	210
	FO−(H_2O) + C_2H_5Cl → C_2H_4 + HOF(H_2O) + Cl^-	609
	CF_3 + CD_3H → CD_3 + CHF_3	522, 524, 551
	CF_3 + C_2H_6 → C_2H_5 + CHF_3	524
	CF_3 + C_3H_8 → $(CH_3)_2CH$ + CHF_3	524
	C_2H_4 + C_4H_6 → C_6H_{10}	620
	N_2O_5 + H_2O → $2HNO_3$	634
	OH + CHF_3 → CF_3 + H_2O	650

[a] See also an SCT calculation in ref 23.

to condensed-phase dynamics,[308,672−694] as discussed in Section 4.1.

As discussed in Section 2.4.4, for H + CH_4 and O + CH_4, VTST/MT calculations are in good agreement with converged quantal ones where the same PES is used.[529−530,664]

2.5. Bimolecular Reactions over Potential Wells

Bimolecular reactions come in a number of different varieties, as illustrated in Figure 5. The simplest case is

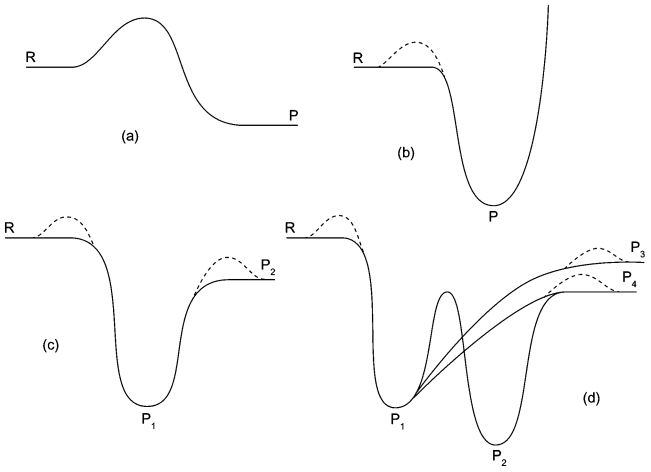

Figure 5. Different types of bimolecular reactions. R denotes reactants; P denotes products.

shown in Figure 5a, where only a simple barrier separates a set of bimolecular products from a set of bimolecular reactants. For such reactions, which have been the sole subject of our discussion up to this point, the rate coefficient is a strong function of the temperature but does not depend on the pressure. However, a common occurrence is that one or more potential wells lie along the reaction path, and this introduces a number of complications in the theoretical analysis. In the presence of a well the reactants can form a long-lived collision complex, which can survive long enough to suffer a number of collisions before it decomposes back into reactants or into products, perhaps resulting instead in stabilization of the complex in the well. The simplest such situation is shown in Figure 5b, where the complex has only the options of reforming reactants or being stabilized. Simple models for the association rate were discussed in Section 2.2.2 of this review, but such reactions are normally treated as the reverse reactions of unimolecular decompositions. For these and more complex reactions, the rate coefficient is a function of both temperature and pressure (or temperature and number density).

The next level of complication involves adding a bimolecular product channel to the association reaction just described, shown in Figure 5c. In this case the collision complex can have one of three fates: stabilization, dissociation back to reactants, or dissociation to bimolecular products. Recently studied examples with reaction profiles of the form of Figure 5c are F^- + $(CH_3)_2SO$[695] and O + OH[696,697] for the case without potential energy barriers and SiH_2 + HCl[698] for the case with barriers. The most general case one can imagine is illustrated in Figure 5d; it includes the possibility of the complex isomerizing to another complex (perhaps multiple times) before it is stabilized or it decomposes, either back to reactants or to one of several sets of bimolecular products. Each intermediate isomer and each bimolecular reactant or product is called an arrangement or a configuration, and each interconversion between two arrangements is called an elementary step. This is the case we want to consider in this section. A recently studied reaction with an energy profile like Figure 1d is H + SO_2.[699] The number of possible arrangements increases rapidly with the total number of atoms, but even a five-atom system like HCO + NO[700] can have an energy diagram much more complicated than Figure 5a. Reactions with both a barrier and wells (intermediates) are particularly interesting,[171] and they may show multimodal lifetime distributions and other manifestations of nonstatistical behavior,[701] but in this section we focus first on barrierless reactions.

2.5.1. RRKM Assumption

The first step to treating a multiple-well, multiple-arrangement reaction theoretically is to treat the component elementary steps individually. Transition-state theory is used to calculate the rate coefficients for these steps. This must be done at the microcanonical or microcanonical/*J*-resolved level, where *J* is the total angular momentum quantum number. A microcanonical/*J*-resolved ensemble takes explicit account of the dependence of reaction rates on total energy or total energy and total angular momentum. These transformations from one arrangement to another are, broadly speaking, of two types: those where there is an "intrinsic" barrier between the configurations and those where there is not; both possibilities are indicated in the diagrams of Figure 5. By the term intrinsic barrier, we mean a potential energy barrier in the exoergic direction. For isomerizations that have a barrier and for fragmentation of a complex to a radical plus a molecule in which the reverse association has a barrier, the transition-state theory methods discussed above can be used directly. For fragmentation to a pair of radicals in which the reverse association has no barrier, special methods are required. We describe these methods below. But first we consider the basic assumption that holds the multiple-well, multiple arrangement theory together.

The fundamental idea that underlies this theory is known as the RRKM assumption or the strong-coupling approximation. This is an assumption about the nature of the dynamics of the collision complexes while they are in the well regions of the potential. It is most easily described and understood from a classical (rather than quantum) perspective, although it may be more valid in a quantum-mechanical system than in a classical one. The RRKM assumption says that the degrees of freedom of a highly excited, isolated molecule or collision complex are so strongly coupled that, no matter how localized in phase space an ensemble of such complexes is prepared, the ensemble will evolve to fill the entire phase space available to it *uniformly* (consistent with conservation of energy and angular momentum) on a time scale much smaller than the characteristic time for reaction (i.e., for an elementary step). Each step thus takes place exclusively from a microcanonical/fixed-*J* ensemble (frequently approximated simply by a microcanonical ensemble). This is illustrated schematically in Figure 6. The isolated pockets of complexes on the left of the figure might correspond to depositing energy in a particular bond or normal mode of the molecule, or they might correspond to isolating the complexes near a transition-state dividing surface through which they were formed. The subsequent trajectories of the complexes are

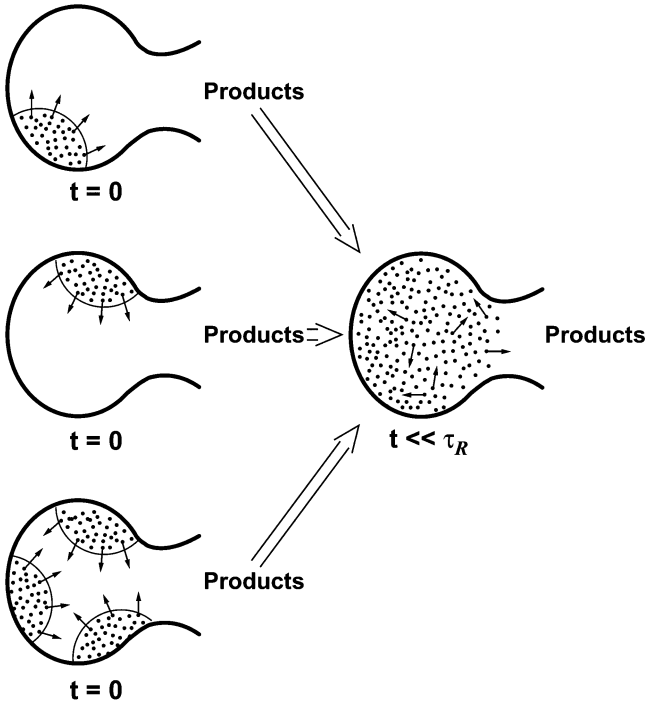

Figure 6. Schematic diagram illustrating RRKM dynamics in phase space. The time τ_R is the characteristic time for reaction to occur.

"chaotic," with the ensemble rapidly becoming uniform in the accessible phase space of a given well.

The RRKM assumption is that the reactant of each elementary step is in microcanonical equilibrium; therefore, the same reaction rates result no matter how energy is deposited in a molecule (or complex). It is thus possible to define universally applicable elementary rate coefficients $k(E,J)$, or $k(E)$, and to bypass the problem of computing the intramolecular dynamics of the complexes entirely. This is an enormous simplification. A consequence of the approximation is that an ensemble of complexes will have an exponential lifetime distribution with a $1/e$ decay time (or lifetime) of $1/k(E,J)$. The classical dynamical implications of RRKM and non-RRKM behavior have been discussed at some length by Bunker and Hase[702] and Hase,[703,704] who pay particular attention to the effects of non-RRKM behavior on lifetime distributions.

The RRKM assumption is generally very good and is expected to get better as the depth of the potential well over which the motion takes place increases. A noteworthy example of the failure of the RRKM assumption is the reaction $H + O_2 \rightleftarrows OH + O$, where the high-frequency O−H vibration does not couple very strongly to the low-frequency O−O motion in the HO_2^* complex.[705,706] However, such failures are likely to be limited to three- or four-atom systems with similar frequency mismatches. Even a methyl group often provides enough anharmonicity to promote efficient intramolecular energy transfer. However, there also appear to be occasional failures of RRKM theory in dissociations of larger molecules such as CF_3CH_3,[707] the chemically activated dissociation of acetone cation,[708] and the conformational isomerization of cyclohexanones[709] and of a dipeptide.[710] In any case, we assume that such failures are the exception rather than the rule.

The combination of the RRKM assumption and transition-state theory is frequently termed RRKM theory.

2.5.2. Variational Transition State Theory for Barrierless Addition Reactions

The absence of a potential energy barrier for the initial association step of a radical−radical or ion−molecule reaction presents certain complications in the application of transition state theory. First, a variational implementation of transition state theory is essential due to the wide variation in the location of the dynamical bottleneck with temperature. Furthermore, a number of the modes transform from free rotations to hindered rotations to librations and eventually to rigid bending vibrations as the system passes through the transition state region, and this phenomenon is typically associated with large vibrational anharmonicity and vibrational Coriolis coupling. Although for a few reactions, such as $CH_3 + H$, decoupled 1D treatments have proven effective,[711] in other instances, decoupled rigid-rotor harmonic-oscillator treatments (as presented in Section 2.4.2) are highly inaccurate.[712] Thus, in general, an accurate treatment of the anharmonicities and the couplings between the various modes, including the reaction coordinate and overall rotation, is a prerequisite for reliable predictions.

The absence of a barrier also makes some simplifications possible. For example, quantum tunneling effects are usually not important for calculating the thermal rate constant. Also, in the transition-state region the two reacting fragments are often interacting only weakly. As a result, an approximate separation of modes into the "conserved" modes, corresponding to the vibrational modes of the fragments, and the remaining modes called "transitional" modes, corresponding to the relative and overall rotational modes, can be used to simplify the analysis. The reaction coordinate, corresponding to the relative translational motion of the fragments (i.e., the interfragment separation) is either considered separately or as part of the transitional modes. (As usual, the overall translational modes are ignored since they factor out of the problem.)

This approximate separation of modes is particularly valuable in allowing for a classical treatment of the transitional modes, while maintaining a quantum treatment of the conserved modes. A quantum treatment of the latter modes is essential due to their generally quite high vibrational frequencies. In contrast, the low-frequency nature of the transitional modes implies that treating them purely classically is acceptable.[713] Importantly, the classical treatment of the transitional modes facilitates the treatment of their anharmonicities and mode−mode couplings via phase-space integral descriptions of the partition functions.[714]

At the canonical level, this assumed separation allows one to evaluate the transition state partition function as the product of the conserved mode and transitional mode partition functions:

$$Q^{\ddagger}(T) = Q^{\ddagger}_{\text{conserved}}(T) Q^{\ddagger}_{\text{transitional}}(T) \qquad (2.5.1)$$

In eq 2.5.1, the double dagger superscript denotes evaluation at the variational transition state, which is where the product on the right-hand side assumes its minimum value, if we keep the zero of energy at reactants. Although eq 2.5.1 is quite useful for calculating the high-pressure limit, the study of the pressure dependence of the reaction kinetics instead requires the implementation of transition-state theory at the microcanonical level or at the microcanonical/J-resolved level. The transition-state partition function then corresponds to the number of available (i.e., energetically accessible)

states, which may be obtained by convolving the number of available states for the transitional modes, $N_{\text{transitional}}$, with the density of states for the conserved modes, $\rho_{\text{conserved}}$:

$$N^{\ddagger}(E,J) = \int_0^E d\epsilon N^{\ddagger}_{\text{transitional}}(\epsilon,J)\rho^{\ddagger}_{\text{conserved}}(E-\epsilon) \quad (2.5.2)$$

The microcanonical rate coefficient, required for the master equation analysis of pressure dependent effects (which is presented below), is given by the standard microcanonical TST expression, which has the form[365]

$$k^{\ddagger}(E) = \frac{N^{\ddagger}(E)}{h\phi^{\text{R}}(E)} \quad (2.5.3)$$

for a bimolecular elementary step, where ϕ^{R} is the reactant density of states per unit energy and volume for the reactant, and the RRKM form[715,716]

$$k^{\ddagger}(E) = \frac{N^{\ddagger}(E)}{h\rho^{\text{R}}(E)} \quad (2.5.4)$$

for a unimolecular elementary step, where $\rho^{\text{R}}(E)$ is the reactant density of states per unit energy. In both of these equations $N^{\ddagger}(E)$ is the number of states of the variational transition state at energies less than or equal to E. The microcanonical/J-resolved analogues are

$$k^{\ddagger}(E,J) = \frac{N^{\ddagger}(E,J)}{h\phi^{\text{R}}(E,J)} \quad (2.5.5)$$

and

$$k^{\ddagger}(E,J) = \frac{N^{\ddagger}(E,J)}{h\rho^{\text{R}}(E,J)} \quad (2.5.6)$$

where now the numbers and densities of states are restricted to a particular value of J. To keep the presentation manageable, we will focus on the bimolecular case and eq 2.5.5, but similar considerations apply to all four of these equations.

Some aspects of the coupling of the conserved modes to the remaining modes are sometimes treated in an approximate fashion. For example, the conserved mode vibrational frequencies and molecular geometries vary with the reaction coordinate. When this variation is ignored, the conserved mode contributions need to be evaluated only for infinitely separated fragments, rather than separately for each transition-state dividing surface that is considered in the variational optimizations. Furthermore, the conserved mode contribution to the canonical transition-state partition function then cancels with the corresponding contribution to the reactant partition function in the evaluation of the high-pressure bimolecular rate coefficient.

Phase space theory (PST) provides a useful, and easily implemented, reference theory for barrierless reactions.[717−725] The basic assumption in phase space theory is that the interaction between the two reacting fragments is isotropic and does not affect the internal fragment motions. This assumption is only valid if the dynamical bottleneck lies at large separations where the interacting fragments have free rotations and unperturbed vibrations. The Gorin model, discussed in Section 2.2.2, is essentially a canonical version of phase space theory for an R^{-6} potential, where R is the separation between the centers of mass of the two fragments. The variable R should not be confused with the gas constant R (used above) or the coordinate set $\mathbf{R}$ (also used above). In eq 2.2.17 and the rest of Section 2.2.2, R was called r; however, we have changed the notation in this section for better correspondence with some of the key references of this section.

The energy for the transitional mode motion on the transition-state dividing surface is given by the sum of the effective centrifugal energy and rotational energies for each of the fragments, $E_{\text{rot}}(j_i,k_i)$, where j_i and k_i are the rotational quantum number and its projection on a body-fixed axis for fragment i. The effective centrifugal potential, $V_{\text{eff}}(R)$, is given by

$$V_{\text{eff}}(R) = V(R) + \frac{\hbar^2 l(l+1)}{2\mu R^2} \quad (2.5.7)$$

where $V(R)$ is the isotropic fragment−fragment interaction energy, μ is the reduced mass of relative translation, and l is the orbital angular momentum quantum number.

The assumption of an isotropic interaction implies that l is a conserved quantum number and therefore the reactive flux can be minimized for each separate l value. In PST the fragment rotational energies are assumed to be independent of R and l, and conserved-mode energies are assumed constant for R greater than its value at the transition state dividing surface. Then the variational minimization reduces to locating the position of the maximum in the effective potential, with corresponding effective potential value $E_l^{\ddagger}$. For the most general case of two nonlinear rotors the phase space theory transitional mode number of states can be written as

$$N^{\text{transitional}}_{\text{PST}}(E,J) = \sum_{j_1}\sum_{j_2}\sum_{k_1}\sum_{k_2}\sum_{l}\Delta(J,j,l)\Delta(j,j_1,j_2)\,\Theta[E - E_{\text{rot}_1}(j_1,k_1) - E_{\text{rot}_2}(j_2,k_2) - E_l^{\ddagger}] \quad (2.5.8)$$

where Θ denotes a Heaviside step function, and the first two terms on the right-hand-side denote triangle inequalities, with j being the angular momentum quantum number corresponding to the vector sum of the fragment rotational angular momenta.

The PST expression for the number of available states can also be obtained from an adiabatic-channel perspective where one considers the number of adiabatic channels whose energy barrier is below the energy E.[726−728] In fact, fully adiabatic theories, where the channel numbers are labeled only according to their energy, provide identical rate coefficients to fully statistical transition state theories.[365] Direct sums such as eq 2.5.8 are readily evaluated computationally, particularly when one realizes that for higher energies the sums can be considered as integrals with nonunit step sizes employed in their evaluation. Alternatively, the quantized formulas can be replaced with classical phase space integrals, which yields further simplifications.[718,723,724]

For ion−molecule reactions long-range expansions of the potentials often provide an adequate description of the interactions in the transition state region. As discussed above, TST treatments for the ion-induced dipole potential yield the Langevin rate. The ion−dipole interaction is generally the next most important term in the potential. The locked-dipole,[729,730] average dipole orientation,[731−734] and effective potential method[735,736] provided early approximate treatments of the effect of the ion−dipole interaction on the capture

rate. These treatments were largely superseded by the pioneering trajectory simulations of Su and Chesnavich.[734,737,738] Related rigid body trajectory simulations of the capture rate for neutral radical−radical reactions have provided useful indications of the limits of accuracy of transition state and adiabatic channel model calculations.[739−744] Gridelet et al.[745] have formulated two criteria for the validity of arbitrary transition state theory for ion−molecule interactions.

A recent long-range TST[746] provides a unified treatment of reactions on long-range potentials. Agreement with trajectory simulations is generally very good. For example, for the particular case of ion−dipole reactions the predictions agree with the trajectory results to within a few percent. This long-range TST is applicable for moderately low temperatures, where the temperature is not so low that quantum effects are significant and not so high that the transition state has moved in to separations where the long-range potential expansion is no longer applicable. Related, but more limited, results had been derived earlier from the perspective of adiabatic channel theories.[747,748]

In reality, the interaction potential for radical−radical reactions is generally quite far from isotropic, and phase space theory provides only an order of magnitude estimate for the capture rate. For ion−molecule reactions the increased strength of the long-range interactions results in a transition state that lies at quite large interfragment separations, where the interaction potential tends to be more isotropic, and the association rate constant of phase space theory is often quite accurate, unless the molecular reactant is either highly nonpolar or nonspherical. In the special case of an ion-induced dipole potential, we can recover the Langevin expression already discussed in Section 2.2.

Recent studies of the high-pressure limit of the $H_3O^+ - H_2O$ association reaction indicate that it is not dominated by ion−dipole forces but rather by the valence part of the potential.[749]

The effect of anisotropies in the interaction potential can readily be accounted for within a classical phase-space integral description of the number of states. At the canonical level the classical partition function for the transitional mode motion on a dividing surface specified by a given value of the separation R may be written as[713]

$$Q_{\text{transitional}}(T,R) = \frac{1}{h^n}\int \mathrm{d}\Omega_{12}\mathrm{d}\Omega_1\mathrm{d}\Omega_2\mathrm{d}\mathbf{p}_{\Omega_{12}}\mathrm{d}\mathbf{p}_{\Omega_1}\mathrm{d}\mathbf{p}_{\Omega_2} \times \exp\{-[K + V(\mathbf{\Omega}_{12},\mathbf{\Omega}_1,\mathbf{\Omega}_2,r)]/k_BT\} \quad (2.5.9)$$

where $\mathbf{\Omega}_i$ denotes the Euler angles $(\theta_i,\varphi_i,\chi_i)$ describing the absolute orientation in space of fragment i, $\mathbf{\Omega}_{12}$ denotes the spherical polar angles describing the absolute orientation of the line-of-centers connecting the centers-of-mass of the two fragments, K is the sum of the fragment and orbital kinetic energies, and n is the number of transitional mode degrees of freedom excluding the reaction coordinate. The transition-state partition function is obtained via minimization of eq 2.5.9 with respect to the dividing-surface parameter R.

The integrals over the momenta in eq 2.5.9 are readily performed analytically to yield:[713]

$$Q_{\text{transitional}}(T,R) = Q_{\text{rot}_1}Q_{\text{rot}_2}\left(\frac{2\pi\mu R^2 k_BT}{\hbar^2}\right) \langle\exp(-\beta V(\mathbf{\Omega}_{12},\mathbf{\Omega}_1,\mathbf{\Omega}_2,r))\rangle_{\mathbf{\Omega}_{12}\mathbf{\Omega}_1\mathbf{\Omega}_2} \quad (2.5.10)$$

where $Q_{\text{rot},i}$, $i = 1,2$ are the rotational partition functions for the fragments, and $\langle ... \rangle_x$ denotes an average over the space x. If the interaction potential is known, Monte Carlo integration provides a simple and efficient procedure for evaluating expressions like eq 2.5.10. Analagous expressions, involving powers of $(E - V)$ or $(E - V - E_{\text{rot}})$ have been derived for the microcanonical and microcanonical/J-resolved transition state partition functions.[750−752] These expressions can also be efficiently evaluated via Monte Carlo integration.

The evaluation of the transition-state partition function according to eq 2.5.10, or its microcanonical or microcanonical/J-resolved analogue, has been termed flexible transition-state theory.[714,753] The earliest application of a flexible transition state theory-like model was provided by Chesnavich and co-workers in their study of ion−dipole capture.[734] Both phase space theory and flexible transition-state theory implicitly assume that the reaction coordinate is the separation between the centers-of-mass of the two reacting fragments. When the transition state lies at large separations, this assumption is perfectly reasonable. However, at closer separations a more reasonable reaction coordinate is more closely related to the distance between the atoms or orbitals involved in the incipient bond. As a result, flexible transition state theory often significantly overestimates (e.g., by a factor of 2) the reaction rate. A discussion of the relation between PST, flexible transition state theory, and a phase space model of Klots[754] is provided elsewhere.[488]

In variable-reaction-coordinate transition state theory (VRC-TST) a more general reaction coordinate is considered.[755−757] This reaction coordinate is specified by a fixed distance between two arbitrarily located pivot points, one on each of the two reacting fragments. When the pivot points are placed at the centers of mass of the corresponding fragments, flexible transition-state theory is recovered. When they are instead located at the atoms involved in the incipient bond, one recovers an approach that is more analogous to an expansion of the potential around the minimum energy path[360,362,369,390,394,758] but with the possibility for a fully coupled anharmonic treatment of the transitional modes. The variational minimization in VRC-TST involves as many as seven parameters; the distance R and two 3D vectors $\mathbf{d}^{(1)}$ and $\mathbf{d}^{(2)}$, connecting the center of mass of each fragment to its pivot point. Fortunately, the directions of the vectors $\mathbf{d}^{(1)}$ and $\mathbf{d}^{(2)}$ are generally clear from physical grounds, and one needs to optimize only the three distances. In particular, the optimal pivot point generally lies somewhere along the vector pointing from the atom involved in the incipient bond to the center of its radical orbital.

The incorporation of this variable reaction coordinate is complicated by the fact that the reaction coordinate is no longer separable from the remaining orientational coordinates of the transitional modes. As a result, expressions like eq 2.5.9 are no longer applicable. Instead, one must return to the original expressions like eq 2.4.17. For a canonical ensemble this implies expressing the partition function as

$$Q(T,s) = \beta\int\frac{\mathrm{d}\mathbf{R}\mathrm{d}\mathbf{p}}{h^n}\exp[-\beta(K+V)]\delta(S-s)\dot{S}\Theta(\dot{S}) \quad (2.5.11)$$

where δ is the Dirac delta function, $S = s$ specifies the dividing surface (so that S is the reaction coordinate), and an overdot denotes a time derivative. (Note that one does not need to specify a reaction path, just a dividing surface.) With eq 2.5.11, analytic integrations over the momenta are

still possible, and, given the interaction potential, the resulting configurational integrals are again readily evaluated via Monte Carlo integration.[759−765]

At the canonical level the expression for the most general case of two nonlinear rotors reduces to[765]

$$Q_{\text{transitional}}(T,s) = 2\left(\frac{k_B T}{\hbar^2}\right)^4\left(\frac{\mu s^2}{\pi^2}\right)\{\prod_{k=1}^{2}\prod_{i=1}^{3}\sqrt{2\pi I_i^{(k)}}\}\langle\Phi \exp(-\beta V(\mathbf{\Omega}_{12},\mathbf{\Omega}_1,\mathbf{\Omega}_2))\rangle_{\mathbf{\Omega}} \quad (2.5.12)$$

where $I_i^{(k)}$ is the principal moment of inertia i of fragment k, s is the distance between the two pivot points, and the kinematic factor Φ is given by

$$\Phi = \sqrt{1 + \mu\sum_{k=1}^{2}\sum_{i=1}^{3}(\mathbf{n}^{(12)} \times \mathbf{d}^{(k)}\cdot\mathbf{n}_i^{(k)})^2/I_i^{(k)}} \quad (2.5.13)$$

where $\mathbf{n}^{(12)}$ is the unit vector pointing from the second pivot point to the first one, and $\mathbf{n}_i^{(k)}$ is the unit vector directed along the principal axis i of the fragment k. Again, similar expressions involving powers in $(E - V)$ or $(E - V - E_{\text{rot}})$ have been obtained for the microcanonical and microcanonical/J-resolved cases.[759−765]

The kinematic factor is unity for center-of-mass pivot points and is otherwise greater than unity. This implies that any reduction in the predicted rate coefficient due to variation in the form of the reaction coordinate is due entirely to increased potential values in the Boltzmann orientational average. Empirically, the optimal dividing surfaces have been found to have a shape that follows the potential energy contours for small angular deviations from the minimum energy path while sampling the highly repulsive interactions at large deviations.[766−768] In many instances, the optimal dividing surfaces are obtained by placing the pivot points near the center of the radical orbitals. For a variety of atom-plus-radical reactions, the contours of the radical orbitals were found to be a good approximation to the optimized dividing-surface shape.[766−768] Indeed, using the radical-orbital contours as a dividing surface might well provide an even more optimal transition-state theory estimate.

The most difficult aspect of the implementation of VRC-TST involves the generation of a suitable potential energy surface. This potential energy surface generally must span the region from 2 to 4 Å in the incipient bond distance and cover all orientations of the two fragments. Early work employed qualitative model surfaces based, for example, on assumed extrapolations and interpolations of the potential from the molecular bonding to the long-range interaction regions.[769−771] Such model studies are similar to empirical implementations of the statistical-adiabatic-channel model[727,728] and to other models assuming an exponential dependence of transitional mode frequencies on the reaction coordinate.[772]

For radical−radical reactions, considerable effort has recently been devoted to obtaining accurate potential energy surfaces from detailed electronic structure calculations. A difficulty is that accurate calculations of potential energy curves for radical−radical reactions generally must involve multireference wave functions;[773−775] standard single-reference-based methods are generally inadequate in the transition-state region for this kind of reaction. When one of the fragments is an atom and the other is nonlinear, the requisite potential energy surface is 3D. In this instance, spline and/or Fourier fits to grid-based ab initio calculations provide an effective procedure for generating the potential. The VRC-TST approach was used in a number of applications to radical-plus-H atom recombination reactions.[766−768] Illustrative results from a study[769,776] of the $CH_3 + H$ reaction are provided in Figure 7. The VRC-TST calculated capture rate is seen to be in good agreement with experiment[777−779] and is also only about 10% greater than the capture rate evaluated from rigid-body trajectory simulations. An earlier study of this reaction[780] found good agreement between quasiclassical trajectory simulations and reaction-path-based variational TST predictions. A recent study has applied this approach to the kinetics of radical reactions with O atoms.[743]

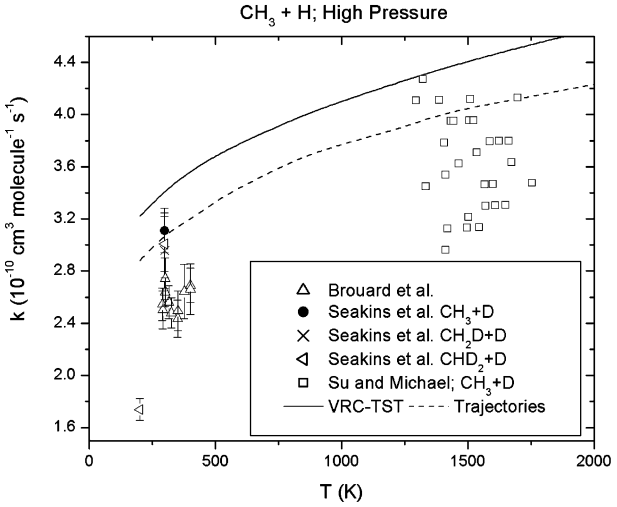

Figure 7. Plot of the $CH_3 + H$ high-pressure rate coefficient versus temperature. The solid line denotes VRC-TST predictions, the dashed line denotes trajectory predictions, and the various symbols denote experimental measurements.

For reactions of two nonlinear fragments the requisite potential energy surface is six-dimensional. In this instance, a grid-based scheme is ineffective both to the large number of points required to appropriately sample the full orientational space and to the inefficiency of simple multidimensional fitting schemes. For a number of such reactions, an alternative approach involving the direct determination of the potential energy for each of the configurations sampled in the Monte Carlo integration has proven to be effective.[744,781−784] The results obtained from this approach for the HNN + OH reaction are illustrated in Figure 8.[783] An accurate estimate of the HNN + OH rate coefficient was a key ingredient in predictions for the calculated branching in the NH_2 + NO reaction. The latter reaction is of central importance in the Thermal De-NOx process. The predicted decrease in the HNN + OH association rate coefficient with increasing temperature as well as the details of the cis/trans branching were both important for reproducing the observed branching for the NH_2 + NO reaction.

For many reactions, there are multiple sites where the two reacting fragments can bind together. For example, in the HNN + OH reaction discussed in the previous paragraph, the OH can bind to either the cis or trans side of the HNN fragment. Other examples of reactions with multiple binding sites are the recombination of resonantly stabilized radicals, such as C_3H_3, and ion−molecule reactions with multiple electrostatic minima. Early VRC-TST work on such reactions assumed a simple separation of the channels, with separate optimizations of the transition-state dividing surface for each channel. However, in many instances the channels are not

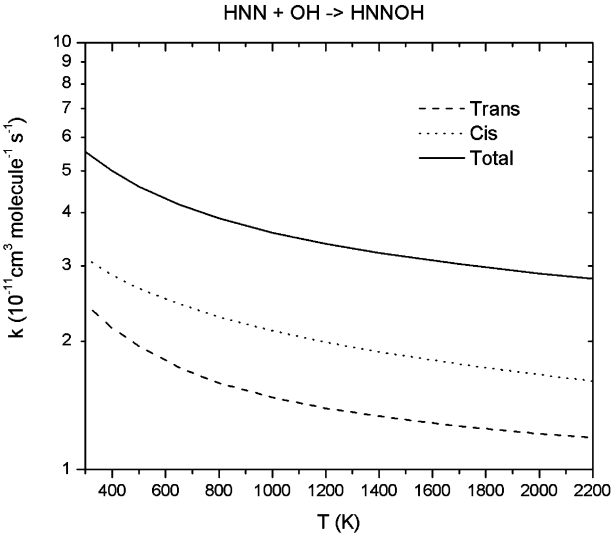

Figure 8. Plot of the HNN + OH high-pressure addition rate coefficients versus temperature. The dashed line denotes the rate to form trans HNNOH, the dotted line denotes the rate to form *cis*-HNNOH, and the solid line denotes the total addition rate.

separable. Furthermore, implementing the assumed separation via approximate infinite potential barriers, at least in principle, negates the variational principle.

Recently, an improved procedure for treating such multiple addition channel reactions was presented.[785] This procedure expresses the overall transition state dividing surface in terms of a composite of individual surfaces with one surface for each of the different binding sites. Each of the individual surfaces is specified in terms of a fixed distance between two points as in the original VRC-TST approach. With this approach the global flux through the overall dividing surface is evaluated, and minimization of this global addition flux is accomplished via variation of the VRC-TST parameters for each of the individual surfaces. This multifaceted dividing surface approach was shown to provide a satisfactory reproduction of the trajectory estimates for the $C_3H_3 + H$ reaction.

2.5.3. Master Equation and Its Application to Reactions over Potential Wells

In Section 2.4, we pointed out that one of the assumptions of transition state theory is that the reactants are distributed among their states according to an equilibrium distribution. We also pointed that this is often a reasonable assumption for simple barrier reactions. As we now turn attention to barrierless association reactions and multiple-well, multiple-arrangement reactions we must reexamine the equilibrium assumption. This will require a consideration of energy transfer collisions and their competition with reaction. This competition, as well as the competition between various possible reactions of the collisional intermediates (e.g., redissociation vs rearrangement even in the absence of energy transfer) is controlled by the master equation, which is the governing equation of the statistical model for multiple-well, multiple-arrangement reactions.

In its most primitive form, the master equation can be written as

$$\frac{dn_i}{dt} = \sum_j (p_{ij} n_j(t) - p_{ji} n_i(t)) \qquad (2.5.14)$$

where $n_i(t)$ is the number density (or population) of state i at time t, and p_{ij} is the probability per unit time of a transition from state j to state i. The evolution of the populations according to eq 2.5.14 is equivalent to a stochastic Markov process. The evolution is Markovian as long as the p_{ij} data do not depend explicitly on the time or on the past history of the populations.[786] For our purposes, such an equation will be applicable as long as the characteristic times for intramolecular motion are much smaller than the average time between collisions. This condition is always satisfied for dilute gases, and thus we can apply the ME under almost all gas-phase conditions, at least until we reach pressures of several hundred atmospheres.

The master equation in the form of eq 2.5.14 has been widely applied to chemical kinetics problems involving diatomic molecules. Detailed analyses of this type are contained in articles on a variety of applications;[544,787−792] these articles also contain a bibliography of previous work on similar topics. In general, eq 2.5.14 could also be nonlinear if the p_{ij} values were functions of the $n_i(t)$ values. This would occur for example in the dissociation of a pure diatomic gas where vibration−vibration energy transfer is important, whereas dissociation of a diatomic molecule dilute in a rare gas is an example of the linear case. Nonlinear problems have been treated theoretically only infrequently in the past,[790,793,794] but they are of some current interest.[795−798] In the following, we discuss molecules more complicated than diatomics, and a linear version of the master equation, which is adequate for the purposes discussed below.

For large, polyatomic molecules (or collision complexes), there are too many states at energies of interest to resolve them all. Consequently, we adopt a contracted, coarse-grained description of these molecular systems. Instead of talking about populations of individual states, we talk about populations of states with energy between E and $E + dE$, or populations of states with energy between E and $E + dE$ and with angular momentum quantum number equal to J. If we had not already indicated our intent to adopt the RRKM approximation, this contracted description would force it on us. It distinguishes the reactivity of states only by the good constants of the motion in the isolated molecule, the total energy and total angular momentum, and quite frequently only by the total energy.

The transition probabilities indicated in eq 2.5.14 are of two types: reactive (unimolecular) and collisional (bimolecular). Radiative processes could also be included, but they are negligible in most nonastrophysical applications. To keep the master equation linear, we envision an experimental situation in which a bimolecular reaction R + X can be studied under pseudo first-order conditions, i.e.

$$n_B \gg n_X \gg n_R \qquad (2.5.15)$$

where n_B is the number density of an inert diluent, n_X is the number density of the reactant present in excess (frequently, but not necessarily, a stable molecule), and n_R is the number density of the limiting reactant (usually a free radical). We assume that R and X, upon collision, form one or another of M configurations of RX. For such conditions, the master equation for the E, J-resolved number density of isomer i of the RX complex can be written as

$$\frac{dn_i(E,J)}{dt} = Z\sum_{J'}\int_{E_0^{(i)}}^{\infty} P_i(E,J;E',J')n_i(E',J')dE' - Zn_i(E,J) - \sum_{j\neq i}^{M} k_{ji}(E,J)n_i(E,J) + \sum_{j\neq i}^{M} k_{ij}(E,J)n_j(E,J) - k_{d_i}(E,J)n_i(E,J) + K_{eq_i}k_{d_i}(E,J)F_i(E,J)n_R n_X - \sum_{p=1}^{N_p} k_{p_i}(E,J)n_i(E,J),\ i = I,...,M \quad (2.5.16)$$

where $n_i(E,J)dE$ is the number density of isomer i of RX with energy between E and $E + dE$ and with angular momentum quantum number J; Z is the collision rate of RX with the bath gas; $E_0^{(i)}$ is the ground-state energy of isomer i; $P_i(E,J;E',J')$ is the probability that a collision will transfer a molecule in well i from a state with energy between E' and $E' + dE'$ and with an angular momentum quantum number J' to a state with energy between E and $E + dE$ and an angular momentum quantum number J; $k_{ij}(E,J)$ is the unimolecular, RRKM rate coefficient for isomerization from well j to well i; $k_{d_i}(E,J)$ is the RRKM rate coefficient for dissociation of isomer i to the original reactants (X and R); $k_{p_i}(E,J)$ is the analogous rate coefficient for dissociation from well i to a set of bimolecular products p; N_p is the number of such product sets; and K_{eq_i} is the equilibrium constant for the X + R $\rightleftarrows$ i reaction. The function $F_i(E,J)$ is the equilibrium distribution in well i at temperature T,

$$F_i(E,J) = \rho_i(E,J)e^{-\beta E}/Q_i(T) \quad (2.5.17)$$

where $Q_i(T)$ is the vibrational−rotational partition function for well i, and $\rho_i(E,J)$ is the corresponding J-resolved density of states.

Most commonly a simpler version of eq 2.5.16 is employed in chemical kinetics problems, one in which E is the only independent variable (and not both E and J), an enormous simplification. It is useful to write it out for clarity:

$$\frac{dn_i(E)}{dt} = Z\int_{E_0^{(i)}}^{\infty} P_i(E,E')n_i(E')dE' - Zn_i(E) - \sum_{j\neq i}^{M} k_{ji}(E)n_i(E) + \sum_{j\neq i}^{M} k_{ij}(E)n_j(E) - k_{d_i}(E)n_i(E) + K_{eq_i}k_{d_i}(E)F_i(E)n_R n_X - \sum_{p=1}^{N_p} k_{p_i}(E)n_i(E),\ i = I,...,M \quad (2.5.18)$$

The term in eq 2.5.16 involving $F_i(E,J)$ (or that involving $F_i(E)$ in eq 2.5.18) is more naturally written as $k_{a_i}(E,J)n_R n_X \rho_{R,X}(E,J)e^{-\beta E}/Q_{R,X}$, where $k_{a_i}(E,J)$ is the association rate coefficient for formation of isomer i from the reactants, $Q_{R,X}$ is the partition function per unit volume of reactants (including relative translational motion), and $\rho_{R,X}(E,J)$ is the corresponding density of states. The form used in eq 2.5.16 comes from applying microscopic reversibility to the association/dissociation reactions; both forms assume that the reactants are maintained in thermal equilibrium. The form shown in the equation has the advantage that is does not require the explicit calculation of $\rho_{R,X}(E,J)$, which is a complicated convolution of the state densities of the two fragments R and X. Nevertheless, we have use for both formulations below.

The second of the inequalities in eq 2.5.15 implies that n_X is a constant, thereby rendering the master equation linear. Thus, it is necessary to supplement the master equation only with an equation for n_R. Assuming again that the reactants are maintained in thermal equilibrium throughout the course of the reaction, we can formulate such an equation as follows:

$$\frac{dn_R}{dt} = \sum_{i=I}^{M}\int_{E_0^{(i)}}^{\infty} k_{d_i}(E)n_i(E)dE - n_R n_X \sum_{i=I}^{M} K_{eq_i}\int_{E_0^{(i)}}^{\infty} k_{d_i}(E)F_i(E)dE \quad (2.5.19)$$

In writing eq 2.5.19 we have restricted ourselves to the 1D problem; the extension to two dimensions (i.e., where both E and J are independent variables) should offer no difficulty. Equations 2.5.16 and 2.5.19 constitute a set of $M + 1$ integrodifferential equations for the unknown populations, $n_i(E)$ and n_R, in the 1D case. Before we solve these equations, we need to consider the collisional terms in the master equation.

2.5.4. Energy Transfer

Collisional energy transfer in highly vibrationally excited molecules and collision complexes is a critical factor in determining rate coefficients for reactions that involve the formation of intermediate complexes that live long enough to suffer one or more collisions. Energy transfer manifests itself in the master equation in the rate coefficient for energy transfer, $k(E,J;E'J')$, which we have implicitly assumed in eq 2.5.16 is factorable into a collision rate, $Z(E',J')$, and a probability density function, $P(E,J;E',J')$. We have gone even one step further and taken $Z(E',J') = Z$, a constant independent of energy and angular momentum. Such a formulation does not pose a limitation if Z is taken to be sufficiently large and if $P(E,J;E',J')$ is chosen accordingly. As far as the master equation is concerned, there is a degree of arbitrariness allowed in defining what one means by a "collision." The only constraint is that the same definition must be used consistently in calculating Z and $P(E,J;E',J')$.

The problem of defining Z unambiguously is strictly a classical mechanical one; it does not exist in quantum mechanics. The problem occurs because of the singularity that exists in classical mechanics at $\Delta E = 0$ in the energy transfer cross section, $\sigma(E,J;\Delta E)$. It is related to the singularity at zero scattering angle in the classical, elastic, differential-scattering cross section. As the impact parameter in classical trajectory calculations is increased, there is less and less energy transferred, and the scattering angle becomes smaller and smaller. There are a very large number of collisions with $\Delta E \approx 0$ and nearly zero scattering angle. One can increase b_{max}, the maximum impact parameter in the trajectory calculations, without limit and not affect the inelastic scattering cross-sections. Classical trajectory calculations do give unique values for the product $Z\langle\Delta E\rangle$, where $\langle\Delta E\rangle$ is the average energy transferred per collision, but not for Z and $\langle\Delta E\rangle$ individually.[799−802] Thus, the questions of how to define a collision, how to calculate Z, and how to choose the "optimum" value of b_{max} in a classical trajectory calculation are intimately connected.

It has become common practice in master-equation analyses to choose Z to be the Lennard-Jones collision rate, Z_{LJ}. However, such a choice has been called into question several times in the past.[799−802] Recognizing that $Z\langle\Delta E\rangle$ or

$\pi b_{max}^2 \langle \Delta E \rangle$, is a constant in trajectory calculations as long as b_{max} is large enough, and defining $\langle \Delta E \rangle_b$ as the average energy transferred per collision for a fixed impact parameter b, Lendvay and Schatz[800] used the criterion that b_{max} be defined by the convergence of the integral,

$$\pi b_{max}^2 \langle \Delta E \rangle = \int_0^{b_{max}} \langle \Delta E \rangle_b \, 2\pi b db \qquad (2.5.20)$$

to within 3% of its limiting constant value as $b_{max} \rightarrow \infty$. They found that, for collisions of highly excited CS_2, SF_6, and SiF_4 molecules with a variety of collision partners, πb_{max}^2 determined from this criterion was always larger than Z_{LJ} and could be larger by as much as a factor of 4.7, with a typical ratio of about 3. However, Nordholm and Schranz[802] subsequently argued that the condition used by Lendvay and Schatz is too stringent and offered a somewhat more complicated alternative, one that frequently yields values only slightly larger than Z_{LJ}. This result is more consistent with the earlier work of Brown and Miller,[799] who studied collisions of highly excited HO_2 molecules with helium. Brown and Miller approached the problem from a different perspective, by considering the energy-transfer cross section, $\sigma(E,J;\Delta E)$, directly. All the unwanted, high impact-parameter trajectories are limited to a narrow region near $\Delta E = 0$ of this function. In fact, as b_{max} is increased beyond a particular point, only values of σ in this region continue to change. Ignoring this "elastic singularity" at $\Delta E = 0$, Brown and Miller fit the remaining inelastic cross sections to an assumed functional form, thus extrapolating the inelastic $\sigma(E,J;\Delta E)$ to $\Delta E = 0$. Integrating over all values of ΔE gives a value for the total inelastic collision cross section, and thus an appropriate value of Z. The values of Z thus obtained by Brown and Miller varied with the E and J of HO_2, but on average they were about 25% larger than Z_{LJ}.

Taking $Z = Z_{LJ}$ is probably a satisfactory choice for collisions of polyatomic molecules with weak colliders such as rare gas atoms and diatomic molecules,[803] but not for collisions between two large polyatomic molecules or for collisions involving highly polar molecules. In such cases the Lennard-Jones potential is not a very good description of the intermolecular interactions. Michael et al.[804] and Durant and Kaufman[805,806] have investigated alternative ways of determining appropriate values for Z. The latter favor calculating the total elastic cross section quantum mechanically and using it to define Z. However, this is probably too complicated for routine use in master-equation modeling. It is worth repeating, however, that only the product ZP, not the individual factors, has meaning for our purposes.

The energy transfer function P remains an elusive quantity, even though it has been the subject of investigation numerous times in the past, both theoretically[799,801,802,807−816] and experimentally.[807,817−828] We shall restrict our discussion to the 1D $P(E,E')$ and forego considering the 2D $P(E,J;E',J')$; very few problems actually require knowledge of the latter anyway. It is common practice in master-equation models to assume a single-exponential-down function for $P(E,E')$, in which[452,829−835]

$$P(E,E') = \frac{1}{C_N(E')} \exp(-\Delta E/\alpha), \quad E \leq E' \qquad (2.5.21)$$

where $C_N(E')$ is a normalization constant and $\Delta E = E' - E$. The activating wing of $P(E,E')$, i.e., the function for $E > E'$, is then determined from detailed balance.[830] The prevalent use of the single-exponential-down model is largely a matter of expedience: the parameter α in the exponential is equal to $\langle \Delta E_d \rangle$, the average energy transferred in a deactivating collision, to a high degree of accuracy in most cases. In general, one can take α to be a function of E' and T, even though doing so is not yet common practice. Evidence from thermal dissociation/recombination experiments suggests strongly that $\langle \Delta E_d \rangle$ increases roughly linearly with T, at least for small molecules with weak colliders.[831] More direct experiments also suggest that there should be an energy dependence[807,831,832] of $\langle \Delta E_d \rangle$. Trajectory calculations confirm this behavior only to a limited extent; the problem is that most such investigations are reported in terms of $\langle \Delta E \rangle$, rather than $\langle \Delta E_d \rangle$. The former has built-in energy and temperature dependence from varying contributions of the activating wing with E and T; the latter does not.

A more serious concern is that $P(E,E')$ is not very accurately described by a single-exponential-down model. Since the Brown−Miller classical-trajectory analysis of He − HO_2 collisional energy transfer, virtually all classical trajectory calculations and direct experiments have concluded that a double-exponential-down formulation is a more realistic description of $P(E,E')$.[799,801,802,809,812,816,821,823,836] Such a model can be written as

$$P(E,E') = \frac{1}{C_N(E')}[(1-f)\exp(-\Delta E/\alpha_1) + f\exp(-\Delta E/\alpha_2)] \quad E \leq E' \qquad (2.5.22)$$

Again, the activating wing of $P(E,E')$ is determined from detailed balance; $C_N(E')$ is a normalization constant, and f, α_1, and α_2 are parameters in the model. However, such a model has not been widely used in master-equation calculations. Thermal dissociation/recombination rate coefficients are not very sensitive to the form of $P(E,E')$,[837] only to $\langle \Delta E_d \rangle$ or $\langle \Delta E \rangle$. This may not be the case for bimolecular reactions over potential wells, especially those where the potential energy barriers to isomerization or fragmentation to bimolecular products lie much lower in energy than the reactants. In fact, Miller and Chandler[838] found significant effects of the high-energy tail of $P(E,E')$ in studying the overtone isomerization of methyl isocyanide. Such photoactivated problems are very similar energetically to the bimolecular collision problems just described. In any event, there have as yet been no systematic investigations of the effects of various forms of $P(E,E')$ on bimolecular reactions over potential wells. Also, there is no systematic prescription for choosing the parameters in eq 2.5.22 for any particular molecular system, an obstacle to implementing the double-exponential-down model.

Luther and co-workers[827] have suggested a third model for $P(E,E')$,

$$P(E,E') = \frac{1}{C_N(E')} \exp\left[-\left(\frac{\Delta E}{\alpha}\right)^Y\right] \quad E \leq E' \qquad (2.5.23)$$

with the activating wing determined from detailed balance, as usual; Y and α are parameters in the model. The advantage of this formulation is a certain degree of flexibility. If $Y = 1$, $P(E,E')$ reduces to a single-exponential-down function. If $Y < 1$, there is a long tail on the distribution, not unlike that of a double exponential, and if $Y > 1$, one gets a highly localized $P(E,E')$ function. In fact, $Y = 2$ corresponds to a

Gaussian. Like the double-exponential model, this function has not been widely used.

Regardless of the considerations raised above, master-equation models of chemical kinetics almost invariably utilize $Z = Z_{LJ}$ and invoke a single-exponential-down model for $P(E,E')$. As noted above, these choices are largely a matter of convenience. They are reinforced by the lack of any systematic procedure for choosing the parameters in the more complicated $P(E,E')$ models and by the fact that Z_{LJ} is probably not too bad a choice for Z if the bath gas is a weak collider, such as one of the rare gas atoms or a diatomic molecule. Energy transfer in highly vibrationally excited molecules is probably the least well understood area of theoretical chemical kinetics.

2.5.5. Solving the Master Equation

The master equation has been formulated and solved in a number of different ways,[506,788−800,839−871] and we especially note some attempts to solve the 2D master equation for some special cases.[750−752,839−847,851,853,855−857,859,860] Most work has been directed toward thermal dissociation reactions, which are just a special case of the methodology described below. An exception is the work on $C_2H_5 + O_2$ by Venkatesh et al.,[856,860] whose methodology for determining rate coefficients is of limited applicability, because it implicitly equates a rate coefficient to a "flux coefficient." We restrict our attention here mainly to the 1D problem, which is probably sufficiently accurate for most purposes. For application to bimolecular reactions over potential wells, there is a very important case for which it is not much more difficult to solve the 2D master equation than it is to solve the 1D problem. That case is the collisionless (or zero-pressure) limit, obtained from eq 2.5.16 by taking the limit $Z \rightarrow 0$. By comparing 2D solutions (which we call microcanonical/J-conservative theory) with 1D solutions (which we call microcanonical theory) in this limit, one can get a good idea of the potential importance of angular momentum conservation on the reaction in general. Since J is a constant of the motion in the absence of collisions, this limit might be expected to give the maximum effect of angular momentum conservation on the thermal rate coefficients. Moreover, under conditions of interest, many important reactions actually occur in this limit.

Another important limit is the high-pressure, or collision-dominated, limit in which $Z \rightarrow \infty$. Rate coefficients in this limit can be calculated directly from the transition-state theory for bimolecular reactions as the rate coefficients for complex formation, or the "capture" rate coefficients. In this limit, thermal equilibrium is established in the first complexes formed before any rearrangement can take place. Consequently, the only products formed are those corresponding to the wells that are directly connected to the reactants.

Our discussion of the collisionless limit follows closely that of Hahn et al.[872] The theoretical development is a generalization of that first given by Miller et al.[873] If one takes $Z = 0$, eq 2.5.16 can be written in the simple vector form,

$$\frac{\mathrm{d}|n(E,J)\rangle}{\mathrm{d}t} = -\mathbf{K}(E,J)|n(E,J)\rangle + n_R n_X |b(E,J)\rangle \rho_{R,X}(E,J) e^{-\beta E}/Q_{R,X} \quad (2.5.24)$$

where $|n(E,J)\rangle$ is (in Dirac notation) the vector of population densities for a given E and J, i.e., each component of the vector corresponds to the population of a different well, and the subscript RX denotes R + X. The elements of the matrix $\mathbf{K}(E,J)$ are algebraic sums of isomerization and dissociation rate coefficients; all its diagonal entries are positive, and all its off-diagonal entries are negative. The vector $|b(E,J)\rangle$ contains the association rate coefficients.

Applying the steady-state approximation to eq 2.5.24, one obtains for the population vector,

$$|n(E,J)\rangle = \mathbf{K}^{-1}(E,J)|b(E,J)\rangle n_R n_X \rho_{R,X}(E,J) e^{-\beta E}/Q_{R,X}(T) \quad (2.5.25)$$

where $\mathbf{K}^{-1}(E,J)$ is the inverse matrix of $\mathbf{K}(E,J)$. The rate of formation of bimolecular products can also be described by a vector equation,

$$\frac{\mathrm{d}|P(E,J)\rangle}{\mathrm{d}t} = \mathbf{D}(E,J)|n(E,J)\rangle \quad (2.5.26)$$

where the components of $|P(E,J)\rangle$ are the number densities per unit energy of the various possible sets of bimolecular products, and $\mathbf{D}(E,J)$ is the matrix whose i,j element is the dissociation rate coefficient from well j to product i. Substituting eq 2.5.25 into eq 2.5.26 results in the expression,

$$\frac{\mathrm{d}|P(E,J)\rangle}{\mathrm{d}t} = \mathbf{D}(E,J)\mathbf{K}^{-1}(E,J)|b(E,J)\rangle n_R n_X \rho_{R,X}(E,J) e^{-\beta E}/Q_{R,X}(T) \quad (2.5.27)$$

Integrating over E and summing over J, one can easily identify a vector of thermal rate coefficients as the factor multiplying $n_R n_X$,

$$|k_0(T)\rangle = \frac{1}{Q_{R,X}(T)} \sum_J (2J+1) \int_0^\infty \mathbf{D}(E,J)\mathbf{K}^{-1}(E,J)|b(E,J)\rangle \rho_{R,X}(E,J) e^{-\beta E}\mathrm{d}E \quad (2.5.28)$$

where the subscript 0 reminds us that we are working in the collisionless limit.

A further simplification results when the appropriate RRKM rate coefficients of eq 2.5.6 are substituted into eq 2.5.28. All the densities of states cancel,[873] and one is left with the result,

$$|k_0(T)\rangle = \frac{1}{hQ_{R,X}(T)} \sum_J (2J+1) \int_0^\infty N_D(E,J) N_K{}^{-1}(E,J)|N_b(E,J)\rangle e^{-\beta E}\mathrm{d}E \quad (2.5.29)$$

where N_D, $N_K{}^{-1}$, and $|N_b\rangle$ are related to $\mathbf{D}$, $\mathbf{K}^{-1}$, and $|b\rangle$ in that the former contain only the numerators $N^{\ddagger}(E,J)$ in the corresponding RRKM rate coefficient expressions of the latter. The vector $|k_0(T)\rangle$ contains the thermal rate coefficients for all the bimolecular product channels. Equation 2.5.29 is very convenient in that one can work only with N_D, N_K, and $|N_b\rangle$ and never have to deal with the densities of states. Evaluating eq 2.5.29 offers no particular difficulty as long as one is careful to avoid singularities in N_K.[872]

Perhaps the most intriguing example of a bimolecular reaction that takes place in its collisionless limit under normal conditions is the reaction between NH_2 and NO.[482,874] This is the key reaction in the Thermal De-NO_x process,[875−878] an important noncatalytic aftertreatment scheme for removing

NO_x from the exhaust gases of stationary combustors; ammonia is the chemical additive. The $NH_2 + NO$ reaction has three energetically accessible product channels,

$$NH_2 + NO \rightarrow N_2 + H_2O \quad \text{(R1a)}$$

$$NH_2 + NO \rightarrow NNH + OH \quad \text{(R1b)}$$

$$NH_2 + NO \rightarrow N_2O + H_2 \quad \text{(R1c)}$$

although only the first two are kinetically significant. Reaction (R1a) is dominant at low temperatures and remarkably involves breaking all three bonds in the reactants and forming three completely new bonds in the products, all in one collision. However, the radical-producing channel, (R1b), is the most significant feature of the reaction. Above a temperature of 1100 K, the chain branching from this channel allows the process to be self-sustaining. Figure 9 shows the

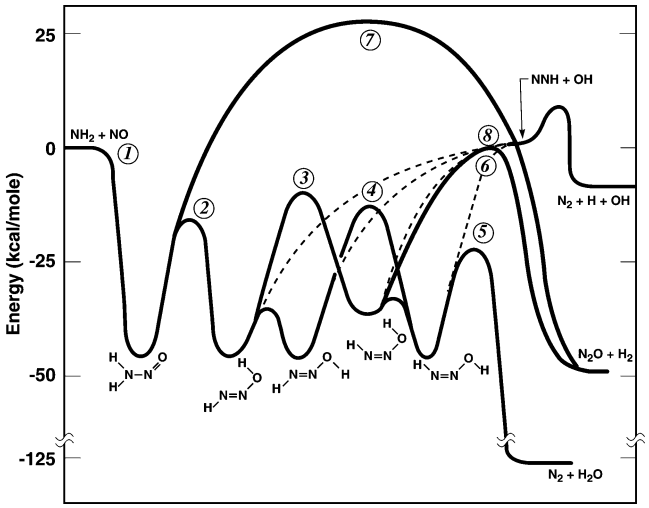

Figure 9. Reaction coordinate diagram for the $NH_2 + NO$ reaction.

reaction coordinate diagram for the reaction. Even at the lowest energies from which a complex can be formed from $NH_2 + NO$, the complex lifetimes are much smaller than the mean time between collisions, $10^{-13} - 10^{-11}$ s compared to 10^{-10} s at one atmosphere pressure.[874] Consequently, one expects the reaction to be in its collisionless regime up to pressures of a few atmospheres. This behavior has been confirmed experimentally at least up to pressures of almost an atmosphere.[874]

Diau and Smith[879] were the first to treat the kinetics of the reaction theoretically using methods like those discussed in this review. Unfortunately, their PES was insufficiently detailed to be quantitatively accurate. Subsequently, Miller and Klippenstein[880] and Fang et al.[783] studied the reaction in detail. The total rate coefficient is largely (but not exclusively) controlled by TS2 (transition state 2) in Figure 9, whereas the product distribution is controlled by a competition between TS4 and fragmentation of the trans HNNOH isomers into NNH + OH through TS8. The latter transition state actually includes four separate reaction paths. Treating this part of the process (both the quantum chemistry and the transition-state theory) accurately is crucial. Making modest adjustments to key features of the PES, Fang et al. were able to predict both the total rate coefficient and the branching fraction ($k_{1b}/(k_{1a} + k_{1b} + k_{1c})$) of the reaction accurately over a wide range of temperatures (see Figures 10 and 11). Interestingly, none of these results are very sensitive to whether angular momentum is conserved.

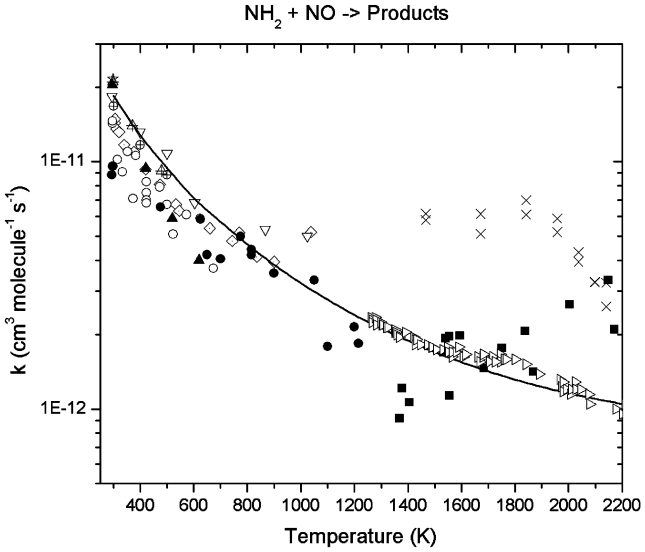

Figure 10. Plot of the total rate coefficient for the $NH_2 + NO$ reaction versus temperature. Symbols denote various experimental measurements, whereas the solid line denotes collisionless-limit master-equation predictions.

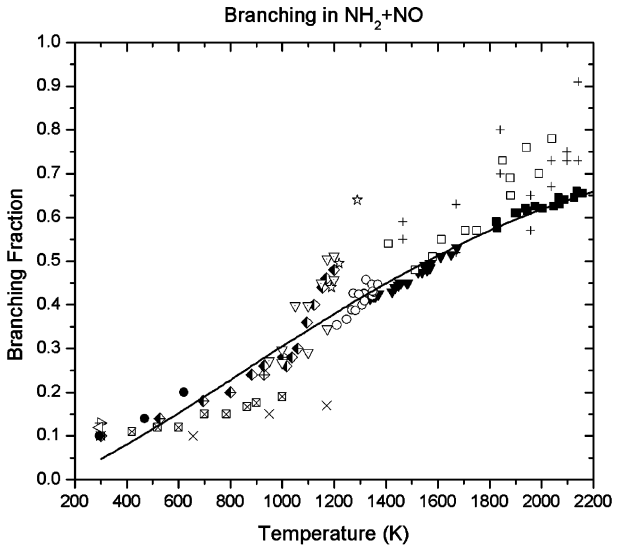

Figure 11. Plot of the branching ratio to form HNN + OH in the $NH_2 + NO$ reaction versus temperature. Symbols denote various experimental measurements, whereas the solid line denotes collisionless-limit master-equation predictions.

Although the collisionless limit is of considerable practical importance, problems in which collisions play a significant, if not dominant, role are even more prevalent. For reasons noted above, we restrict ourselves to a discussion of the 1D master equation (microcanonical theory, not microcanonical/*J*-conservative theory). Also, it is convenient to assume that we have added terms to the master equation, analogous to the $K_{eq_i}k_{d_i}(E)F_i(E)n_R n_X$ term on the right-hand side of eq 2.5.18, that describe reassociation of the bimolecular products. Furthermore, let us assume that for each set of bimolecular products one of the components is maintained in great excess, analogous to n_X for the reactants. These assumptions keep the master equation linear and allow us to deal with all chemical configurations (wells, bimolecular reactants, and bimolecular products) on an equal footing. Such analyses could easily be performed, but it is common practice to assume that any set of bimolecular products

represents an "infinite sink", i.e., that such products, once they are formed, never return to the wells. We deal with this approximation after we treat the more general case.

Equations 2.5.18 and 2.5.19 and an equation analogous to (2.5.19) for each set of bimolecular products can be combined into one (vector) master equation. After the integrals in these equations are approximated as discrete sums with a grid spacing δE, one can manipulate the master equation algebraically into the deceptively simple form,[862]

$$\frac{\mathrm{d}|w(t)\rangle}{\mathrm{d}t} = \mathbf{G}|w(t)\rangle \tag{2.5.30}$$

where **G** is a real, symmetric (Hermitian) matrix, and $|w(t)\rangle$ is the vector of unknown populations,

$$|w(t)\rangle = \left[y_I(E_O^{(I)}),...,y_I(E_l),...,y_i(E_0^{(I)}),...,y_i(E_l),..., \left(\frac{n_X}{Q_{R,X}\delta E}\right)^{1/2} X_R,...\right]^T \tag{2.5.31}$$

In eq 2.5.31, $y_i(E,t) = x_i(E,t)/f_i(E)$ and $f_i^2(E) = F_i(E)Q_i(T)$; $x_i(E,t)\delta E$ is the fraction of the initial reactant concentration that is present in well i with energy between E and $E + \delta E$ at time t, and X_R is the fraction that is present as R at time t. The three dots at the end indicate that there is a component of the vector of the same form as $(n_X/Q_{RX}\delta E)^{1/2}X_R$ for each set of bimolecular products.

The Hermiticity of the transition matrix **G** facilitates the solution of eq 2.5.30. One can find its eigenvalues and construct an orthonormal set of eigenvectors of **G** from the solutions of the eigenvalue equation,

$$\mathbf{G}|g_j\rangle = \lambda_j|g_j\rangle \tag{2.5.32}$$

One can then expand $|w(t)\rangle$ in this basis and obtain the solution of eq 2.5.30 in the form

$$|w(t)\rangle = \hat{T}|w(0)\rangle \tag{2.5.33}$$

where $|w(0)\rangle$ is the initial-condition vector, and $\hat{T}$ is the time evolution operator,

$$\hat{T} = \sum_{j=0}^{N-1} e^{\lambda_j t}|g_j\rangle\langle g_j| \tag{2.5.34}$$

where N is the order of the matrix,

$$N = \sum_{i=1}^{M} N_i + N_p + 1 \tag{2.5.35}$$

and N_i is the number of grid points in well i; the final 1 in the sum is for the reactants.

All the eigenvalues of **G** are nonpositive, i.e., either zero or negative. There is always one zero eigenvalue, $\lambda_0 = 0$; the corresponding eigenvector corresponds to a state of complete thermal and chemical equilibrium. The remainder of the eigenvalues must be negative, $\lambda_j < 0$, with $j = 1,...,N - 1$; otherwise, the solution (eqs 2.5.33 and 2.5.34) would blow up as $t \rightarrow \infty$. We refer to the second largest (i.e., the least negative) eigenvalue of **G** as λ_1, the third largest as λ_2, and so on; the corresponding eigenvectors are $|g_1\rangle,|g_2\rangle,...,$ etc. Widom[881−883] describes these eigenpairs as "normal modes of relaxation" of the system. They describe the system's approach to equilibrium from an arbitrary initial condition.

From the solution vector one can obtain the macroscopic populations directly for the bimolecular components and by integration,

$$X_i(t) = \int_{E_i^{(0)}}^{\infty} x_i(E,t)\mathrm{d}E \tag{2.5.36}$$

for the wells. Even though N may be an extremely large number, typically in the thousands in a practical problem, not all of these relaxation modes describe chemical change, i.e., changes in the macroscopic populations. The vast majority simply describe the relaxation of the internal degrees of freedom of the molecules corresponding to the wells, i.e., relaxation of the internal energy. We refer to these eigenmodes as internal energy relaxation eigenmodes (IEREs). The remainder are chemically significant eigenmodes (CSEs). When the eigenvalues corresponding to the IEREs and CSEs are vastly different in magnitude,[881−883] the internal degrees of freedom relax much more rapidly than the chemical ones. Such a situation does not always exist. However, when these conditions do prevail, it is an enormous simplification for determining the thermal rate coefficients from the eigenvalues and eigenvectors of **G**. Moreover, even when the eigenvalues do not satisfy these conditions, modifications to the general method can be made to determine the rate coefficients of interest, as discussed below, after eq 2.5.51.

If there are S "species", or chemical configurations, in a problem,

$$N_{chem} = S - 1 \tag{2.5.37}$$

chemically significant eigenmodes in addition to λ_0, $|g_0\rangle$. Each of these modes describes the approach to chemical equilibrium of one species with one or more other species. To see the validity of eq 2.5.37, it is useful to consider a specific case. Suppose we have a problem where $S = 4$. Chemical equilibrium can be brought about in one of two distinct ways. In the first way, the fastest-relaxing mode brings one species into equilibrium with another. The second fastest CSE equilibrates these two species with a third, and the slowest eigenpair describes the equilibration of the first three species with the last. In the other way of approaching chemical equilibrium for this problem, the third and fourth species equilibrate through the second eigenmode, and the two pairs equilibrate via the slowest-relaxing eigenmode. Either way, $N_{chem} = S - 1$. In more complicated problems the number of possible ways that the system can approach complete chemical equilibrium becomes quite large. Nevertheless, there are $S - 1$ chemically significant eigenmodes.

For the same problem, i.e., one with S chemical configurations, there are N_k reversible elementary reactions occurring simultaneously, where

$$N_k = \sum_{n=1}^{S-1} n = \frac{S(S-1)}{2} \tag{2.5.38}$$

If $S = 2$, both N_{chem} and N_k are equal to unity, and it is not difficult to obtain the forward and reverse rate coefficients from the single eigenvalue, λ_1, and the equilibrium constant.[881] However, N_k increases quadratically with S and if,

for example, $S = 10$, then $N_k = 45$. It is this large number of elementary reactions, all occurring simultaneously, that makes it difficult to obtain the phenomenological rate coefficients from the raw time histories that come from solutions to the master equation, but it is these rate coefficients that we want for use in modeling macroscopic chemical phenomena.

Under conditions where the IEREs relax faster than the CSEs, the macroscopic populations can be written as

$$X_i(t) = \sum_{j=0}^{N_{\text{chem}}} a_{ij} e^{\lambda_j t}, \quad i = I,...,M,R,P_1,..., \quad (2.5.39)$$

after the IEREs have been relaxed to zero. The coefficient $a_{i0} = X_i(\infty)$ is the equilibrium population of configuration i, and

$$a_{ij} = -\Delta X_{ij}; \quad j \neq 0 \quad (2.5.40)$$

where ΔX_{ij} is the change in population that accompanies the time evolution of eigenmode j from $t = 0$ to $t = \infty$ for a specific initial condition. The values of the various ΔX_{ij} thus depend on the initial condition, but they can be calculated readily from the solution to the master equation, eqs 2.5.33 and 2.5.34. It is the λ_j and a_{ij} values that are required to calculate the phenomenological rate coefficients.

Klippenstein and Miller[884,885] have derived two different methods of determining the rate coefficients from the chemically significant eigenpairs. In the first method, which we call the initial-rate method, one utilizes different initial conditions in evaluating a_{ij} in eq 2.5.39. Differentiating this equation with respect to time and taking the limit $t \rightarrow 0$ results in the rate-coefficient expressions,

$$k_{\text{T}i} = \sum_{j=1}^{N_{\text{chem}}} \lambda_j \Delta X_{ij}^{(i)}$$
$$k_{il} = -\sum_{j=1}^{N_{\text{chem}}} \lambda_j \Delta X_{lj}^{(i)} \quad (2.5.41)$$

where $k_{\text{T}i}$ is the total rate coefficient for removal of species i, and k_{il} is the $i \rightarrow l$ rate coefficient. The superscript (i) on $\Delta X_{ij}^{(i)}$ indicates that species i must be the initial reactant. This method is strictly applicable only as long as $|\lambda_{N_{\text{chem}}}| \ll |\lambda_{N_{\text{chem}}+1}|$ since one must be able to identify a suitable time to take as $t = 0$. In other words, there must exist a time period where all the IEREs have relaxed to zero, but no reaction has occurred. This condition is not as restrictive as it appears. In fact, it is generally presumed to be a necessary condition for a rate-coefficient description of the chemical kinetics to apply.

The second approach taken by Klippenstein and Miller is what we call the long-time method, for reasons that will become apparent below. This method consists of recognizing that eq 2.5.39 is identical in form to the solution of a system of first-order rate equations. One can then solve the inverse problem of finding the phenomenological rate coefficients for the system of reactions that generated the given solution. Klippenstein and Miller solved this problem and obtained the results,

$$k_{\text{T}i} = -\sum_{j=0}^{N_{\text{chem}}} \lambda_j a_{ij} b_{ji}$$
$$k_{il} = \sum_{j=0}^{N_{\text{chem}}} \lambda_j a_{lj} b_{ji} \quad (2.5.42)$$

where, if the a_{ij} are taken to be the elements of a matrix $\mathbf{A}$, the b_{ij} are the elements of its inverse, $\mathbf{B} = \mathbf{A}^{-1}$. Note that eqs 2.5.42 apply to any and all initial conditions and, more importantly, that eq 2.5.39 (and thus eqs 2.5.42) is applicable as long as $|\lambda_{N_{\text{chem}}}| < |\lambda_{N_{\text{chem}}+1}|$, a less restrictive condition than that necessary for the applicability of the initial-rate method. As long as the rotational−vibrational relaxation period is over before the chemistry is finished, there will be at least a short period of time, late in the reaction, when a phenomenological description of the chemical kinetics will apply, with the rate coefficients given by eqs 2.5.42.

For most conditions that are of practical interest, the initial-rate method and the long-time method yield the same values for the rate coefficients. However, as the magnitude of $\lambda_{N_{\text{chem}}}$ approaches that of $\lambda_{N_{\text{chem}}+1}$ the long-time method will continue to yield good values for the rate coefficients when the initial-rate method will fail. Nevertheless, the initial-rate approach is generally the method of choice, simply because it is easier to apply under most conditions.[884−886]

In a seminal paper in 1974, Bartis and Widom[887] used an approach to the rate-coefficient problem similar to the long-time method of Klippenstein and Miller, but with an additional assumption. The essence of this assumption is that, during the course of reaction, the state populations are not perturbed greatly from their equilibrium values.[884] One can probably take this to mean that their result will apply when only states that are not heavily populated at equilibrium are affected significantly by the reaction. With this assumption, Bartis and Widom derived rate-coefficient expressions analogous to eqs 2.5.42 that satisfy detailed balance *exactly*, i.e., the forward rate coefficient divided by the reverse rate coefficient is equal to the equilibrium constant. Although it has not been proven here that the rate-coefficient expressions given above satisfy detailed balance, they normally do. They *will* satisfy detailed balance (at least) under the conditions that the Bartis-Widom analysis applies.

The rate coefficients that are derived from eqs 2.5.41 and 2.5.42 are first-order or pseudo first-order rate coefficients. In cases where the reactions are really bimolecular, the rate coefficients calculated from these expressions must be divided by n_{X} or its equivalent to get the true bimolecular rate coefficients. This minor modification is the only price we pay for the "linearization" of the master equation described above.

At this point it is convenient to consider a particular example to illustrate the methods, to show how one can approximate bimolecular products as infinite sinks, and to describe what happens when $\lambda_{N_{\text{chem}}}$ becomes equal to $\lambda_{N_{\text{chem}}+1}$. Figure 12 is a reaction coordinate diagram for the reaction of propargyl radicals (C_3H_3) with hydrogen atoms.[885] One set of bimolecular products, $^3C_3H_2$ (propargylene) + H_2, is formed by direct abstraction on a separate (triplet) PES from the others. Thus, the rate coefficient for this reaction can be calculated independently of the rest by the methods discussed at the beginning of this review. However, the theoretical treatment of the remainder of the reaction requires the methods described just above.

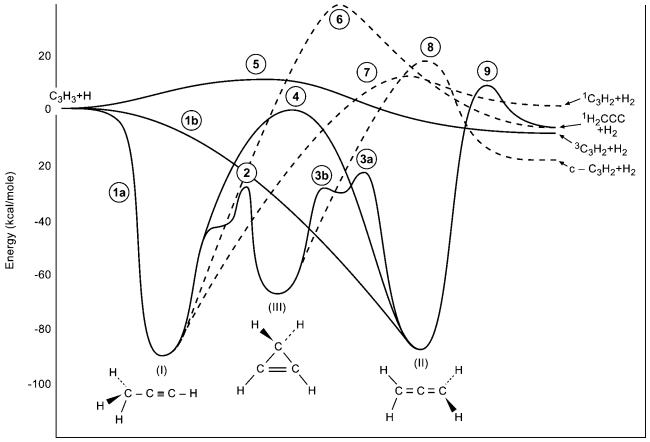

Figure 12. Schematic diagram of the C_3H_4 potential energy surface.

In studying this reaction Miller and Klippenstein[885] lumped all three of the remaining sets of bimolecular products into a single infinite sink. Thus, for the purposes of the master equation analysis, there are effectively only five species, $S_{\text{eff}} = 5$ and $N_{\text{chem}} = 4$. At low temperature, if one starts with an initial condition consisting of all $C_3H_3 + H$, one finds that the fastest-relaxing eigenpair, $\lambda_4,|g_4\rangle$, describes the equilibration of $C_3H_3 + H$ with propyne, C_3H_4p (well I of Figure 12), although other products may be formed simultaneously. The next fastest-relaxing eigenpair ($\lambda_3,|g_3\rangle$) describes the equilibration of these two species with cyclopropene (c-C_3H_4), well III, while $\lambda_2,|g_2\rangle$ equilibrates the first three configurations with allene (C_3H_4a), well II. The last CSE ($\lambda_1,|g_1\rangle$) describes the slow leak of this equilibrated "four-component" system into the infinite sink.

One can employ the methodology described above even in the absence of complete chemical equilibrium at long times. This can be illustrated for the case where there is only one set of products in the sink. In this case, the macroscopic populations satisfy the global conservation equation

$$X_{\text{R}} + X_{\text{p}} + \sum_{i=I}^{M} X_i = 1 \qquad (2.5.43)$$

Differentiating this equation with respect to time and then integrating from $t = 0$ to $t = \infty$, one obtains

$$\Delta X_{\text{R}} + \Delta X_{\text{p}} + \sum_{i=I}^{M} \Delta X_i = 0 \qquad (2.5.44)$$

Because the terms in eq 2.5.39 (or eq 2.5.34) are linearly independent functions of time as long as no two CSEs are equal, eq 2.5.44 must be satisfied not only globally but also by each eigenmode individually, i.e.,

$$(\Delta X_{\text{R}} + \Delta X_{\text{p}} + \sum_{i=I}^{M} \Delta X_i)_j = 0 \qquad (2.5.45)$$

Thus one can calculate ΔX_{pj} from eq 2.5.45; the other terms in the equation come from the solution to the master equation, as indicated above. These results, coupled with the long-time limits,

$$X_p(\infty) = 1$$
$$X_R(\infty) = X_i(\infty) = 0, (i = I,...M) \qquad (2.5.46)$$

can be inserted into eqs 2.5.41 and 2.5.42 to obtain the thermal rate coefficients.

The situation is not quite so simple if there are multiple sets of products coupled together in an infinite sink. The above procedure gives only the total rate coefficient for all products; it says nothing about the individual rate coefficients; however, it is not too much more difficult to extract those. From eqs 2.5.33 and 2.5.34, one can write $x_i(E,t)$ during the rate-coefficient period as

$$x_i(E,t) = \sum_{j=1}^{N_{\text{chem}}} c_{ij}(E) e^{\lambda_j t} \qquad (2.5.47)$$

where $c_{ij}(E)$ comes from eigenvector j and the initial condition. The total rate of formation of product p is (see eq 2.5.18)

$$\frac{dX_p}{dt} = \sum_{i=I}^{M} \int_{E_i^{(0)}}^{\infty} k_{p_i}(E) x_i(E,t) dE \qquad (2.5.48)$$

Substituting eq 2.5.47 into eq 2.5.48, one obtains

$$\frac{dX_p}{dt} = \sum_{j=1}^{N_{\text{chem}}} e^{\lambda_j t} \sum_{i=I}^{M} \int_{E_i^{(0)}}^{\infty} k_{p_i}(E) c_{ij}(E) dE \qquad (2.5.49)$$

Integrating this equation term-by-term from $t = 0$ to $t = \infty$ results in

$$X_p(\infty) = \sum_{j=1}^{N_{\text{chem}}} \Delta X_{pj} \qquad (2.5.50)$$

where

$$\Delta X_{pj} = -\frac{1}{\lambda_j} \sum_{j=1}^{N_{\text{chem}}} \int_{E_i^{(0)}}^{\infty} k_{p_i}(E) c_{ij}(E) dE \qquad (2.5.51)$$

The sum and integral in eq 2.5.51 are relatively easily evaluated, and eqs 2.5.50 and 2.5.51 can be used in eqs 2.5.41 and 2.5.42 to determine the phenomenological rate coefficients.

Figure 13 shows the eigenvalue spectrum for the $C_3H_3 + H$ problem as a function of temperature at a pressure of 1 atm and n_X corresponding to a partial pressure of 1 Torr. In this diagram, the eigenvalues are labeled by their magnitude at any given temperature rather than by function. If we had labeled the curves by their equilibration function, there would be some curve crossing in the diagram. For temperatures above 1200 K it is $\lambda_4,|g_4\rangle$, not $\lambda_3,|g_3\rangle$, that brings about the equilibration of cyclopropene with propyne, as indicated in the diagram. At $T \approx 2200$ K, λ_4 merges with the continuum of IEREs, a common occurrence in complicated, high-temperature reactions. In principle, this creates a problem for the rate-coefficient analysis discussed above in that all the CSEs are no longer discernible from the IEREs. However, the problem can be repaired relatively easily. The merging of λ_4 with the continuum of IEREs means that the reaction c-$C_3H_4 \rightleftarrows C_3H_4p$ equilibrates on IERE time scales. Therefore, the two species cease to be distinct in the kinetic sense discussed above, and we can combine them into a single "superspecies" for kinetic purposes, taking $S = 4$ instead of 5 in the analysis. This reduces the number of terms

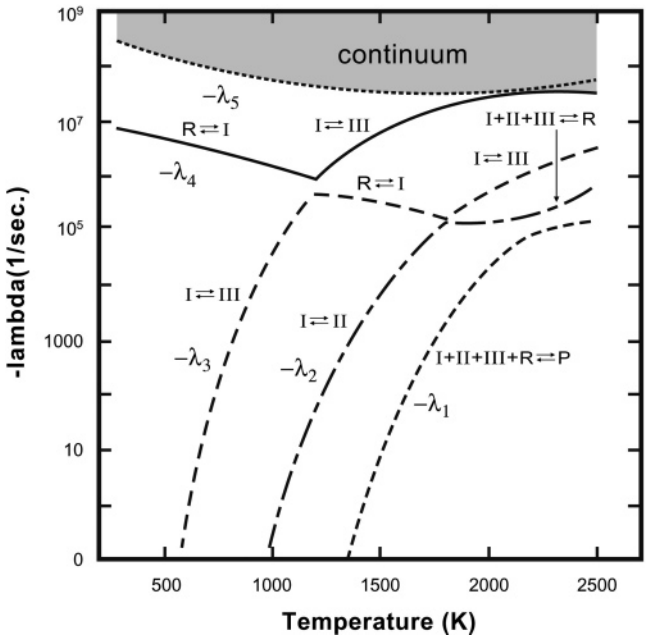

Figure 13. Eigenvalue spectrum for the $C_3H_3 + H$ problem at a pressure of 1 atm.

in the sum of eq 2.5.41 by one and reduces the **A** and **B** matrices associated with eq 2.5.42 by one row and one column. This procedure is very useful (even necessary) in extending the rate-coefficient regime to high temperatures. Of course, at sufficiently high temperatures there is no real distinction between CSEs and IEREs; all chemical processes equilibrate on IERE time scales.

The theoretical methodology described above eliminates the ambiguity that exists in more ad hoc methods of calculating rate coefficients. In Figure 12, for example, TS4 is irrelevant in the analysis; including it or excluding it gives the same results. That being the case, how does one distinguish between single-step processes such as $C_3H_4a \rightarrow C_3H_4p$ and its corresponding two-step process, $C_3H_4a \rightarrow c\text{-}C_3H_4 \rightarrow C_3H_4p$, when the reaction must pass through the $c\text{-}C_3H_4$ configuration in both cases? The above procedures automatically make the correct distinctions without any need for further arbitrary assumptions concerning energies or lifetimes. Similarly, one never needs to ask or answer the question, "Can allene dissociate 'directly' to $C_3H_3 + H$ through TS1a?", or does such an occurrence necessarily involve intermediate isomerization?

Figure 13 illustrates another important point concerning dissociation. For temperatures higher than about 1800 K, λ_2 and $|g_2\rangle$ describe the equilibration of allene with propyne and cyclopropene, whereas λ_3 and $|g_3\rangle$ describe the dissociation of the equilibrated threesome to $C_3H_3 + H$. At $T =$ 2200K, $-\lambda_3$ is larger than $-\lambda_2$ by roughly a factor of 6, i.e., the isomerization reactions equilibrate considerably faster than dissociation can occur. As a result, most experiments are sensitive only to $-\lambda_2$ and not to the dissociation rate coefficients individually, regardless of which of the three isomers is prepared as the reactant. This makes it very difficult to measure the rate coefficients directly. Nevertheless, the theory yields good rate coefficients for the dissociation of the individual isomers to $C_3H_3 + H$. The results are discussed and compared with experiment by Miller and Klippenstein.[885]

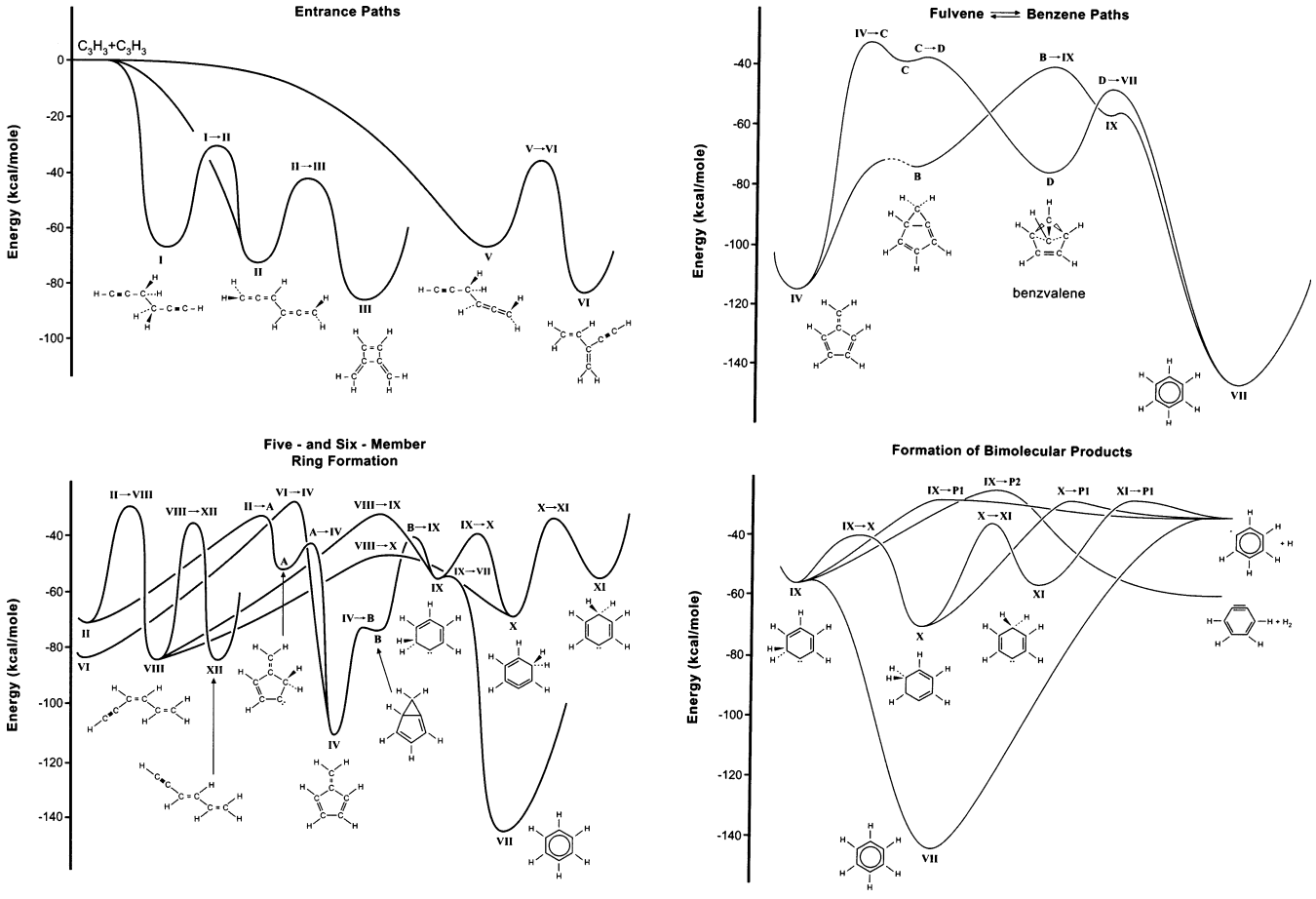

Figure 14. Schematic diagram of the potential energy surface for $C_3H_3 + C_3H_3$ recombination.

The most complex reaction to which the methods of this review have been applied is the $C_3H_3 + C_3H_3$ recombination.[886] The analysis of this reaction involves 12 potential wells and 2 sets of bimolecular products. The PES is shown diagrammatically in Figure 14, which has four parts. There are 13 CSEs in this reaction, one of which has an anomalously large magnitude because of a very shallow well. The others begin to merge with the continuum of IEREs at temperatures as low as 1000 K, a factor that must be accounted for correctly in the analysis. Nevertheless, rate coefficients and product distributions for this reaction have been obtained by Miller and Klippenstein.[886]

A plot of the total rate coefficient as a function of temperature and pressure is shown in Figure 15. The curve

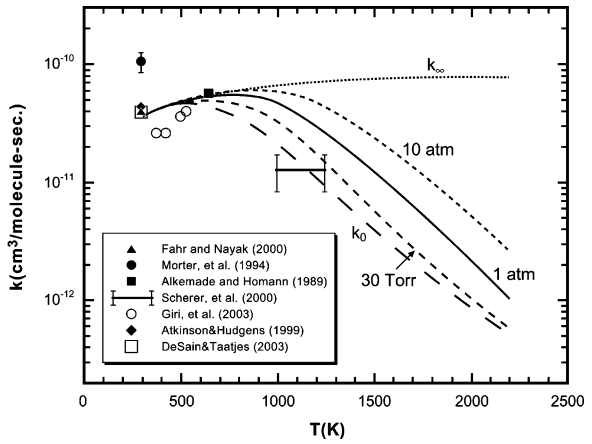

Figure 15. The total rate coefficient for $C_3H_3 + C_3H_3 \rightarrow$ products.

labeled k_0 is the collisionless limit, and the one labeled k_∞ is the high-pressure limit, i.e., the rate coefficient for complex formation (or the capture rate coefficient). Up to temperatures of about 500 K, there is no difference between $k_0(T)$ and $k_\infty(T)$, indicating that any complex, once formed, ultimately reacts—the products could be bimolecular or they could be stabilized C_6H_6 isomers. At temperatures above 500 K, the $k_\infty(T)$ and $k_0(T)$ curves increasingly separate. In the absence of collisions, many $C_6H_6^*$ complexes redissociate to $C_3H_3 + C_3H_3$ before they can go on to products. The primary effect of collisions is to stabilize many of these nonreactive complexes in the wells. Thus, the rate coefficient for any finite, nonzero pressure lies somewhere between the two limits, as shown on the plot.

Product distributions for the propargyl recombination reaction are shown in Figure 16 as a function of pressure for two temperatures, 300 and 2000 K. At any temperature, only the bimolecular products (principally phenyl + H) are formed at zero pressure. As the pressure is increased slightly, the first stabilization products to appear correspond to the complexes with the longest RRKM lifetimes, typically, the isomers with the deepest wells. In the present case, these isomers are benzene (well VII), fulvene (well IV), and 2-ethynyl-1,3-butadiene (well VI). However, as the pressure is increased further the C_6H_6 isomers located early on the reaction path increasingly become the favored stabilization products. At sufficiently high pressure, the only significant products are 1,5-hexadiyne (well I), 1,2,4,5-hexatetraene (well II), and 1,2-hexadiene-5-yne (well V), which are formed directly from $C_3H_3 + C_3H_3$. As the temperature is increased, the trends with pressure do not change, but the low-pressure products tend to persist to higher pressures, as shown in

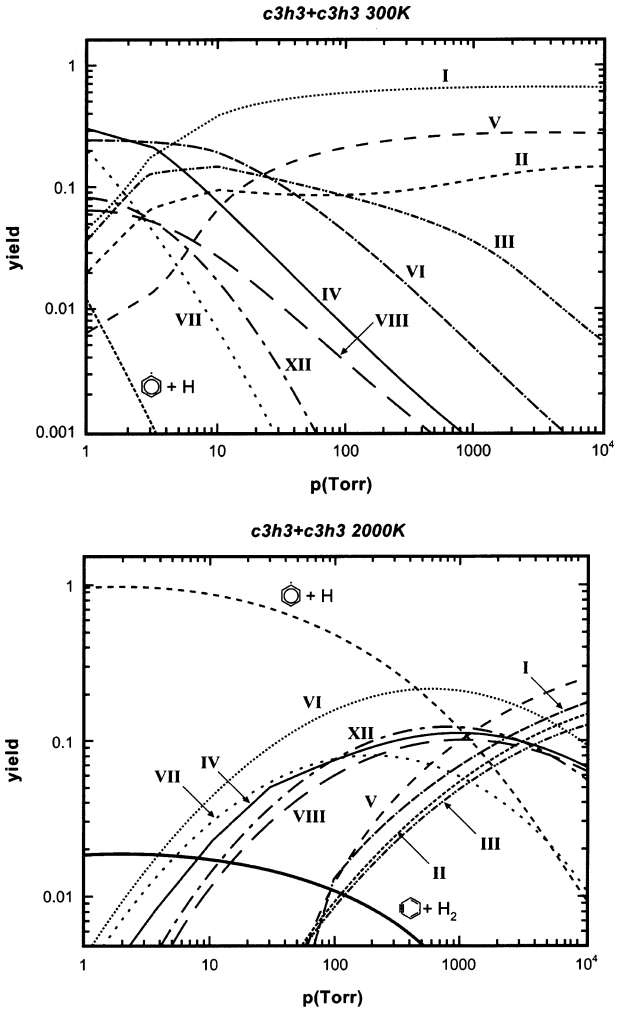

Figure 16. Product distributions for propargyl recombination as a function of pressure. The roman numerals denote stabilization products corresponding to the wells of Figure 14.

Figure 16. Phenyl + H, which amounts to only 4% of the products at $T = 300$ K and a pressure of 1 Torr, is the dominant product up to a pressure of almost one atmosphere at 2000 K.

As the pressure on a gas increases, collisional energy transfer processes equilibrate the reactant better, and the limiting high-pressure rate constants from the master equation should agree with transition state theory. This is actually a plateau rather than a final limit, though, because eventually the rate constants must become diffusion controlled and small at ultrahigh pressures or in liquids.[888−891] However, this physical behavior can easily be masked by changes in the potentials of mean force due to strong interactions, complexation, clustering, condensation, caging, and solvation.[888−892] Supra-high-pressure reactions can also exhibit effects due to transients in the nascent distributions of energized molecules.[893]

3. Gas-Phase State-Selected Reactions and Product State Distributions

In the last section, we discussed how to evaluate thermal rate constants by QCT calculations or by VTST on an adiabatic potential energy surface. However, thermal rate constants are highly averaged quantities, and it is interesting and often important to quantify the contribution of individual states to the total rate. This is discussed for vibrational and

rotational states in Section 3.1. When one considers excited electronic states, one is faced with reactions that cannot be adequately described by a single potential energy surface; this kind of reaction is considered in Section 3.2.

3.1. Electronically Adiabatic Reactions

State-selected rate constants allow one to assess, for example, how the excitation of a given normal mode affects the dynamics of the chemical reaction. For some reactions and some initial vibrational modes state-selected thermal rate constants may be evaluated by a statistical vibrationally diabatic model[894] that assumes that the vibrational modes preserve their characters along the reaction coordinate. This model is obtained from harmonic CVT by replacing the vibrational partition function for state-selected diabatic vibrational mode m in quantum state n_m by $\exp[-(1/2 + n_m)\beta\hbar\omega_m]$. In other cases, a statistical-adiabatic theory is more appropriate.[895−898] Both approaches are probably only applicable to high-frequency modes; low-frequency modes tend to be neither adiabatic nor diabatic. The most reasonable approach for a high-frequency mode is to assume that it is adiabatic, except at narrowly avoided vibrational state crossings, from the start of the collision only until the system reaches a region of high curvature of the reaction path[899] because reaction-path curvature causes vibrational nonadiabaticity.[36,363,364,900,901]

Duncan and Truong[902] and Corchado et al.[903] have calculated state-selected rate constants for the $Cl + CH_4 \rightarrow HCl + CH_3$ reaction. For this reaction vibrational excitation of the C−H stretch and the lowest frequency bending mode of CH_4 accelerate the forward reaction, whereas excitation of the CH_3 umbrella slows down the reaction at temperatures below 800 K and accelerates it for temperatures above 900 K. Similar results have been obtained by Espinosa-García[904] for the $CH_3 + HBr \rightarrow CH_4 + Br$ reaction, in accord with quantum-mechanical calculations.

In the case of atom−diatom and diatom−diatom[905] reactions, it is possible to go further and analyze not only the role played by asymptotic (reactant and product) states but also the role played by individual levels of the quantized transition states in both thermal and state-selected processes. We define a quantized transition state as a dynamical bottleneck with quantized levels. Then we write the canonical rate constant $k(T)$ in terms of the microcanonical one $k(E)$[395]

$$k(T) = \frac{\int_0^\infty \exp(-\beta E)\rho^{\mathrm{R}}(E)k(E)dE}{\Phi^{\mathrm{R}}(T)} \qquad (3.1.1)$$

where $\rho^{\mathrm{R}}(E)$ is the reactant density of states per unit energy. The microcanonical rate constant may be written as[393,906]

$$k(E) = [h\phi^{\mathrm{R}}(E)]^{-1}N(E) \qquad (3.1.2)$$

with

$$N(E) = \sum_{\alpha}\sum_{\alpha'} P_{\alpha\alpha'}(E) \qquad (3.1.3)$$

where $P_{\alpha\alpha'}(E)$ is the completely quantum-number-resolved reaction probability from reactant channel α to product channel α', where "channel" denotes a complete set of quantum numbers for a reactant or product. Since the reactants are bimolecular, α includes the orbital angular momentum quantum numbers of relative translation as well as electronic, vibrational, rotational, and spin quantum numbers. Comparing eqs 3.1.2 and 3.1.3 to eqs 2.4.73 or 2.5.3 shows that transition state theory would be exact if $N^{\mu\mathrm{VT}}(E)$ were equal to $N(E)$. However, $N^{\mu\mathrm{VT}}(E)$ contains the assumptions that we can separate out a classical reaction coordinate (no tunneling) and that there is no recrossing at the dynamical bottleneck defined by the minimum value of the number of states along the reaction coordinate.

On the basis of the above equations, we can write the microcanonical TST rate constant as[365,715,716,907,908] eq 2.5.3 where $N^{\ddagger}(E)$ is now the transition state approximation to the sum over open quantized levels (states) at the transition state:

$$N^{\ddagger}(E) = \sum_{\tilde{\alpha}} \Theta(E - E_{\tilde{\alpha}}) \qquad (3.1.4)$$

where $E_{\tilde{\alpha}}$ is a quantized energy level at the transition state. Note that degenerate levels are included a number of times equal to their degeneracy. To improve on the two approximations mentioned at the end of the previous paragraph, we introduce a transmission coefficient $\kappa_{\tilde{\alpha}}$ for each level of the transition state so that[393,566,567,909−912]

$$N(E) \cong \sum_{\tilde{\alpha}} \kappa_{\tilde{\alpha}}(E) \qquad (3.1.5)$$

For reactions with barriers and hydrogenic motion in the reaction coordinate, the former approximation (no tunneling) is often more serious than the latter (no recrossing). The simplest way to include tunneling in the transmission coefficient is with an effective parabolic potential for motion along a reaction coordinate s:

$$V = E_{\tilde{\alpha}} - \frac{1}{2}k_{\tilde{\alpha}}^{\ddagger}s^2 \qquad (3.1.6)$$

where $k_{\tilde{\alpha}}^{\ddagger}$ is the negative effective force constant. The transmission coefficient for potential (3.1.6) is given by[512]

$$\kappa_{\tilde{\alpha}}(E) = 1/\{1 + \exp[(E_{\tilde{\alpha}} - E)/W_{\tilde{\alpha}}]\} \qquad (3.1.7)$$

where $W_{\tilde{\alpha}} = \hbar|\omega_{\tilde{\alpha}}|/2\pi$ with $\omega_{\tilde{\alpha}}$ being the imaginary frequency equal to $(k_{\tilde{\alpha}}^{\ddagger}/\mu)^{1/2}$. We should keep in mind that the force constant in eq 3.1.6 is an effective force constant, as is the frequency $\omega_{\tilde{\alpha}}^{\ddagger}$. An approximate theory for estimating these quantities has been presented[913] based on a multidimensional semiclassical theory of tunneling.

For simple reactions, the accurate cumulative reaction probability for a given potential energy surface can be calculated by converged quantum mechanical scattering, and if one examines the microcanonical/J-resolved rate constant $k^J(E)$ defined such that

$$k(E) = \sum_J (2J + 1)k^J(E) \qquad (3.1.8)$$

one can see clear structure in the rate constant that matches well with the structure predicted by combining eqs 2.5.6, 3.1.5, and 3.1.7.[395,566,567,909−912] These studies show clearly that the quantized transition states control the structure of the microcanonical rate constants as a function of energy. Furthermore, they show that we can understand the state-to-state dynamics with the highest possible resolution allowed by quantum mechanics, namely, from a specific channel of reactants to a specific level of the quantized transition state, to a specific channel of the product.[566,567,912]

The equations just presented may also be used to derive the ground-state tunneling approximation introduced in Section 2.4.4. According to eqs 3.1.1 through 3.1.3, $k(T)$ is an appropriately normalized sum of

$$P_\alpha(E) = \sum_{\alpha'} P_{\alpha\alpha'}(E) \tag{3.1.9}$$

This normalized sum is denoted in shorthand as

$$k(T) = \langle\langle P_\alpha(E) \rangle\rangle \tag{3.1.10}$$

where $\ll ... \gg$ denotes a generalized "average." Next we multiply and divide by the TST approximation to $k(T)$, which gives

$$k(T) = \frac{\langle\langle P_\alpha(E) \rangle\rangle}{\langle\langle P_\alpha^{\ddagger}(E) \rangle\rangle} k^{\ddagger}(T) \tag{3.1.11}$$

where the denominator is another way to write $k^{\ddagger}(T)$. In the ground-state approximation, we replace the ratio of averages by the ratio for a representative case.

The ground-state is a good representative case because tunneling makes the largest relative contribution to the rate constant at low T (where the overbarrier process has a very small Boltzmann factor), and at low T the system must either be in the ground state or in a state that is energetically similar to the ground state. As the temperature is increased, more states contribute, but also $\kappa(T) \rightarrow 1$. Since $\kappa(T)$ based on the ground state also tends to unity as T increases, there is no great harm in basing it on the ground state at all temperatures. This is equivalent to setting

$$\kappa_{\tilde{\alpha}}(E) = \kappa_0[E - (E_{\tilde{\alpha}} - E_0)] \tag{3.1.12}$$

where $\tilde{\alpha} = 0$ denotes the ground state. If this is inadequate one can use eq 3.1.5 with a less restrictive approximation.

Since this review is mainly concerned with thermal rate constants, the above discussion is mainly concerned with practical methods that are designed for calculating thermal rate constants. For a more complete understanding of a reaction, one must consider more than the valley around the minimum energy path and the dominant multidimensional tunneling paths. In particular, as stated by Sun et al.,[914] "it is necessary to study the actual motion of the atoms on a reactive system's PES." This is generally done by trajectory calculations, but wave packet simulations are becoming reasonably common as well, especially for small systems. The motion of such systems may take one far from the minimum energy path,[159,914−925] and several studies have indicated the presence of interesting secondary pathways for the formation of products in bimolecular reactions passing over potential wells. These "roaming fragment" paths, where a departing fragment abstracts an atom from the other departing fragment, are not well described with standard statistical treatments. In a detailed study, comparing direct dynamics simulations with experimental observations, Marcy et al. demonstrated that the reaction of $O(^3P)$ with CH_3 produces H_2 + HCO predominantly via the abstraction of an H atom from formaldehyde (H_2CO) by the departing H atom.[917] Recent related experimental and trajectory studies have provided clear evidence for the existence of such a "roaming atom" channel in the photodissociation of formaldehyde (i.e., $H_2CO \rightarrow HCO + H \rightarrow H_2 + CO$, where the last step involves an H abstraction by the H from HCO).[921]

A related mechanism provides an explanation for some old experimental observations of Kable and Houston for the photodissociation of CH_3CHO.[924] Similarly, the roaming fragment mechanism provides an explanation for the observation of H_2O as a product in a number of O^- + hydrocarbon reactions.[918] Preliminary results from a number of direct dynamics simulations indicate that roaming fragment pathways are ubiquitous, apparently arising wherever the reverse bimolecular reaction of the product fragments has a barrierless abstraction channel.[925] In particular, roaming fragment branching ratios of at least a few percent were observed in direct B3LYP simulations of the $C_2H_5 + O$, $NH_2 + HO_2$, $HCCO + O_2$, and $CH_3 + C_2H_3$ bimolecular reactions. The branching between these roaming fragment channels and the simple dissociation channels in the decomposition of closed shell molecules may have an important effect on combustion modeling, since in the one case two closed shell molecules are formed, whereas, in the other case two radicals are formed. Knyazev has provided a theoretical model for this branching and applied it to the $CH_3 + O$ reaction.[919]

Discussions of the factors controlling vibrational and rotational energy release and utilization in chemical reactions are presented elsewhere.[36,926−929]

The last topic in this subsection is the prediction of final vibrational−rotational energy distributions or the prediction of the dependence of the reaction rate on rotational energy or low-frequency modes of the reactant that are not expected to remain adiabatic or diabatic even up to the dynamical bottleneck or the first local maximum in the reaction-path curvature. TST is not designed for these problems, and one generally uses classical trajectories for these purposes. Reviews of general principles[36,926−928] and modern methods[32,33,930,931] for trajectory calculations are available. A discussion of the reaction $CN + H_2 \rightarrow HCN + H$ has been presented as a case study where good agreement is obtained between trajectory calculations and approximate quantum scattering theory.[34] Interesting recent case studies involve $OH + D_2 \rightarrow HOD + D$[932] and the $H + H_2O$ reaction.[933]

Trajectory calculations have shown that very high excitation energies may convert a reaction from being thermally activated with a threshold to showing capture behavior such as occurs in barrierless reactions.[934]

3.2. Electronically Nonadiabatic Reactions

Up to this point, we have employed the assumption that the Born−Oppenheimer (adiabatic) approximation is valid, which implies that a single potential energy surface controls the reaction dynamics. However, there are many reactions, called non-Born−Oppenheimer reactions or electronically nonadiabatic reactions, in which dynamics does not proceed on a single potential energy surface. These reactions include many photochemical and chemiluminescent processes, in particular, bimolecular reactions initiated in an electronically excited state[935,936] and those that produce an electronically excited species (sometimes called chemiluminescent reactions) and also unimolecular photodissociations and photoisomerizations.[937−939] Just as for electronically adiabatic reactions the ultimately preferred approach would be quantum mechanical scattering theory. Although quantum mechanical methods are available,[940] their cost has so far prohibited converged calculations except for atom−diatom reactions.[941−943] Therefore, we will focus on semiclassical methods[944] in which the nuclear motion is treated classically, whereas the transitions between electronic states are treated by quantum mechanics.

We will begin by using the adiabatic potential energy surfaces, V_γ, which, in the notation of eq 2.3.2, are defined by

$$V_\gamma \equiv V_{NR} + E_\gamma^{(el)} \tag{3.2.1}$$

Note that V_1 was just called V in earlier sections of this review, except in eqs 2.4.49−2.4.51. For a general polyatomic system without symmetry, and neglecting spin−orbit interactions, if there are N atoms, the potential energy surfaces depend on $3N - 6$ internal coordinates, and the potential surfaces may intersect in a $3N - 8$ dimensional subspace;[945] these are called conical intersections because the surfaces separate like a conical bifunnel in the other two internal degrees of freedom. Conical intersections, though not required in the general case, should not be rare.[946,947]

The semiclassical methods make a distinction between the quantum mechanical variables **r** (electronic coordinates) and the classical mechanical variables **R** (nuclear coordinates). The latter are described by classical trajectories $\mathbf{R}(t)$, and the former are described by the time-dependent Schrödinger equation

$$i\hbar\dot{\Psi}(\mathbf{r},t) = H^{(el)}(\mathbf{r},\mathbf{R})\Psi(\mathbf{r},t) \tag{3.2.2}$$

where Ψ and $H^{(el)}$ are respectively the electronic wave function and electronic Hamiltonian, and an overdot denotes a time derivative. Expanding the electronic wave function in two electronically adiabatic eigenstates

$$\Psi(\mathbf{r},t) = \sum_{\gamma=1}^{2} a_\gamma(t)\phi_\gamma(\mathbf{r};\mathbf{R}(t)) \tag{3.2.3}$$

where the coefficient a_γ is an electronic amplitude yields the following electron density

$$|\Psi(\mathbf{r},t)|^2 = \sum_{\gamma=1}^{2}\sum_{\gamma'=1}^{2} a_\gamma(t)a_{\gamma'}^*(t)\phi_\gamma(\mathbf{r};\mathbf{R}(t))\phi_{\gamma'}^*(\mathbf{r};\mathbf{R}(t)) \tag{3.2.4}$$

where * denotes a complex conjugate. Therefore, the electronic density matrix is

$$\rho_{\gamma\gamma'}(t) = a_\gamma(t)a_{\gamma'}^*(t) \tag{3.2.5}$$

Substituting eq 3.2.3 into eq 3.2.2 and using eq 3.2.5, the Hermitian character of ρ, the anti-Hermitian character of **d**, and the semiclassical approximation

$$\frac{d}{dt} = \dot{\mathbf{R}}\cdot\nabla_{\mathbf{R}} \tag{3.2.6}$$

for the time derivative yield the following coupled equations for the time evolution of the density matrix elements:[948]

$$\dot{\rho}_{11} = -2\mathrm{Re}(\rho_{21}\dot{\mathbf{R}}\cdot\mathbf{d}_{21}) \tag{3.2.7}$$

where Re denotes the real part and

$$\dot{\rho}_{12} = (\rho_{11} - \rho_{22})\dot{\mathbf{R}}\cdot\mathbf{d}_{12} + i\rho_{12}(V_2 - V_1)/\hbar \tag{3.2.8}$$

with similar equations for $\dot{\rho}_{22}$ and $\dot{\rho}_{21}$, where

$$d_{\gamma\gamma'} = \langle\phi_\gamma|\nabla_{\mathbf{R}}|\phi_{\gamma'}\rangle \tag{3.2.9}$$

The matrix elements $d_{\gamma\gamma'}$ are called the nonadiabatic coupling matrix elements, or—when multiplied by $\hbar/i$—the nuclear momentum couplings. These matrix elements are typically of the order of magnitude of unity in atomic units,[949] but they are large *near* conical intersections of the two states involved, and they are infinitely large *at* conical intersections.[950−953] Far from conical intersections the effects of the nonadiabatic terms are expected to be small enough that the Born−Oppenheimer approximation is a good approximation,[949] because the nonadiabatic matrix elements of eq 3.2.29 are multiplied by $\dot{\mathbf{R}}$ or $1/\mu$,[949] which are small in atomic units. These considerations can be expressed in more mathematical terms[949] by making expansions in fractional powers of the ratio of electronic to nuclear mass, a technique first introduced by Born and Oppenheimer.[58]

The solution of the two coupled equations for the electronic amplitudes by first-order perturbation theory gives the Massey criterion[954,955] for adiabatic behavior, which may be written in modified form as[956,957]

$$\xi_{12} = (V_1 - V_2)/\hbar|d_{12}\cdot\dot{\mathbf{R}}| \tag{3.2.10}$$

If $\xi_{12} \gg 1$ the system can be considered adiabatic and the Born−Oppenheimer approximation should be reasonable. Nevertheless, even when the electronically nonadiabatic transition probabilities are small, it is often important to be able to calculate them.

The adiabatic wave functions ϕ_γ and the adiabatic potential energy surfaces V_γ can be written as the eigenvalues of the diabatic potential surface matrix

$$\mathbf{U} = \begin{pmatrix} U_{11} & U_{12} \\ U_{12} & U_{22} \end{pmatrix} \tag{3.2.11}$$

specifically

$$V_\gamma = \frac{1}{2}[(U_{11} + U_{22}) - ((U_{22} + U_{11})^2 - 4(U_{11}U_{22} - U_{12}^2))^{1/2}] \tag{3.2.12}$$

The transformation between adiabatic (ϕ_γ) and diabatic (ψ_γ) wave functions is

$$\phi_\gamma(\mathbf{r};\mathbf{R}) = \sum_{\gamma'}\psi_{\gamma'}(\mathbf{r};\mathbf{R})T_{\gamma'\gamma}(\mathbf{R}) \tag{3.2.13}$$

where

$$T_{\gamma'\gamma}(\mathbf{R}) = \begin{pmatrix} \cos\theta(\mathbf{R}) & \sin\theta(\mathbf{R}) \\ -\sin\theta(\mathbf{R}) & \cos\theta(\mathbf{R}) \end{pmatrix} \tag{3.2.15}$$

with a mixing angle $\theta(\mathbf{R})$ given by

$$\tan 2\theta(\mathbf{R}) = \frac{2U_{12}}{U_{11} - U_{22}} \tag{3.2.15}$$

A variety of methods have been proposed for carrying out diabatic transformations.[274,953,958−972]

The key assumption one makes when one uses a diabatic representation is that the effect of the vector coupling $\langle\psi_\gamma|\nabla_R|\psi_{\gamma'}\rangle$ may be neglected as compared to the effect of the scalar coupling $U_{\gamma\gamma'}$. It is impossible, in general, to find a transformation that makes all components of the vector coupling zero over a finite region of space.[973,974] But one can find transformations that reduce it everywhere to the order of 1 atomic unit or less, and it always gets multiplied by a quantity like $1/\mu$, which is small in atomic units, or

like $\dot{R}$, which is small in atomic units in the chemical energy range. Even at the high energy of 10 eV, the speed of a proton is only 0.02 atomic units.

Although there is no unique way to specify the diabatic representation, it is useful to define it such that the momentum coupling has a negligible effect and that the diabatic electronic wave functions are smoothly varying functions of **R**. The adiabatic states diagonalize the electronic Hamiltonian but are coupled by the nuclear momentum, whereas diabatic states have no nuclear momentum coupling although they are coupled by off-diagonal elements (U_{12}) of the electronic Hamiltonian. In the adiabatic representation the coupling is given by a nonsmooth vector $\mathbf{d}_{12}$, whereas it is a smooth scalar in the diabatic representation; the vector coupling is less convenient than the scalar one, but the adiabatic representation has the advantage that one can optimize the adiabatic wave functions by the variational principle. The advantages of both representations may be combined by defining diabatic basis sets in terms of adiabatic basis sets using orthogonal or unitary transformations.[957,958,960,969,971,972]

If we assume a 1D model in which U_{11} crosses U_{22} with U_{12} approximately constant, we obtain the Landau−Zener[975−977] one-way transition probability P_{LZ}, which is the single-passing probability of a nonadiabatic transition from the adiabatic state 1 to the adiabatic state 2, and is given by

$$P_{LZ} = 1 - \exp\left[-\frac{2\pi U_{12}^{\,2}}{\hbar\dot{Z}\left|\frac{dU_{11}}{dZ} - \frac{dU_{22}}{dZ}\right|}\right] \quad (3.2.16)$$

where Z is the component of **R** along the path, and all quantities are evaluated at the crossing point. Important further improvements of the Landau−Zener model were presented in subsequent years.[978−983]

Another general class of models is appropriate for the Rosen−Zener−Demkov case where the two diabatic surfaces do not cross.[984,985] Although such simple models are useful for showing the nature of the dependence of transition probabilities on key variables, they are too simplified to provide quantitative results for real systems, and the best available option for practical work is nonadiabatic trajectory calculations.

A key reason multidimensional trajectory calculations are required is the prevalence of conical intersections, which are intrinsically multidimensional. When one encounters a local minimum (along a path) of the gap between two adiabatic potential energy surfaces, almost always this will be because one has passed near a conical intersection, rather than a true avoided crossing corresponding to a finite local minimum in the gap.[947] In an adiabatic representation, the nonadiabatic coupling becomes singular at conical intersections,[950,951] but this singularity can always be removed by transformation to a diabatic representation.[274,949−953,969,970,986] Furthermore, one can show[949] by expansion[58] in powers of m_e/μ, where m_e is the mass of an electron and μ is a nuclear mass, that in normal molecular situations, apart from the singularity, the effect of the rest of the nonadiabatic coupling can be expected to be small in the Born−Oppenheimer sense. Therefore, the nonadiabatic coupling is often dominated by small regions around a conical intersection (regions in which the singular leading term in the nonadiabatic coupling dominates the other terms). Furthermore, in high-symmetry cases or when only the lowest-energy part of the seam of conical intersections is important, one can understand the interactions between the electronic states in terms of an easily obtained[274,951,969,970] diabatic basis. This provides a route to simple models as well as to quantitative treatments. Even when one needs more complicated algorithms to obtain diabatic states that remove all the singular coupling,[972] diabatic states still often provide useful models as well as the starting point for quantitative dynamics.

The conversion of electronic energy to nuclear-motion energy by decay from an electronically excited singlet or doublet state to the ground electronic state is called internal conversion, radiationless decay, or an electronically nonadiabatic transition. Internal conversion is often the critical first step in photochemical processes. The proposals, in various forms, by Teller,[946,987] Zimmerman,[988] and Michl[989] that internal conversions in regions close to conical intersections are characteristic steps in many photochemical reactions was one of the first steps forward in describing photochemical processes in terms of geometric features in excited-state potential energy surfaces.[990−993] Decay of electron excitation energy in the vicinity of a conical intersection involves entangled electronic and nuclear motion on a time scale of tens of femtoseconds and has been studied in a variety of systems.[994−1030]

However, one must also be careful not to oversimplify. First of all, the most critical region is the region near the conical intersection seam in which the singular terms[274,949−951,969,970] dominate the coupling, not just the conical intersection seam itself. Second, the region around the *lowest-energy* conical-intersection point may be insufficient even for a zero-order picture[1031−1033] As an analogy, it is worthwhile to compare the situation to that for thermally activated single-surface reactions, where we know that transition state theory, which emphasizes the low-energy region around a saddle point or the lowest energy portion of a variational transition seam, is very useful when reaching the transition state is a rare event in the free energy sense.[1034] A similar approach can be applied to certain electronically nonadiabatic reactions.[1035] However, returning to the electronically adiabatic case, if one wants to calculate branching ratios when the total energy significantly exceeds the energy of the controlling dynamical bottlenecks,[413] then a transition state picture may be less appropriate, and one needs to invoke less reliable statistical assumptions.[413,717−720,1036] Closely related problematic systems involve potential energy surfaces where dynamical branching is controlled by trajectories leaving a plateau region in various directions or by trajectories that reach points of no return from unequilibrated regions of phase space.[417,418,959,1037−1039] These kinds of scenarios are probably even more prominent in electronically nonadiabatic systems, where the total energy is often sufficient to reach large portions of one or more conical intersection seams rather than just their lowest-energy part. In such cases one needs to map out the characteristics of the seam or seams more fully. Even in such cases, statistical theories are available,[1040−1047] but they are not always valid because the probability of decay at one or another portion of the seam may be determined by initial conditions (as determined, for example, by Franck−Condon factors) or by inertial or other dynamical factors, not just by statistics. Thus, one requires trajectory calculations, such as the surface hopping or decay-of-mixing methods discussed below, or wave packet calculations.

Finally, it is important to keep in mind that although conical intersections are not rare, very many interesting processes do not involve them because the seam of diabatic crossing does not intersect a seam of zero diabatic coupling at an accessible geometry or because the diabats do not cross. Nevertheless, a diabatic picture can still be very useful. Furthermore, in cases such as this, multidimensional dynamics calculations (nonadiabatic trajectories or wave packets) are very important because 1D models of the dynamics do not appear to be generally valid even in the absence of conical intersection.[941]

The use of diabatic potential energy surfaces is expected to greatly ease the fitting of potential energy surfaces because (i) diabatic surfaces are much smoother than adiabatic ones and (ii) the couplings in diabatic representations are smooth, scalar functions, whereas in adiabatic representations they are rapidly varying, singular, vector functions. However, one promising approach to fitting the adiabatic surfaces, at least for exploratory dynamics, is the SRP method (see discussion in Section 2.3), which has been extended to non-Born−Oppenheimer problems by Martínez-Nuñez et al.[1048]

Nonadiabatic trajectory methods based on ensembles of independent trajectories are especially relevant in the search for simple guiding pictures because they lead to visualizable dynamics. Two standard methods based on classical trajectories are the trajectory surface hopping (TSH)[957,1049−1054] approach and Ehrenfest method or self-consistent potential (SCP)[956,957,1054,1055] approach. The TSH method was initially suggested by Nikitin[1049] and Tully and Preston.[1050] In these early studies, the trajectories were propagated on the adiabatic surfaces, and probability for trajectories to hop was evaluated by the Landau−Zener model. A more complete theory in which the trajectories are coupled to eqs 3.2.3 for arbitrary surface characteristics was proposed later[1051] and successively refined[1052,1053,1056−1059] In general, trajectories may be propagated on either the adiabatic or diabatic surfaces.

Tully's fewest switches scheme[956,1052] is particularly appealing because it employs the fewest number of switches necessary to obtain ensemble-averaged consistency between the quantum and classical degrees of freedom in the limit of $V_1(\mathbf{R}) = V_2(\mathbf{R})$. In this method, self-consistency is accomplished by propagating an ensemble of trajectories on the diagonal potential matrix elements, with each trajectory being independent of the others, and with the probability that a trajectory that is propagating on one potential surface will hop to another being determined such that the fraction of trajectories propagating on surface γ is (if energy conservation permits) given by $\rho_{\gamma\gamma}$.

A serious problem with the TSH method is that hops from the lower surface to the upper surface can be forbidden by conservation of energy or momentum (frustrated hops), and this destroys the self-consistency of the coupled treatment of electronic and nuclear motion.[1060] These frustrated hops have two causes:[957] (1) the original fewest-switches method[1052] does not allow tunneling into a new electronic state, which is a consequence of a classical trajectory approach, and (2) it does not properly treat electronic state dephasing, which is a result of the formulation of the hopping probability. The frustrated hops associated with (1) are considered physically meaningful and the transition between states should be allowed, whereas the hops associated with (2) are not physically meaningful and should be ignored. New surface hopping methods identify the frustrated hops associated with tunneling and attempt to improve the self-consistency of the method by allowing nonlocal surface hops.[1057,1058] This problem is also partially ameliorated by methods that propagate wave packets instead of trajectories,[1061−1065] although these are more expensive.

The semiclassical Ehrenfest method is quite different; in particular, in this method the effective PES is given by the expectation value of the electronic Hamiltonian computed with the current density matrix, with no hops. Because the trajectories are propagated on this averaged potential, the results are independent of the choice of representation (adiabatic or diabatic) of the electronic wave function. This is an important advantage because the surface hopping methods can be very inaccurate if one chooses to use the wrong representation. The most apppropriate basis in which to carry out the calculations would be the "pointer" basis,[1066,1067] but this is usually not known. An approximate rule, called the Calaveras County criterion, for determining this basis has been presented.[1068]

The biggest drawback of the semiclassical Ehrenfest method is that trajectories propagating on an average surface may *finish* on an average surface, which corresponds to being in a mixed electronic state that is not an allowed final state because it is not an eigenvalue of the asymptotic electronic Hamiltonian. In such a case the final electronic, vibrational, rotational, and translational energies of the products are not realistic. This problem has been solved by including decay-of-mixing terms in eqs 3.2.7 and 3.2.8.[1069,1070] The mixed state is thereby resolved into one or another pure electronic state as the trajectory leaves the region of interstate coupling. Adding the decay of mixing terms makes the trajectories depend on representation (adiabatic or diabatic), but the dependence is small.

The self-consistent decay of mixing (SCDM) method[948] and the coherent switching decay of mixing (CSDM) method[1071] both incorporate such decay terms, but they require only about the same amount of computational effort and data as the other methods we have discussed. The decay of mixing rate must be based on two different kinds of consideration; it has a physical component corresponding to physical population dynamics and dephasing,[1072] but this is not identical to the algorithmic decay rate required in order that an ensemble of trajectories with a specific semiclassical prescription for electronic state switching and nuclear motion will correctly simulate a quantum mechanical wave packet.[948,1071] The decay of mixing algorithm is based on both considerations. It has performed quite well in comparison to accurate quantum dynamics for electronically nonadiabatic atom−diatom reactions,[948,1067,1071,1073,1074] and the SCDM and CSDM are the most accurate available nonadiabatic trajectory methods.

There is a fundamental difference between nonadiabatic coupling in internal coordinates (vibronic interactions, as discussed so far) and nonadiabatic coupling caused by overall rotation. Most attention has been paid to the former. The terms in the rotational kinetic energy that couple internal motions such as vibrations and electronic degrees of freedom are called Coriolis terms. In polyatomic molecules, electronic Coriolis coupling has been much less widely studied than vibronic interactions, although the surface hopping method can include this kind of transition.[1075] The different mechanisms have been compared elsewhere.[957,983,1076]

The discussion has centered so far on spin-conserving processes, which are often promoted by intersections occurring in at most $3N - 8$ dimensions. In contrast, singlet triplet

intersections may occur on a $(3N - 7)$-dimensional seam. Electronic structure calculations may be used to characterize the intersections,[1077−1082] especially by calculating the minimum on the seam of surface crossing (MSX). Dynamical theories for predicting the probabilities of spin-forbidden processes have been developed.[1078,1080,1081,1083]

4. Condensed-Phase Bimolecular Reactions

Many reactions of interest occur either in solution or at a gas−surface interface. In some reactions, the solvent or the surface has only a small effect, but usually it has a large effect. For instance in liquids, the rates of unimolecular reactions between nonpolar species are sometimes roughly independent of the type of solvent, but in the case of polar molecules the rates may be speeded up or slowed down by large factors in liquid solution as compared to the gas phase, even for nonpolar solvents. One example is the Claisen rearrangement of the polar molecule allyl vinyl ether to 4-pentenal, which is speeded up by about 3 orders of magnitude in aqueous solvation as compared to the gas phase; even in the nonpolar solvent hexadecane it is speeded up by about one order magnitude.[1084,1085] Bimolecular reactions involving ions and polar molecules generally depend strongly on the solvent. The key consideration is often the difference in solvation free energy of the transition state and the reactants, but in bimolecular reactions one must also consider long-range interactions and gradients of concentration. Reactions in solids show similar effects although the slower diffusion through solids is often a dominant consideration. The effect of a solid surface, such as ice, a metal oxide, or a metal, on reactivity is often so large that the surface is considered to be a catalyst. Processes at metal surfaces often show strong effects of Born−Oppenheimer breakdown.[1086] Overviews of the application of transition state theory to liquid-phase and solid−gas interface reactions are available elsewhere,[347,349,356,1034,1087−1098] and key theoretical developments are summarized in the context of this review in the following two subsections.

4.1. Reactions in Liquids

In general, a reaction in solution can be modeled by the following mechanism

$$A + B \underset{k_{-D}}{\overset{k_D}{\rightleftharpoons}} AB \xrightarrow{k_2} \text{Products} \tag{4.1.1}$$

where AB is the transient complex formed by the encounter of the two molecules. The rate of this reaction may be derived by applying the steady-state condition to the complex, which yields

$$k = \frac{k_D k_2}{k_{-D} + k_2} \tag{4.1.2}$$

A typical value of k_D is 4×10^9 M^{-1} s^{-1}. If $k_2 \gg k_{-D}$ the reaction is controlled by diffusion. In the opposite case of $k_{-D} \gg k_2$ the bimolecular reaction rate is

$$k_{eq} = Kk_2 \tag{4.1.3}$$

where $K = k_D/k_{-D}$. When eq 4.1.3 holds the existence of the complex becomes irrelevant (the numerator of K exactly cancels the denominator of k_2), which is a special case of the general rule that an intermediate before the rate-determining step has no effect on the rate.

When the reaction is diffusion controlled, the concentration of B molecules in the vicinity of A molecules becomes depleted.[1099,1100] The equation governing the diffusion of B molecules toward A is Fick's first law of diffusion. The number of B molecules per unit time reaching a spherical surface of area $4\pi R^2$ at a distance R from A is

$$J = 4\pi D_{AB} R^2 \frac{d[B]}{dR} \tag{4.1.4}$$

where D_{AB} is the binary diffusion coefficient. By solving eq 4.1.4 with an appropriate boundary condition[1101] at $r = \sigma_{col}$, where σ_{col} is a collision diameter, one can again derive eq 4.1.2 where

$$k_D = 4\pi\sigma D_{AB} \tag{4.1.5}$$

Equation 4.1.5 is appropriate in the case where intermolecular forces are neglected for $R > \sigma_{col}$. If $V(\sigma_{col})$ cannot be neglected, as for the reaction of two ions of charge q_A and q_B for which

$$V(\sigma_{col}) = \frac{q_A q_B}{\epsilon \sigma_{col}} \tag{4.1.6}$$

where ϵ is the dielectric constant, then eq 4.1.2 is replaced by

$$k = \frac{k_D k_2 e^{-\beta V(\sigma_{col})}}{k_D + k_2 e^{-\beta V(\sigma_{col})}} \tag{4.1.7}$$

For slow reactions, there should be a substantial barrier for the second step of reaction 4.1.1, and therefore $k_D \gg k_2 \exp[-\beta V(\sigma_{col})]$, and eq 4.1.7 reduces to

$$k = k_2 \exp[-\beta V(\sigma_{col})] \tag{4.1.8}$$

This equation has been used to interpret reactions between ions. The substitution of eq 4.1.6 into eq 4.1.8 allows one to obtain an effective value of σ_{col} by plotting the logarithm of k versus $1/\epsilon$.

When $k_2 \ll k_{-D}$, reactions in solution can be modeled by TST. Even when this relation does not hold, TST may be used to model k_2. Using the formalism of eq 2.2.4, we can express the entire effect of solvation on the reaction rate (either k_{eq} or k_2) as follows:

$$\Delta\Delta G_{act} \equiv G^o_{act}(l) - \Delta G^o_{act}(g) \tag{4.1.9a}$$

$$= \Delta G^{\ddagger,o}_T(l) - \Delta G^{\ddagger,o}_T(g) - RT \ln [\gamma(T,l) - \gamma(T,g)] \tag{4.1.9b}$$

where l and g denote the liquid-phase and gas-phase environments, respectively. With this fundamental equation available to organize the discussion, we can distinguish three levels of dynamical theory for calculating bimolecular reaction rates in liquid solutions. These levels will be called separable equilibrium solvation (SES), equilibrium solvation path (ESP), and nonequilibrium solvation (NES.)

A key result needed to relate condensed-phase thermochemistry to the gas phase is the equation for the solvation of a single substance.[1097,1102]

$$G^o_T(l) = G^o_T(g) + \Delta G^o_S(T) \tag{4.1.10}$$

where ΔG_S^o is the standard-state free energy of solvation of the substance in question. Therefore, the free energy change of eq 2.1.7 becomes

$$\Delta G_T^o(l) = \Delta G_T^o(g) + \Delta\Delta G_S^o \qquad (4.1.11)$$

where the first delta in the last term, like that in eq 2.1.7, denotes the difference between product and reactants, and the second delta in this term, like the one in eq 4.1.10, refers to the solvation process. By the quasithermodynamic analogue we also have

$$\Delta G_T^{\ddagger,o}(l) = \Delta G_T^{\ddagger,o}(g) + \Delta^\dagger \Delta G_S^o \qquad (4.1.12)$$

where $\Delta^\ddagger$ denotes the difference between the transition state and reactants.

Equation 4.1.12 also applies to generalized transition states. However, to calculate transmission coefficients we need not just the free energy of activation profile but also effective potentials for estimating tunneling contributions and recrossing factors. For this purpose, we use the canonical mean shape approximation[1103]

$$W(\mathbf{R}) = V(\mathbf{R}) + \Delta G_S^o(\mathbf{R},T) + \beta\frac{\partial G_S^o(\mathbf{R},T)}{\partial\beta} \qquad (4.1.13)$$

where $V(\mathbf{R})$ is the gas-phase potential energy of the solute, $\mathbf{R}$ denotes the collection of all the atomic coordinates of the solute, $W(\mathbf{R})$ is the effective potential of the solute in the liquid phase, and $\Delta G_S^o(\mathbf{R},T)$ is the standard-state free energy of solvation of the rigid solute. In practice, one approximates eq 4.1.13 by the zero-order canonical mean shape approximation[1103]

$$W(\mathbf{R},T) = V(\mathbf{R}) + \Delta G_S^o(\mathbf{R},T) \qquad (4.1.14)$$

The right-hand side of eq 4.1.14 is called[1104] the potential of mean force. Thus the zero-order canonical-mean-shape approximation consists of setting the effective potential equal to the potential of mean force.

If the solute has N atoms, the potential of mean force $W(\mathbf{R},T)$ is a function of $3N$ coordinates and corresponds to averaging the solvent forces over a thermal ensemble of solvent coordinates. Another useful quantity is the 1D potential of mean force $W(z)$ which corresponds to averaging over not only the solvent but also $3N - 1$ of the solute coordinates, leaving a function of a single pre-selected coordinate, usually taken as a physically motivated reaction coordinate. Most generally z could be a function not only of the $3N$ solute coordinates but also of solvent coordinates; it could even be a collective solvent coordinate.

In the SES approximation,[1105] one calculates the first term of eq 4.1.9b by using the approximation

$$G_T^o(l) = G_T^o(g) + \Delta G_S^o(\mathbf{R}_e,T) \qquad (4.1.15)$$

for reactants, where $\mathbf{R}_e$ is the equilibrium gas-phase geometry, and by the approximation

$$G_T^{\ddagger,o}(l) = G_T^{\ddagger,o} + \Delta^\dagger \Delta G_S^o(\mathbf{R}^\ddagger,T) \qquad (4.1.16)$$

for transition states, where $\mathbf{R}^\ddagger$ is the gas-phase transition-state geometry. For the second term of eq 4.1.9b, the effective potential used to calculate the transmission coefficient is obtained by eq 4.1.13 or eq 4.1.14, and the transmission coefficient is based on the gas-phase minimum energy path. Separable equilibrium solvation often provides quite useful results with a minimum of effort.[1106]

The separable assumption for the solute reaction path is removed in the ESP approximation.[347,611,1092,1103,1105] In particular, one introduces eq 4.1.14 at all stages of the calculation. Thus, for example, one finds a new minimum energy path using $W(\mathbf{R})$ instead of $V(\mathbf{R})$.

The SES and ESP approximations assume a clear separation of solute and solvent in that the generalized transition state dividing surface is defined entirely in terms of solute coordinates $\mathbf{R}$. This restriction is sometimes important, and even the best dividing surface defined in this way may involve significant amounts of recrossing. This effect is called solvent friction or nonequilibrium solvation. There are several possible ways to treat this kind of effect, the most obvious of which involve treating some or all of the solvent coordinates explicitly on the same footing as the solute. Treating a few solvent molecules explicitly and the rest implicitly by means of $\Delta G_S^o(T)$ or $\Delta G_S(\mathbf{R},T)$ functions is called a mixed discrete-continuum model[1107−1110] a semi-continuum model,[1110] or a cluster-continuum model.[1111] The collection of the solute and all explicit solvent molecules is called the supermolecule. A serious problem with this approach is that the number of conformers grows very rapidly as one adds more solvent molecules to the supermolecule due to the large number of solvation sites and solvent molecules orientations, and the potential surface becomes very anharmonic, so it becomes impractical to compute solute partition functions by the usual methods. This problem can become serious with even as few as two or three solvent molecules.

Another approach to nonequilibrium solvation is to include collective solvent coordinates (as opposed to actual atomic coordinates of individual solvent molecules) in the solute (or supermolecule) Hamiltonian.[1112−1120] Such collective coordinates can represent, e.g., the electric polarization of the solvent, which is not necessarily in equilibrium with solute motion. The collective solvent approach may be used to derive a simple approximation, called Grote−Hynes theory,[1093,1095,1121] to the nonequilibrium solvation effect based on the friction on the reaction coordinate z in the vicinity of the maximum of the 1D potential of mean force $W(z)$. Typically the Grote−Hynes transmission coefficient is in the range $0.3 < \Gamma < 1$. Chuang and Truhlar[1119] made a quantized VTST study of the reaction $H + CH_3OH \rightarrow H_2 + CH_2OH$ in water at 298 K with 21 solute degrees of freedom and one collective solvent mode. They calculated $\Gamma_{friction} \cong 0.4$ without tunneling and $\Gamma_{friction} \cong 0.5$ with tunneling.

A question that arises is whether nonequilibrium solvation is included in the free energy of activation or in the transmission coefficient.[1098] When a solvent degree of freedom is important for specifying the least-recrossed dividing surface, but it is not included in the computational reaction coordinate, the effect shows up as a reduced transmission coefficient. If the effect is recognized, though, and coupled motion is included in the reaction coordinate, then the effect shows up in the free energy of activation.

Another approach to nonequilibrium solvation has been presented by Warshel and co-workers, first for electronically nonadiabatic electron-transfer reactions[680,1122] and then for electronically adiabatic reactions.[308,1123−1125] In this approach, the solvent is included in the reaction coordinate, even for

electronically adiabatic reactions, as an electronically diabatic energy gap[1120] computed from an empirical valence bond representation of the potential energy surface. This approach has advantages when nonequilibrium solvation effects are large.

Finally, there are cases where it is necessary to treat the whole system explicitly. Two frameworks are available for calculating rate constants in such cases. One is called ensemble-averaged variational transition state theory (EA-VTST).[1126−1130] This method lends itself well to including quantum effects; for this purpose the system is divided into a primary zone and a secondary zone, and quantum effects are included in the former. In a first stage one uses a preselected reaction coordinate *z*, called a distinguished reaction coordinate, to compute a 1D potential of mean force $W(z)$. Then one calculates the reaction rate by eq 2.2.3 with the approximation:

$$\Delta G_{act}(T) = \max_z W(z) - \min_z W(z) \qquad (4.1.17)$$

where the maximum corresponds to the transition state and the minimum corresponds to reactants. The theory is general enough to accommodate any reasonable choice of reaction coordinate for z; note though that eq 4.1.17 is only valid for a planar density surface, which implies a rectilinear reaction coordinate, as assumed in eq 2.4.16. For a more general dividing surface, there is an additional term,[378−381] which is often neglected (see Section 2.4.5). One can incorporate tunneling in this theory and allow for the participation of secondary-zone coordinates in the reaction coordinate by stages that employ a static-secondary-zone (SSZ) approximation or an equilibrium-secondary-zone (ESZ) approximation.[1126,1129,1130]

Equation 4.1.17 has been used frequently, in a variety of contexts, to study organic bimolecular reactions in liquid solutions,[1106,1131−1145] with various levels of approximation in the calculation of $W(z)$. For example, *z* may be a distinguished reaction coordinate, or the reaction coordinate may be optimized in the gas-phase or in the liquid-phase solution. Furthermore, one can distinguish various degrees of coupling between the solute and the solvent in modeling the potential energy surface, which is discussed further below. In addition, dual-level methods originally developed (see Section 2.4.5) for gas-phase calculations may be used to improve the accuracy in an efficient way.[1144]

In some cases, when it is not clear a priori how to choose the progress variable *z*, one first explores the detailed dynamical mechanism by calculating the potential of mean force as a function of two[1129,1146−1148] or more[1145,1149] variables.

An example of a complicated reaction coordinate that can be used to describe a complex process is the modified-center-of-excess-charge reaction coordinate developed to study long-range proton-transfer kinetics.[1150]

Although thorough coverage of enzyme dynamics is beyond the scope of the present review, we note that there has been considerable recent progress in including tunneling[489,1098,1126−1130,1151−1156] and recrossing[489] in the transmission coefficient even for reactions as complicated as enzyme-catalyzed reactions.

The second general formalism for calculating reaction rates when a collection of paths and the entire system must be explicitly considered is transition path sampling,[689,690,1157−1159] in which one statistically samples an ensemble of reaction paths without defining a progress coordinate such as the coordinate used in umbrella sampling. Having found the ensemble of paths, one calculates the transmission coefficient and reaction rate as a flux correlation function (see Section 2.4.8). This formalism, like EA-VTST, is particularly motivated by the fact that liquid-phase reactions involve a myriad of saddle points, often differing only in terms of solvent conformations, and each saddle point has its own minimum-energy path. There is an ensemble of system trajectories in the valley corresponding to each saddle point and associated minimum-energy path, and this ensemble may be treated by VTST, but there is an even more diverse ensemble associated with the ensemble of saddle points and minimum energy reaction paths. EA-VTST and transition path sampling provide statistical mechanical algorithms for including the contributions of trajectories sampling this broad ensemble of reaction valleys.

Another important dynamical issue is decoherence, whose effects have recently been elucidated by Han and Brumer[1160] for a model collinear reaction in a solvent that causes decoherence but not solute−solvent energy transfer. The effect of the solvent is to increase the energy dispersion in the solute. In the tunneling regime (below threshold), this increases the fraction of the wave packet with energy above the barrier and hence increases the reaction probability.

For reactions in liquid-phase solution, progress has required not only new formulations of the dynamics but also new methods for calculating the potential energy surface. In some cases, one uses a model for the potential energy surface and obtains the required free energies by statistical averaging. In other cases, for example, when using continuum approximations for the solvent,[1097] one directly calculates the free energy of solvation without an explicit model for the potential energy of solvation. Explicit models of the solvent, especially molecular mechanics,[1161] are also in widespread use, and the coupling between the degrees of freedom treated by molecular mechanics and those treated by quantum mechanics may be handled at various levels of sophistication.[1162−1165] The effective fragment model[1166] provides a way to model ab initio solvation effects in a computationally efficient way, and it has been validated for the bimolecular Menshutkin reaction in aqueous solution.[1167]

Electron transfer reactions present a very special class of reactions in that they may be electronically nonadiabatic and may show large nonequilibrium effects.[1112,1168−1172] There is a considerable amount of interesting work using theoretical approaches originally developed for electron transfer to treat broader classes of reactions.[347,1120,1122,1125,1171−1183]

4.2. Reactions on Surfaces and in Solids

Adsorption is the process of attachment of particles to a surface; the inverse process is desorption. For a gas molecule A(g) (adsorbate), which is binding to the surface S (the adsorbent), the processes of adsorption and desorption can be represented by the chemical equation

$$A(g) + S \rightarrow A{\cdot}S \qquad (4.2.1)$$

and its reverse, respectively. The molecules of the gas can attach to the surface in two ways: (1) by physisorption, i.e., the molecules of A are bound to the adsorbent by van der Waals interactions, which in general are weak, and (2) by chemisorption, that is, the molecules stick to the surface by forming chemical bonds. In general, the association to form

a physisorption complex has a loose transition state, and VTST is needed to define a transition state, whereas chemisorption reactions often (not always) have tight transition states, and the saddle point provides a starting point for identifying the transition state.

Bimolecular chemical reactions at a surface[1184−1186] can take place by two mechanisms,[1184,1187,1188] the Langmuir−Hinshelwood (LH) mechanism

$$B{\cdot}S + A{\cdot}S \rightarrow \text{products} \qquad (4.2.2)$$

or the Eley-Rideal (ER) mechanism

$$B(g) + A{\cdot}S \rightarrow \text{products} \qquad (4.2.3)$$

Although the LH mechanism is very common,[1189−1198] both theoretical[1199−1212] and experimental[1187,1213−1220] studies show that the ER mechanism is also possible, and it tends to lead to higher energy release because the B-S chemisorption energy needs not be overcome. An intermediate mechanism is possible in which B is partially accommodated to the surface (trapped as "hot precursor") but not completely equilibrated to it prior to reaction.[1221−1225] Both wave packet[1201,1203,1205,1211,1212,1223] and trajectory[1199,1200,1202,1204,1206−1209,1223−1225] calculations have been used to study the ER and hot precursor mechanisms. Electronic structure calculations can be very helpful in sorting out the mechanisms.[1226,1227]

Extended LEPS potentials have been used recently for several purposes such as the study of reactions of H_2 and D_2 at a Cu(001) surface.[1228−1230] The Shepard method, discussed at length in Section 2.3, has also extended to molecule−surface interactions.[1231,1232]

For the case of diatomic molecules interacting with a solid surface, it is possible to build a six-dimensional PES as a function of two position vectors; one of them, $\mathbf{R}(X,Y,Z)$, points from the molecular center to some point over the surface (with the Z axis chosen perpendicular to the surface), whereas the other vector, $\mathbf{r}$, usually defined in spherical coordinates (r,θ,ϕ), indicates the position of atom B relative to atom A in the AB diatomic molecule. The usual procedure is to fix X, Y, θ, and ϕ, so the molecule remains in the particular configuration with respect to the surface, and several ab initio points are calculated on a grid of different r and Z values. The procedure is then repeated for different X, Y, θ, ϕ configurations. Busnego et al.[1233] developed the corrugation-reducing procedure (CRP) that allows an efficient and accurate interpolation of this 6D PES. Specifically, the potential is divided into three parts:

$$V^{6D} = I^{6D} + J_A^{3D} + J_B^{3D} \qquad (4.2.4)$$

where I^{6D} is an interpolation function that contains all the formation with the exception of the atom−substrate interactions, which are incorporated in J_A^{3D} and J_B^{3D}, respectively. The success of the CRP is based on the smoothness of I^{6D} when compared with the highly corrugated V^{6D} potential. The function J_A^{3D} and J_B^{3D} are constructed by applying the CRP again, i.e.,

$$J^{3D} = I^{3D} + \sum_{i=1}^{n} Q^{2D}(R_i) \qquad (4.2.5)$$

where I^{3D} is the atomic equivalent of I^{6D}, and $Q^{2D}(R_i)$ represents the interaction between the adsorbing atom and the ith atom of the surface. The electronic structure energies may be calculated by DFT with a generalized gradient approximation. This procedure has been used to build the PESs of H_2 + Pd(111),[1196,1233] H_2 + Pt(111), H_2 + Cu(100),[1234,1235] H_2 + Pt(211),[1236] and H_2 + Ru(0001)[1237] systems.

Variational transition state theory with multidimensional tunneling is well suited for the study of molecular reactions at surfaces.[1024,1197,1238]

Chemical reaction dynamics have also been studied at liquid surfaces.[1239−1241]

4.3. Tunneling at Low Temperature

At low enough temperature, tunneling often causes exceptionally large amounts of concave curvature in Arrhenius plots. In analyzing this, some workers assume that the tunneling contribution is independent of temperature.[1242] Unfortunately, this is not true. The rate constant becomes independent of temperature when all reaction occurs out of the ground state. Since all medium-sized or large molecules have low-frequency modes, once must go to very low temperatures (significantly below 100 K, maybe even below 10 K, depending on the molecule and the process) for all the molecules to react out of the ground state.

We may distinguish three regimes:

Regime I: Most of the reaction occurs from the ground state of reactants. We can call this the ground-state tunneling regime. The rate constant is independent of temperature in this regime.

Regime II: Most of the reaction occurs by tunneling but out of a range of possible initial states. We can call this the activated tunneling regime. With very rare exceptions, this is the regime we need to be concerned about when we consider tunneling in organic chemistry. The rate constant is not independent of temperature in this regime, even if more than 99% of the reactive events occur by tunneling.

Regime III: Most of the reaction occurs by an overbarrier process.

One could also say that there are three components in the rate constant: tunneling from the ground state, tunneling from other states, and the overbarrier component. At low enough temperature, any reaction must occur in regime I, but of course the solvent may freeze before one gets there. If one considers reaction on a solid surface or simple reactions within solids (such as low-temperature matrices), this freezing does not get in the way of watching the transition from III to II to I as the temperature lowers. Then it can be shown that the rate constant does become a constant at low enough temperature, although this is very rarely observed.[1243] What is usually observed, both under these conditions and at higher temperatures in liquids, is a concave Arrhenius plot where (as the temperature is lowered) we see a flattening that corresponds to the beginning of an approach to a constant value.

We can describe this at a higher level of mathematical precision as follows. If the Arrhenius plot is straight at high T (an approximation, but often one we are willing to make, at least in the present context) and is straight and constant in the low-T limit, then it has no curvature (a straight line has a zero second derivative) in either of these limits. Some place between these two regimes, it must have the maximum absolute value of the curvature. We can call this the transition temperature. This is *not* a point to associate with the transition from tunneling not being important to tunneling

dominating (III → II); actually this is the transition from regime II to regime I.[1244] Since tunneling dominates in regime II, this transition temperature is not the onset of tunneling. Tunneling is important at a much higher temperature than this. For example, hydrogen transfer reactions (and also proton and hydride transfer reactions) with barriers of a few kcal/mol or higher are almost always dominated by tunneling at room temperature.

All real Arrhenius plots are curved. If a reaction is measured over a narrow temperature range, the curvature of the Arrhenius plot will often be less than experimental errors and so not be observable. A higher-than-usual curvature at low temperature is often an indication of tunneling, and it may even be a strong indication, but this is a quantitative issue, not simply an issue of equating curvature with tunneling. Reactions with observable curvature are sometimes proceeding mainly over the barrier (for example, Arrhenius plots are often quite curved at combustion temperatures due to anharmonicity—not tunneling); and reactions without observable curvature are often nevertheless proceeding mainly by tunneling.

5. Concluding Remarks

There has been great progress in our ability to model the kinetics of bimolecular reactions. This derives from (i) improved methods for generating and using reactive potential energy surfaces, especially implicit potential energy surfaces generated by direct dynamics, (ii) improved dynamical algorithms, including practical methods for finding variational transition states, well-validated multidimensional methods for including tunneling, and master equation methods for treating nonequilibrium distributions, especially in multiwell, multi-arrangement reactions, and (iii) efficient methods for interfacing i and ii. We anticipate continued improvements in all three areas.

6. Glossary of Acronyms

Acronyms that are not used after they are defined are not included here.

Glossary

B3LYP	Becke 3-parameter Lee−Yang−Parr density functional
C	classical
C	coherent switching with decay of mixing
CCUS	competitive CUS
CRP	corrugation-reducing procedure
CSE	chemically significant eigenmode
CUS	canonical unified statistical theory
CVT	canonical variational (transition state) theory
DFT	density functional theory
ESP	equilibrium solvation path
EVB	empirical valence bond
FR	free rotor
G	ground state
GT	generalized transition-state theory
HF	Hartree−Fock
HO	harmonic oscillator
HR	hindered rotor
IC	interpolated corrections
ICVT	improved CVT
IERE	internal energy relaxation eigenmode
ER	Eley−Rideal
ILCT1D	LCT based on 1D interpolation
ILCT2D	LCT based on 2D interpolation
LCG3	version 3 of the LCT approximation when used with the ground-state approximation for the transmission coefficient
LCG4	version 4 of the LCT approximation when used with the ground-state approximation for the transmission coefficient
LCT	large-curvature tunneling
LEP	London−Eyring−Polanyi
LEPS	London−Eyring−Polanyi−Sato
LH	Langmuir−Hinshelwood
MCCM	multicoefficient correlation method
MCMM	multi-configuration molecular mechanics
ME	master equation
MEP	minimum-energy path
MM	molecular mechanics
MP2	Møller−Plesset second-order perturbation theory (for electronic structure)
MT	multidimensional tunneling
μOMT	microcanonically optimized OMT
μVT	microcanonical variational (transition-state) theory
NES	nonequilibrium solvation
OMT	optimized MT
PES	potential energy surface
PST	phase-space theory
PT2	second-order perturbation theory (for vibration)
QCT	quasiclassical trajectory
R	reactant
RODS	reorientation (of the) dividing surface
RRKM	Rice−Ramsperger−Kassel−Marcus
SCDM	self-consistent decay of mixing
SCT	small-curvature tunneling
SES	separable equilibrium solvation
S_N2	bimolecular nucleophilic substitution
SPT	simple perturbation theory
SRP	specific reaction parameter(s)
TSH	trajectory surface hopping
TST	transition state theory
UD	unified dynamical theory
US	(microcanonical) unified statistical theory
VB	valence bond
VCI	vibrational configuration interaction
VRC	variable-reaction ccordinate
VTST	variational TST
WFT	wave function theory
WKB	Wentzel−Brillouin−Kramers

7. Acknowledgments

The authors are grateful to Yan Zhao, Jingzhi Pu and Ahren Jasper for helpful assistance. A.F.-R. also thanks the Ministerio de Educación Ciencia for a Ramón y Cajal Research Contract and for the research project #BQU2003-01639. The work at Sandia and the University of Minnesota is supported by the Division of Chemical Sciences, Geosciences, and Biosciences, the Office of Basic Energy Sciences of the U. S. Department of Energy. Sandia is a multi-program laboratory operated by Sandia Corporation, a Lockheed Martin Company, for the United States Department of Energy's National Nuclear Security Administration under Contract No. DE-AC04-94-AL85000. The work at the University of Minnesota is supported by Grant No. DOE-DE-FG02-85ER13579. Additional support was provided by the Air Force Office of Scientific Research by a Small Business Technology grant to Scientific Applications and Research Assoc., Inc.

8. References

(1) Boyd, R. K. *Chem. Rev.* **1977**, *77*, 93.
(2) Irikura, K. K., Frurip, D. J., Eds.; *Computational Thermochemistry*; American Chemical Society: Washington, 1998.

(3) Pople, J. A. *Rev. Mod. Phys.* **1999**, *71*, 1267.
(4) Curtiss, L. A.; Redfern, P. C.; Raghavachari, K. *J. Chem. Phys.* **2005**, *123*, 124107.
(5) Arrhenius, S. *Z. Phys. Chem.* **1889**, *4*, 226.
(6) Tolman, R. C. *Statistical Mechanics with Applications to Physics and Chemistry*; Chemical Catalog Co.: New York, 1927; pp 260−270.
(7) Truhlar, D. G. *J. Chem. Educ.* **1978**, *55*, 309.
(8) Pollak, E.; Pechukas, P. *J. Am. Chem. Soc.* **1978**, *100*, 2984.
(9) Karas, A. J.; Gilbert, R. G.; Collins, M. A. *Chem. Phys. Lett.* **1992**, *193*, 181.
(10) *Atom-Molecule Colllision Theory*; Bernstein, R. B., Ed.; Plenum: New York, 1979.
(11) Johnston, H. S. *Gas-Phase Reacton Rate Theory*; Ronald Press: New York, 1966.
(12) Eliason, M. A.; Hirschfelder, J. O. *J. Chem. Phys.* **1959**, *30*, 1426.
(13) Kuppermann, A. *J. Phys. Chem.* **1979**, *83*, 171.
(14) Christov, S. G. *Collision Theory and Statistical Theory of Chemical Reactions*; Springer-Verlag: Berlin, 1980.
(15) Kuppermann, A.; Greene, E. F. *J. Chem. Educ.* **1968**, *45*, 361.
(16) Ross, J.; Light, J. C.; Schuler, K. E. In *Kinetic Processes in Gases and Plasmas*; Hochstim, A. R., Ed.; Academic: New York, 1969; pp 281−320.
(17) LeRoy, R. L. *J. Phys. Chem.* **1969**, *73*, 4338.
(18) Menzinger, M.; Wolfgang, R. *Angew. Chem., Int. Ed. Engl.* **1969**, *8*, 438.
(19) Langevin, P. *Ann. Chem. Phys.* **1905**, *5*, 245.
(20) Gioumousis, G.; Stevenson, D. P. *J. Chem. Phys.* **1958**, *29*, 294.
(21) Henglein, A. In *Physical Chemistry. An Advanced Treatise*; Eyring, H., Henderson, D., Jost, W., Eds.; Academic Press: New York, 1975; Vol. VIB, pp 509−551.
(22) Stevenson, D. P.; Schissler, D. O. *J. Chem. Phys.* **1958**, *29*, 282.
(23) Hyatt, D.; Lacmann, K. *Z. Naturforsch.* **1968**, *23a*, 2080.
(24) Gorin, E. *Acta Phys. USSR* **1938**, *9*, 681.
(25) Gorin, E. *J. Chem. Phys.* **1939**, *7*, 256.
(26) Gorin, E.; Kauzmann, W.; Walter, J.; Eyring, H. *J. Chem. Phys.* **1939**, *7*, 633.
(27) Johnston, H. S.; Goldfinger, P. *J. Chem. Phys.* **1962**, *37*, 700.
(28) Garrett, B. C.; Truhlar, D. G. *J. Am. Chem. Soc.* **1979**, *101*, 4534.
(29) Benson, S. W. *Can. J. Chem.* **1983**, *61*, 881.
(30) Smith G. P.; Golden, D. M. *Int. J. Chem. Kinet.* **1978**, *10*, 489.
(31) Karplus, M.; Porter, R. N.; Sharma, R. D. *J. Chem. Phys.* **1965**, *43*, 3259.
(32) Truhlar, D. G.; Muckerman, J. T. In *Atom-Molecule Collision Theory*; Bernstein, R. B., Ed.; Plenum: New York, 1979; pp 505−566.
(33) Raff, L. M.; Thompson, D. L. In *Theory of Chemical Reaction Dynamics*; Baer, M., Ed.; CRC Press: Boca Raton, 1985; Vol. 3, pp 1−121.
(34) Schatz, G. C.; Horst, M. T.; Takayanagi, T. In *Modern Methods for Multidimensional Dynamics Calculations in Chemistry*; Thompson, D. L., Ed.; World Scientific: Singapore, 1998; pp 1−33.
(35) Xie, T.; Bowman, J.; Duff, J. W.; Braunstein, M.; Ramachandran, B. *J. Chem. Phys.* **2005**, *122*, 14301.
(36) Truhlar, D. G.; Dixon, D. A. In *Atom-Molecule Collision Theory: A Guide for the Experimentalist*; Bernstein, R. B., Ed.; Plenum: New York, 1979; pp 595−646.
(37) Gao, Y.; Thompson, D. L.; Sewell, T. D. *J. Chem. Phys.* **1996**, *104*, 576.
(38) Giese, K.; Kühn, O. *J. Chem. Theory Comput.* **2006**, *2*, 717.
(39) Light, J. C. In *Atom-Molecule Collision Theory: A Guide for the Experimentalist*; Bernstein, R. B., Ed.; Plenum: New York, 1979; pp 467−476.
(40) Wyatt, R. E. In *Atom-Molecule Colllision Theory: A Guide for the Experimentalist*; Bernstein, R. B., Ed.; Plenum: New York, 1979; pp 477−503.
(41) Kouri, D. J.; Sun, Y.; Mowrey, R. C.; Zhang, J. Z. H.; Truhlar, D. G.; Haug, K.; Schwenke, D. W. In *Mathematical Frontiers in Computational Chemical Physics*; Truhlar, D. G., Ed.; Springer-Verlag: New York, 1988; pp 207−243.
(42) Parker, G. A.; Pack, R.; T Laganà, A.; Archer, B. J.; Kress, J. D.; Bacic, Z. In *Supercomputer Algorithms for Reactivity, Dynamics, and Kinetics of Small Molecules*; Laganà, A., Ed.; Kluwer: Dordrecht, 1989; pp 105−129.
(43) Schwenke, D. W.; Mladenovic, M.; Zhao, M.; Truhlar, D. G.; Sun, Y.; Kouri, D. J. In *Supercomputer Algorithms for Reactivity, Dynamics, and Kinetics of Small Molecules*; Laganà, A., Ed.; Kluwer: Dordrecht, 1989; pp 131−168.
(44) Truhlar, D. G.; Schwenke, D. W.; Kouri, D. J. *J. Phys. Chem.* **1990**, *94*, 7346.
(45) Miller, W. H. *Annu. Rev. Phys. Chem.* **1990**, *41*, 245.
(46) Nyman, G.; Yu, H. G. *Rep. Prog. Phys.* **2000**, *63*, 1001.
(47) Althorpe, S. C.; Clary, D. C. *Annu. Rev. Phys. Chem.* **2003**, *54*, 493.
(48) Zhang, D. H.; Zhang, J. Z. H. In *Dynamics of Molecules and Chemical Reactions*; Wyatt, R. E., Zhang, J. Z. H., Eds.; Dekker: New York, 1996; p 231.
(49) Mladenovic, M.; Zhao, M.; Truhlar, D. G.; Schwenke, D. W.; Sun, Y.; Kouri, J. D. *J. Phys. Chem.* **1988**, *92*, 7035.
(50) Mielke, S. L.; Lynch, G. C.; Truhlar, D. G.; Schwenke, D. W. *J. Phys. Chem.* **1994**, *98*, 8000.
(51) Bañares, L.; D'Mello, M. J. *Chem. Phys. Lett.* **1997**, *277*, 465.
(52) Huarte-Larrañaga, F.; Manthe, U. *J. Chem. Phys.* **2002**, *116*, 2863.
(53) Mielke, S. L.; Peterson, K. A.; Schwenke, D. W.; Garrett, B. C.; Truhlar, D. G.; Michael, J. V.; Shi, M.-C.; Sutherland, J. W. *Phys. Rev. Lett.* **2003**, *91*, 62301.
(54) Yamamoto, T. *J. Chem. Phys.* **1960**, *33*, 281.
(55) Miller, W. H. *J. Chem. Phys.* **1974**, *74*, 1823.
(56) Huarte-Larrañaga, F. Manthe, U. *J. Chem. Phys.* **2003**, *118*, 8261.
(57) Chakraborty, A.; Truhlar, D. G. *Proc. Natl. Acad. Sci. U.S.A.* **2005**, *102*, 6744.
(58) Born, M.; Oppenheimer, R. *Ann. Phys.* **1927**, *84*, 457.
(59) Born, M.; Huang, K. *Dynamical Theory of Crystal Lattices*; Oxford University Press: New York, 1954.
(60) Slater, J. C. *Quantum Theory of Matter*; Mc-Graw-Hill: New York, 1908; p 378.
(61) Kolos, W. *Adv. Quantum Chem.* **1970**, *5*, 99.
(62) Mead, C. A. In *Mathematical Frontiers in Computational Chemical Physics*; Truhlar, D. G., Ed.; Springer-Verlag: New York, 1988; pp 1−17.
(63) Roothaan, C. C. J. *Rev. Mod. Phys.* **1951**, *23*, 69.
(64) Roothaan, C. C. J. *Rev. Mod. Phys.* **1960**, *32*, 178.
(65) Pople, J. A.; Nesbet, R. K. *J. Chem. Phys.* **1954**, *22*, 571.
(66) Møller, C.; Plesset, M. S. *Phys. Rev.* **1934**, *46*, 618.
(67) Pople, J. A.; Binkley, J. S.; Seeger, R. *Int. J. Quantum Chem. Symp.* **1976**, *10*, 1.
(68) Dewar, M. J. S.; Zoebisch, E. G.; Healy, E. F.; Stewart, J. J. P. *J. Am. Chem. Soc.* **1985**, *107*, 3902.
(69) Stewart, J. J. P. *J. Comput. Chem.* **1989**, *10*, 209.
(70) Stewart, J. J. P. *J. Comput.-Aided Mol. Des.* **1990**, *4*, 1.
(71) Cízek, J. *Adv. Chem. Phys.* **1969**, *14*, 35.
(72) Bartlett, R. J. In *Theory and Applications of Computational Chemistry*: *The First Forty* Years; Dykstra, C., Frenking, G., Kim, K. S., Scuseria, G. E., Eds.; Elsevier: Amsterdam, 2005; p 1191.
(73) Raghavachari, K.; Trucks, G. W.; Pople, J. A.; Head-Gordon, M. *Chem. Phys. Lett.* **1989**, *157*, 479.
(74) Halkier, A.; Helgaker, T.; Jørgensen, P.; Klopper, W.; Koch, H.; Olson, J.; Wilson, A. K. *Chem. Phys. Lett.* **1998**, *286*, 243.
(75) Fast, P. L.; Sánchez, M. L.; Truhlar, D. G. *J. Chem. Phys.* **1999**, *111*, 2921, **2000**, *113*, 3931(E).
(76) Piecuch, P.; Kowalski, K.; Pimienta, I. S. U.; Fan, P.-D.; Lodriquito, M.; McGuire, M. J.; Kucharski, S. A.; Kus, T.; Musial, M. *Theor. Chem. Acc.* **2004**, *112*, 349.
(77) Kinal, A.; Piecuch, P. *J. Phys. Chem. A* **2006**, *110*, 367.
(78) Piecuch, P.; Wloch, M.; Gour, J. R.; Kinal, A. *Chem. Phys. Lett.* **2006**, *418*, 467.
(79) Almlöf, J. E.; Taylor, P. R. *J. Chem. Phys.* **1987**, *86*, 4070.
(80) Dunning, T. H., Jr. *J. Chem. Phys.* **1989**, *90*, 1007.
(81) Wilson, A. K.; Woon, D. E.; Peterson, K. A.; Dunning, T. H., Jr. *J. Chem. Phys.* **1999**, *110*, 7667.
(82) Kendall, R. A.; Dunning, T. H., Jr.; Harrison, R. T. *J. Chem. Phys.* **1992**, *96*, 6792.
(83) Frisch, M. J.; Pople, J. A.; Binkley, J. S. *J. Chem. Phys.* **1984**, *80*, 3265.
(84) Lynch, B. J., Zhao, Y.; Truhlar, D. G. *J. Phys. Chem. A* **2003**, *107*, 1384.
(85) Curtiss, L. A.; Raghavachari, K.; Redfern, P. C.; Rassolov, V.; Pople, J. A. *J. Chem.* Phys. **1998**, *109*, 7764.
(86) Zhao, Y.; Pu, J.; Lynch, B. J.; Truhlar, D. G. *Phys. Chem. Chem. Phys.* **2004**, *6*, 673.
(87) Lynch, B. J.; Zhao, Y.; Truhlar, D. G. *J. Phys. Chem. A* **2005**, *109*, 1643.
(88) Easton, R. E.; Giesen, D. J.; Welch, A.; Cramer, C. J.; Truhlar, D. G. *Theor. Chim.* Acta **1996**, *93*, 281.
(89) Lynch, B. J.; Truhlar, D. G. *Theor. Chem. Acc.* **2004**, *111*, 335.
(90) Schafer, A.; Horn, H.; Ahlrichs, R. *J. Chem. Phys.* **1992**, *97*, 2571.
(91) Jensen, F. *J. Chem. Phys.* **2005**, *122*, 74111.
(92) Gordon, M. S.; Truhlar, D. G. *J. Am. Chem. Soc.* **1986**, *108*, 5412.
(93) Rossi, I.; Truhlar, D. G. *Chem. Phys. Lett.* **1995**, *234*, 64.
(94) Corchado, J. C.; Truhlar, D. G. *ACS Symp. Ser.* **1998**, *712*, 106.
(95) Fast, P. L.; Corchado, J.; Sánchez, M. L.; Truhlar, D. G. *J. Phys. Chem. A* **1999**, *103*, 3139.
(96) Tratz, C. M.; Fast, P. L.; Truhlar, D. G. *Phys. Chem. Commun.* **1999**, *2*, 14.
(97) Lynch, B. J.; Truhlar, D. G. *J. Phys. Chem. A* **2003**, *107*, 3898.
(98) Montgomery, J. A., Jr.; Ochterski, J. W.; Petersson, G. A. *J. Chem. Phys.* **1994**, *101*, 5900.

(99) Ochterski, J. W.; Petersson, G. A.; Montgomery, J. A., Jr. *J. Chem. Phys.* **1996**, *104*, 2598.
(100) Montgomery, J. A., Jr.; Frisch, M. J.; Ochterski, J. W.; Petersson, G. A. *J. Chem. Phys*. **1999**, *110*, 2822.
(101) Fast, P. L.; Corchado, J.; Sánchez, M. L.; Truhlar, D. G. *J. Phys. Chem. A* **1999**, *103*, 5129.
(102) Fast, P. L.; Sánchez, M. L.; Corchado, J.; Truhlar, D. G. *J. Chem. Phys.* **1999**, *110*, 11679.
(103) Fast, P. L.; Sánchez, M. L.; Truhlar, D. G. *Chem. Phys. Lett.* **1999**, *306*, 407.
(104) Fast, P. L.; Truhlar, D. G. *J. Phys. Chem. A* **2000**, *104*, 6111.
(105) Li, T.-H.; Chen, R.-R.; Hu, W.-P. *Chem. Phys. Lett.* **2005**, *412*, 430.
(106) Curtiss, L. A.; Raghavachari, K.; Redfern, P. C.; Pople, J. A. *J. Chem. Phys.* **2000**, *112*, 1125.
(107) Curtiss, L. A.; Redfern, P. C.; Rassolov, V.; Kedziora, G.; Pople, J. A. *J. Chem. Phys.* **2001**, *114*, 9287.
(108) Curtiss, L. A.; Redfern, P. C.; Raghavachari, K.; Pople, J. A. *J. Chem. Phys.* **2001**, *114*, 108.
(109) Curtiss, L. A.; Raghavachari, K.; Trucks, G. W. J. A. Pople, *J. Chem. Phys.* **1991**, *94*, 7221.
(110) Martin, J. M. L.; de Oliveira, G. *J. Chem. Phys.* **1999**, *111*, 1843.
(111) Lynch, B. J.; Truhlar, D. G. In *Recent Advances in Electron Correlation Methodology*; Wilson, A. K., Peterson, K. A., Eds.; ACS Symposium Series; American Chemical Society: Washington, in press.
(112) Schwenke, D. W.; Steckler, R.; Brown, F. B.; Truhlar, D. G. *J. Chem. Phys.* **1986**, *84*, 5706.
(113) Lynch, G. C.; Steckler, R.; Schwenke, D. W.; Varandas, A. J. C.; Truhlar, D. G.; Garrett, B. C. *J. Chem. Phys.* **1991**, *94*, 7136.
(114) Stark, R.; Werner, H. J. *J. Chem. Phys.* **1996**, *104*, 6515.
(115) Lynch, B. J.; Truhlar, D. G. *J. Phys. Chem. A* **2002**, *106*, 842.
(116) Kállay, M.; Gauss, J.; Szalay, P. *J. Chem. Phys.* **2003**, *119*, 2991.
(117) Lu, S.-I. *J. Chem. Phys.* **2005**, *122*, 194323.
(118) Cardoen, W.; Gdanitz, R.; Simons, J. *J. Phys. Chem. A* **2006**, *110*, 564.
(119) Blais, N. C.; Truhlar, D. G. *J. Chem. Phys.* **1973**, *58*, 1090.
(120) Schaefer, H. F., III *J. Phys. Chem.* **1985**, *89*, 5336.
(121) Sparks, R. K.; Heyden, C. C.; Shobatake, K.; Neumark, D. M.; Lee, Y. T. In *Horizons of Quantum Chemistry*; Fukui, K., Pullman, B., Eds.; Reidel: Dordrecht, 1980; p 91.
(122) Kohn, W.; Sham, L. J. *Phys. Rev.* **1965**, *140*, A1133.
(123) Kohn, W.; Becke, A. D.; Parr, R. G. *J. Phys. Chem.* **1996**, *100*, 12974.
(124) Becke, A. D. *J. Chem. Phys.* **1993**, *98* 5648.
(125) Staroverov, V. N.; Scuseria, G. E.; Tao, J.; Perdew, J. P. *J. Chem. Phys.* **2003**, *119*, 12129.
(126) Stevens, P. J.; Devlin, F. J.; Chabalowski, C. F.; Frisch, M. J. *J. Phys. Chem.* **1994**, *98*, 11623.
(127) Adamo, C.; Barone, V. *J. Chem. Phys.* **1998**, *108*, 664.
(128) Lynch, B. J.; Fast, P. L.; Harris, M.; Truhlar, D. G. *J. Phys. Chem. A* **2000**, *104*, 4811.
(129) Enzerhof, M.; Scuseria, G. E. *J. Chem. Phys.* **1999**, *110*, 5029.
(130) Adamo, C.; Cossi, M.; Barone, V. *J. Mol. Struct. (THEOCHEM*) **1999**, *493*, 145.
(131) Wilson, P. J.; Bradley, T. J.; Tozer, D. J. *J. Chem. Phys.* **2001**, *115*, 9233.
(132) Becke, A. D. *J. Chem. Phys.* **1996**, *104*, 1040.
(133) Zhao, Y.; Lynch, B. J.; Truhlar, D. G. *J. Phys. Chem. A* **2004**, *108*, 2715.
(134) Zhao, Y.; Truhlar, D. G. *J. Phys. Chem. A* **2004**, *108*, 6908.
(135) Boese, A. D.; Martin, J. M. L. *J. Chem. Phys.* **2004**, *121*, 3405.
(136) Zhao, Y.; Truhlar, D. G. *J. Phys. Chem. A* **2005**, *109*, 5656.
(137) Zhao, Y.; Schultz, N. E.; Truhlar, D. G. *J. Chem. Phys. Comput*. **2006**, *2*, 364.
(138) Lynch, B. J.; Truhlar, D. G. *J. Phys. Chem. A* **2001**, *105*, 2936.
(139) Zhao, Y.; Lynch, B. J.; Truhlar, D. G. *J. Phys. Chem. A* **2004**, *108*, 4786.
(140) Zhao, Y.; Lynch, B. J.; Truhlar, D. G. *Phys. Chem. Chem. Phys.* **2005**, *7*, 43.
(141) Hratchian, H. P.; Schlegel, H. B. In *Theory Theory and Applications of Computational Chemistry*: *The First Forty Years*; Dykstra, C. E., Frenking, G., Kim, K. S., Scuseria, G. E., Eds.; Elsevier: Amsterdam, 2005; p 195.
(142) Mills, G.; Jónsson, H. *Phys. Rev. Lett.* **1994**, *72*, 1124.
(143) Mills, G.; Jónsson, H.; Schenter, G. K. *Surf. Sci.* **1995**, *324*, 305.
(144) Henkelman, G.; Uberagua, B. P.; Jónsson, H. *J. Chem. Phys.* **2000**, *113*, 9901.
(145) Henkelman, G.; Jónsson, H. *J. Chem. Phys.* **2000**, *113*, 9978.
(146) González-Garcia, N.; Pu, J.; González-Lafont, A.; Lluch, J. M.; Truhlar, D. G. *J. Chem. Theory Comput*. **2006**, *2*, 895.
(147) Truhlar, D. G.; Steckler, R.; Gordon, M. S. *Chem. Rev*. **1987**, *87*, 217.
(148) Schatz, G. C. *Rev. Mod. Phys*. **1989**, *61*, 669.
(149) Wilson, E. B., Jr.; Decius, J. C.; Cross, P. C. *Molecular Vibrations*; McGraw-Hill: New York, 1955.
(150) Diem, M. *Introduction to Modern Vibrational Spectroscopy*; John Wiley & Sons: New York, 1993.
(151) London, F. *Z. Elektrochem.* **1929**, *35*, 551.
(152) Truhlar, D. G.; Wyatt, R. E. *Adv. Chem. Phys.* **1977**, *36*, 141.
(153) Eyring, H.; Polanyi, M. *Naturwissenschaften* **1930**, *18*, 914.
(154) Sato, S. *Bull. Chem. Soc. Jpn.* **1955**, *281*, 450.
(155) Sato, S. *J. Chem. Phys.* **1955**, *23*, 592.
(156) Kuntz, P. N.; Nemeth, E. M.; Polanyi, J. C.; Rosner, S. D.; Young, C. E. *J. Chem. Phys*. **1966**, *44*, 1168.
(157) Parr, C. A.; Truhlar, D. G. *J. Phys. Chem.* **1971**, *75*, 1844.
(158) Weston, R. E., Jr. *J. Phys. Chem.* **1979**, *83*, 61.
(159) Pomerantz, A. E.; Camden, J. P.; Chiou, A. S.; Ausfelder, F.; Chawla, A.; Hase, W. L.; Zare, R. N. *J. Am. Chem. Soc.* **2005**, *127*, 16368.
(160) Laganà, A.; García, E.; Ciccarelli, L. *J. Phys. Chem.* **1987**, *91*, 312.
(161) Skouteris, D.; Pacifini, L.; Laganà, A. *Mol. Phys*. **2004**, *102*, 2237.
(162) Baldridge, K. K.; Gordon, M. S.; Steckler, R.; Truhlar, D. G. *J. Phys. Chem.* **1989**, *93*, 5107.
(163) Truhlar, D. G.; Gordon, M. S. *Science* **1990**, *249*, 491.
(164) González-Lafont, A.; Truong, T. N.; Truhlar, D. G. *J. Phys. Chem.* **1991**, *95*, 4618.
(165) Truhlar, D. G. In *The Reaction Path in Chemistry*; Heidrich, D., Ed.; Kluwer: Dordrecht, 1995; pp 229−255.
(166) Hase, W. L.; Song, K.; Gordon, M. S. *Comput. Sci. Eng*. **2003**, *5*, 36.
(167) Wang, L.; Liu, J.-y.; Li, Z.-s.; Sun, C.-c. *J. Chem. Theory Comput*. **2005**, *1*, 201.
(168) Wang, I. S. Y.; Karplus, M. *J. Am. Chem. Soc.* **1973**, *95*, 8160.
(169) Leforestier, C. *J. Chem. Phys.* **1978**, *68*, 4406.
(170) Bolton, K.; Schlegel, H. B.; Hase, W. L.; Song, K. *Phys. Chem. Chem. Phys*. **1999**, *1*, 999.
(171) Sun, L.; Hase, W. L.; Sung, K. *J. Am. Chem. Soc*. **2001**, *123*, 5753.
(172) Liu, J.; Song, K.; Hase, W. L.; Anderson. S. L. *J. Phys. Chem. A* **2005**, *109*, 11376.
(173) Camden, J. P.; Bechtel, H. A.; Brown, D. J. A.; Martin, M. R.; Zare, R. N.; Hu, W.; Lendvay, G.; Troya, D.; Schatz, G. C. *J. Am. Chem. Soc.* **2005**, *127*, 11898.
(174) Camden, J. P.; Hu, W.; Bechtel, H. A.; Brown, D. J. A.; Martin, M. R.; Zare; Lendvay, G.; Troya, D.; Schatz, G. C. *J. Chem. Phys. A* **2006**, *110*, 677.
(175) Hu, W.; Lendvay, G.; Troya, D.; Schatz, G. C.; Camden, J. P.; Bechtel, H. A.; Brown, D. J. A.; Martin, M. R.; Zare, R. N. *J. Phys. Chem. A* **2006**, *110*, 3017.
(176) Yu, H.-G.; Muckerman, J. T.; Francisco, J. S. *J. Phys. Chem*. **2005**, *109*, 5230.
(177) Zhao, Y.; Truhlar, D. G., unpublished data.
(178) Lynch, B. J.; Truhlar, D. G. *J. Phys. Chem. A* **2003**, *107*, 8996.
(179) Zhao, Y.; González-García, N.; Truhlar, D. G. *J. Phys. Chem. A* **2005**, *109*, 2012.
(180) Boese, A. D.; Martin, J. M. L.; Handy, N. C. *J. Chem. Phys.* **2003**, *119*, 3005.
(181) Schatz, G. C. *Lecture Notes Chem*. **2000**, *75*, 15.
(182) McLaughlin, D. R.; Thompson, D. L. *J. Chem. Phys.* **1973**, *59*, 4393.
(183) Sathyamurthy, N.; Raff, L. M. *J. Chem. Phys.* **1975**, *631*, 464.
(184) Sorbie, K. S.; Murrell, J. N. *Mol. Phys.* **1976**, *31*, 905.
(185) Schinke, R.; Lester, W. A., Jr. *J. Chem. Phys.* **1980**, *72*, 3754.
(186) Murrell, J. N.; Carter, S.; Farantos, S. C.; Huxley, P.; Varandas, *A. Molecular Potential Energy Functions*; Wiley: Chichester, 1984.
(187) Bowman, J. M.; Bittman, J. S.; Harding, L. B. *J. Chem. Phys.* **1986**, *85*, 911.
(188) Laganà, A. *J. Chem. Phys.* **1991**, *95*, 2216.
(189) Ischtwan, J.; Colllins, M. A. *J. Chem. Phys.* **1994**, *100*, 8080.
(190) Jordan, M. J. T.; Thompson, K. C.; Collins, M. A. *J. Chem. Phys.* **1995**, *102*, 5647.
(191) Nguyen, K. A.; Rossi, I.; Truhlar, D. G. *J. Chem. Phys*. **1995**, *103*, 5522.
(192) Ho, T.-S.; Rabitz, H. *J. Chem. Phys.* **1996**, *104*, 2584.
(193) Frishman, A.; Hoffman, D. K.; Kouri, D. J. *J. Chem. Phys.* **1997**, *107*, 804.
(194) Ishida, T.; Schatz, G. C. *J. Chem. Phys.* **1997**, *107*, 3558.
(195) Thompson, K. C.; Collins, M. A. *J. Chem. Soc., Faraday Trans.* **1997**, *93*, 871.
(196) Ishida, T.; Schatz, G. C. *Chem. Phys. Lett.* **1998**, *298*, 285.
(197) Bettens, R. P. A.; Collins, M. A. *J. Chem. Phys.* **1998**, *108*, 2424.
(198) Laganà, A.; de Aspuru, G. O.; García, E. *J. Chem. Phys.* **1998**, *108*, 3886.
(199) Thompson, K. C.; Jordan, M. J. T.; Collins, M. A. *J. Chem. Phys.* **1998**, *108*, 8302.
(200) Bettens, R. P. A.; Collins, M. A. *J. Chem. Phys.* **1998**, *109*, 9728.
(201) de Aspuru, G. O.; Clary, D. C. *J. Phys. Chem. A* **1998**, *102*, 9631.
(202) Eckert, F.; Werner, H. J. *Chem. Phys. Lett.* **1999**, *302*, 208.
(203) Ishida, T.; Schatz, G. C. *Chem. Phys. Lett.* **1999**, *314*, 369.

(204) Bettens, R. P. A.; Collins, M. A. *J. Chem. Phys.* **1999**, *111*, 816.
(205) Lin, S. Y.; Park, S. C.; Kim, M. S. *J. Chem. Phys.* **1999**, *111*, 3787.
(206) Millam, J. M.; Bakken, V.; Chen, W.; Hase, W. L.; Schlegel, H. B. *J. Chem. Phys.* **1999**, *111*, 3800.
(207) Bettens, R. P. A.; Hansen, T. A.; Collins, M. A. *J. Chem. Phys.* **1999**, *111*, 6322.
(208) Szalay, V. *J. Chem. Phys.* **1999**, *111*, 8804.
(209) Collins, M. A.; Zhang, D. H. *J. Chem. Phys.* **1999**, *111*, 9924.
(210) Kim, Y.; Corchado, J. C.; Villa, J.; Xing, J.; Truhlar, D. G. *J. Chem. Phys.* **2000**, *112*, 2718.
(211) Rhee, Y. M. *J. Chem. Phys.* **2000**, *113*, 6021.
(212) Yang, M.; Zhang, D. H.; Collins, M. A.; Lee, S.-Y. *J. Chem. Phys.* **2001**, *115*, 174.
(213) Palma, J.; Clary, D. C. *J. Chem. Phys.* **2001**, *115*, 2188.
(214) Albu, T.; Corchado, J. C.; Truhlar, D. G. *J. Phys. Chem. A* **2001**, *105*, 8465.
(215) Ishida, T.; Schatz, G. C. *J. Comput. Chem.* **2002**, *24*, 1077.
(216) Yagi, K.; Taketsugu, T.; Hirao, K. *J. Chem. Phys.* **2002**, *116*, 3963.
(217) Ho, T. S.; Hollenbeck, T.; Rabitz, H.; Chau, S. D.; Skodje, R. T.; Zyubin, A. S.; Mebel, A. M. *J. Chem. Phys.* **2002**, *116*, 4124.
(218) Collins, M. A. *Theor. Chem. Acc.* **2002**, *108*, 313.
(219) Bañares, L.; Aoiz, F. J.; Vázquez, S. A.; Ho, T.-S.; Rabitz, H. *Chem. Phys. Lett.* **2003**, *374*, 243.
(220) Kim, M. S.; Moon, J. H. *Int. J. Mass Spectrom.* **2003**, *225*, 191.
(221) Ho, T.-S.; Rabitz, H.; Aoiz, F. J.; Bañares, L.; Vázquez, S. A.; Harding, L. B. *J. Chem. Phys.* **2003**, *119*, 3063.
(222) Colllins, M. A.; Radom, L. *J. Chem. Phys.* **2003**, *118*, 6222.
(223) Wu, T.; Manthe, U. *J. Chem. Phys.* **2003**, *119*, 14.
(224) Kim, K. H.; Lee, Y. S.; Ishida, T.; Jeung, G.-H. *J. Chem. Phys.* **2003**, *119*, 4689.
(225) Lakin, M. J.; Troya, D.; Schatz, G. C.; Harding, L. B. *J. Chem. Phys.* **2003**, 119, 5848.
(226) Ho, T. S.; Rabitz, H. *J. Chem. Phys.* **2003**, *119*, 6433.
(227) Ramachandran, B.; Peterson, K. A. *J. Chem. Phys.* **2003**, *119*, 9590.
(228) Maisuradze, G. G.; Thompson, D. L.; Wagner, A. F.; Minkoff, M. *J. Chem. Phys.* **2003**, *119*, 10002.
(229) Maisuradze, G. G.; Thompson, D. L. *J. Phys. Chem. A* **2003**, *107*, 7118.
(230) García, E.; Rodríguez, A.; Hernández, M. L.; Laganà, A. *J. Phys. Chem. A* **2003**, *107*, 7248.
(231) Kerkeni, B.; Clary, D. C. *J. Phys. Chem. A* **2003**, *107*, 10851.
(232) Valero, R.; van Hemert, M. C.; Kroes, G. *J. Chem. Phys. Lett.* **2004**, *393*, 236.
(233) Kim, K. H.; Kim, Y. *J. Chem. Phys.* **2004**, *120*, 623.
(234) Kerkeni, B.; Clary, D. C. *J. Chem. Phys.* **2004**, *120*, 2308.
(235) Troya, D.; Millán, J.; Baños, I.; Gonzalez, M. *J. Chem. Phys.* **2004**, *120*, 5181.
(236) Kawano, A.; Guo, Y.; Thompson, D. L.; Wagner, A. F.; Minkoff, M. *J. Chem. Phys.* **2004**, *120*, 6414.
(237) Rheinecker, J.; Xie, T.; Bowman, J. M. *J. Chem. Phys.* **2004**, *120*, 7018.
(238) Brown, A.; McCoy, A. B.; Braams, B. J.; Jin, Z.; Bowman, J. M. *J. Chem. Phys.* **2004**, *121*, 4105.
(239) Guo, Y.; Kawano, A.; Thompson, D. L.; Wagner, A. F.; Minkiff, M. *J. Chem. Phys.* **2004**, *121*, 5091.
(240) Maisuradze, G. G.; Kawano, A.; Thompson, D. L.; Wagner, A. F.; Minkoff, M. *J. Chem. Phys.* **2004**, *121*, 10329.
(241) Lin, H.; Albu, T.; Truhlar, D. G. *J. Phys. Chem. A* **2004**, *108*, 4112.
(242) Huang, X.; Braams, B. J.; Bowman, J. M. *J. Chem. Phys.* **2005**, *122*, 44308.
(243) Raff, L. M.; Malshe, M.; Hagan, M.; Doughan, D. I.; Rockley, M. G.; Komanduri, R. *J. Chem. Phys.* **2005**, *122*, 84104.
(244) Espinosa-Garcia, J.; Rangel, C.; Navarette, M.; Corchado, J. C. *J. Chem. Phys.* **2005**, *122*, 134315.
(245) Kerkeni, B.; Clary, D. C. *J. Chem. Phys.* **2005**, *123*, 64305.
(246) Evenhuis, C. R.; Lin, X.; Zhang, D. H.; Yarkony, D.; Collins, M. A. *J. Chem. Phys.* **2005**, *123*, 134110.
(247) Park, S. C.; Braams, B, J,; Bowman, J. M. *J. Chem. Theory Comput.* **2005**, *1*, 40163.
(248) Castillo, J. F.; Aoiz, F. J.; Bañares, L.; Martínez-Núñez, E.; Fernández-Ramos, A.; Vázquez, S. *J. Phys. Chem. A* **2005**, 109, 8459.
(249) Balabanov, N. B.; Shepler, B. C.; Peterson, K. A. *J. Phys. Chem. A* **2005**, *109*, 8765.
(250) Moyano, G. E.; Collins, M. A. *Theor. Chem. Acc.* **2005**, *113*, 225.
(251) García E.; Sánchez, C.; Rodríguez, A.; Laganà, A. *Int. J. Quantum Chem.* **2006**, *106*, 623.
(252) Zhang, X.; Braams, B. J.; Bowman, J. M. *J. Chem. Phys.* **2006**, *124*, 21104.
(253) Kawano, A.; Tokmakov, I. V.; Thompson, D. L.; Wagner, A. F.; Minkoff, M. *J. Chem. Phys.* **2006**, *124*, 54105.
(254) Oyanagi, C.; Yagi, K.; Taketsugu, T.; Hirao, K. *J. Chem. Phys.* **2006**, *124*, 64311.
(255) Kim, Y.; Kim, Y. *J. Phys. Chem. A* **2006**, *110*, 600.
(256) Medvedev, D. M.; Harding, L. B.; Gray, S. K. *Mol. Phys.* **2006**, *104*, 73.
(257) Tautermann, C. S.; Wellenzohn, B.; Clary, D. C. *Mol. Phys.* **2006**, *104*, 151.
(258) Franke, R.; Nielson, G. *Int. J. Numer. Methods Eng.* **1980**, *15*, 1961.
(259) Renka, R. J. *ACM Trans. Math. Software* **1988**, *14*, 139.
(260) Shepard, D. *Proc. ACM Natl. Conf.* **1968**, *517*.
(261) Truhlar, D. G.; Horowitz, C. J. *J. Chem. Phys.* **1978**, *68*, 2466, **1979**, *71*, 1514(E).
(262) Masgrau, L.; González-Lafont, A.; Lluch, J. M. *J. Comput. Chem.* **1999**, *20*, 1685.
(263) Alvarez-Idaboy, J. R.; Mora-Diez, N.; Boyd, R. J.; Vivier-Bunge, A. *J. Am. Chem. Soc.* **2001**, *23*, 2018.
(264) Aoiz, F. J.; Bañares, L.; Herrero, V. J. *Int. Rev. Phys. Chem.* **2005**, *24*, 119.
(265) Ellison, F. O. *J. Am. Chem. Soc.* **1963**, *85*, 3540.
(266) Kuntz, P. J. In *Atom-Molecule Collision Theory*; Bernstein, R. B., Ed.; Plenum: New York, 1979; pp 79−110.
(267) Tully, J. C. *Adv. Chem. Phys.* **1980**, *42*, 63.
(268) Whitlock, P. A.; Muckerman, J. T.; Fisher, E. R. *J. Chem. Phys.* **1982**, *76*, 4468.
(269) Kuntz, P. *J. Chem. Phys.* **1999**, *240*, 19.
(270) Pickup, B. T. *Proc. R. Soc. London Ser. A* **1973**, *333*, 69.
(271) Varandas, A. J. C.; Voronin, A. I.; Caridade, P. J. S. B. *J. Chem. Phys.* **1998**, *108*, 7623.
(272) Liu, Y.; Lohr, L. L.; Barker, J. R. *J. Phys. Chem. B* **2005**, *109*, 8304.
(273) Mielke, S. L.; Garrett, B. C.; Peterson, K. A. *J. Chem. Phys.* **1999**, *111*, 3806.
(274) Varandas, A. J. C.; Brown, F. B.; Mead, C. A.; Truhlar, D. G.; Blais, N. C. *J. Chem. Phys.* **1987**, *86*, 6258.
(275) Varandas, A. J. C. *Adv. Chem. Phys.* **1988**, *74*, 255.
(276) Pastrana, M. R.; Quintales, L. A. M.; Brandão, J.; Varandas, A. J. C. *J. Phys. Chem.* **1990**, *94*, 8073.
(277) Varandas, A. J. C. *Int. Rev. Phys. Chem.* **2000**, *19*, 199.
(278) Varandas, A. J. C.; Rodriques, S. P. J. *J. Phys. Chem. A* **2006**, *110*, 485.
(279) Aguado, A.; Paniagua, M. *J. Chem. Phys.* **1992**, *96*, 1265.
(280) Aguado, A.; Tablero, C.; Paniagua, M. *Comput. Phys. Commun.* **1998**, *108*, 259.
(281) Aguado, A.; Tablero, C.; Paniagua, M. *Comput. Phys. Commun.* **2001**, *134*, 97.
(282) Hayes, M. Y.; Deskevich, M. P.; Nesbitt, D. J.; Takahashi, K.; Skodje, R. T. *J. Phys. Chem.* **2006**, *110*, 436.
(283) Wall, F. T.; Porter, R. N. *J. Chem. Phys.* **1962**, *36*, 3256.
(284) Truhlar, D. G.; Kupperman, A. *J. Chem. Phys.* **1972**, *56*, 2232.
(285) Bowman, J. M.; Kuppermann, A. *Chem. Phys. Lett.* **1975**, *34*, 523.
(286) Wright, J. S.; Gray, S. K. *J. Chem. Phys.* **1978**, *69*, 67.
(287) Garrett, B. C.; Truhlar, D. G.; Wagner, A. F.; Dunning, T. H., Jr. *J. Chem. Phys.* **1983**, *78*, 4400.
(288) Joseph, T.; Truhlar, D. G.; Garrett, B. C. *J. Chem. Phys.* **1988**, *88*, 6982.
(289) Koizumi, H.; Schatz, G. C.; Walch, S. P. *J. Chem. Phys.* **1991**, *95*, 4130.
(290) Maierle, C. S.; Schatz, G. C.; Gordon, M. S.; McCabe, P.; Connor, J. N. L. *J. Chem. Soc. Faraday Trans.* **1997**, *793*, 709.
(291) Dobbyn, A. J.; Connor, J. N. L.; Besley, N. A.; Knowles, P. J.; Schatz, G. C. *Phys. Chem. Chem. Phys.* **1999**, *1*, 957.
(292) Garrett, B. C.; Truhlar, D. G.; Magnuson, A. W. *J. Chem. Phys.* **1983**, *76*, 2321.
(293) Johnston, H. S.; Parr, C. *J. Am. Chem. Soc.* **1963**, *85*, 2544.
(294) Pauling, L. *J. Am. Chem. Soc.* **1947**, *69*, 542.
(295) Duin, A. C. T. v.; Dasgupta, S.; Lorant, F.; Goddard, W. A., III *J. Phys. Chem. A* **2001**, *105*, 9396.
(296) Rogers, S.; Wang, D.; Kuppermann, A.; Walch, S. *J. Phys. Chem. A* **2000**, 104, 2308.
(297) Raff, L. M. *J. Chem. Phys.* **1974**, *60*, 2220.
(298) Warshel, A.; Weiss, R. M. *J. Am. Chem. Soc.* **1980**, *102*, 6218.
(299) Warshel, A. In *Computer Modeling of Chemical Reactions in Enzymes and Solutions*; Wiley-Interscience: New York, 1991.
(300) Chakraborty, A.; Zhao, Y.; Lin, H.; Truhlar, D. G. *J. Chem. Phys.* **2006**, *124*, 44315.
(301) Coulson, C. A.; Danielsson, U. *Arkiv Fysik* **1954**, *8*, 239.
(302) Porter, R. N.; Karplus, M. *J. Chem. Phys.* **1964**, *40*, 1105.
(303) Raff, L. M.; Stivers, L.; Porter, R. N.; Thompson, D. L.; Sims, L. B. *J. Chem. Phys.* **1970**, *52*, 3449.
(304) Blais, N. C.; Truhlar, D. G. *J. Chem. Phys.* **1973**, *58*, 1090.
(305) Pross, A.; Shaik, S. *J. Am. Chem. Soc.* **1982**, *104*, 1129.
(306) Chang, Y.-T.; Miller, W. H. *J. Phys. Chem.* **1990**, *94*, 5884.
(307) Chang, Y. T.; Minichino, C.; Miller, W. H. *J. Chem. Phys.* **1992**, *96*, 4341.
(308) Hwang, J. K.; King, G.; Creighton, S.; Warshel, A. *J. Am. Chem. Soc.* **1988**, *110*, 5297.
(309) Åqvist, J.; Warshel, A. *Chem. Rev.* **1993**, *93*, 2523.

(310) Lobaugh, J.; Voth, A. *J. Chem. Phys.* **1996**, *104*, 2056.
(311) Hinsen, K.; Roux, B. *J. Comput. Chem.* **1997**, *18*, 368.
(312) Guo, Y.; Thompson, D. L. *J. Chem. Phys.* **2003**, *118*, 1673.
(313) Truhlar, D. G. *J. Phys. Chem. A* **2003**, *106*, 5048.
(314) Shurki, A.; Crown, H. A. *J. Phys. Chem. B* **2005**, *109*, 23638.
(315) Maupin, C. M.; Wong, K. F.; Soudackov, A. V.; Kim, S.; Voth, G. A. *J. Phys. Chem.* A **2006**, *110*, 631.
(316) Espinosa-García, J. *J. Phys. Chem. A* **2001**, *105*, 8748.
(317) Rángel, C.; Navarrete, M.; Espinosa-García, J. *J. Phys. Chem. A* **2005**, *109*, 1441.
(318) Rángel, C.; Espinosa-García, J. *J. Phys. Chem. A* **2006**, *110*, 537.
(319) Rángel, C.; Navarrete, M.; Corchado, J. C.; Espinosa-García, J. *J. Chem. Phys.* **2006**, *124*, 124306.
(320) Rangel, C.; Espinosa-Garcia, J. *J. Phys. Chem. A* **2006**, *110*, 537.
(321) Wilson, E. B., Jr.; Decius, J. C.; Cross, P. C. *Molecular Vibrations: The Theory of Infrared and Raman Vibrational Spectra*; McGraw-Hill: New York, 1955.
(322) Dostrovsky, I.; Hughes, E. D.; Ingold, C. K. *J. Chem. Soc*. **1946**, *173*,
(323) Westheimer, F. H.; Mayer, J. E. *J. Chem. Phys.* **1946**, *14*, 733.
(324) Warshel, A.; Lifson, S. *J. Chem. Phys.* **1970**, *53*, 582.
(325) Olson, W.; Flory, P. *Biopolymers* **1972**, *11*, 25.
(326) Allinger, N. L. *Adv. Phys. Org. Chem.* **1976**, *13*, 1.
(327) Weiner, S. J.; Kollman, P. A.; Case, D. A.; Singh, U. C. Ghio, C.; Alagona, G.; Profeta, S.; Weiner, P. *J. Am. Chem. Soc*. **1984**, *106*, 765.
(328) Brooks, B. R.; Bruccoleri, R. E.; Olofson, B. D.; States, D. J.; Swaminathan, S.; Karplus, M. *J. Comput. Chem*. **1986**, *7*, 591.
(329) Bowen, J. P.; Allinger, N. L. *Rev. Comput. Chem*. **1991**, *2*, 81.
(330) Dinur, U.; Hogler, A. T. *Rev. Comput. Chem*. **1991**, *2*, 99.
(331) Troya, D.; Schatz, G. C. *J. Chem. Phys.* **2004**, *120* 7696.
(332) Sun, L.; Schatz, G. C. *J. Phys. Chem. B* **2005**, *109*, 8431.
(333) Martínez-Núñez, E.; Fernández-Ramos, A.; Cordeiro, M. N. D. S.; Vázquez, A.; Aoiz, F. J.; Bañares, L. *J. Chem. Phys.* **2003**, *119*, 10618.
(334) Yan, T.; Doubleday: C.; Hase, W. L. *J. Phys. Chem. A* **2004**, *108*, 9863.
(335) Troya, D.; García-Molina, E. *J. Phys. Chem. A* **2005**, *109*, 3015.
(336) Rossi, I.; Truhlar, D. G. *Chem. Phys. Lett.* **1995**, *233*, 231.
(337) Bash, P. A.; Ho, L. L.; MacKerell, A. D.; Levine, D.; Hallstrom, P. *Proc. Natl. Acad. Sci. U.S.A.* **1996**, *93*, 3698.
(338) Joseph, T.; Steckler, R.; Truhlar, D. G. *J. Chem. Phys.* **1987**, *87*, 7036.
(339) Espinosa-Garcia, J. *J. Chem. Phys.* **2002**, *116*, 10664.
(340) Zhao, Y.; Yamamoto, T.; Miller, W. H. *J. Chem. Phys.* **2004**, *120*, 3100.
(341) Rangel, C.; García-Bernáldez, J. C.; Espinosa-García, J. *Chem. Phys. Lett.* **2006**, *422*, 581.
(342) Pu, J.; Truhlar, D. G. *J. Chem. Phys.* **2002**, *116*, 1468.
(343) Wu, T.; Werner, H.-J.; Manthe, U. *Science* **2004**, *306*, 2227.
(344) Eyring, H. *J. Chem. Phys.* **1935**, *3*, 107.
(345) Evans, M. G.; Polanyi, M. *Trans. Faraday Soc.* **1935**, *31*, 875.
(346) Fowler, R. H. *Trans. Faraday Soc.* **1938**, *34*, 124.
(347) Kreevoy, M. M.; Truhlar, D. G. In Investigation of Rates and Mechanisms of Reactions, Part 1; Bernasconi, C. F., Ed.; Techniques of Chemistry Series 4th ed., Vol. 6; John Wiley and Sons: New York, 1986; pp 13−95.
(348) Pilling, M. J.; Seakins, P. W. *Reaction Kinetics*; Oxford University Press: Oxford, 1995; pp 76−77.
(349) Horiuti, J. *Bull. Chem. Soc. Jpn.* **1938**, *13*, 210.
(350) Wigner, E. P. *Trans. Faraday Soc.* **1938**, *34*, 29.
(351) Keck, J. C. *J. Chem. Phys.* **1960**, *32*, 1035.
(352) Keck, J. C. *Adv. Chem. Phys.* **1967**, *13*, 85.
(353) Pechukas, P. In *Dynamics of Molecular Collisions, Part B*; Miller, W. H., Ed.; Plenum: New York, 1976; Modern Theoretical Chemistry, Vol. 2, p 269.
(354) Tucker, S. C.; Truhlar, D. G. In *Theoretical Concepts for Understanding Organic Reactions*; Bertrán, J., Csizmadia, I. G., Eds.; Kluwer Academic Publishers: Norwell, MA, 1989; pp 291−346.
(355) Garrett, B. C. *Theor. Chem. Acc.* **2000**, *103*, 200.
(356) Garrett, B. C.; Truhlar, D. G. In *Theory and Applications of Computational Chemistry*; *The First Forty Years*; Dykstra, C. E.; Frenking, G., Kim, K. S., Scuseria, G. E., Eds.; Elsevier: Amsterdam, 2005; p 67.
(357) Pechukas, P.; Pollak, E. *J. Chem. Phys.* **1979**, *71*, 2062.
(358) Pechukas, P. *Annu. Rev. Phys. Chem.* **1981**, *32*, 159.
(359) Pechukas, P. *Ber. Bunsen-Ges. Phys. Chem*. **1982**, *86*, 372.
(360) Isaacson, A. D.; Truhlar, D. G. *J. Chem. Phys.* **1982**, *76*, 1380.
(361) Jepson, D. W.; Hirschfelder, J. O. *Proc. Natl. Acad. Sci. U.S.A.* **1959**, *45*, 249.
(362) Marcus, R. A. *J. Chem. Phys.* **1966**, *45*, 4500.
(363) Hofacker, G. L.; Michel, K. W. *Ber. Bunsen-Ges. Phys. Chem*. **1974**, *78*, 174.
(364) Duff, J. W.; Truhlar, D. G. *J. Chem. Phys.* **1975**, *62*, 2477.
(365) Garrett, B. C.; Truhlar, D. G. *J. Phys. Chem.* **1979**, *83*, 1052. Garrett, B. C.; Truhlar, D. G. *J. Phys. Chem.* **1983**, *87*, 4553(E).
(366) Wigner, E. P. *J. Chem. Phys.* **1937**, *5*, 720.
(367) Denbigh, K. *The Principles of Chemical Equilibrium*; 3rd ed., Cambridge University Press: London, 1971; p 455.
(368) Berry, R. S.; Rice, S. A.; Ross, J. *Physical Chemistry*, 2nd ed.; Oxford University Press: New York, 2000; pp 575, 916.
(369) Garrett, B. C.; Truhlar, D. G. *J. Chem. Phys.* **1979**, *70*, 1593.
(370) Shavitt, I. *J. Chem. Phys.* **1968**, *49*, 4048.
(371) Truhlar, D. G.; Kupperman, A. *J. Am. Chem. Soc*. **1971**, *93*, 1840.
(372) Fukui, K. *Acc. Chem. Res.* **1981**, *14*, 363.
(373) Garrett, B. C.; Truhlar, D. G. *J. Phys. Chem.* **1979**, *83*, 3058.
(374) Steel, C.; Laidler, K. J. *J. Chem. Phys.* **196**, *134*, 1827.
(375) Tweedale, A.; Laidler, K. J. *J. Chem. Phys.* **1970**, *53*, 2045.
(376) Greenhill, P. G.; Gilbert, A. G. *J. Phys. Chem.* **1986**, *90*, 3104.
(377) Jordan, M. J. T.; Smith, S. C.; Gilbert, R. G. *J. Phys. Chem.* **1991**, *95*, 8685.
(378) Schenter, G. K.; Garrett, B. C.; Truhlar, D. G. *J. Chem. Phys.* **2003**, *119*, 5828.
(379) Vanden-Eijnden, E.; Tal, F. A. *J. Chem. Phys.* **2005**, *123*, 184103.
(380) Watney, J. B.; Soudackov, A. V.; Wong, K. F.; Hammes-Schiffer, S. *Chem. Phys. Lett.* **2006**, *418*, 268.
(381) Roca, M.; Moliner, V.; Ruíz-Pernía, J. J.; Silla, E.; Tuñón, I. *J. Phys. Chem. A* **2006**, *110*, 503.
(382) Masgrau, L.; González-Lafont, A.; Lluch, J. M. *Chem. Phys. Lett.* **2002**, *353*, 154.
(383) Truhlar, D. G.; Isaacson, A. D.; Garrett, B. C. In *Theory of Chemical Reaction Dynamics*; Baer, M., Ed.; CRC Press: Boca Raton, 1985; Vol. 4, pp 65−137.
(384) Page, M.; McIver, J. W., Jr. *J. Chem. Phys.* **1988**, *88*, 922.
(385) Garrett, B. C.; Redmon, M. J.; Steckler, R.; Truhlar, D. G.; Baldridge, K. K.; Bartol, D.; Schmidt, M. W.; Gordon, M. S. *J. Phys. Chem.* **1988**, *92*, 1476.
(386) Melissas, V. S.; Truhlar, D. G.; Garrett, B. C. *J. Chem. Phys.* **1992**, *96*, 5758.
(387) Page, M. *Comput. Phys. Commun.* **1994**, *84*, 115.
(388) Villa, J.; Truhlar, D. G. *Theor. Chem. Phys.* **1997**, *97*, 317.
(389) Fast, P. L.; Truhlar, D. G. *J. Chem. Phys.* **1998**, *109*, 3721.
(390) Miller, W. H.; Handy, N. C.; Adams, J. E. *J. Chem. Phys.* **1980**, *72*, 99.
(391) Pechukas, P.; McLafferty, F. J. *J. Chem. Phys.* **1973**, *58*, 1622.
(392) Forst, W. In *Theory of Unimolecular Reactions*; Academic Press: New York, 1973; Chapter 6.
(393) Miller, W. H. *J. Chem. Phys.* **1975**, *62*, 1899.
(394) Miller, W. H. In *Potential Energy Surfaces and Dynamic Calculations*; Truhlar, D. G., Ed.; Plenum: New York, 1979; pp 265−286.
(395) Chatfield, D. C.; Friedman, R. S.; Truhlar, D. G.; Garrett, B. C.; Schwenke, D. W. *J. Am. Chem. Soc.* **1991**, *113*, 486.
(396) Aoiz, F. J.; Saez-Rabanos, V.; Martinez-Haya, B.; Gonzalez-Lezana, T. *J. Chem. Phys*. **2005**, *123*, 94101.
(397) Miller, W. H. *Acc. Chem. Res.* **1993**, *26*, 174.
(398) Sato, S. *Chem. Phys. Lett.* **2004**, *387*, 216.
(399) Sato, S. *Chem. Phys.* **2005**, *315*, 65.
(400) Garrett, B. C.; Truhlar, D. G.; Grev, R. S.; Magnuson, A. W. *J. Phys. Chem.* **1980**, *84*, 1730; Garrett, B. C.; Truhlar, D. G.; Grev, R. S.; Magnuson, A. W. *J. Phys. Chem.* **1983**, *87*, 4554(E).
(401) Lu, D.-h.; Truong, T. N.; Melissas, V. S.; Lynch, G. C.; Liu, R.-P.; Garrett, B. C.; Steckler, R.; Isaacson, A. D.; Rai, S. N.; Hancock, G. C.; Lauderdale, J. G.; Joseph, T.; Truhlar, D. G. *Comput. Phys. Commun.* **1992**, *71*, 235.
(402) Fernández-Ramos, A.; Ellingson, B. A.; Garrett, B. C.; Truhlar, D. G.; *Rev. Comput. Chem*., in press.
(403) Fernández-Ramos, A.; Martínez-Núñez, E.; Marques, J. M. C.; Vázquez, S. A. *J. Chem. Phys*. **2003**, *118*, 6280.
(404) Dunning, T. H., Jr.; Peterson, K. A. *J. Chem. Phys.* **1998**, *108*, 4761.
(405) Truhlar, D. G. *Chem. Phys. Lett.* **1998**, *294*, 45.
(406) Hitsuda, K.; Takahashi, T.; Matsumi, T.; Wallington, T. J. *J. Phys. Chem.* **2001**, *105*, 5131.
(407) Hasanayn, F.; Streitwieser, A.; Al-Rifai, R. *J. Am. Chem. Soc*. **2005**, *127*, 2249.
(408) Truong, T. N. *J. Chem. Phys.* **2000**, *113*, 4957.
(409) Zhang, S.; Truong, T. N. *J. Phys. Chem. A* **2003**, *107*, 1138.
(410) Violi, A.; Truong, T. N.; Sarofim, A. F. *J. Phys. Chem. A* **2004**, *108*, 4846.
(411) Kungwan, N.; Truong, T. N. *J. Phys. Chem. A* **2005**, *109*, 7742.
(412) Huynh, L. K.; Ratkiewicz, A.; Truong, T. N. *J. Phys. Chem. A* **2006**, *110*, 473.
(413) Hu, W.-P.; Truhlar, D. G. *J. Am. Chem. Soc.* **1996**, *118*, 860.
(414) Yanai, T.; Taketsugu, T.; Hirao, K. *J. Chem. Phys.* **1997**, *107*, 1137.
(415) Yamataka, H.; Alda, M.; Dupuis, M. *Chem. Phys. Lett.* **1999**, *300*, 583.
(416) Bakken, V.; Danovich, D.; Shaik, S.; Schlegel, H. B. *J. Am. Chem. Soc.* **2001**, *123*, 130.

(417) Singleton, D. A.; Hang, C.; Szymanski, M. J.; Greenwald, E. E. *J. Am. Chem. Soc.* **2003**, *125*, 1176.
(418) Singleton, D. A.; Hang, C.; Szymanski, M. J.; Meyer, M. P.; Leach, A. G.; Kuwata, K. T.; Chen, J. S.; Greer, A.; Foote, C. S.; Houk, K. N. *J. Am. Chem. Soc.* **2003**, *125*, 1319.
(419) González-Lafont, A.; Moreno, M.; Lluch, J. M. *J. Am. Chem. Soc.* **2004**, *126*, 13089.
(420) Li, J.; Li, X.; Shaik, S.; Schlegel, H. B. *J. Phys. Chem. A* **2004**, *108*, 8526.
(421) Li, J.; Shaik, S.; Schlegel, H. B. *J. Phys. Chem. A* **2006**, *110*, 2801.
(422) Chakraborty, A.; Truhlar, D. G.; Bowman, J. M.; Carter, S. *J. Chem. Phys.* **2004**, *121*, 2071.
(423) Lynch, V. A.; Mielke, S. L.; Truhlar, D. G. *J. Chem. Phys.* **2004**, *121* 5148.
(424) Chakraborty, A.; Truhlar, D. G. *J. Chem. Phys.* **2006**, *124*, 184310.
(425) Landau, L. D.; Lifshitz, E. M. *Quantum Mechanics: Non-Relativistic Theory*, 2nd ed.; Addison-Wesley: Reading, MA, 1965; p 163.
(426) Connor, J. N. L. *Chem. Phys. Lett.* **1969**, *4*, 419.
(427) Garrett, B. C.; Truhlar, D. G. *J. Chem. Phys.* **1984**, *81*, 309.
(428) Herzberg, G. In *Molecular Spectra and Molecular Structure. I. Spectra of Diatomic* Molecules; Van Nostrand: Reinhold: Princeton, 1950.
(429) Garrett, B. C.; Truhlar, D. G. *J. Phys. Chem.* **1979**, *83*, 1079; Garrett, B. C.; Truhlar, D. G. *J. Phys. Chem.* **1980**, *84*, 682(E).
(430) Truhlar, D. G. *J. Mol. Spectrosc.* **1971**, *38*, 415.
(431) Garrett, B. C.; Truhlar, D. G. *J. Phys. Chem.* **1979**, *83*, 1915.
(432) Garrett, B. C.; Truhlar, D. G. *J. Phys. Chem.* **1991**, *95*, 10374.
(433) Truhlar, D. G. *J. Comput. Chem.* **1991**, *12*, 266.
(434) Pitzer, K. S.; Gwinn, W. D. *J. Chem. Phys.* **1942**, *10*, 428.
(435) Pitzer, K. S. *Quantum Chemistry*; Prentice Hall: Englewood Cliff, NJ, 1953.
(436) Pitzer, K. S.; Gwinn, W. D. *J. Chem. Phys.* **1942**, *10*, 428.
(437) Pitzer, K. S. *J. Chem. Phys.* **1946**, *14*, 239.
(438) Kilpatrick, J. E.; Pitzer, K. S. *J. Chem. Phys.* **1949**, *17*, 1064.
(439) Herschbach, D. R.; Johnston, H. S.; Pitzer, K. S.; Powell, R. E. *J. Chem. Phys.* **1956**, *25*, 736.
(440) East, A. L. L.; Radom, L. *J. Chem. Phys.* **1997**, *106*, 6655.
(441) Robertson, S. H.; Wardlaw, D. M. *Chem. Phys. Lett.* **1992**, *199*, 391.
(442) Chuang, Y.-Y.; Truhlar, D. G. *J. Chem. Phys.* **2000**, *112*, 1221; erratum in press.
(443) Katzer, G.; Sax, A. F. *Chem. Phys. Lett.* **2003**, *368*, 473.
(444) McClurg, R. B.; Flagan, R. C.; Goddard, W. A., III. *J. Chem. Phys.* **1997**, *106*, 6675.
(445) Ayala, P. Y.; Schlegel, H. B. *J. Chem. Phys.* **1998**, *108*, 2314.
(446) Ellingson, B.; Lynch, V. A.; Mielke, S. M.; Truhlar, D. G. *J. Chem. Phys.*, in press.
(447) Zhang, Q.; Zhang, R. Q.; Chan, K. S.; Bello, I. *J. Phys. Chem. A* **2005**, *109*, 9112.
(448) Beyer, T.; Swinehart, D. F. *Commun. ACM* **1973**, *16*, 379.
(449) Stein, S. E.; Rabinovitch, B. S. *J. Chem. Phys.* **1973**, *58*, 2438.
(450) Whitten, G. Z.; Rabinovitch, B. J. *J. Chem. Phys.* **1963**, *38*, 2466.
(451) Forst, W. *J. Comput. Chem.* **1996**, *17*, 954.
(452) Knyazev, V. D.; Dubinski, I. A.; Slagle, I. R.; Gutman, D. *J. Phys. Chem.* **1994**, *98*, 5279.
(453) Knyazev, V. D. *J. Phys. Chem. A* **1998**, *102*, 3916.
(454) McClurg, R. B. *J. Chem. Phys.* **1998**, *208*, 1748.
(455) Doll, J. D. *Chem. Phys. Lett.* **1980**, *72*, 139.
(456) Miller, J. A.; Klippenstein, S. J. *J. Phys. Chem. A* **2000**, *104*, 7525.
(457) Jordan, M. J. T.; Smith, S. C.; Gilbert, R. G. *J. Phys. Chem.* **1991**, *95*, 8685.
(458) Knyazev, V. D.; Tsang, W. *J. Phys. Chem. A* **1998**, *102*, 9167.
(459) Farantos, S. C.; Murrell, J. N.; Hajduk, J. C. *Chem. Phys.* **1982**, *68*, 109.
(460) Parneix, P.; Van-Oanh, N.-T.; Brechignac, P. *Chem. Phys. Lett.* **2002**, *357*, 78.
(461) Börjesson, L. E. B.; Nordholm, S.; Anderson, L. L. *Chem. Phys. Lett.* **1991**, *186*, 65.
(462) Pacey, P. D. *J. Chem. Phys.* **1982**, *77*, 3540.
(463) Pacey, P. D.; Wagner, B. D. *J. Chem. Phys.* **1984**, *80*, 1477.
(464) Truhlar, D. G.; Brown, F. B.; Steckler, R.; Isaacson, A. D. In *The Theory of Chemical Reaction Dynamics*; Clary, D. C., Ed.; NATO ASI Series C170; Reidel: Dordrecht, 1986; p 285.
(465) Isaacson, A. D. *J. Phys. Chem. A* **2006**, *110*, 379.
(466) Nielsen, H. H. *Encl. Phys.* **1959**, *37*, 173.
(467) Isaacson, A. D.; Truhlar, D. G.; Scanlon, K.; Overend, J. *J. Chem. Phys.* **1981**, *75*, 3017.
(468) Zhang, Q.; Day, P.; Truhlar, D. G. *J. Chem. Phys.* **1993**, *98*, 4948.
(469) Isaacson, A. D.; Hung, S.-C. *J. Chem. Phys.* **1994**, *101*, 3928.
(470) Isaacson, A. L. *J. Chem. Phys.* **1997**, *107*, 3832.
(471) Truhlar, D. G.; Isaacson, A. D. *J. Chem. Phys.* **1991**, *94*, 357.
(472) Isaacson, A. L. *J. Chem. Phys.* **2002**, *117*, 8778.
(473) Barone, V. *J. Chem. Phys.* **2004**, *120*, 3059.
(474) Kuhler, K. M.; Truhlar, D. G.; Isaacson, A. D. *J. Chem. Phys.* **1996**, *104*, 4664.
(475) Carter, S.; Culik, S. J.; Bowman, J. M. *J. Chem. Phys.* **1997**, *107*, 10458.
(476) Carter, S.; Bowman, J. M.; Handy, N. C. *Theor. Chem. Acc.* **1998**, *100*, 191.
(477) Carter, S.; Bowman, J. M. *J. Phys. Chem. A.* **2000**, *104*, 2355.
(478) Feynman, R. P.; Hibbs, A. R. *Quantum Mechanics and Path Integrals*; McGraw-Hill: New York, 1965.
(479) Topper, R. Q. *Adv. Chem. Phys.* **1999**, *105*, 117.
(480) Mielke, S. L.; Srinivasan, J.; Truhlar, D. G. *J. Chem. Phys.* **2000**, *112*, 8768.
(481) Mielke, S. L.; Truhlar, D. G. *J. Chem. Phys.* **2001**, *114*, 621.
(482) Miller, J. A. *Faraday Discuss.* **2001**, *119*, 461.
(483) Mielke, S. L.; Truhlar, D. G. *Chem. Phys. Lett.* **2003**, *378*, 317.
(484) Lynch, V. A.; Mielke, S. L.; Truhlar, D. G. *J. Phys. Chem. A* **2005**, *109*, 10092.
(485) Isaacson, A. D.; Truhlar, D. G. *J. Chem. Phys.* **1981**, *75*, 4090.
(486) Song, K.; Peslherbe, G. H.; Hase, W. L.; Dobbyn, A. J.; Stumpf, M.; Schinke, R. *J. Chem. Phys.* **1995**, *103*, 8891.
(487) Speybroeck, V. V.; Neck, D. V.; Waroquier, M. *J. Phys. Chem. A.* **2002**, *106*, 8945.
(488) Peslherbe, G. H.; Hase, W. L. *J. Chem. Phys.* **1994**, *101*, 8535.
(489) Garcia-Viloca, M.; Gao, J.; Karplus, M.; Truhlar, D. G. *Science* **2004**, *303*, 186.
(490) Evans, M. G. *Trans. Faraday Soc.* **1938**, *34*, 73.
(491) Garrett, B. C.; Truhlar, D. G. *Acc. Chem. Res.* **1980**, *13*, 440.
(492) Hirschfelder, J. O.; Wigner, E. *J. Chem. Phys.* **1939**, *7*, 616.
(493) Miller, W. H. *J. Chem. Phys.* **1976**, *65*, 2216.
(494) Garrett, B. C.; Truhlar, D. G. *J. Chem. Phys.* **1982**, *76*, 1853.
(495) Smith, I. W. M. *J. Chem. Soc., Faraday Trans.* **1981**, *277*, 747.
(496) Frost, R. J.; Smith, I. W. M. *Chem. Phys.* **1987**, *111*, 389.
(497) Truhlar, D. G.; Garrett, B. C. *Faraday Discuss. Chem. Soc.* **1987**, *84*, 464.
(498) Greenwald, E. E.; North, S. W.; Georgievskii, Y.; Klippenstein, S. J. *J. Phys. Chem. A* **2005**, *109*, 6034.
(499) Fernández-Ramos, A.; Varandas, A. J. C. *J. Phys. Chem. A* **2002**, *106*, 4077.
(500) Masgrau, L.; González-Lafont, A.; Lluch, J. M. *J. Phys. Chem. A* **2003**, *107*, 4490.
(501) Orchando-Pardo, M.; Nebot-Gil, I.; González-Lafont, A.; Lluch, J. M. *J. Phys. Chem.* A **2004**, *108*, 5117.
(502) Keck, J. C. *Discuss. Faraday Soc.* **1962**, *33*, 173.
(503) Keck, J. C. *Adv. At. Mol. Phys.* **1972**, *8*, 39.
(504) Anderson, J. B. *J. Chem. Phys.* **1973**, *58*, 4684.
(505) Anderson, J. B. *J. Chem. Phys.* **1975**, *62*, 2446.
(506) Anderson, J. B. *Adv. Chem. Phys.* **1995**, *91*, 381.
(507) Wigner, E. P. *Z. Phys. Chem. Abt. B* **1932**, *19*, 203.
(508) Marcus, R. A. *J. Chem. Phys.* **1966**, *45*, 4493.
(509) Garrett, B. C.; Truhlar, D. G. *J. Phys. Chem.* **1979**, *83*, 2921.
(510) Garrett, B. C.; Truhlar, D. G.; Grev, R. S. *J. Phys. Chem.* **1980**, *84*, 1749.
(511) Skodje, R. T.; Truhlar, D. G.; Garrett, B. C. *J. Chem. Phys.* **1982**, *77*, 5955.
(512) Kemble, E. C. *Fundamental Principles of Quantum Mechanics with Elementary Applications*; Dover: New York, 1958.
(513) Marcus, R. A.; Coltrin, M. E. *J. Chem. Phys.* **1977**, *67*, 2609.
(514) Skodje, R. T.; Truhlar, D. G.; Garrett, B. C. *J. Phys. Chem.* **1981**, *85*, 3019.
(515) Liu, Y.-P.; Lynch, G. C.; Truong, T. N.; Lu, D.-h.; Truhlar, D. G.; Garrett, B. C. *J. Am. Chem. Soc.* **1993**, *115*, 2408.
(516) Marcus, R. A. *Discussions Faraday Soc.* **1967**, *44*, 7.
(517) Bondi, D. K.; Connor, J. N. L.; Garrett, B. C.; Truhlar, D. G. *J. Chem. Phys.* **1983**, *78*, 5981.
(518) Garrett, B. C.; Truhlar, D. G. *J. Chem. Phys.* **1983**, *79*, 4931.
(519) Garrett, B. C.; Abusalbi, N.; Kouri, D. J.; Truhlar, D. G. *J. Chem. Phys.* **1985**, *83*, 2252.
(520) Garrett, B. C.; Joseph, T.; Truong, T. N.; Truhlar, D. G. *Chem. Phys.* **1989**, *136*, 271.
(521) Truong, T. N.; Lu, D.-h.; Lynch, G. C.; Liu, Y.-P.; Melissas, V. S.; Steward, J. J. P.; Steckler, R.; Garrett, B. C.; Isaacson, A. D.; González-Lafont, A.; Rai, S. N.; Hancock, G. C.; Joseph, T.; Truhlar, D. G. *Comput. Phys. Commun.* **1993**, *75*, 143.
(522) Liu, Y.-P.; Lu, D.-h.; González-Lafont, A.; Truhlar, D. G.; Garrett, B. C. *J. Am. Chem. Soc.* **1993**, *115*, 7806.
(523) Fernández-Ramos, A.; Truhlar, D. G. *J. Chem. Phys.* **2001**, *114*, 1491.
(524) Fernandez-Ramos, A.; Truhlar, D. G. *J. Chem. Theory Comp.* **2005**, *1*, 1063.
(525) Sansón, J. A.; Sánchez, M.-L.; Corchado, J. C. *J. Chem. Phys.* **2006**, *110*, 589.
(526) Allison, T. C.; Truhlar, D. G. In *Modern Methods for Multidimensional Dynamics Computations in Chemistry*; Thompson, D. L., Ed.; World Scientific: Singapore, 1998; pp 618−712.

(527) Bowman, J.; Wang, D.; Huang, X.; Huarte-Larrañaga, H.; Manthe, U. *J. Chem. Phys.* **2001**, *114*, 9083.
(528) Huarte-Larrañaga, F. *J. Chem. Phys.* **2002**, *117*, 4635.
(529) Pu, J.; Corchado, J. C.; Truhlar, D. G. *J. Chem. Phys.* **2001**, *115*, 6266.
(530) Pu, J.; Truhlar, D. G. *J. Chem. Phys.* **2002**, *117*, 1479.
(531) Espinosa-García, J.; García-Bernáldez, J. C. *Phys. Chem. Chem. Phys.* **2000**, *2*, 2345.
(532) Child, M. S. *Mol. Phys.* **1967**, *12*, 401.
(533) Garrett, B. C.; Truhlar, D. G.; Grev, R. S.; Schatz, G. C.; Walker, R. B. *J. Phys. Chem.* **1981**, *85*, 3806.
(534) Takayanagi, T.; Kurosaki, Y. *Phys. Chem. Chem. Phys.* **1999**, *1*, 1099.
(535) Balakrishnan, N.; Dalgarno, A. *Chem. Phys. Lett.* **2001**, *341*, 652.
(536) Skokov, S.; Zou, S.; Bowman, J. M.; Allison, T. C.; Truhlar, D. G.; Lin, Y.; Ramachandran, B.; Garrett, B. C.; Lynch, B. J. *J. Phys. Chem. A* **2001**, *105*, 2298.
(537) Xie, T.; Bowman, J. M.; Peterson, K. A.; Ramachandra, B. *J. Chem. Phys.* **2003**, *119*, 9601.
(538) Balakrishnan, N.; Dalgarno, A. *J. Phys. Chem. A* **2003**, *107*, 7101.
(539) Wei, L.; Jasper, A. W.; Truhlar, D. G. *J. Phys. Chem. A* **2003**, *107*, 7236.
(540) Bowman, J. M. *Chem. Phys.* **2005**, *308*, 255.
(541) Weck, P. F.; Balakrishnan, N. *J. Chem. Phys.* **2005**, *122*, 154309.
(542) Weck, P. F.; Balakrishnan, N. *J. Chem. Phys.* **2005**, *122*, 234310.
(543) Mayer, I. *J. Chem. Phys.* **1974**, *60*, 2564.
(544) Lim, C.; Truhlar, D. G. *J. Phys. Chem.* **1985**, *89*, 5.
(545) Truhlar, D. G.; Garrett, B. C. *J. Am. Chem. Soc.* **1989**, *111*, 1232.
(546) Natanson, G. A.; Garrett, B. C.; Truong, T. N.; Joseph, T.; Truhlar, D. G. *J. Chem. Phys.* **1991**, *94*, 7875.
(547) Jackels, C. J.; Gu, Z.; Truhlar, D. G. *J. Chem. Phys.* **1995**, *102*, 3188.
(548) Nguyen, K. A.; Jackels, C. F.; Truhlar, D. G. *J. Chem. Phys.* **1996**, *104*, 6491.
(549) Chuang, Y.-Y.; Truhlar, D. G. *J. Chem. Phys.* **1997**, *107*, 83.
(550) Corchado, J. C.; Coitiño, E. L.; Chuang, Y.-Y.; Fast, P. L.; Truhlar, D. G. *J. Phys. Chem. A* **1998**, *102*, 2424.
(551) Hu, W.-P.; Liu, Y.-P.; Truhlar, D. G. *J. Chem. Soc., Faraday Trans.* **1994**, *90*, 1715.
(552) Chuang, Y.-Y.; Truhlar, D. G. *J. Phys. Chem. A* **1997**, *101*, 3808.
(553) Chuang, Y.-Y.; Truhlar, D. G. *J. Phys. Chem. A* **1997**, *101*, 8741.
(554) Chuang, Y.-Y.; Corchado, J. C.; Truhlar, D. G. *J. Phys. Chem. A* **1999**, *103*, 1140.
(555) González-García, N.; González-Lafont, A.; Lluch, J. M. *J. Phys. Chem. A* **2006**, *110*, 798.
(556) Hu, W.-P.; Truhlar, D. G. *J. Am. Chem. Soc.* **1995**, *117*, 10726.
(557) Zhao, X. G.; Lu, D.-h.; Liu, Y.-P.; Lynch, G. C.; Truhlar, D. G. *J. Chem. Phys.* **1992**, *97*, 6369.
(558) Fernández-Ramos, A.; Truhlar, D. G.; Corchado, J. C.; Espinosa-García, J. *J. Phys. Chem. A* **2002**, *106*, 4957.
(559) Truhlar, D. G. *J. Chem. Phys.* **1970**, *53*, 2041.
(560) Hofacker, L. *Z. Naturforsch.* **1963**, *18a*, 607.
(561) Wu, S.; Marcus, R. A. *J. Chem. Phys.* **1970**, *53*, 4026.
(562) Duff, J. W.; Truhlar, D. G. *Chem. Phys. Lett.* **1973**, *23*, 327.
(563) Garrett, B. C.; Truhlar, D. G. *Proc. Natl. Acad. Sci. U.S.A.* **1979**, *76*, 4755.
(564) Bowman, J. M.; Kuppermann, A.; Adams, J. T.; Truhlar, D. G. *Chem. Phys. Lett.* **1973**, *20*, 229.
(565) Lynch, G. C.; Halvick, P.; Truhlar, D. G.; Garrett, B. C.; Schwenke, D. W.; Kouri, D. J. *Z. Naturforsch.* **1989**, *44a*, 427.
(566) Chatfield, D. C.; Friedman, R. S.; Truhlar, D. G.; Schwenke, D. W. *Faraday Discuss. Chem. Soc.* **1991**, *91*, 289.
(567) Chatfield, D. C.; Friedman, R. S.; Lynch, G. C.; Truhlar, D. G.; Schwenke, D. W. *J. Chem. Phys.* **1993**, *98*, 342.
(568) Mortensen, E. M.; Pitzer, K. S. *Chem. Soc. Spec. Publ.* **1962**, *16*, 57.
(569) Walker, R. B.; Hayes, E. F. *J. Phys. Chem.* **1984**, *88*, 1194.
(570) Bowman, J. M. *Adv. Chem. Phys.* **1985**, *61*, 151.
(571) Zhang, D. H.; Zhang, J. Z. H. *J. Chem. Phys.* **1994**, *100*, 2697.
(572) Nyman, G.; Clary, D. C.; Levine, R. D. *Chem. Phys.* **1995**, *191*, 223.
(573) Yu, H.-G.; Nyman, G. *J. Chem. Phys.* **2000**, *112*, 238.
(574) Aguillon, F.; Sizun, M. *J. Chem. Phys.* **2000**, *112*, 10179.
(575) Szichman, H.; Gilibert, M.; Gonzalez, M.; Giménez, X.; Navarro, A. A. *J. Chem. Phys.* **2000**, *113*, 176.
(576) Skokov, S.; Bowman, J. M. *J. Chem. Phys.* **2000**, *113*, 4995.
(577) Yu, H.-G.; Nyman, G. *J. Chem. Phys.* **2000**, *113*, 8936.
(578) Nyman, G.; Yu, H.-G. *Rep. Prog. Phys.* **2000**, *63*, 1001.
(579) Takayanagi, T.; Wada, A. *Chem. Phys.* **2001**, *269*, 37.
(580) Domenico, D. D.; Hernández, M. I.; Campós-Martínez, J. *Chem. Phys. Lett.* **2001**, *342*, 177.
(581) Yu, H.-G. *J. Chem. Phys.* **2001**, *114*, 2967.
(582) Wang, D.; Bowman, J. M. *J. Chem. Phys.* **2001**, *115*, 2055.
(583) Yu, H.-G.; Nyman, G. *J. Phys. Chem. A* **2001**, *105*, 2240.
(584) Skokou, S.; Bowman, J. M. *J. Phys. Chem. A* **2001**, *105*, 2502.
(585) Huarte-Larrañaga, F.; Manthe, U. *J. Phys. Chem. A* **2001**, *105*, 2522.
(586) Buonomo, E.; Clary, D. C. *J. Phys. Chem. A* **2001**, *105*, 2694.
(587) Szichman, H.; Baer, R. *J. Chem. Phys.* **2002**, *117*, 7614.
(588) Palma, J.; Echave, J.; Clary, D. C. *J. Phys. Chem. A* **2002**, *106*, 8256.
(589) Bowman, J. M. *Theor. Chem. Acc.* **2002**, *108*, 125.
(590) Valero, R.; McCormack, D. A.; Kroes, G.-J. *J. Chem. Phys.* **2004**, *120*, 4263.
(591) Kerkeni, B.; CLary, D. C. *J. Chem. Phys.* **2004**, *121*, 6809.
(592) Kerkeni, B.; Clary, D. C. *J. Phys. Chem. A* **2004**, *108*, 8966.
(593) Hennig, C.; Schmatz, S. *J. Chem. Phys.* **2005**, *122*, 234307.
(594) Kerkeni, B.; Clary, D. C. *Mol. Phys.* **2005**, *103*, 1745.
(595) Hennig, C.; Schmatz, S. *Phys. Chem. Chem. Phys.* **2005**, *7*, 1552.
(596) Valero, R.; Kroes, G.-J. *Chem. Phys. Lett.* **2006**, *417*, 43.
(597) Kerkeni, B.; Clary, D. C. *Chem. Phys. Lett.* **2006**, *421*, 499.
(598) Takayanagi, T. *J. Phys. Chem. A* **2006**, *110*, 361.
(599) Kerkeni, B.; Clary, D. C. *Phys. Chem. Chem. Phys.* **2006**, *8*, 917.
(600) Viggiano, A. A.; Paschkewitz, J.; Morris, R. A.; Paulson, J. F.; González-Lafont, A.; Truhlar, D. G. *J. Am. Chem. Soc.* **1991**, *113*, 9404.
(601) Corchado, J. C.; Espinosa-Garcia, J.; Hu, W.-P.; Rossi, I.; Truhlar, D. G. *J. Phys. Chem.* **1995**, *99*, 687.
(602) Steckler, R.; Thurman, G. A.; Watts, J. D.; Bartlett, R. J. *J. Chem. Phys.* **1997**, *106*, 3926.
(603) Sekusak, S.; Liedl, K. R.; Rode, B. M.; Sabljic, A. *J. Phys. Chem. A* **1997**, *101*, 4245.
(604) Chuang, Y.-Y.; Truhlar, D. G. *J. Phys. Chem. A* **1998**, *102*, 242.
(605) González-Lafont, A.; Villà, J.; Lluch, J. M.; Bertrán, J.; Steckler, R.; Truhlar, D. G. *J. Phys. Chem. A* **1998**, *102*, 3420.
(606) Roberto-Neto, R.; Coitiño, E. L.; Truhlar, D. G. *J. Phys. Chem. A* **1998**, *102*, 4568.
(607) Corchado, J. C.; Espinosa-Garcia, J.; Roberto-Neto, O.; Chuang, Y.-Y.; Truhlar, D. G. *J. Phys. Chem. A* **1998**, *102*, 4899.
(608) Espinosa-Garcia, J.; Coitiño, E. L.; González-Lafont, A.; Lluch, J. M. *J. Phys. Chem. A* **1998**, *102*, 10715.
(609) Wu, Y.-R.; Hu, W. P. *J. Am. Chem. Soc.* **1999**, *121*, 10168.
(610) Masgrau, L.; González-Lafont, A.; Lluch, J. M. *J. Phys. Chem. A* **1999**, *103*, 1044.
(611) Chuang, Y.-Y.; Radhakrishnan, M. L.; Fast, P. L.; Cramer, C. J.; Truhlar, D. G. *J. Phys. Chem. A* **1999**, *103*, 4893.
(612) Villà, J.; Corchado, J. C.; González-Lafont, A.; Lluch, J. M.; Truhlar, D. G. *J. Phys. Chem. A* **1999**, *103*, 5061.
(613) Sekusak, S.; Cory, M. G.; Bartlett, R. J.; Sabljic, A. *J. Phys. Chem. A* **1999**, *103*, 11394.
(614) Kurosaki, Y.; Takayanagi, T. *J. Chem. Phys.* **2000**, *113*, 4060.
(615) Huang, C.-H.; You, R.-M.; Lian, P.-Y.; Hu, W.-P. *J. Phys. Chem. A* **2000**, *104*, 7200.
(616) Yin, H.-M.; Yang, B.-H.; Han, K.-L.; He, G.-Z.; Guo, J.-Z.; Liu, C.-P.; Gu, Y.-S. *Phys. Chem. Chem. Phys.* **2000**, *2*, 5093.
(617) Troya, D.; Lakin, M. J.; Schatz, G. C.; Gonzalez, M. *J. Chem. Phys.* **2001**, *115*, 1828.
(618) Sekusak, S.; Sabljic, A. *J. Phys. Chem. A* **2001**, *105*, 1968.
(619) Lien, P.-Y.; You, R.-M.; Hu, W.-P. *J. Phys. Chem. A* **2001**, *105*, 2391.
(620) Huang, C.-H.; Tsai, L.-C.; Hu, W.-P. *J. Phys. Chem. A* **2001**, *105*, 9945.
(621) González-Lafont, A.; Lluch, J. M.; Espinosa-Garcia, J. *J. Phys. Chem. A* **2001**, *105*, 10553.
(622) Zhang, X.; Ding, Y.-H.; Li, Z.-S.; Huang, X.-R.; Sun, C. C. *Phys. Chem. Chem. Phys.* **2001**, *3*, 965.
(623) Roberto-Neto, O.; Machado, F. B. C. *Theor. Chem. Acc.* **2001**, *107*, 15.
(624) Pu, J.; Truhlar, D. G. *J. Chem. Phys.* **2002**, *117*, 10675.
(625) Wu, Y.; Ding, Y.-H. Xiao, J.-F.; Li, Z.-S.; Huang, X.-R.; Sun, C.-C. *J. Comput. Chem.* **2002**, *23*, 1366.
(626) Zhang, Q.; Zhang, D.; Wang, S.; Gu, Y. *J. Phys. Chem. A* **2002**, *106*, 122.
(627) Masgrau, L.; González-Lafont, A.; Lluch, J. M. *J. Phys. Chem. A* **2002**, *106*, 11760.
(628) Masgrau, L.; González-Lafont, A.; Lluch, J. M. *Theor. Chem. Acc.* **2002**, *108*, 38.
(629) Xu, F.; Lin, M. C. *Int. J. Chem. Kinet.* **2003**, *35*, 184.
(630) Wu, J.-Y.; Liu, J.-Y.; Li, Z.-S.; Huang, X.-R.; Sun, C.-C. *J. Comput. Chem.* **2003**, *24*, 593.
(631) Masgrau, L.; González-Lafont, A.; Lluch, J. M. *J. Phys. Chem. A* **2003**, *107*, 4490.
(632) Choi, Y. M.; Park, J.; Lin, M. C. *J. Phys. Chem. A* **2003**, *107*, 7755.
(633) Zhang, Q.; Gu, Y.; Wang, S. *J. Phys. Chem. A* **2003**, *107*, 8295.
(634) Voegele, A. F.; Tautermann, C. S.; Loerting, T.; Liedl, K. R. *Phys. Chem. Chem. Phys.* **2003**, *5*, 487.
(635) Li, H.-Y.; Pu, M.; Ji, Y.-Q.; Xu, Z.-F.; Feng, W.-L. *Chem. Phys.* **2004**, *307*, 35.
(636) Pei, K.; Li, H. *Chem. Phys. Lett.* **2004**, *387*, 70.

(637) Nguyen, H. M. T.; Zhang, S.; Peeters, J.; Truong, T. N.; Nguyen, M. T. *Chem. Phys. Lett.* **2004**, *388*, 94.
(638) Zhang, Q.; Zhang, R. Q.; Gu, Y. *J. Phys. Chem. A* **2004**, *108*, 1064.
(639) Xu, Z. F.; Park, J.; Lin, M. C. *J. Chem. Phys.* **2004**, *120*, 6593.
(640) Ochando-Pardo, M.; Nebot-Gil, I.; González-Lafont, A.; Lluch, J. M. *J. Phys. Chem. A* **2004**, *108*, 5117.
(641) Roberto-Neto, O.; Machado, F. B. C.; Ornellas, F. R. *Chem. Phys. Lett.* **2005**, *409*, 38.
(642) Lin, H.; Zhao, Y.; Ellingson, B. A.; Pu, J.; Truhlar, D. G. *J. Am. Chem. Soc.* **2005**, *127*, 2830.
(643) Galano, A.; Alvarez-Idaboy, J. R.; Ruiz-Santoyo, Ma. E.; Vivier-Bunge, A. *J. Phys. Chem. A* **2005**, *109*, 169.
(644) He, H.-Q.; Liu, J.-Y.; Li, Z.-S.; Sun, C.-C. *J. Phys. Chem. A* **2005**, *109*, 3235.
(645) Zhang, H.; Wu, J.-Y.; Li, Z.-S.; Liu, J.-Y.; Sheng, L.; Sun, C.-C. *THEOCHEM* **2005**, *728*, 25.
(646) Xie, J.; Feng, D.; Feng, S.; Zhang, J. *Chem. Phys*. **2006**, *323*, 185.
(647) Sellevåg, R. S.; Nyman, G.; Nielsen, C. J. *J. Phys. Chem. A* **2006**, *110*, 141.
(648) Galano, A.; Cruz-Torres, A.; Alvarez-Idaboy, J. R. *J. Phys. Chem. A* **2006**, *110*, 1917.
(649) He, H.-q.; Liu, J.-y.; Li, Z.; Sun, C.-c. *THEOCHEM*. **2006**, *763*, 59.
(650) Albu, T. V.; Swaminathan, S. *Theor. Chem. Acc*., in press.
(651) Mielke, S. L.; Lynch, G. C.; Truhlar, D. G.; Schwenke, D. W. *Chem. Phys. Lett.* **1993**, *216*, 441.
(652) Park, T. J.; Light, J. C. *J. Chem. Phys.* **1989**, *91*, 974.
(653) Chatfield, D. C.; Truhlar, D. G.; Schwenke, D. W. *J. Chem. Phys.* **1991**, *94*, 2040.
(654) Day, P. N.; Truhlar, D. G. *J. Chem. Phys.* **1991**, *94*, 2045.
(655) Park, T. J.; Light, J. C. *J. Chem. Phys.* **1991**, *94*, 2946.
(656) Mielke, S. L.; Lynch, G. C.; Truhlar, D. G.; Schwenke, D. W. *J. Phys. Chem.* **1994**, *98*, 8000.
(657) Mielke, S. L.; Allison, T. C.; Truhlar, D. G.; Schwenke, D. W. *J. Phys. Chem.* **1996**, *100*, 13558.
(658) Day, P. N.; Truhlar, D. G. *J. Chem. Phys.* **1991**, *95*, 5097.
(659) Manthe, U.; Seideman, T.; Miller, W. H. *J. Chem. Phys.* **1993**, *99*, 10078. Manthe, U.; Seideman, T.; Miller, W. H. *J. Chem. Phys.* **1994**, *101*, 4759.
(660) Manthe, U.; Matzkies, F. *J. Chem. Phys.* **2000**, *113*, 5725.
(661) Goldfield, E. M.; Gray, S. K. *J. Chem. Phys.* **2002**, *117*, 1604.
(662) Bowman, J. M.; Wang, D.; Huang, X.; Huarte-Larrañaga, F.; Manthe, U. *J. Chem. Phys.* **2001**, *114*, 9683.
(663) Wu, T.; Werner, H.-J.; Manthe, U. *J. Chem. Phys.* **2006**, *124*, 164307.
(664) Huarte-Larrañaga, F.; Manthe, U. *J. Chem. Phys.* **2002**, *117*, 4635.
(665) Medvedev, D. M.; Gray, S. K.; Goldfield, E. M.; Lakin, M. J.; Troya, D.; Schatz, G. C. *J. Chem. Phys.* **2004**, *120*, 1231.
(666) Miller, W. H.; Schwartz, S. P.; Tromp. J. W. *J. Chem. Phys.* **1983**, *79*, 4889.
(667) Tromp, J. W.; Miller, W. H. *Faraday Discuss. Chem. Soc.* **1987**, *84*, 441.
(668) Park, T. J.; Light, J. C. *J. Chem. Phys.* **1992**, *96*, 8853.
(669) Re, M.; Laria, D. *J. Chem. Phys.* **1996**, *105*, 4584.
(670) Thompson, W. H.; Miller, W. H. *J. Chem. Phys.* **1997**, *106*, 142.
(671) Woittequand, F.; Monnerville, M.; Briquez, S. *Chem. Phys. Lett.* **2006**, *417*, 492.
(672) Kubo, R.; Toyozawa, Y. *Prog. Theor. Phys*. **1955**, *13*, 160.
(673) Zwanzig, R. *Annu. Rev. Phys. Chem.* **1965**, *16*, 67.
(674) Kapral, R.; Hudson, S.; Ross, J. *J. Chem. Phys.* **1970**, *53*, 4387.
(675) Kapral, R. *J. Chem. Phys.* **1972**, *56*, 1842.
(676) Rosenstein, R. A. *Ber. Bunsen-Ges. Phys. Chem*. **1973**, *77*, 493.
(677) Chandler, D. *J. Chem. Phys.* **1978**, *68*, 2959.
(678) Northrup, S. H.; Hynes, J. T. *J. Chem. Phys.* **1980**, *73*, 2700.
(679) Montgomery, J. A. Jr.; Holmgren, S. L.; Chandler, D. *J. Chem. Phys.* **1980**, *73*, 3868.
(680) Warshel, A.; Hwang, J.-K. *J. Chem. Phys.* **1986**, *59*, 4938.
(681) Wolynes, P. *J. Chem. Phys.* **1987**, *87*, 6559.
(682) Wilson, M. A.; Chandler, D. *Chem. Phys*. **1990**, *149*, 11.
(683) Warshel, A.; Chu, Z. T. *J. Chem. Phys.* **1990**, *93*, 4003.
(684) Ando, K.; Kato, S. *J. Chem. Phys.* **1991**, *95*, 5966.
(685) Hwang, J.-K.; Chu, Z. T.; Yadav, A.; Warshel, A. *J. Phys. Chem.* **1991**, *95*, 8445.
(686) Borgis, D. *Stud. Phys. Theor. Chem.* **1992**, *78*, 345.
(687) Luzar, A.; Chandler, D. *J. Chem. Phys.* **1993**, *98*, 8160.
(688) Borgis, D. *AIP Conf. Proc.* **1994**, *298*, 205.
(689) Dellago, C.; Bolhuis, P. G.; Csajka, F. S.; Chandler, D. *J. Chem. Phys.* **1998**, *108*, 1964.
(690) Bolhuis, P. G.; Dellago, C.; Chandler, D. *Faraday Discuss*. **1998**, *110*, 421.
(691) Vuilleumier, R.; Borgis, D. *J. Chem. Phys.* **1999**, *111*, 4251.
(692) Winter, N.; Benjamin, I. *J. Chem. Phys.* **2005**, *122*, 184717.
(693) Hanna, G.; Kapral, R. *J. Chem. Phys.* **2005**, *122*, 244505.
(694) Yang, S.; Yamamoto, T.; Miller, W. H. *J. Chem. Phys.* **2006**, *124*, 84102.
(695) Ren, J.; Brauman, J. I. *J. Am. Chem. Soc.* **2004**, *126*, 2640.
(696) Miller, J. A.; Pilling, M. J.; Troe, J. *Proc. Combust. Inst*. **2005**, *30*, 43.
(697) Lin, S. Y.; Rackham, E. J.; Guo, H. *J. Phys. Chem. A* **2005**, *109*, in press.
(698) Beccera, R.; Cannady, J. P.; Walsh, R. *J. Phys. Chem. A* **2004**, *108*, 3897.
(699) Murakami, Y.; Onishi, S.; Fujii, N. *J. Phys. Chem. A* **2004**, *108*, 8141.
(700) Xu, Z. F.; Hsu, C.-H.; Lin, M. C. *J. Chem. Phys.* **2005**, *122*, 234308.
(701) Carpenter, B. K. *Annu. Rev. Phys. Chem.* **2005**, *56*, 57.
(702) Bunker, D. L.; Hase, W. L. *J. Chem. Phys.* **1973**, *59*, 4621.
(703) Hase, W. L. In *Modern Theoretical Chemistry-Dynamics of Molecular Collisions, Part B*; Miller, W. H., Ed.; Plenum Press: New York, 1976; pp 121−169.
(704) Hase, W. L. In *Potential Energy Surfaces and Dynamics Calculations*; Truhlar, D. G., Ed.; Plenum Press: New York, 1979; pp 1−35.
(705) Miller, J. A.; Garrett, B. C. *Int. J. Chem. Kinet*. **1997**, *29*, 275.
(706) Miller, J. A.; Klippenstein, S. J. *Int. J. Chem. Kinet*. **1999**, *31*, 753.
(707) Kiefer, J. H.; Katopidis, C.; Santhanam, S.; Srinivasan, N. K.; Tranter, R. S. *J. Phys. Chem. A* **2004**, *108*, 2443.
(708) Nummela, J. A.; Carpenter, B. K. *J. Am. Chem. Soc.* **2002**, *124*, 8512.
(709) Baer, T.; Potts, A. R. *J. Phys. Chem. A* **2000**, *104*, 9397.
(710) Dian, B. C.; Longarte, A.; Winter, P. R.; Zwier, T. S. *J. Chem. Phys.* **2004**, *120*, 133.
(711) Hase, W. L.; Mondro, S. L.; Duchovic, R. J.; Hirst. D. M. J. *Am. Chem. Soc*. **1987**, *109*, 2916.
(712) Yu, J.; Klippenstein, S. J. *J. Phys. Chem.* **1991**, *95*, 9882.
(713) Klippenstein, S. J.; Marcus, R. A. *J. Chem. Phys.* **1987**, *87*, 3410.
(714) Wardlaw, D. M., Marcus, R. A. *Adv. Chem. Phys.* **1988**, *70*, 231.
(715) Marcus, R. A. *J. Chem. Phys.* **1952**, *20*, 359.
(716) Rosenstock, H. M.; Wallenstein, M. B.; Wahrhaftig, A. L.; Eyring, H. *Proc. Natl. Acad. Sci. U.S.A.* **1952**, *38*, 667.
(717) Pechukas, P.; Light, J. C. *J. Chem. Phys.* **1965**, *42*, 3281.
(718) Light, J. C.; Lin, J. *J. Chem. Phys.* **1965**, *43*, 3209.
(719) Nikitin, E. E. *Teor. Eksp. Khim. Acad. Nauk. Ukr. SSR* **1965**, *1*, 428.
(720) Pechukas, P.; Rankin, R., Light, J. C. *J. Chem. Phys.* **1966**, *44*, 794.
(721) Truhlar, D. G. *J. Chem. Phys.* **1969**, *51*, 4617.
(722) Truhlar, D. G.; Kuppermann, A. *J. Phys. Chem.* **1969**, *73*, 1722.
(723) Chesnavich, W. J.; Bowers, M. T. *J. Am. Chem. Soc*. **1977**, *99*, 1705.
(724) Chesnavich, W. J.; Bowers, M. T. *J. Chem. Phys.* **1977**, *66*, 2306.
(725) Chesnavich, W. J.; Bowers, M. T. *Prog. React. Kinet*. **1982**, *11*, 137.
(726) Marcus, R. A. *J. Chem. Phys.* **1965**, *43*, 1598.
(727) Quack, M.; Troe, J. *Ber. Bunsen. Phys. Chem*. **1974**, *78*, 240.
(728) Quack, M.; Troe, J. *Ber. Bunsen. Phys. Chem*. **1975**, *79*, 469.
(729) Moran, T. F.; Hamill, W. H. *J. Chem. Phys.* **1963**, *39*, 1413.
(730) Gupta, S. K.; Jones, E. G.; Harrison, A. G.; Myher, J. J. *Can. J. Chem.* **1965**, *45*, 3107.
(731) Su, T.; Bowers, M. T. *J. Chem. Phys.* 58 **1973**, *3027*.
(732) Su, T.; Bowers, M. T. *Int. J. Mass Spectrom. Ion Phys.* **1975**, *17*, 211.
(733) Su, T.; Bowers, M. T. In *Gas-Phase Ion Chemistry*; Bowers, M. T., Ed.; Academic Press: New York, 1979; Vol. 1, pp 83−118.
(734) Chesnavich, W. J.; Su, T.; Bowers, M. T. *J. Chem. Phys.* **1980**, *72*, 2641.
(735) Celli, F.; Weddle, G.; Ridge, D. P. *J. Chem. Phys.* **1980**, *73*, 801.
(736) Markovic, N.; Nordholm, S. *J. Chem. Phys.* **1989**, *91*, 6813.
(737) Su, T.; Chesnavich, W. J. *J. Chem. Phys.* **1982**, *76*, 5183.
(738) Su, T. *J. Chem. Phys.* **1988**, *88*, 4102, 5355.
(739) Klippenstein, S. J. *J. Chem. Phys.* **1994**, *101*, 1996.
(740) Maergoiz, A. I.; Nikitin, E. E.; Troe, J.; Ushakov, V. G. *J. Chem. Phys.* **1998**, *108*, 5265.
(741) Maergoiz, A. I.; Nikitin, E. E.; Troe, J.; Ushakov, V. G. *J. Chem. Phys.* **1998**, *108*, 9987.
(742) Maergoiz, A. I.; Nikitin, E. E.; Troe, J.; Ushakov, V. G. *J. Chem. Phys.* **2002**, *117*, 4201.
(743) Harding, L. B.; Klippenstein, S. J.; Georgievskii, Y. *Proc. Combust. Inst*. **2004**, *30*, 985.
(744) Harding, L. B.; Georgievskii, Y.; Klippenstein, S. J. *J. Phys. Chem. A* **2005**, *109*, 4646.
(745) Gridelet, E.; Lorquet, J. C.; Leyh, B. *J. Chem. Phys.* **2005**, *122*, 94106.
(746) Georgievskii, Y.; Klippenstein, S. J. *J. Chem. Phys.* **2005**, *122*, 194103.
(747) Clary, D. C. *Annu. Rev. Phys. Chem.* **1990**, *41*, 61.
(748) Troe, J. *Adv. Chem. Phys.* **1997**, *101*, 819.
(749) Hamon, S.; Speck, T.; Mitchell, J. B. A.; Rowe, B. Troe, J. *J. Chem. Phys.* **2005**, *123*, 54303.
(750) Smith, S. C. *J. Chem. Phys.* **1991**, *95*, 3404.
(751) Smith, S. C. *J. Chem. Phys.* **1992**, *97* 2406.
(752) Smith, S. C. *J. Phys. Chem*. **1993**, *97*, 7034.
(753) Aubanel, E. E.; Wardlaw, D. M. *J. Phys. Chem.* **1989**, *93*, 3117.
(754) Klots, C. E. *J. Chem. Phys.* **1976**, *64*, 4269.
(755) Klippenstein, S. J. *Chem. Phys. Lett.* **1990**, *170*, 71.

(756) Klippenstein, S. J. *J. Chem. Phys.* **1991**, *94*, 6469.
(757) Klippenstein, S. J. *J. Chem. Phys.* **1992**, *96*, 367.
(758) Rai, S. N.; Truhlar, D. G. *J. Chem. Phys.* **1983**, *79*, 6046.
(759) Klippenstein, S. J. *Chem. Phys. Lett.* **1993**, *214*, 418.
(760) Klippenstein, S. J. *J. Phys. Chem.* **1994**, *98*, 11459.
(761) Smith, S. C. *J. Chem. Phys.* **1999**, *111*, 1830.
(762) Smith, S. C. *J. Phys. Chem. A* **2000**, *104*, 10489.
(763) Robertson, S. H.; Wardlaw, D. M.; Wagner, A. F. *J. Chem. Phys.* **2002**, *117*, 593.
(764) Robertson, S.; Wagner, A. F.; Wardlaw, D. M. *J. Phys. Chem. A* **2002**, *106*, 2598.
(765) Georgievskii, Y.; Klippenstein, S. J. *J. Chem. Phys.* **2003**, *118*, 5442.
(766) Harding, L. B.; Klippenstein, S. *J. Proc. Combust. Inst.* **1998**, *27*, 151.
(767) Klippenstein, S. J.; Harding, L. B. *Phys. Chem. Chem. Phys.* **1999**, *1*, 989.
(768) Klippenstein, S. J.; Harding, L. B. *Proc. Combust. Inst.* **2000**, *28*, 1503.
(769) Wardlaw, D. M.; Marcus, R. A. *J. Phys. Chem.* **1986**, *90*, 5383.
(770) Klippenstein, S. J.; Khundkar, L. R.; Zewail, A. H.; Marcus, R. A. *J. Chem. Phys.* **1988**, *89*, 4761.
(771) Klippenstein, S. J.; Marcus, R. A. *J. Chem. Phys.* **1989**, *91*, 2280.
(772) Claire, P. d. S.; Peslherbe, G. H.; Wang, H.; Hase, W. L. *J. Am. Chem. Soc.* **1997**, *119*, 5007.
(773) Das, G.; Wahl, G. C. *J. Chem. Phys.* **1966**, *44*, 3050.
(774) Brown, F. B.; Truhlar, D. G. *Chem. Phys. Lett.* **1985**, *113*, 441.
(775) Schmidt, M. W.; Gordon, M. S. *Annu. Rev. Phys. Chem.* **1998**, *49*, 233.
(776) Klippenstein, S. J.; Georgievskii, Y.; Harding, L. B. *Proc. Combust. Inst.* **2002**, *29*, 1229.
(777) Brouard, M.; Macpherson, M. T.; Pilling, M. J. *J. Phys. Chem.* **1989**, *93*, 4047.
(778) Seakins, P. W.; Robertson, S. H.; Pilling, M. J.; Wardlaw, D. M.; Nesbitt, F. L.; Thorn, R. P.; Payne, W. A.; Stief, L. J. *J. Phys. Chem. A* **1997**, *101*, 9974.
(779) Su, M.-C.; Michael, J. V. *Proc. Combust. Inst.* **2001**, *29*, 1219.
(780) Hu, X.; Hase, W. L. *J. Chem. Phys.* **1991**, *95*, 8073.
(781) Klippenstein, S. J.; East, A. L. L.; Allen, W. D. *J. Chem. Phys.* **1996**, *105*, 118.
(782) Klippenstein, S. J.; Harding, L. B. *J. Phys. Chem. A* **1999**, *103*, 9388.
(783) Fang, D.-C.; Harding, L. B.; Klippenstein, S. J.; Miller, J. A. *Faraday Discuss.* **2001**, *119*, 207.
(784) Klippenstein, S. J.; Georgievskii, Y.; Harding, L. B. *Phys. Chem. Chem. Phys.* **2006**, *8*, 1133.
(785) Georgievskii, Y.; Klippenstein, S. J. *J. Phys. Chem. A* **2003**, *107*, 9776.
(786) Pilling, M. J.; Robertson, S. H. *Annu. Rev. Phys. Chem.* **2003**, *54*, 245.
(787) Truhlar, D. G.; Blais, N. C.; Hajduk, J.-C. J.; Kiefer, J. H. *Chem. Phys. Lett.* **1979**, *63*, 337.
(788) Lim, C.; Truhlar, D. G. *J. Phys. Chem.* **1983**, *87*, 2683.
(789) Lim, C.; Truhlar, D. G. *J. Chem. Phys.* **1983**, *79*, 3296.
(790) Lim, C.; Truhlar, D. G. *J. Phys. Chem.* **1984**, *88*, 778.
(791) Lim, C.; Truhlar, D. G. *Chem. Phys. Lett.* **1985**, *114*, 253.
(792) Haug, K.; Truhlar, D. G.; Blais, N. C. *J. Chem. Phys.* **1987**, *86*, 2697; **1992**, *96*, 5556(E).
(793) Ramakrishna, M.; Babu, S. V. *Chem. Phys.* **1979**, *36*, 259.
(794) Kuznetsov, N. M.; Samusenko, A. M. *Teor. Eksp. Khim.* **1982**, *18*, 259.
(795) Davis, M. J.; Skodje, R. T. *Z. Phys. Chem.* **2001**, *215*, 233.
(796) Davis, M. J.; Klippenstein, S. J. *J. Phys. Chem. A* **2002**, *106*, 5860.
(797) Davis, M. J. *J. Chem. Phys.* **2002**, *116*, 7828.
(798) Davis, M. J.; Kiefer, J. H. *J. Chem. Phys.* **2002**, *116*, 7814.
(799) Brown, N. J.; Miller, J. A. *J. Chem. Phys.* **1984**, *80*, 5568.
(800) Lendvay, G.; Schatz, G. C. *J. Phys. Chem.* **1992**, *96*, 3752.
(801) Lendvay, G.; Schatz, G. C. In *Vibrational Energy Transfer in Large and Small Molecules*; Barker, J. R., Ed.; J. A. I. Press: Greenwich, Connecticut, 1995, 2B; pp 481−513.
(802) Nordholm, S.; Schranz, H. W. In *Vibrational Energy Transfer in Large and Small Molecules*; Barker J. R., Ed.; J. A. I. Press: Greenwich, Connecticut, 1995; Vol. 2A, pp 245−281.
(803) Troe, J. *J. Phys. Chem.* **1979**, *83*, 114.
(804) Michael, J. V.; Su, M.-C.; Sutherland, J. W.; Carroll, J. J.; A. F. Wagner, *J. Phys.* Chem. A **2002**, *106*, 5297.
(805) Durant, J. L.; Kaufman, F. *Chem. Phys. Lett.* **1987**, *142*, 246.
(806) Hsu, K.-J.; Anderson, S. M.; Durant, J. L.; Kaufman, F. *J. Phys. Chem.* **1989**, *93*, 1018.
(807) Oref, I.; Tardy, D. C. *Chem. Rev.* **1990**, *90*, 1407.
(808) Gilbert, R. G. *Int. Rev. Phys. Chem.* **1991**, *10*, 319.
(809) Lendvay, G.; Schatz, G. C. *J. Phys. Chem.* **1994**, *98*, 6530.
(810) Clarke, D. L.; Thompson, K. C.; Gilbert, R. G. *Chem. Phys. Lett.* **1991**, *182*, 357.
(811) Oref, I. In *Vibrational Energy Transfer in Large and Small Molecules*; Barker, J. R., Ed.; J. A. I Press: Greenwich, Connecticut, 1995; Vol. 2B, pp 285−298.
(812) Lenzer, T.; Luther, K.; Troe, J.; Gilbert, R. G.; Lim, K. L. *J. Chem. Phys.* **1995**, *103*, 626.
(813) Bernshtein, V.; Oref, I.; Lendvay, G. *J. Phys. Chem.* **1996**, *100*, 9738.
(814) Bernshtein, V.; Oref, I. *J. Chem. Phys.* **1998**, *108*, 3543.
(815) Grigoleit, U.; Lenzer, T.; Luther, K. *Z. Phys. Chem.* **2000**, *213*, 1065.
(816) Higgins, C.; Ju, Q.; Seiser, N.; Flynn, G. W.; Chapman, S. *J. Phys. Chem. A* **2001**, *105*, 2858.
(817) Luther, K.; Reihs, K. *Ber. Bunsen-Ges. Phys. Chem.* **1988**, *92*, 442.
(818) Löhmannsröben, H. G.; Luther, K. *Chem. Phys. Lett.* **1988**, *144*, 473.
(819) Brenner, J. D.; Erinjeri, J. P.; Barker, J. R. *Chem. Phys.* **1993**, *175*, 99.
(820) Mullin, A. S.; Park, J.; Chou, J. Z.; Flynn, G. W.; Weston, R. E. *J. Chem. Phys.* **1993**, *53*, 175.
(821) Mullin, A. S.; Michaels, C. A.; Flynn, G. W. *J. Chem. Phys.* **1995**, *102*, 6032.
(822) Michaels, C. A.; Flynn, G. W. *J. Chem. Phys.* **1997**, *106*, 3558.
(823) Hold, U.; Lenzer, T.; Luther, K.; Reihs, K.; Symonds, A. *Ber. Bunsen-Ges. Phys. Chem.* **1997**, *101*, 552.
(824) Hold, U.; Lenzer, T.; Luther, K.; Reihs, K.; Symonds, A. C. *J. Chem. Phys.* **2000**, *112*, 4076.
(825) Lenzer, T.; Luther, K.; Reihs, K.; Symonds, A. C. *J. Chem. Phys.* **2000**, *112*, 4090.
(826) Barker, J. R.; Yoder, L. M.; King, K. D. *J. Phys. Chem. A* **2001**, *103*, 796.
(827) Grigoleit, U.; Lenzer, T.; Luther, K.; Mützel, M.; Takahara, A. *Phys. Chem. Chem. Phys.* **2001**, *3*, 2192.
(828) Lenzer, T.; Luther, T. *Phys. Chem. Chem. Phys.* **2004**, *6*, 955.
(829) Rabinovitch, B. S.; Tardy, D. C. *J. Chem. Phys.* **1966**, *45*, 3720.
(830) Gilbert, R. G.; Smith, S. C. *Theory of Unimolecular and Recombination Reactions*; Blackwell, UK, 1990.
(831) Hanning-Lee, M. A.; Green, N. J. B.; Pilling, M. J.; Robertson, S. H. *J. Phys. Chem.* **1993**, *97*, 860.
(832) Feng, Y.; Nüranen, J. T.; Benesura, A.; Knyazev, V. D.; Gutman, D.; Tsang, W. *J. Phys. Chem.* **1993**, *97*, 871.
(833) Tsang, W.; Kiefer, J. H. In *Chemical Dynamics and Kinetics of Small Radicals*, Part I; Wagner, A. F., Liu, K., Eds.; World Scientific: Singapore, 1995; pp 58−119.
(834) Knyazev, V. D.; Slagle, I. R. *J. Phys. Chem.* **1996**, *100*, 16899.
(835) Knyazev, V. D.; Tsang, W. *J. Phys. Chem. A* **2000**, *104*, 10747.
(836) Troe, J. *J. Chem. Phys.* **1992**, *97*, 288.
(837) Miller, J. A.; Klippenstein, S. J.; Raffy, C. *J. Phys. Chem. A* **2002**, *106*, 4904.
(838) Miller, J. A.; Chandler, D. W. *J. Chem. Phys.* **1986**, *85*, 4502.
(839) Dove, J. E.; Jones, D. J. *Chem. Phys. Lett.* **1972**, *17*, 134.
(840) Ashton, T.; McElwain, D. L. S.; Pritchard, H. O. *Can. J. Chem.* **1973**, *51*, 237.
(841) Pritchard, H. O. *Spec. Period. Rep. React. Kinet.* **1975**, *1*, 243.
(842) Dove, J. E.; Raynor, S. *J. Phys. Chem.* **1979**, *83*, 127.
(843) Kutz, H. D.; Burns, G. *J. Chem. Phys.* **1981**, *74*, 3947.
(844) Smith, S. C.; Gilbert, R. G. *Int. J. Chem. Kinet.* **1988**, *20*, 307.
(845) Schwenke, D. W. *J. Chem. Phys.* **1990**, *92*, 7267.
(846) Sharma, S. P.; Schwenke, D. W. *J. Thermophys. Heat Transfer* **1991**, *5*, 469.
(847) Robertson, S. H.; Shushin, A. I.; Wardlaw, D. M. *J. Chem. Phys.* **1993**, *98*, 8673.
(848) McIlroy, A.; Tully, F. P. *J. Chem. Phys.* **1993**, *99*, 3597.
(849) Barker, J. R.; King, K. D. *J. Chem. Phys.* **1995**, *103*, 4953.
(850) Bedanov, V. M.; Tsang, W.; Zachariah, M. R. *J. Phys. Chem.* **1995**, *99*, 11452.
(851) Martin, P. G.; Schwarz, D. H.; Mundy, M. E. *Appita J.* **1996**, *461*, 265.
(852) Shizgal, B. D.; Lordet, F. *J. Chem. Phys.* **1996**, *104*, 3579.
(853) Jeffrey, S. J.; Gates, K. E.; Smith, S. C. *J. Phys. Chem.* **1996**, *100*, 7090.
(854) Tsang, W.; Bedanov, V.; Zachariah, M. R. *Ber. Bunsen-Ges. Phys. Chem.* **1997**, *101*, 491.
(855) Robertson, S. H.; Pilling, M. J.; Green, N. J. B. *Mol. Phys.* **1996**, *89*, 1531.
(856) Venkatesh, P. K.; Dean, H. M.; Cohen, M. H.; Case, R. W. *J. Chem. Phys.* **1997**, *107*, 8904.
(857) Robertson, S. H.; Pilling, M. J.; Gates, K. E.; Smith, S. C. *J. Comput. Chem.* **1997**, *18*, 1004.
(858) Gates, K. E.; Robertson, S. H.; Smith, S. C.; Pilling, M. J.; Beasley, M. S.; Maschhoff, K. *J. Phys. Chem. A* **1997**, *101*, 5765.
(859) Pack, R. T.; Walker, R. B.; Kendrick, B. K. *J. Chem. Phys.* **1998**, *109*, 6714; **2000**, *113*, 1668(E).
(860) Venkatesh, P. K.; Dean, A. M.; Cohen, M. H.; Carr, R. W. *J. Chem. Phys.* **1999**, *111*, 8313.
(861) Frankcombe, T. J.; Smith, S. C. *J. Comput. Chem.* **2000**, *21*, 592.

(862) Miller, J. A.; Klippenstein, S. J.; Robertson, S. H. *J. Phys. Chem. A* **2000**, *104*, 7525; Miller, J. A.; Klippenstein, S. J.; Robertson, S. H. *J. Phys. Chem. A* **2000**, *104*, 9806 (E).
(863) Frankcombe, T. J.; Smith, S. C.; Gates, K. E.; Robertson, S. H. *Phys. Chem. Chem. Phys.* **2000**, *2*, 793.
(864) Blitz, M. A.; Beasley, M. S.; Pilling, M. J.; Robertson, S. H. *Phys. Chem. Chem. Phys.* **2000**, *2*, 905.
(865) Tsang, W.; Mokrushin, V. *Proc. Combust. Inst.* **2000**, *28*, 1717.
(866) Frankcombe, T. J.; Smith S. C. *Comput. Phys. Commun.* **2001**, *141*, 159.
(867) Frankcombe, T. J.; Smith, S. C. *Faraday Discuss.* **2001**, *119*, 159.
(868) Barker, J. R. *Int. J. Chem. Kinet.* **2001**, *33*, 232.
(869) Barker, J. R.; Ortiz, N. F. *Int. J. Chem. Kinet.* **2001**, *33*, 246.
(870) Senosaian, J. P.; Musgrave, C. B.; Golden, D. M. *Int. J. Chem. Kinet.* **2003**, *35*, 464.
(871) Frankcombe, T. J.; Smith S. C. *J. Chem. Phys.* **2003**, *119*, 12729.
(872) Hahn, D. K.; Klippenstein, S. J.; Miller, J. A. *Faraday Discuss.* **2002**, *119*, 79.
(873) Miller, J. A.; Parrish, C.; Brown, N. J. *J. Phys. Chem.* **1986**, *90*, 3339.
(874) Miller, J. A. *Proc. Combust. Inst.* **1996**, *26*, 461.
(875) Lyon, R. K. U.S. Patent 3,900,554, March 16, 1975.
(876) Miller, J. A.; Bowman, C. T. *Prog. Energy Combust. Sci.* **1989**, *15*, 287.
(877) Miller, J. A.; Glarborg, P. In *Gas-Phase Chemical Reaction Systems; Experiments and Models 100 Years after Max Bodenstein*; Wolfrum, J., Volpp, H.-R., Ranacher, R., Warnatz, J., Eds.; Springer: New York, 1996; pp 318−333.
(878) Miller, J. A.; Glarborg, P. *Int. Chem. Kinet.* **1999**, *31*, 757.
(879) Diau, E. W.-G.; Smith S. C. *J. Phys. Chem.* **1996**, *100*, 12349.
(880) Miller, J. A.; Klippenstein, S. J. *J. Phys. Chem. A* **2000**, *104*, 2061.
(881) Widom, B. *Science* **1965**, *148*, 1555.
(882) Widom, B. *J. Chem. Phys.* **1971**, *55*, 44.
(883) Widom, B. *J. Chem. Phys.* **1974**, *61*, 672.
(884) Klippenstein, S. J.; Miller, J. A. *J. Phys. Chem. A* **2002**, *106*, 9267.
(885) Miller, J. A.; Klippenstein, S. J. *J. Phys. Chem. A* **2003**, *107*, 2680.
(886) Miller, J. A.; Klippenstein, S. J. *J. Phys. Chem. A* **2003**, *107*, 7783.
(887) Bartis, J. T.; Widom, B. *J. Chem. Phys.* **1974**, *60*, 3474.
(888) Troe, J. In *Kinetics of Gas Reactions*; Just, W., Ed.; *Physical Chemistry An Advanced Treatise* 6B; Academic: New York, 1975; pp 835−929.
(889) Troe, J. *J. Phys. Chem.* **1986**, *90*, 357.
(890) Oum, K.; Sekiguchi, K.; Luther, K.; Troe, *J. Phys. Chem. Chem. Phys.* **2003**, *5*, 2931.
(891) Oum, K.; Luther, K.; Troe, J. *J. Phys. Chem. A* **2004**, *108*, 2690.
(892) Lienau, C.; Zewail, A. H. *J. Phys. Chem.* **1996**, *100*, 18629.
(893) Dutton, M. L.; Bunker, D. L.; Harris, H. H. *J. Phys. Chem.* **1972**, *76*, 2614.
(894) Truhlar, D. G.; Isaacson, A. D. *J. Chem. Phys.* **1982**, *77*, 3516.
(895) Garrett, B. C.; Truhlar, D. G. *J. Phys. Chem.* **1985**, *89*, 2204.
(896) Garrett, B. C.; Truhlar, D. G. *Int. J. Quantum Chem.* **1986**, *29*, 1463.
(897) Steckler, R.; Truhlar, D. G.; Garrett, B. C. *J. Chem. Phys.* **1986**, *84*, 6712.
(898) Garrett, B. C.; Truhlar, D. G.; Varandas, A. J. C.; Blais, N. C. *Int. J. Chem. Kinet.* **1986**, *18*, 1065.
(899) Garrett, B. C.; Truhlar, D. G.; Bowman, J. M.; Wagner, A. F. *J. Phys. Chem.* **1986**, *90*, 4305.
(900) Morokuma, K.; Kato, S. In *Potential Energy Surfaces and Dynamics Calculations*; Truhlar, D. G., Ed.; Plenum: New York, 1981; p 243.
(901) Rangel, C.; Espinosa-Garcia, J. *J. Chem. Phys.* **2005**, *122*, 134315.
(902) Duncan, W. T.; Truong, T. N. *J. Chem. Phys.* **1995**, *103*, 9642.
(903) Corchado, J. C.; Truhlar, D. G.; Espinosa-García, J. *J. Chem. Phys.* **2000**, *112*, 9375.
(904) Espinosa-García, J. *J. Chem. Phys.* **2002**, *117*, 2076.
(905) Zhang, D. H.; Yang, M.; Lee, S.-Y. *J. Chem. Phys.* **2002**, *116*, 2388.
(906) Marcus, R. A. *J. Chem. Phys.* **1966**, *45*, 2138.
(907) Marcus, R. A.; Rice, O. K. J. *Phys. Collid. Chem.* **1951**, *55*, 894.
(908) Magee, J. L. *Proc. Natl. Acad. Sci. U.S.A.* **1952**, *38*, 764.
(909) Chatfield, D. C.; Friedman, R. S.; Schwenke, D. W.; Truhlar, D. G. *J. Phys. Chem.* **1992**, *96*, 2414.
(910) Chatfield, D. C.; Friedman, R. S.; Lynch, G. C.; Truhlar, D. G. *J. Phys. Chem.* **1992**, *96*, 57.
(911) Chatfield, D. C.; Friedman, R. S.; Mielke, S. L.; Lynch, G. C.; Allison, T. C.; Truhlar, D. G. In *Dynamics of Molecules and Chemical Reactions*; Wyatt, R. E., Zhang, J. Z. H., Eds.; Marcel Dekker: New York, 1996; pp 323−386.
(912) Chatfield, D. C.; Mielke, S. L.; Allison, T. C.; Truhlar, D. G. *J. Chem. Phys.* **2000**, *112*, 8387.
(913) Skodje, R. T.; Truhlar, D. G. *J. Phys. Chem.* **1981**, *85*, 624.
(914) Sun, L.; Song, K.; Hase, W. L. *Science* **2002**, *296*, 875.
(915) Parr, C. A.; Polanyi, J. C.; Wong, W. H. *J. Chem. Phys.* **1973**, *58*, 5.
(916) Blais, N. C.; Truhlar, D. G. *J. Chem. Phys.* **1974**, *61*, 4186.
(917) Marcy, T. P.; Diaz, R. R.; Heard, D.; Leone, S. R.; Harding, L. B.; Klippenstein, S. J. *J. Phys. Chem. A* **1991**, *105*, 8361.
(918) Lee, J.; Grabowski, J. J. *Chem. Rev.* **1992**, *92*, 1611.
(919) Knyazev, V. D. *J. Phys. Chem. A* **2002**, *106*, 8741.
(920) Ammal, S. C.; Yamataka, H.; Aida, M.; Dupuis, M. *Science* **2003**, *299*, 1555.
(921) Townsend, D.; Lahankar, S. A.; Lee, S. K.; Chambreau, S. D.; Suits, A. G.; Zhang, X.; Rheinecker, J.; Harding, L. B.; Bowman, J. M. *Science* **2004**, *306*, 1158.
(922) Zhang, X.; Rheinecker, J. L.; Bowman, J. M. *J. Chem. Phys.* **2005**, *122*, 114313.
(923) Chambreau, S. D.; Townsend, D.; Lahankar, S. A.; Lee, S. K.; Suits, A. G. *Phys. Scr.* **2006**, *73*, C89.
(924) Kable, S. H.; Houston, P., manuscript in press.
(925) Klippenstein, S. J.; Harding, L. B., unpublished results.
(926) Polanyi, J. C. *Acc. Chem. Res.* **1972**, *5*, 161.
(927) Levine, R. D.; Bernstein, R. B. *Molecular Reaction Dynamics and Chemical Reactivity*; Oxford University Press: New York, 1987.
(928) Smith, I. W. M. In *Bimolecular Collisions*; Ashford, M. N. R., Baggott, J. E., Eds.; *Adv. Gas-Phase Photochem. Kinet. 2*; Royal Society of Chemistry: London, 1989; pp 53−104.
(929) Camden, J. P.; Bechtel, H. A.; Brown, D. J. A.; Zare, R. N. *J. Chem. Phys.* **2006**, *124*, 34311.
(930) Mayne, H. R. In *Dynamics of Molecules and Chemical Reaction*; Wyatt, R. E., Zhang, J. Z. H., Eds.; Dekker: New York, 1996; pp 589−616.
(931) Peslherbe, G. H.; Wang, H.; Hase, W. L. *Adv. Chem. Phys.* **1999**, *105*, 171.
(932) Lakin, M. J.; Troya, D.; Lendvay, G.; Gonzalez, M.; Schatz, G. C. *J. Chem. Phys.* **2001**, *115*, 5160.
(933) Castillo, J. F.; Collins, M. J.; Aoiz, F. J.; Bañares, L. *J. Chem. Phys.* **2003**, *118*, 7303.
(934) Bene, E.; Lendvay, G.; Póta, G. *J. Phys. Chem. A.* **2005**, *109*, 8336.
(935) Donovan, R. J.; Husain, D. *Chem. Rev.* **1970**, *70*, 489.
(936) Husian, D.; Roberts, G. In *Bimolecular Collisions*; Ashford, M. N. R., Baggott, J. E., Eds.; *Adv. Gas-Phase Photochem. Kinet. 2*; Royal Society of Chemistry: London, 1989; pp 263−336.
(937) Schinke, R. *Photodissociation Dynamics*, Cambridge University Press: Cambridge, 1993.
(938) Domcke, W.; Yarkony, D. R.; Köppel, H., Eds.; *Conical Intersections*; World Scientific: River Edge, NJ, 2004.
(939) *Computational Methods in Photochemistry*; Kutateladze, A. G., Ed.; *Molecular and Supramolecular Photochemistry 13*; Taylor & Francis: Boca Raton, 2005.
(940) Tawa, G. J.; Mielke, S. L.; Truhlar, D. G.; Schwenke, D. W. *Adv. Mol. Vib. Collision Dyn.* **1994**, *2B*, 45.
(941) Mielke, S. L.; Tawa, G. J.; Truhlar, D. G.; Schwenke, D. W. *Chem. Phys. Lett.* **1995**, *234*, 57.
(942) Mielke, S. L.; Truhlar, D. G.; Schwenke, D. W. *J. Phys. Chem.* **1995**, *99*, 16210.
(943) Jasper, A. W.; Truhlar, D. G. *J. Chem. Phys.* **2005**, *122*, 44101.
(944) Child, M. S. In *Atom-Molecule Collision Theory*; Bernstein, R. B., Ed.; Plenum: New York, 1979; pp 427−465.
(945) Mead, C. A. *J. Chem. Phys.* **1979**, *70*, 2276.
(946) Teller, E. *J. Phys. Chem.* **1937**, *41*, 109.
(947) Truhlar, D. G.; Mead, C. A. *Phys. Rev. A* **2003**, *68*, 32501.
(948) Zhu, C.; Jasper, A. W.; Truhlar, D. G. *J. Chem. Phys.* **2004**, *120*, 5543.
(949) Kendrick, B. K.; Mead, C. A.; Truhlar, D. G. *Chem. Phys.* **2002**, *277*, 31.
(950) Mead, C. A. *J. Chem. Phys.* **1983**, *78*, 807.
(951) Thompson, T. C.; Truhlar, D. G.; Mead, C. A. *J. Chem. Phys.* **1985**, *82*, 2392.
(952) Yarkony, D. R. *J. Phys. Chem. A* **1997**, *101*, 4263.
(953) Yarkony, D. R. *Mol. Phys.* **1998**, *93*, 971.
(954) Massey, H. S. W. *Rep. Prog. Phys.* **1949**, *12*, 248.
(955) Mott, N. F.; Massey, H. S. W. *The Theory of Atomic Collisions*, 3rd. ed.; Oxford, London, 1965; p 665.
(956) Tully, J. C. In *Modern Methods for Multidimensional Dynamics Computations in Chemistry*; Thompson, D. L., Ed.; World Scientific: Singapore, 1998; pp 34−72.
(957) Jasper, A.; Kendrick, B. K.; Mead, C. A.; Truhlar, D. G. In *Modern Trends in Chemical Reaction Dynamics*; Yang, X., Liu, K., Eds.; World Scientific: Singapore, 2003; p 329−391.
(958) Smith, F. T. *Phys. Rev.* **1969**, *179*, 111.
(959) Nikitin, E. E. *Adv. Quantum Chem.* **1970**, *5*, 135.
(960) Garrett, B. C.; Redmon, M. J.; Truhlar, D. G.; Melius, C. F. *J. Chem. Phys.* **1981**, *74*, 412.
(961) Werner, H.-J.; Meyer, W. *J. Chem. Phys.* **1981**, *74*, 5802.
(962) Delos, J. B. *Rev. Mod. Phys.* **1981**, *53*, 287.
(963) Garrett, B. C.; Truhlar, D. G. *Theoretical Chemistry: Advances and Perspectives* **1981**, *6A*, 215.

(964) Cimaraglia, R.; Malrieu, J. P.; Spiegelman, F. *J. Phys. B* **1985**, *18*, 3073.
(965) Sidis, V. *Adv. Chem. Phys.* **1992**, *82*, 73.
(966) Pacher, T.; Cederbaum, L. S.; Köppel, H. *Adv. Chem. Phys.* **1993**, *84*, 293.
(967) Domcke, W.; Woywood, C. *Chem. Phys. Lett.* **1993**, *216*, 362.
(968) Atchity, G. J.; Ruedenberg, K. *Theor. Chem. Acc.* **1997**, *97*, 47.
(969) Thiel, A.; Köppel, H. *J. Chem. Phys.* **1999**, *110*, 9371.
(970) Köppel, H.; Gronki, J.; Mahapatra, S. *J. Chem. Phys.* **2001**, *115*, 2377.
(971) Nakamura, H.; Truhlar, D. G. *J. Chem. Phys.* **2001**, *115*, 10353.
(972) Nakamura, H.; Truhlar, D. G. *J. Chem. Phys.* **2003**, *118*, 6816.
(973) Mead, C. A.; Truhlar, D. G. *J. Chem. Phys.* **1982**, *77*, 6090.
(974) Kendrick, B. K.; Mead, C. A.; Truhlar, D. G. *Chem. Phys. Lett.* **2000**, *330*, 629.
(975) Landau, L. D. *Phys. Z. Sowjetunion* **1932**, *2*, 46.
(976) Zener, C. *Proc. Royal Soc. London A* **1932**, *137*, 696.
(977) Stückelberg, E. C. G. *Helv. Phys. Acta* **1932**, *5*, 369.
(978) Nikitin, E. E. *Opt. Spektrosk.* **1961**, *10*, 443.
(979) Ovchinnikova, M. Ya. *Opt. Spektrosk.* **1961**, *17*, 447.
(980) Bykhovskii, V. K.; Nikitin, E. E.; Ovchinnikova, M. Ya. *Z. Eksp. Teor. Fiz.* **1964**, *47*, 750.
(981) Delos, J. B.; Thorson, W. R. *Phys. Rev. A* **1972**, *6*, 728.
(982) Nakamura, H.; Zhu, C. *Comm. At. Mol. Phys.* **1996**, *32*, 249.
(983) Nakamura, H. In *Dynamics of Molecules and Chemical Reactions*; Wyatt, R. E., Zhang, J. Z. H., Eds.; Marcel Dekker: New York, 1996; pp 473−529.
(984) Rosen, N.; Zener, C. *Phys. Rev.* **1932**, *40*, 502.
(985) Demkov, Y. N. *Soviet Phys. JETP* **1964**, *18*, 138.
(986) Yarkony, D. R. *J. Chem. Phys.* **1996**, *105*, 10456.
(987) Teller, E. *Isr. J. Chem.* **1969**, *7*, 227.
(988) Zimmerman, H. E. *Acc. Chem. Res.* **1972**, *5*, 393.
(989) Michl, J. *Mol. Photochem.* **1972**, *4*, 243.
(990) Bernardi, F.; De, S.; Olivucci, M.; Robb, M. A. *J. Am. Chem. Soc.* **1990**, *112*, 1737.
(991) Salem, L. *Electrons in Chemical Reactions: First Principles*; Wiley: New York, 1982.
(992) Michl, J.; Bonacic-Koutecky, V. *Electronic Aspects of Organic Photochemistry*; Wiley: New York, 1990.
(993) Olivucci, M.; Sinocropi, A. In *Computational Photochemistry*; Oluvicci, M., Ed.; Theoretical and Computational Chemistry 16; Elsevier: Amsterdam, 2005; p 1.
(994) Blais, N. C.; Truhlar, D. G.; Mead, C. A. *J. Chem. Phys.* **1988**, *89*, 6204.
(995) Schneider, R.; Domcke, W.; Köppel, H. *J. Chem. Phys.* **1990**, *92*, 1045.
(996) Mielke, S. L.; Tawa, G. J.; Truhlar, D. G.; Schwenke, D. W. *Int. J. Quantum Chem. Symp.* **1993**, *115*, 6436.
(997) Mielke, S. L.; Tawa, G. J.; Truhlar, D. G.; Schwenke, D. W. *J. Am. Chem. Soc.* **1993**, *115*, 6436.
(998) Smith, B. R.; Bearpark, M. J.; Robb, M. A.; Bernardi, F.; Olivucci, M. *Chem. Phys. Lett.* **1995**, *242*, 27.
(999) Clifford, S.; Bearpark, M. J.; Bernardi, F.; Olivucci, M.; Robb, M. A.; Smith, B. R. *J. Am. Chem. Soc.* **1996**, *118*, 7553.
(1000) Ferretti, A.; Gianucci, G.; Lami, A.; Persico, M.; Villani, G. *J. Chem. Phys.* **1996**, *104*, 5517.
(1001) Martinez, T. J.; Ben-Nun, M.; Levine, R. D. *J. Phys. Chem. A* **1997**, *101*, 6389.
(1002) Topaler, M. S.; Allison, T. C.; Schwenke, D. W.; Truhlar, D. G. *J. Chem. Phys.* **1998**, 109, 3321. Topaler, M. S.; Allison, T. C.; Schwenke, D. W.; Truhlar, D. G. *J. Chem. Phys.* **2000**, *113*, 3928-(E).
(1003) Worth, G. A.; Meyer, H.-D.; Cederbaum, L. S. *J. Chem. Phys.* **1998**, *109*, 3518.
(1004) Thompson, K.; Martinez, T. J. *J. Chem. Phys.* **1999**, *110*, 1376.
(1005) Santoro, F.; Petrongolo, C. *J. Chem. Phys.* **1999**, *110*, 4419.
(1006) Alijah, A.; Nikitin, E. E. *Mol. Phys.* **1999**, *96*, 1399.
(1007) Ferretti, A.; Lami, A.; Villani, G. *Chem. Phys.* **2000**, *259*, 201.
(1008) Hofmann, A.; Vivie-Riedle, R. D. *J. Chem. Phys.* **2000**, *112*, 5054.
(1009) Thoss, M.; Miller, W. H.; Stock, G. *J. Chem. Phys.* **2000**, *112*, 10282.
(1010) Hofmann, A.; Vivie-Riedel, R. D. *Chem. Phys. Lett.* **2001**, *346*, 299
(1011) Hartmann, M.; Pittner, J.; Bonacic-Koutecky, V. *J. Chem. Phys.* **2001**, *114*, 2123.
(1012) Cattarius, C.; Worth, G. A.; Meyer, H.-D.; Cederbaum, L. S. *J. Chem. Phys.* **2001**, *115*, 2088.
(1013) Kühl, A.; Domcke, W. *J. Chem. Phys.* **2002**, *116*, 263.
(1014) Köppel, H.; Döscher, M.; Bâldea, I.; Meyer, H.-D.; Szalay, P. G. *J. Chem. Phys.* **2002**, *117*, 2657.
(1015) Mahapatra, S.; Ritschel, T. *Chem. Phys.* **2003**, *289*, 291.
(1016) Balzer, B.; Hahn, S.; Stock, G. *Chem. Phys. Lett.* **2003**, *379*, 351.
(1017) Boggio-Pasqua, M.; Ravaglia, M.; Bearpark, M. J.; Garavelli, M.; Robb, M. A. *J. Phys. Chem. A* **2003**, *107*, 11139.
(1018) Worth, G. A.; Cederbaum, L. S. *Annu. Rev. Phys. Chem.* **2004**, *55*, 127.
(1019) Toniolo, A.; Thompson, A. L.; Martinez, T. J. *Chem. Phys.* **2004**, *304*, 133.
(1020) Toniolo, A.; Olsen, S.; Manohar, L.; Martinez, T. J. *Faraday Discuss.* **2004**, *127*, 149.
(1021) Mahapatra, S. *Int. Rev. Phys. Chem.* **2004**, *23*, 483.
(1022) Vallet, V.; Lan, Z.; Mahapatra, S.; Sobolewski, A. L.; Domcke, W. *J. Chem. Phys.* **2005**, *123*, 144307.
(1023) Barbatti, M.; Granucci, G.; Persico, M.; Lischka, H. *Chem. Phys. Lett.* **2005**, 401, 276.
(1024) Coe, J.; Martinez, T. J. *J. Am. Chem. Soc.* **2005**, *127*, 4560.
(1025) Jasper, A. W.; Truhlar, D. G. *J. Chem. Phys.* **2005**, *122*, 44101.
(1026) Gelman, D.; Katz, G.; Kosloff, R.; Ratner, M. A. *J. Chem. Phys.* **2005**, *123*, 134112.
(1027) Bâldea, I.; Koppel, H. *J. Chem. Phys.* **2006**, *124*, 64101.
(1028) Tamura, H.; Nanbu, S.; Ishida, T.; Nakamura, H. *J. Chem. Phys.* **2006**, *124*, 84313.
(1029) Coe, J.; Martinez, T. J. *J. Phys. Chem. A* **2006**, *110*, 618.
(1030) Worth, G. A.; Welch, G.; Paterson, M. J. *Mol. Phys.* **2006**, *104*, 1095.
(1031) Migani, A.; Sinicropi, A.; Ferré, N.; Cembran, A.; Garavelli, M.; Olivucci, M. *Faraday Discuss.* **2004**, *127*, 179.
(1032) Toniolo, A.; Olsen, S.; Manohor, L.; Martinez, T. J. *Faraday Discuss. Chem. Soc.* **2004**, *127*, in press.
(1033) Worth, G. A.; Bearpark, M. J.; Robb, M. A. In *Computational Photochemistry*; Oluvicci, M., Ed.; Theoretical and Computational Chemistry 16; Elsevier: Amsterdam, 2005; p 171.
(1034) Truhlar, D. G.; Garrett, B. C.; Klippenstein, S. J. *J. Phys. Chem.* **1996**, *100*, 12771.
(1035) Morokuma, K.; Cui, Q.; Liu, Z. *Faraday Discuss.* **1998**, *110*, 71.
(1036) Truhlar, D. G. *J. Am. Chem. Soc.* **1975**, *97*, 6310.
(1037) Carpenter, B. K. *Angew. Chem., Int. Ed.* **1998**, *37*, 3340.
(1038) Doubleday: C. *J. Phys. Chem. A* **2001**, *105*, 6333.
(1039) Carpenter, B. K. *J. Phys. Org. Chem.* **2003**, *16*, 858.
(1040) Tully, J. C. *J. Chem. Phys.* **1974**, *61*, 61.
(1041) Zahr, G. E.; Preston, R. K.; Miller, W. H. *J. Chem. Phys.* **1975**, *62*, 1127.
(1042) Desouter-Lecomte, M.; Sannen, C.; Lorquet, J. C. *J. Chem. Phys.* **1983**, *79*, 894.
(1043) Heller, E. J.; Brown, R. C. *J. Chem. Phys.* **1983**, *79*, 3336.
(1044) Lorquet, J. C.; Leyh-Nihant, B. *J. Phys. Chem.* **1988**, *92*, 4778.
(1045) Sahm, D. K.; Thompson, D. C. *Chem. Phys. Lett.* **1993**, *201*, 175.
(1046) Sahm, D. K.; Thompson, D. L. *Chem. Phys. Lett.* **1993**, *205*, 241.
(1047) Topaler, M. S.; Truhlar, D. G. *J. Chem. Phys.* **1997**, *107*, 392.
(1048) Martínez-Nuñez, E.; Vázquez, S.; Granucci, G.; Persico, M.; Estevez, C. M. *Chem. Phys. Lett.* **2005**, *412*, 35.
(1049) Nikitin, E. E. *Chem. Phys. Lett.* **1967**, *1*, 179.
(1050) Tully, J. C.; Preston, R. K. *J. Chem. Phys.* **1971**, *55*, 562.
(1051) Blais, N. C.; Truhlar, D. G. *J. Chem. Phys.* **1983**, *79*, 1334.
(1052) Tully, J. C. *J. Chem. Phys.* **1990**, *93*, 1061.
(1053) Chapman, S. *Adv. Chem. Phys.* **1992**, *82*, 423.
(1054) Meyer, H.-D.; Miller, W. H. *J. Chem. Phys.* **1979**, *70*, 3214. Gerber, R. B.; Buch, V.; Ratner, M. A. *J. Chem. Phys.* **1982**, *77*, 3022. Buch, V.; Gerber, R. B.; Ratner, M. A. *Chem. Phys. Lett.* **1983**, *101*, 44. Micha, D. A. *J. Chem. Phys.* **1983**, *78*, 7138. Durup, J. *Chem. Phys. Lett.* **1990**, *173*, 537. Alimi, R.; Gerber, R. B.; Hammerich, A. D.; Kosloff, R.; Ratner, M. A. *J. Chem. Phys.* **1990**, *93*, 6484. García-Vela, A.; Gerber, R. B.; Imre, D. G. *J. Chem. Phys.* **1992**, *97*, 7242. Topaler, M. S.; Hack, M. D.; Allison, T. C.; Liu, Y.-P.; Mielke, S.; Schwenke, D. W.; Truhlar, D. G. *J. Chem. Phys.* **1997**, *106*, 8699.
(1055) Li, X.; Tully, J. C.; Schlegel, H. B.; Frisch, M. J. *J. Chem. Phys.* **2005**, *123*, 84106.
(1056) Parlant, G.; Gislason, E. A. *J. Chem. Phys.* **1989**, *91*, 4416.
(1057) Zhu, C.; Nobusada, K.; Nakamura, H. *J. Chem. Phys.* **2001**, *115*, 3031. Zhu, C.; Kamisaka, H.; Nakamura, H. *J. Chem. Phys.* **2001**, *115*, 11036.
(1058) Jasper, A. W.; Stechmann, S. N.; Truhlar, D. G. *J. Chem. Phys.* **2002**, *116*, 5424.
(1059) Jasper, A. W.; Truhlar, D. G. *Chem. Phys. Lett.* **2003**, *369*, 60.
(1060) Hack, M. D.; Jasper, A. W.; Volobuev, Y. L.; Schwenke, D. W.; Truhlar, D. G. *J. Phys. Chem. A* **1999**, *103*, 6309.
(1061) Ben-Nun, M.; Martinez, T. J. *J. Chem. Phys.* **1998**, *108*, 7244. Ben-Nun, M.; Quenneville, J.; Martinez, T. J. *J. Phys. Chem. A* **2000**, *104*, 5061.
(1062) Hack, M. D.; Wensmann, A. M.; Truhlar, D. G. *J. Chem. Phys.* **2001**, *115*, 1172.
(1063) Ben-Nun, M.; Martinez, T. J. *Adv. Chem. Phys.* **2002**, *121*, 439.
(1064) Worth, G. A.; Robb, M. A.; Burghardt, I. *Faraday Discuss.* **2004**, *127*, 307.

(1065) Coe, J. D.; Martinez, T. J. *J. Phys. Chem.* **2006**, *110*, 618.
(1066) Zurek, W. H. *Phys. Rev. D* **1981**, *24*, 1516.
(1067) Jasper, A. W.; Zhu, C.; Nangia, S.; Truhlar, D. G. *Faraday Discuss.* **2004**, *127*, 1.
(1068) Hack, M. D.; Truhlar, D. G. *J. Phys. Chem. A* **2000**, *104*, 7917.
(1069) Volobuev, Y. L.; Hack, M. D.; Topaler, M. S.; Truhlar, D. G. J. *Chem. Phys.* **2000**, *112*, 9716.
(1070) Hack, M. D.; Truhlar, D. G. *J. Chem. Phys.* **2001**, *114*, 2894.
(1071) Zhu, C.; Nangia, S.; Jasper, A. W.; Truhlar, D. G. *J. Chem. Phys.* **2004**, *121*, 7658.
(1072) Fiete, G. A.; Heller, E. *J. Phys. Rev. A* **2003**, *68*, 022112.
(1073) Zhu, C.; Jasper, A. W.; Truhlar, D. G. *J. Chem. Theory Comp.* **2005**, *1*, 527.
(1074) Jasper, A. W.; Nangia, S.; Zhu, C.; Truhlar, D. G. *Acc. Chem. Res.* **2005**, *38*, in press.
(1075) Achirel, P.; Habitz, P. *Chem. Phys.* **1983**, *78*, 213.
(1076) Nakamura, H. *Adv. Chem. Phys.* **1992**, *82*, 243.
(1077) Mebel, A. M.; Luna, A.; Lin, M. C.; Morokuma, K. *J. Chem. Phys.* **1996**, *105*, 6439.
(1078) Morokuma, K.; Cui, Q.; Lin, Z. *Faraday Discuss.* **1998**, *110*, 71.
(1079) Kaledin, A. L.; Cui, Q.; Heaven, M. C.; Morokuma, K. *J. Chem. Phys.* **1999**, *111*, 5004.
(1080) Harvey, J. N.; Aschi, M. *Phys. Chem. Chem. Phys.* **1999**, *1*, 5555.
(1081) Li, Q.-S.; Zhang, F.; Fang, W. H.; Yu, J.-G. *J. Chem. Phys.* **2006**, *124*, 54324.
(1082) Garcia, L.; Sambrano, J. R.; Andrés, J.; Beltran, A. *Organometallics* **2006**, *25*, 1643.
(1083) Cui, Q.; Morokuma, K.; Bowman, J. M.; Klippenstein, S. J. *J. Chem. Phys.* **1999**, *110*, 9469.
(1084) Severance, D. L.; Jorgensen, W. L. *J. Am. Chem. Soc.* **1992**, *114*, 10966.
(1085) Storer, J. W.; Giesen, D. J.; Hawkins, G. D.; Lynch, G. C.; Cramer, C. J.; Truhlar, D. G.; Liotard, D. A. *ACS Symp. Ser.* **1994**, *568*, 24.
(1086) Tully, J. C. *Annu. Rev. Phys. Chem.* **2000**, *51*, 153.
(1087) Evans, M. G. *Trans. Faraday Soc.* **1938**, *34*, 49.
(1088) Truhlar, D. G.; Hase, W. L.; Hynes, J. T. *J. Phys. Chem.* **1983**, *87*, 2664; **1983**, *87*, 5523 (E).
(1089) Hynes, J. T. In *Theory of Chemical Reaction Dynamics*; Baer, M., Ed.; CRC Press: Boca Raton, FL, 1985; Vol. 4, pp 171−234.
(1090) Connors, K. A. *Chemical Kinetics*; VCH: New York, 1990; p 200.
(1091) Wonchoba, S. E.; Hu, W.-P.; Truhlar, D. G. In *Theoretical Approaches to Interface Phenomena*; Sellers, H. L., Golab, J. T., Eds.; Plenum: New York, 1994; pp 1−34.
(1092) Garrett, B. C. *Int. Rev. Phys. Chem.* **1994**, *13*, 263.
(1093) Tucker, S. C. In *New Trends in Kramers' Reaction Rate Theory*; Talkner, P, Hánggi, P., Eds.; Kluwer: Dordrecht, 1995; pp 5−46.
(1094) Cramer, C. J.; Truhlar, D. G. In *Solvent Effects and Chemical Reactivity*; Tapia, O., Bertrán, J., Eds.; Kluwer: Dordrecht, 1996; pp 1−80.
(1095) Hynes, J. T. In *Solvent Effects and Chemical Reactivity*; Tapia, O., Bertrán, J., Eds.; Kluwer: Dordrecht, 1996; pp 231−258.
(1096) Garrett, B. C.; Truhlar, D. G. In *Encyclopedia of Computational Chemistry*; Schleyer, P. v. R., Allinger, N. L., Clark, T., Gasteiger, J., Kollman, P. A., Schaefer, H. F., III, Eds.; Wiley: Chichester, 1998; Vol. 5; pp 3094−3104.
(1097) Cramer, C. J.; Truhlar, D. G. *Chem. Rev.* **1999**, *99*, 2161.
(1098) Truhlar, D. G. In *Isotope Effects in Chemistry and Biology*; Kohen, A., Limbach, H.-H., Eds.; CRC/Taylor & Francis: Boca Raton, 2006; p 579.
(1099) Noyes, R. M. *Prog. React. Kinet.* **1961**, *1*, 129.
(1100) Hammes, G. G. *Principles of Chemical Kinetics*; Academic: New York, 1978; p 62.
(1101) Truhlar, D. G. *J. Chem. Educ.* **1985**, *62*, 104.
(1102) Cramer, C. J.; Truhlar, D. G. In *Free Energy Calculations in Rational Drug Design*; Reddy, W. R., Erion, M. D., Eds.; Kluwer: New York, 2001; pp 63−95.
(1103) Truhlar, D. G.; Liu, Y.-P.; Schenter, G. K.; Garrett, B. C. *J. Phys. Chem.* **1994**, *98*, 8396.
(1104) Hill, T. L. *An Introduction to Statistical Mechanics*; Addison-Wesley: Reading, 1960; pp 312−313.
(1105) Chuang, Y.-Y.; Cramer, C. J.; Truhlar, D. G. *Int. J. Quantum Chem.* **1998**, *70*, 887.
(1106) Chandrasekhar, J.; Jorgensen, W. L. *J. Am. Chem. Soc.* **1985**, *107*, 2974.
(1107) Tortonda, F. R.; Pascual-Ahuir, J.-P.; Silla, E.; Tuñon, I. *J. Phys. Chem.* **1995**, *99*, 12525.
(1108) Li, G.-S.; Ruiz-Lopez, M. F.; Maigret, B. *J. Phys. Chem. A* **1997**, *101*, 7885.
(1109) Sicinska, D.; Paneth, P.; Truhlar, D. G. *J. Phys. Chem. B* **2002**, *106*, 2708.
(1110) Martinez, J. M.; Pappalardo, R. R.; Marcos, E. S. *J. Phys. Chem. A* **1997**, *101*, 4444.
(1111) Pliego, J. R., Jr.; Riveros, J. M. *J. Phys. Chem. A* **2001**, *105*, 7241.
(1112) Marcus, R. A. *J. Chem. Phys.* **1956**, *24*, 966.
(1113) Zusman, L. D. *Chem. Phys.* **1980**, *49*, 295.
(1114) Alexandrov, I. V. *Chem. Phys.* **1980**, *51*, 449.
(1115) Lee, S.; Hynes, J. T. *J. Chem. Phys.* **1988**, *88*, 6863.
(1116) Truhlar, D. G.; Schenter, G. K.; Garrett, B. C. *J. Chem. Phys.* **1993**, *98*, 5756.
(1117) Garrett, B. C.; Schenter, G. K. *ACS Symp. Ser.* **1994**, *568*, 122.
(1118) Ando, K. *J. Chem. Phys.* **1997**, *106*, 116.
(1119) Chuang, Y.-Y.; Truhlar, D. G. *J. Am. Chem. Soc.* **1999**, *121*, 10157.
(1120) Schenter, G. K.; Garrett, B. C.; Truhlar, D. G. *J. Phys. Chem. B* **2001**, *105*, 9672.
(1121) Grote, R. F.; Hynes, J. T. *J. Chem. Phys.* **1980**, *76*, 2715.
(1122) Warshel, A. *J. Phys. Chem.* **1982**, *86*, 2218.
(1123) Warshel, A. *Proc. Natl. Acad. Sci. U.S.A.* **1984**, *81*, 444.
(1124) Muller, R. P., Warshel, A. *J. Chem. Phys.* **1996**, *99*, 17516.
(1125) Villà, J.; Warshel, A. *J. Phys. Chem. B* **2001**, *105*, 7887.
(1126) Alhambra, C.; Corchado, J.; Sanchez, M. L.; Garcia-Viloca, M.; Gao, J.; Truhlar, D. G. *J. Phys. Chem. B* **2001**, *105*, 11326.
(1127) Truhlar, D. G.; Gao, J.; Alhambra, C.; Garcia-Viloca, M.; Corchado, J.; Sanchez, M. L.; Villà, J. *Acc. Chem. Res.* **2002**, *35*, 341.
(1128) Garcia-Viloca, M.; Alhambra, C.; Truhlar, D. G.; Gao, J. *J. Comput. Chem.* **2003**, *24*, 177.
(1129) Poulsen, T. D.; Garcia-Viloca, M.; Gao, J.; Truhlar, D. G. *J. Phys. Chem. B* **2003**, *107*, 9567.
(1130) Truhlar, D. G.; Gao, J.; Garcia-Viloca, M.; Alhambra, C.; Corchado, J.; Sanchez, M. L.; Poulsen, T. D. *Int. J. Quantum Chem.* **2004**, *100*, 1136.
(1131) Madura, J. D.; Jorgensen, W. L. *J. Am. Chem. Soc.* **1986**, *108*, 2517.
(1132) Gao, J. *J. Am. Chem. Soc.* **1991**, *113*, 7796.
(1133) Hwang, J.-K.; Warhsel, A. *J. Phys. Chem.* **1993**, *97*, 10053.
(1134) Kong, Y. S.; Warshel, A. *J. Am. Chem. Soc.* **1995**, *117*, 6234.
(1135) Muller, R. P.; Warshel, A. *J. Phys. Chem.* **1995**, *99*, 17516.
(1136) Weslowski, T.; Muller, R. P.; Warshel, A. *J. Phys. Chem.* **1996**, *100*, 15444.
(1137) Jensen, C.; Liu, J.; Houk, K. N.; Jorgensen, W. L. *J. Am. Chem. Soc.* **1997**, *119*, 12982.
(1138) Stanton, R. V.; Peräkylä, M.; Bakoweis, D.; Kollman, P. A. *J. Am. Chem. Soc.* **1998**, *120*, 3448.
(1139) Bakoweis, D.; Kollman, P. A. *J. Am. Chem. Soc.* **1999**, *121*, 5712.
(1140) Pak, Y.; Voth, G. A. *J. Phys. Chem. A* **1999**, *103*, 925.
(1141) Peräkylä, M.; Kollman, P. A. *J. Phys. Chem. A* **1999**, *103*, 8067.
(1142) Byun, K.; Gao, J. *J. Mol. Graph. Model.* **2000**, *18*, 50.
(1143) Vayner, G.; Houk, K. N.; Jorgensen, W. L.; Brauman, J. I. *J. Am. Chem. Soc.* **2004**, *126*, 9054.
(1144) Marti, S.; Moliner, V.; Tuñón, I. *J. Chem. Theory Comput.* **2005**, *1*, 1008.
(1145) Ensing, B.; Klein, M. L. *Proc. Natl. Acad. Sci. U.S.A.* **2005**, *102*, 6755.
(1146) Martin, F. P.-D.; Dumas, R.; Field, M. J. *J. Am. Chem. Soc.* **2000**, *122*, 7688.
(1147) Rajamani, R.; Naidoo, K. J.; Gao, J. *J. Comput. Chem.* **2003**, *24*, 1775.
(1148) Acevedo, O.; Jorgensen, W. L. *Org. Lett.* **2004**, *6*, 2881.
(1149) Ensing, B.; Laio, A.; Gervasio, F. L.; Parrinello, M.; Klein, M. L. *J. Am. Chem. Soc.* **2004**, *126*, 9492.
(1150) König, P. H.; Ghosh, N.; Hoffmann, M.; Elstner, M.; Tajkhorshid, E.; Frauenheim, Th.; Cui, Q. *J. Phys. Chem. A* **2006**, *110*, 548.
(1151) Antoniou, D.; Schwartz, S. D. In *Theoretical Methods in Condensed Phase Chemistry*; Schwartz, S. D., Ed.; Kluwer: Dordrecht, 2000; p 69.
(1152) Nicoll, R. M.; Hindle, S. A.; MacKenzie, G.; Hillier, I. H.; Burton, N. A. *Theor. Chem. Acc.* **2001**, *106*, 105.
(1153) Gao, J.; Truhlar, D. G. *Annu. Rev. Phys. Chem.* **2002**, *53*, 467.
(1154) Cui, Q.; Karplus, M. *Adv. Protein Chem.* **2003**, *66*, 315.
(1155) Masgrau, L.; Basran, J.; Huthi, P.; Sutcliff, M. J.; Scrutton, N. S. *Arch. Biochem. Biophys. Acta* **2004**, *428*, 41.
(1156) Hammes-Schiffer, S. *Acc. Chem. Res.* **2006**, *39*, 93.
(1157) Bolhuis, D. G.; Chandler, D.; Dellago, C.; Geissler, P. L. *Annu. Rev. Phys. Chem.* **2002**, *53*, 291.
(1158) Best, R. B.; Hummer, G. *Proc. Natl. Acad. Sci. U.S.A.* **2005**, *102*, 6732.
(1159) Zahn, D. *J. Chem. Theory Comput.* **2006**, *2*, 107.
(1160) Han, H.; Brumer, P. *J. Chem. Phys.* **2005**, *122*, 144316.
(1161) Kaminski, G.; Jorgensen, W. L. *J. Phys. Chem.* **1996**, *100*, 18010.
(1162) Jorgensen, W. L. *ACS Symp. Ser.* **1999**, *721*, 74.
(1163) Mulholland, A. J. *Theor. Comput. Chem.* **2001**, *9*, 597.
(1164) Sato, H. *Understanding Chem. React.* **2003**, *24*, 61.
(1165) Lin, H.; Truhlar, D. G. *Theor. Chem. Acc.*, in press.
(1166) Day, P. N.; Jensen J. H.; Gordon, M. S.; Webb, S. P.; Stevens, W. J.; Krauss, M.; Garner, D. R.; Basch, H.; Cohen, D. *J. Chem. Phys.* **1996**, *105*, 1969. Webb, S. P.; Gordon, M. S. *J. Phys. Chem. A* **1999**, *103*, 1265.

(1167) Gordon, M. S.; Freitag, M. A.; Bandyopadhyay, P.; Jensen, J. H.; Kairys, V.; Stevens, W. J. *J. Phys. Chem. A* **2001**, *105*, 293.
(1168) Marcus, R. A. *Annu. Rev. Phys. Chem.* **1964**, *15*, 155.
(1169) Newton, M. D.; Sutin, N. *Annu. Rev. Phys. Chem.* **1984**, *35*, 437.
(1170) Rips, I.; Jortner, J. *J. Chem. Phys.* **1987**, *87*, 2090.
(1171) Kornyshev, A. A., Tosi, M., Ulstrup, J., Eds.; *Electron and Ion Transfer in Condensed Media*; World Scientific: Singapore, 1997.
(1172) May, V.; Kühn, O. *Charge and Energy Transfer Dynamics in Molecular Systems*; Wiley-VCH: Berlin, 2000.
(1173) Marcus, R. A. *J. Phys. Chem.* **1968**, *72*, 891.
(1174) Cohen, A. O.; Marcus, R. A. *J. Phys. Chem.* **1968**, *72*, 4249.
(1175) Albery, W. J.; Kreevoy, M. M. *Adv. Phys. Org. Chem.* **1978**, *6*, 87.
(1176) Guthrie, J. P. *J. Am. Chem. Soc.* **1996**, *118*, 12886.
(1177) Borgis, D.; Hynes, J. T. *J. Phys. Chem.* **1996**, *100*, 1118.
(1178) Marcus, R. A. *J. Phys. Chem. A* **1997**, *101*, 4072.
(1179) Hammes-Schiffer, S. *ChemPhysChem* **2002**, *3*, 33.
(1180) Cohen, B.; Leiderman, P.; Huppert, D. *J. Phys. Chem. A* **2003**, *107*, 1433.
(1181) Braun-Sand, S.; Strajbl, M.; Warshel, A. *Biophys. J.* **2004**, *87*, 2221.
(1182) Kiefer, P. M.; Hynes, J. T. *J. Phys. Chem. A* **2004**, *108*, 11793.
(1183) Braun-Sand, S.; Olsson, M. H. M.; Warshel, A. *Adv. Phys. Org. Chem.* **2005**, *40*, 201.
(1184) Roberts, M. W. *Chemistry of the Metal-Gas Interface*; Oxford University Press: Oxford, 1978; p 40.
(1185) Bamford, C. H., Tipper, C. F. H., Compton, R. G., Eds.; *Simple Processes at the Gas−Solid Interface*; Elsevier: Amsterdam, 1984.
(1186) Bamford, C. H.; Tipper, C. F. H.; Compton, R. G. *Reactions of Solids with Gases*; Elsevier: Amsterdam, 1984.
(1187) Rettner, C. T.; Auerbach, D. J.; Tully, J. C.; Kleyn, A. W. *J. Phys. Chem.* **1996**, *100*, 13021.
(1188) Remorov, R. G.; Bardwell, M. W. *J. Phys. Chem. B* **2005**, *109*, 20036.
(1189) Boudart, M.; Djega-Mariadassou, *Kinetics of Heterogeneous Catalytic Reactions*; Princeton University Press: Princeton, 1984.
(1190) Campbell, I. M. *Catalysis at Surfaces*; Chapman and Hall: London, 1988.
(1191) Ertl, G. *Surf. Sci.* **1994**, *299/300*, 742.
(1192) Kang, H. C.; Weinberg, W. H. *Surf. Sci.* **1994**, *299/300*, 755.
(1193) Robert, M. W. *Surf. Sci.* **1994**, *299/300*, 769.
(1194) Madix, R. J. *Surf. Sci.* **1994**, *299/300*, 785.
(1195) Santen, R. A. v.; Niemantsverdriet, J. W. *Chemical Kinetics and Catalysis*; Plenum: New York, 1995.
(1196) Crespos, C.; Busnengo, H. F.; Dong, W.; Salin A. *J. Chem. Phys.* **2001**, *114*, 10954.
(1197) Sakong, S.; Gross, A. *J. Catal.* **2005**, *231*, 420.
(1198) Tautermann, C. S.; Clary, D. C. *J. Chem. Phys.* **2005**, *122*, 134702.
(1199) Elkowitz, A. B.; McCreery, J. H.; Wolken, G., Jr. *Chem. Phys.* **1975**, *17*, 423.
(1200) Tully, J. C. *J. Chem. Phys.* **1980**, *73*, 6333.
(1201) Kratzer, P.; Brenig, W. *Surf. Sci.* **1991**, *254*, 275.
(1202) Shin, H. K. *J. Chem. Phys.* **1992**, *96*, 3330.
(1203) Jackson, B.; Persson, M. *J. Chem. Phys.* **1992**, *96*, 2378.
(1204) Chang, X. Y.; Perry, M.; Peploski, J.; Thompson, D. L.; Raff, L. M. *J. Chem. Phys.* **1993**, *99*, 4748.
(1205) Jackson, B.; Persson, M.; Kay, B. *J. Chem. Phys.* **1994**, *100*, 7687.
(1206) Shalashilin, D. V.; Jackson, B.; Persson, M. *Faraday Discuss.* **1998**, *110*, 287.
(1207) Kim, W. K.; Ree, J.; Shin, H. K. *J. Phys. Chem. A* **1999**, *103*, 411.
(1208) Shalashilin, D. V.; Jackson, B.; Persson, M. *J. Chem. Phys.* **1999**, *110*, 11038.
(1209) Rutigliano, M.; Cacciatore, M.; Billing, G. D. *Chem. Phys. Lett.* **2001**, *340*, 13.
(1210) Ree, J.; Kim, Y. H.; Shin, H. K. *Chem. Phys. Lett.* **2002**, *353*, 368.
(1211) Meijer, A. J. H. M.; Farebrother, A. J.; Clary, D. J. *J. Phys. Chem. A* **2002**, *106*, 8996.
(1212) Sha, X.; Jackson, B. *Surf. Sci.* **2002**, *496*, 318.
(1213) Kuipers, E. W.; Vardi, A.; Danon, A.; Amirau, A. *Phys. Rev. Lett.* **1991**, *66*, 116.
(1214) Rettner, C. T.; Auerbach, D. J. *Surf. Sci.* **1996**, *357−358*, 602.
(1215) Rettner, C. T.; Auerbach, D. J. *J. Chem. Phys.* **1996**, *104*, 2732.
(1216) Biener, J.; Lutlerloh, C.; Schenk, A.; Pöhlman, K.; Küppers, J. *Surf. Sci.* **1996**, *365*, 255.
(1217) Takamine, Y.; Namiki, A. *J. Chem. Phys.* **1997**, *107*, 8935.
(1218) Buntin, S. A. *J. Chem. Phys.* **1998**, *108*, 1601.
(1219) Hayakawa, E.; Khannon, F.; Yoshifuki, T.; Shimokawa, S.; Namiki, A. *Phys. Rev. B.* **2001**, *65*, 33405.
(1220) Kolovas-Vellianitis, D.; Küppers, J. *J. Phys. Chem. B* **2003**, *107*, 2559.
(1221) Harris, J.; Kasemo, B. *Surf. Sci.* **1981**, *105*, L281.
(1222) Harris, J.; Kasemo, B.; Törnquist, E. *Surf. Sci.* **1981**, *105*, L288.
(1223) Jackson, B.; Persson, M. *J. Chem. Phys.* **1995**, *103*, 6257.
(1224) Kratzer, P.; Brenig, W. *Z. Phys. B* **1996**, *99*, 571.
(1225) Kratzer, P. *J. Chem. Phys.* **1997**, *106*, 6752.
(1226) Persson, M.; Strömquist, J.; Bengtsson, L.; Jackson, B.; Shalashilin, D. V.; Hammer, B. *J. Chem. Phys.* **1999**, *110*, 2240.
(1227) Nakajima, T.; Tanaka, T.; Yamashita, K. *Surf. Sci.* **2000**, *444*, 99.
(1228) Dai, J.; Zhang, J. Z. H. *J. Chem. Phys.* **1995**, *102*, 6280.
(1229) Somers, M. F.; Kingma, S. M.; Pijper, E.; Kroes, G. J.; Lemoine, D. *Chem. Phys. Lett.* **2002**, *360*, 390.
(1230) Perrier, A.; Bonnet, L.; Rayez, J.-C. *J. Phys. Chem. A* **2006**, *110*, 1608.
(1231) Crespos, C.; Collins, M. A.; Pijper, E.; Kroes, G. J. *J. Chem. Phys.* **2004**, *120*, 2392.
(1232) Díaz, C.; Vincent, J. K.; Krishanamohan, G. P.; Olsen, R. A.; Kroes, G. J.; Honkala, K.; Nørskov, J. K. *Phys. Rev. Lett.* **2006**, *96*, 096102.
(1233) Busnengo, H. F.; Salin, A.; Dong, W. *J. Chem. Phys.* **2000**, *112*, 7641.
(1234) Olsen, R. A.; Busnengo, H. F.; Salin, A.; Somers, M. F.; Kroes, G. J.; Baerends, E. J. *J. Chem. Phys.* **2002**, *116*, 3841.
(1235) Somers, M. F.; Olsen, R. A.; Busnengo, H. F.; Baerends, E. J.; Kroes, G. J. *J. Chem. Phys.* **2004**, *121*, 11379.
(1236) McCormack, D. A.; Olsen, R. A.; Baerends, E. J. *J. Chem. Phys.* **2005**, *122*, 194708.
(1237) Luppi, M.; Olsen, R. A.; Baerends, E. J. *Phys. Chem. Chem. Phys.* **2006**, *8*, 688.
(1238) Voegele, A. F.; Tautermann, C. S.; Loerting, T.; Leidl, K. R. *Chem. Phys. Lett.* **2003**, *372*, 569.
(1239) Gordon, D. J.; Minton, T. K.; Alagia, M.; Balucani, M.; Casavecchia, P.; Volpi, G. G. *J. Chem. Phys.* **2000**, *112*, 5975.
(1240) Benjamin, I. *Prog. React. Kinet. Mech.* **2002**, *27*, 87.
(1241) Nathanson, G. M. *Annu. Rev. Phys. Chem.* **2004**, *55*, 231.
(1242) Doering, W. v. E.; Zhao, X. *J. Am. Chem. Soc.* **2006**, *128*, 9080.
(1243) Zuev, P. S.; Sheridan, R. S.; Albu, T. V.; Truhlar, D. G.; Hrovat, D. A.; Borden, W. T. *Science* **2003**, *299*, 867.
(1244) Wonchoba, S. E.; W.-P. Hu, W.-P.; Truhlar, D. G. *Phys. Rev. B* **1995**, *51*, 9985.

CR050205W